The Generation of Cell Lines Permitting Isolation of Genetically Intact Human Cytomegalovirus (HCMV)

A thesis submitted in candidature for the degree of

Master of Philosophy (MPhil)

by

Dawn Roberts

December 2020

Division of Infection and Immunity,

School of Medicine,

Cardiff University

Acknowledgements

I would like to express my most sincere thanks to my supervisors for the opportunity to undertake this MPhil project. I would like to thank Dr Richard Stanton in particular for his support, optimism and never-ending enthusiasm, all of which made this project possible. Thank you for always having the time for me, even though you were always incredibly busy! I am also very grateful to Prof Gavin Wilkinson for his honesty, encouragement and guidance.

I would like to thank the other members of the laboratory, past and present, particularly Dr Virginia-Maria Vlachava and Miss Ourania Kolliniatiin for shRNA construct design and shRNA protein purification respectively. Thanks also to Dr Eddie Wang, Dr Simone Forbes, Dr Evelina Statkute, Miss Anzelika Rubina and Miss Lauren Kerr. Their assistance and support were invaluable, and I could not have done this without them.

I would like to acknowledge my collaborator Dr Michael Weekes, Cambridge University, for providing constructs for this work.

Thank you to my family and close friends for their love and support throughout. Thanks also to the girls and boys at Personal Pole for keeping me active not only during write-up but also lockdown!

Finally, thanks to my husband Jon, the best '*gwr tŷ*' in the world! Thank you for being you.

Summary

Human cytomegalovirus (HCMV) is a clinically important human pathogen that can cause severe disease in immunologically deficient individuals. Studies into the virus are hindered by the rapid and reproducible mutations that occur *in vitro*, resulting in viruses which behave differently from those found *in vivo.* Mutations rapidly occur in the RL13 and UL128L gene regions, leading to increased growth kinetics and altered cellular tropism respectively.

In order to work with genetically intact HCMV, genomes have been BAC cloned, and repaired to genetically match the original clinical sample. This does not, however, prevent the emergence of new mutants. To overcome this, RL13 and UL128L are conditionally suppressed during virus growth using a tetracycline repressor based system. Although effective, this requires the genome to be available as a BAC clone, preventing their use with primary clinical isolates.

This thesis aimed to generate cell lines to enable work with genetically stable clinical isolates without the need for BAC cloning, to produce an indicator cell line for the rapid detection of replicating virus, and to convert existing laboratory-adapted viruses to more closely represent wild-type isolates.

As an alternative to tet repression, cell lines expressing shRNA targeting RL13/UL128L were used to suppress protein expression during infection, however these attempts were unsuccessful. Indicator cell lines were produced that expressed GFP following infection, however the level of GFP induction was too weak for these lines to be used reliably.

However, a UL128 expressing cell line was successfully produced, which complemented the loss of this gene from our existing bank of lab-adapted viruses. As a result, it became possible to infect a range of cell types with existing viruses, therefore enabling studies into viral dissemination, pathogenesis and disease prevention, without the need to re-generate existing constructs in new virus backgrounds.

Table of contents

Table of Figures

Table of tables

Symbols/Acronyms/Abbreviations

+	Containing
°C	Degrees centigrade
Δ	Gene deletion
<	Less than
>	Greater than
ψ	Packaging signal
‘	Prime
α	Alpha
A	Adenine
AIDS	Acquired immunodeficiency syndrome
ANOVA	Analysis of variance
ARPE-19	Adult retinal pigment epithelium
ATCC	American type culture collection
AVEXIS	Avidity-based extracellular interaction screen
β	Beta
B-cell	B lymphocyte
BAC	Bacterial artificial chromosome
BD	Becton Dickinson
C	Cytosine
CD	Cluster of differentiation
CID	Cytomegalic inclusion disease
CO_2	Carbon dioxide
CPE	Cytopathic effect
cPPT	Central polypurine tract

CRALBP	Cellular retinaldehyde-binding protein
CRISPR	Clustered regularly interspaced short palindromic repeats
CXCL1	Chemokine (C-X-C motif) ligand 1
δ	Delta
DABCO	1,4-diazabicyclo-[2,2,2]-octane
DAPI	4′,6-Diamidino-2-phenyindole
DC	Dendritic cell
DDAO	7-hydroxy-9H(I,3-dichloro-9,9-dimethylacridin-2-one)
ddH_2O	Double distilled (ultra pure) water
DE	Delayed early
DMEM	Dulbecco's Modified Eagle Medium
DMSO	Dimethyl sulphoxide
DNA	Deoxyribonucleic acid
DPBS	Dulbecco's phosphate-buffered saline
dsRNA	Double stranded ribonucleic acid
E	Early
EBV	Epstein-Barr virus
EC	Endothelial cell
ECACC	European Collection of Authenticated Cell Cultures
E. coli	Escherichia coli
EDTA	Ethylenediamine tetraacetic acid
eGFP	Enhanced green fluorescent protein
EGFR	Epidermal growth factor receptor
ER	Endoplasmic reticulum
ERAD	Endoplasmic-reticulum-associated protein degradation

F	Flow cytometry
FACS	Fluorescence-activated cell sorting
FBS	Foetal bovine serum
FCAR	Immunoglobulin alpha Fc receptor
FDA	Food and drug administration
FSC	Forward scatter
γ	Gamma
g	Gram
G	Guanine
GAGs	Glycosaminoglycans
GCV	Ganciclovir
GFP	Green fluorescent protein
GM-CSF	Granulocyte macrophage colony-stimulating factor
gp	Glycoprotein
Gy	Gray
HCMV	Human cytomegalovirus
HCMV-IGT	Human cytomegalovirus immunoglobulin therapy
HEK	Human embryo kidney
HF	Human fetal foreskin fibroblasts
HHV-5	Human herpesvirus 5
HIV	Human immunodeficiency virus
h.p.i	Hours post infection
HRP	Horseradish peroxidase
HSC	Hematopoietic stem cell
HSCT	Hematopoietic stem cell transplant

HSPG	Heparan sulphate proteoglycans
HSV	Herpes simplex virus
HT	Human tissue
ICAM	Intercellular Adhesion Molecule
IE	Immediate early
IF	Immunofluorescence
IL	Interleukin
IMS	Industrial methylated spirit
iNos	Inducible nitric oxide synthase
IPTG	Isopropyl β-D-1-thiogalactopyranoside
IRES	Internal ribosome entry site
IRL	Inverted repeat long
IRS	Inverted repeat short
i.u	International units
Kb	Kilobase
Kbp	Kilobase pair
KV	Kilovolt
L	Late
LB	Lysogeny broth/Luria-Bertani medium
LILRB3	Leukocyte Immunoglobulin Like Receptor B3
LG	L-Glutamine
LTR	Long terminal repeat
MCS	Multiple cloning site
MES	2-(*N*-morpholino)ethanesulfonic acid
MHC	Major histocompatibility complex

MIEP	Major immediate early promoter
ml	Milliliter
mm	Millimeter
moDC	Monocyte-derived dendritic cell
MOI	Multiplicity of infection
mRNA	Messenger ribonucleic acid
ms	Millisecond
NAD	Nicotinamide adenine dinucleotide
NADP	Nicotinamide adenine dinucleotide phosphate
NCBI	National Center for Biotechnology Information
NEB	New England Biolabs
NEC	Nuclear egress complex
ng	Nanogram
NK	Natural Killer
nm	Nanometer
NRG-2	Neuregulin-2
Nrp-2	Neuropilin-2
ns	Non-significance
OD	Optical density
OR	Olfactory receptor
ORF	Open reading frame
OriLyt	Origin of lytic repliaction
p	Protein not known to be phosphorylated or glycosylated
P	Probability
PBMC	Peripheral blood mononuclear cells

PBS-T	Phosphate buffered saline containing tween
PCR	Polymerase chain reaction
PDGFRα	Platelet-derived growth factor receptor alpha
PFU	Plaque forming units
PGK	Phosphoglycerate kinase
pH	Potential/power of hydrogen
pp	Phosphoprotein
PPE	Personal protective equipment
PS	Penicillin and streptomycin
PVDF	Polyvinylidene fluoride or polyvinylidene difluoride
qPCR	Quantitative polymerase chain reaction
®	Registered
RISC	RNA-induced silencing complex
RL	Repeat long
RNAi	Ribonucleic acid interference
RPE-1	Retinal pigment epithelium-1
rpm	Revolutions per minute
RPMI	Roswell park memorial institute
RT	Room temperature
RT-qPCR	Quantitative reverse transcription polymerase chain reaction
SDS	Sodium dodecyl sulphate
SDS-PAGE	Sodium dodecyl sulphate–polyacrylamide gel electrophoresis
SFFV	Spleen focus-forming virus
shRNA	Short hairpin ribonucleic acid
siRNA	Short interfering ribonucleic acid

SOC	Super optimal broth
SOT	Solid organ transplant
SSC	Side scatter
SV40TAg	Simian Vacuolating Virus 40 large T antigen
T	Thymine
T-cell	T lymphocyte
TAE	Tris-acetate buffer
TD	Transduced
Tet	Tetracycline
TGFβRIII	Transforming growth factor beta receptor III
THBD	Thrombomodulin
™	Trademark
TNFα	Tumor necrosis factor apha
TNFR-1	Tumor necrosis factor receptor 1
TRS	Terminal repeat short
TRL	Terminal repeat long
UL	Unique long
UL128L	Unique long 128 locus
µm	Micrometre
µM	Micromolar
US	Unique short
UV	Ultra violet
VAC	Viral assemble complex
VCAM	Vascular cell adhesion molecule
VGC	Valganciclovir

V/V	Volume per volume
VZV	Varicella-zoster virus
WB	Western blot
WKRU	Wales kidney research unit
WPRE	Woodchuck Hepatitis Virus Posttranscriptional Regulatory Element
WT	Wild-type
xg	Times gravity

Chapter 1 - Introduction

1.1 Human Cytomegalovirus (HCMV)

Human cytomegalovirus, also referred to as human herpes virus 5 (HHV-5), is a prevalent betaherpes virus with global distribution (1). Infection is typically asymptomatic during primary infection in healthy individuals, progressing into a latent infection, with intermittent reactivation throughout the lifetime of the host (1-2). HCMV is an opportunistic pathogen that can cause severe disease in individuals with an impaired (e.g. HIV patients), diminished (e.g. solid organ transplant patients) or under developed (e.g. neonates) immune system (1-5). Disorders from HCMV infection range from pneumonia, sensorineural hearing loss, cerebral palsy and death (3-7). With HCMV affecting almost 1 in every 1000 births in the UK (7), the economic and social burden of treating the long-term effects associated with infection is vast. No licensed HCMV vaccine currently exists, making it a major health priority worldwide. (1, 8)

1.1.1 Herpesvirus family

Derived from the Greek *herpein*, meaning 'to creep', the family *Herpesviridae*, in the order *Herpesvirales,*encompasses a large number of DNA viruses that replicate in the nucleus of cells from a broad range of hosts including birds, mammals and reptiles (9, 10). *Alloherpesviridea*, that include the herpesviruses of fish and amphibians, and *Malacoherpesviridea*, which contain a herpesvirus capable of infecting oysters, also belong to the order *Herpesvirales*. The family *Herpesviridae* comprises three subfamilies: *Alphaherpesvirinae*, *Betaherpesvirinae* (of which HCMV belongs), and *Gammaherpesvirinae* (11). *Betaherpesviruses* have narrow host ranges and are well adapted to their host. As a result, they exhibit long replication cycles and cell-associated modes of infection, which may help evade the host immune system (12).

Herpesvirus virions are composed of a complex architecture that defines the family. The structure is composed of a relatively large, double-stranded, linear DNA genome enclosed by an icosahedral (T = 16) capsid, which itself is coated by a protein rich layer termed the tegument. Encompassing the entire

structure is the viral envelope, embedded with viral glycoproteins that are necessary for binding to the host cell (1, 11).

Viral phenotypic characteristics such as replication strategy, morphology, host range and the type of disease caused, define the subfamily to which a virus is assigned (12, 13). There are currently 25 species within the *Betaherpesvirinae* subfamily, distributed among the four genera; *Cytomegalovirus*, *Muromegalovirus*, *Proboscivirus* and *Roseolovirus*, with two species as yet unassigned to a particular genus (1, 14). At the time or writing, eleven species have been assigned to the *Cytomegalovirus* genus (1, 14).

1.1.2 Discovery and isolation of HCMV

German pathologist, Dr Hugo Ribbert was the first to describe the appearance of enlarged cells with intranuclear inclusions from sections of a kidney from a stillborn infant in a meeting at the *Natural History Society of Prussian Rhineland and Westphalia*, Germany, 1881 (15). In 1904, Jesionek and Kiolemenoglou reported similar observations in the kidneys, liver and lungs of an 8 month old fetus suffering from hereditary syphilis (16). Löwenstein later reported identical observations in four infants, and concluded that the inclusions were either protozoan in origin, or due to syphilitic induced changes (17). Goodpasture and Talbot provided evidence in 1921 that these abnormal cell structures could be due to chronic inflammation, as a similar phenotype was observed in the salivary glands of guinea pigs. These structures were given the name cytomegalia (large cell) (18). Later that year, Lipschütz noted the similarity of the intranuclear inclusion to that seen in herpetic lesions, and proposed a viral origin for the disease (19). Von Glahn *et al* reiterated this proposal in 1925 (20), but it wasn't until a year later that the first experimental evidence to support this idea was provided by Cole and Kuttner (21). They successfully induced inclusion body formation in young guinea pigs following injection of matter from the salivary gland of older guinea pigs. The pair also noted the lack of pathogenesis when the injected material was injected into other species, but the significance of this observation was not fully realized at the time.

The term ‘Cytomegalic inclusion disease (CID)’ was coined in 1950 by Wyatt *et al*, following clinical observations whereby the presence of enlarged cells correlated with congenital infection in a variety of animals including newborn humans, monkeys, mice, guinea pigs and hamsters (22). Following technological advances and improvements in tissue culture methods for viral isolation, electron microscopy analysis of enlarged pancreatic cells by Minder in 1953 confirmed that viruses were responsible for the aforementioned aetiology observed (23).

Margaret Smith was the first to successfully isolate and propagate virus from the salivary gland of mice in 1954 (24). In 1956, Smith succeeded in growing both human salivary gland derived and kidney derived viruses, and noted that the virus was only able to grow on human, but not murine tissue, illustrating the host specificity of the virus (25-6). Following two independent reports of successful viral isolation and propagation (27-8), Weller provided the first evidence of strain differences among viral isolates. The term ‘cytomegalovirus’ was proposed and adopted in 1960 (17, 19-21).

HCMV is now established as the prototype member of the betaherpesvirus family (1).

1.2 Epidemiology, clinical significance and treatment of cytomegalovirus infection

1.2.1 Epidemiology

HCMV is a prevalent human pathogen, which infects 56–94% of individuals worldwide (29). Seroprevalence varies with age, gender, race, socioeconomic status and geographical location. High seroprevalence is observed in developing countries such as Saudi Arabia (30) and Brazil (31), while lower seroprevalence has been reported in developed countries such as England (32), Australia and Germany (33). The virus is readily transmitted in early life in developing countries, likely due to population density, number of household

members and unclean living conditions. In contrast, wealthy, developed countries show low (~30-40%) seroprevalence in young children (6-11 years) with incidence increasing to >90% with age (>80 years) (34-5). Infection rates in developed nations are therefore inversely related to socioeconomic status (36-41).

In the USA, a study by Staras *et al* in 2006 (40) showed that after correcting for income, geographical location and family size, increased rates of infection were found in African America and Hispanic populations compared to Caucasian individuals between the ages of 15 and 59, suggesting that genetics may play a role in the transmission of the virus (38, 40-1). In support of this idea, two recent independent studies from Ireland (42) and Iran (43) have shown that the most common human leukocyte antigen genes among Caucasians, HLA-A1 and -B8 (44), correlate with HCMV seronegativity, potentially offering an explanation for the lower rates of infection observed in these countries compared to other developed nations. A number of studies have shown lower rates of infection in males compared to females, with only a minimal decrease in the percentage difference between the two genders observed with age (40). However the interpretation of epidemiological studies such as these are subject to debate, due to the possibility of bias or confounding variables.

1.2.2 Transmission and primary infection

Transmission naturally occurs through direct contact with CMV infected bodily fluids such as blood, urine, saliva, tears, cervical secretions, semen, and breast milk. Medical intervention can also result in viral spread through solid-organ or hematopoietic stem cell transplantation (10, 35, 45-6). Based on rhesus models and independent work by Cannon and Mayer, it is presumed that most individuals contract HCMV orally (47-8). Viral replication following primary infection persists between 1-2 months. It is during this period that viraemia occurs, characterized by the dissemination, and low titre shedding of the virus through bodily fluids (49). Concurrently, a proportion of the virus

enters latent infection in the myeloid lineage, where gene expression is restricted, replication is prevented, but the genome is maintained (50-1). As with all human herpesviruses, HCMV persists for the lifetime of the host following initial infection.

1.2.3 HCMV infection in immunologically competent individuals

In the majority of immunologically competent individuals, infection is generally asymptomatic, as viral replication is rapidly controlled by the host immune system and involves antibodies, natural killer (NK) cells and HCMV specific γδ, $CD4^+$ and $CD8^+$ T cells (10, 52-3). In a small percentage of individuals, a mononucleosis-like syndrome has been reported following infection, leading to enlargement of the spleen, fever, fatigue, sore throat and swollen lymph nodes. Other disorders such as cardiovascular, gastrointestinal, neurological and/or liver complications have also been documented (54-6). More recently, the role of HCMV as an oncomodulator in various types of cancer has been proposed (57-8).

1.2.4 HCMV infection in immunologically compromised, suppressed and naïve individuals

HCMV is a clinically significant pathogen that can be life-threatening to immunologically compromised, suppressed and naïve individuals due to their inability to mount an effective immune response against the virus (1-5).

1.2.4.1 HCMV infection in immunologically naïve individuals

It had been shown by the early part of the twentieth century that intracellular inclusions present in the tissue of deceased neonates were a result of congenital infection, with HCMV subsequently identified as the causative agent (see section 1.1.2). The consequence of HCMV infection during fetal development remains unclear, however, studies indicate that the disease caused, and its severity, is dependent on the gestational stage that the

pathogen was acquired. Analysis of infected infant material has established that HCMV can lead to sensorineural hearing loss, neurological damage and visual impairment in infected infants. Such health issues can occur following primary infection, re-activation or re-infection with an alternative strain of the virus (1, 59). HCMV is now established as the leading infectious cause of congenital malformation in the developed world (60-2).

Congenital HCMV infection affects between 0.2% and 2.2% of all live births. Around a tenth of these are symptomatic at birth (<30 days of age), while a further 12.7% go on to display symptoms in later life (61-5). In primary maternal infection, the risk of transplacental infection is relatively low during the first and second trimester (30-40% of all transmissions), however, the risk of serious foetal disease is high, with up to 30% death rates observed. In contrast, transplacental infection rate during the final trimester is vast (up to 70% of all transmissions), but disease severity is much reduced (64, 66). Intrapartum HCMV transmission can occur in seropositive women due to cervical shedding of the virus during childbirth, with infant viral shedding observed between three and six weeks of age (67).

A notable mode of HCMV transmission is via the breast milk of seropositive mothers. Of the ~30-40% of children from developed countires that acquire HCMV by the age of 11, 69% of these contract HCMV in their first year of life (68). Newly infected newborns rarely display symptoms following infection, but have the ability to shed the virus readily through infected saliva and urine for months or even years. Caregivers and other children are subsequently at high risk of catching the virus, thus increasing the incidence of the virus globally (66-70).

1.2.4.2 HCMV infection in immunologically compromised and suppressed individuals

Over half a century ago, cytomegalovirus was identified as a major cause of morbidity and mortality in transplant patients post-operatively, and this continues to be the case today (71-5). The type of disease caused by HCMV

is dependent on the nature of the transplantation, sero-status of both the donor and recipient, the immunosuppressive medication administered and further underlying health complications (76). The percentage of lung or heart-lung transplant patients infected with HCMV post operatively is between 50-75%, while fewer patients acquire the pathogen following pancreas/kidney-pancreas transplantation (50%). Much lower rates of acquisition (9-32%) are seen in heart, liver, haematopoietic stem cell (HSC) or kidney transplant patients (77).

In solid organ transplantation (SOT), the sero-status of both the donor and recipient is crucial to the overall success of the procedure, with seronegative recipients at greatest risk of viremia following transplantation of an organ from a seropositive donor. Conversely, HCMV seropositive haematopoietic stem cell transplantation (HSCT) recipients are at greatest risk of viremia if receiving seronegative stem cells from the donor. In the absence of prophylaxis, diseases associated with HCMV usually occur between 1-3 months post operatively (78-79). Diseases associated with HCMV in immunosuppressed individuals include colitis, encephalitis, hepatitis, retinitis, gastrointestinal tract disease and pneumonia (76, 80).

HCMV is an opportunistic pathogen in patients progressing from HIV infection to Acquired Immunodeficiency Syndrome (AIDS), and is characterised by high levels of HCMV viraemia (81). The lack of a functioning immune system, namely a very low CD4 cell count (<50/mm^3), allows HCMV replication to occur, leading to a variety of clinical manifestations including retinitis, enteritis, encephalitis, pancreatitis, pneumonia and end-organ failure among others (82-87). Over the past quarter of a century however, the widespread use of antiretroviral therapy has dramatically reduced the incidence of these maladies (85-6).

1.2.5 HCMV treatment and prophylaxis

Nearly all available HCMV drug treatments to treat or prevent HCMV disease target the viral replication cycle (2). Intravenously administered ganciclovir

(GCV) is the preferred drug of choice in the immunocompromised, however the oral alternative, valganciclovir (VGC), may be used in less severe cases or as prophylaxis treatment in HIV and solid organ transplant patients (88). Both GCV and VGC are guanosine analogues that are phosphorylated by the viral UL97 kinase, followed by cellular kinases, leading to HCMV DNA replication arrest (2, 89). GCV and VCV work by targeting the HCMV DNA polymerase UL54, resulting in the termination of viral DNA synthesis (90).

The less prescribed drugs Foscarnet, a nucleoside pyrophosphate and cidofovir, a nucleoside monophosphate also inhibit viral DNA polymerases, relying only on cellular kinases for activation (91).

The adverse effects associated with the aforementioned antivirals are well documented, however for many individuals, the benefits greatly outweigh the negatives. To mitigate the adverse effects, drug use is limited and carefully selected according to the affected organ(s) of the patient. Negative effects include, but are not limited to, anemia, thrombocytopenia, liver toxicity (GVC, VGVC) (92), diarrhoea (VGVC) (92), leucopenia, nephrotoxicity, electrolyte imbalances (Foscarnet) (93), neutropenia and renal toxicity (GCV, VGCV, cidofovir) (94). Such antiviral toxicity prevents their use in congenital HCMV infections, leaving neonates with no protection against the virus. Drug resistance in HCMV is common following sustained therapeutic use and occurs when the administered drug can no longer fully suppress viral replication (2, 91), Resistance is acquired following mutations in the viral UL97 (GCV, VGC) or UL54 genes (Foscarnet, cidofovir). It is clear therefore, that there is scope for the development of newer antivirals with better safety profiles and alternative modes of action.

Leflunomide, an anti-rheumatoid arthritis drug, which is both an immunosuppressive and antiviral, has yielded mixed results in clinical trials (95). It has been shown to be effective in post renal transplant HCMV infections due to its ability to inhibit HCMV nucleocapsid tegumentation (96-7), however, a more recent (2017) study of allogeneic stem cell transplant recipients has concluded that leflunomide has limited value therapeutically,

due to its inability to control the virus when HCMV copies exceed 2000/mL (96). Efforts to evaluate the effectiveness of the drug as preemptive treatment in a transplant setting therefore warrant further investigation. Following successful clinical trials, the viral terminase inhibitor, letermovir has recently been licensed for use in haematopoietic stem cell transplant patients in North America and the European union (97). Maribavir, a benzimidazole riboside, inhibits the HCMV kinase UL97 (98-9,) and demonstrates reduced toxicity compared with GCV and VGCV (100). Phase II and III clinical trials indicate that the effectiveness of Maribavir is dependent on its dose, with the appropriate dose for therapeutic and preemptive use as yet undetermined (101).

Exactly twenty years ago, the US Institute of Medicine designated the development of an HCMV vaccine the highest priority based on cost savings. Despite the clear financial and health burden associated with HCMV, no licenced vaccine currently exists, although there are several in development (102). The first HCMV vaccines were live-attenuated vaccines based on the highly passaged laboratory adapted strain, AD169 (103-4). These were quickly replaced with vaccines based on the strain Towne, which remains the best-studied HCMV vaccine candidate to date.

Towne based vaccines have been shown to promote humoral and cellular mediated immunity and can protect against HCMV under certain conditions. A significant limitation with all Towne vaccinations to date, however, is the lack of sustained immunogenicity when compared with naturally occurring infections. Recent co-administration of the pro-inflammatory cytokine, IL-12 with the Towne vaccine by Jacobson *et al* has shown increased Towne immunogenicity through enhanced antibody and T cell production (105).

Administration of the highly conserved and immunogenic envelope glycoprotein B, (gB), in conjunction with either the MF59 or aluminium hydroxide (alum) adjuvants, so called subunit vaccines, have undergone clinical trials. Only MF59 was able to induce antibody titres and neutralizing antibodies at levels comparable with natural infection and has consequently

undergone further evaluation (106). As with the Towne vaccine, initial investigations revealed decreasing neutralizing antibody titres over time, however T cell production levels remained constant (107-8). A number of subsequent phase II clinical trials have also yielded promising results, with a 50% and 43% reduction, respectively, in HCMV infection in young mothers and young girls (12-17 years) (109-10) and a reduction in the level and duration of HCMV viremia in patients undergoing kidney or liver transplantation (110). Epitope-based gB vaccines, with particular focus on the antigenic domains 1-5 are the focus of current HCMV subunit vaccines (111).

In addition to gB, T cell targets pp65 (ppUL83) and the immediate early 1 (IE-1) protein have undergone evaluation as subunit vaccine candidates (112). Plasmid DNA vaccines which contain pp65 and gB have also been tested in phase II trials in hematopoietic stem cell transplant patients and have been shown to reduce viremia. Phase III clinical trials and commercialisation is now in progress (113-4).

Despite being food and drug administration (FDA) approved for pre-emptive HCMV treatment in high-risk lung, heart and intestinal patients in the US (115-6), the addition of intravenous HCMV immunoglobulin therapy (HCMV-IGT) to standard antiviral (GCV/VGCV) treatment remains controversial, as no study to date has demonstrated additional benefit to the patient when compared to standard treatment alone. The use of HCMV-IGT in a congenital infection has yielded mixed results (117-8).

A novel RNA based vaccine vector containing gB and a pp65-IE-1 fusion protein has recently been evaluated in rhesus macaques. Initial studies appear promising as both CD4+ and CD8+ T cell responses were detected in all subjects (119).

With no vaccine immediately forthcoming, prevention of infection though enhanced hygiene and education is the only current means of protection against primary and alternative strain HCMV infections.

1.3 HCMV basic biology

HCMV virions typically range between 150-300nm in diameter and consist of a large, linear, double stranded DNA core protected by the nucleo- or C-capsid (120). The capsid is a symmetrical (T = 16) icosahedral structure measuring 100-110nm in diameter, and made up of five core gene products; pUL46, pUL48A, pUL85, pUL86, pUL104 (121). These are organised into 320 triplexes bound by 162 capsomeres (150 hexamers and 12 pentamers). A portal complex resides on a single pentamer, enabling viral genome movement to/from the capsid (122-3) (Figure 1). The amorphus tegument is approximately 50nm thick and like the capsid, is made from a plethora of virally encoded proteins, plus a modest number of viral and cellular RNAs obtained during virion production in the viral assembly complex (VAC) (124). The functional roles of less than half the tegument proteins have been determined to date, however it is predominated by the pp65, pp150 and pp71 proteins (125-6). Tegument proteins have been implicated in the delivery of viral DNA from the capsid to the nucleus (127), initiation and control of viral replication (128-31), immune evasion (132) and egress of virions from the nucleus and cell (133).

The host-derived bilayer virion envelope is approximately 10nm thick and encompasses the tegument layer (134) (Figure 1). In line with other herpesviruses, it is embedded with viral glycoproteins for cellular attachment and as with the tegument proteins, a number of envelope glycoproteins have been implicated in immune evasion (131). Of the twenty-five envelope glycoproteins (g) identified to date, five (gB, gH, gL, gM and gN) are vital components during initial infection (135).

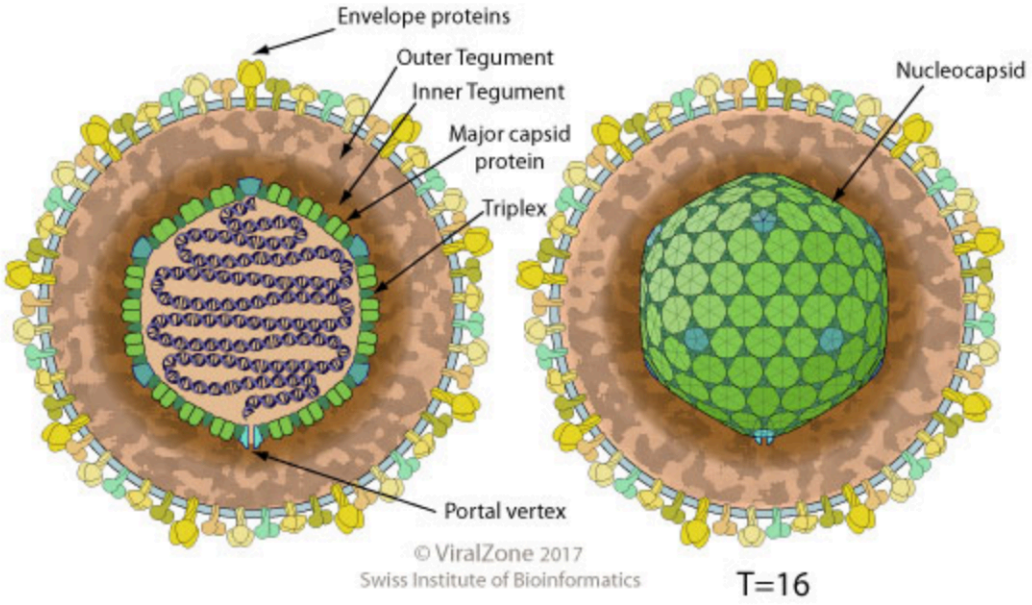

Figure 1. Human cytomegalovirus virion structure

The structure of the HCMV virion with the key components identified. Image taken from https://viralzone.expasy.org/180?outline=all_by_species

1.4 Genetic diversity of HCMV

Isolate, clinical, laboratory adapted and high/low passage strains are terms frequently used in HCMV research. In the context of this thesis, the interchangeable terms ‘isolate’, ‘clinical’ and ‘low passage’ all refer to HCMV that have been isolated from pathological specimens and undergone limited replication *in vitro,* thereby retaining the majority of their genetic integrity. ‘Laboratory adapted’ and ‘high passage’ strains in contrast, describe isolates that have been extensively passaged *in vitro* and have acquired substantial mutations within the genome.

1.4.1 HCMV genome organization

The HCMV genome, which consists of approximately 235Kbp, is among the largest of all the human DNA viruses and encodes between 175 - 750 open reading frames (ORFs), at least 26 mature microRNAs, four long non-coding RNAs (RNA1.2, RNA2.7, RNA4.9 and RNA5.0) and two origin of lytic replication (oriLyt) RNA (1, 136-42). The numbers quoted to describe the HCMV genome vary widely across the literature depending on the evolving definitions of the terms ‘gene’ and ‘ORF’. Historical texts use the ‘classical’ and ‘neoclassical’ definition of a gene, while more recent literature refer to the terms ‘canonical’ and ‘non-canonical’ to define the gene complement, with canonical referring to genes for which a high level of evidence exists that they encode functional proteins. Non-canonical refers to a large number of additional genes that have been identified by ribosome profiling, but may or may not encode functional proteins (143).

The linear, double strandedgenome consists of two unique (U) segments, termed long (L) and short (S), each of which are flanked by inverted repeats, termed terminal/internal repeat long (TRL/IRL) and terminal/internal repeat short (TRS/IRS). Both repeats are also referred to as *ab*/*b’a’* and *a’c*/*ca* respectively (1, 12). A diagrammatic representation of the

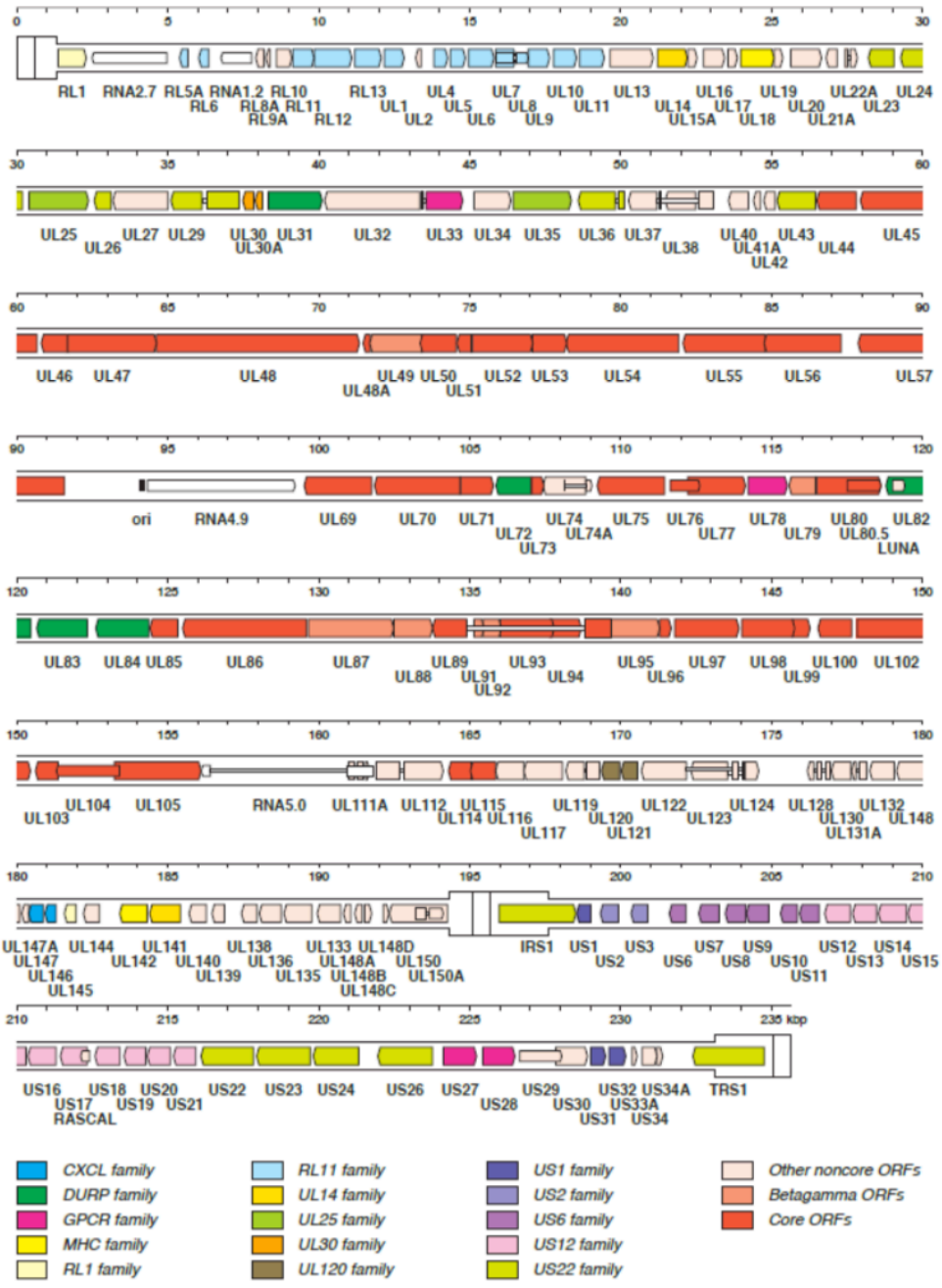

Figure 2. Genetic map of wild-type HCMV

The genetic content of HCMV strain Merlin, demonstrating a TRL–UL–IRL–IRS–US–TRS genomic configuration. Reproduced from (1). Gene families are codified by colour, narrow arrows depict the unique short/long regions while broad arrows represent the long/short repeat regions. Core genes are highlighted in red, non-core genes in beige and introns are depicted by narrow white bars.

genome is given in Figure 2, and lists the canonical genes. The proportion of the genome shared between the repeating sequences corresponds to the *a* sequence, while the other repeat regions are referred to as *b* or *c* sequences. The prime (‘) signifies inverted version of the DNA. Within the repeat sequences are two conserved cis-acting signals, designated pac 1 and pac 2, which are required for HCMV genome cleavage and maturation (144-5). Pac 1 and 2 also promote the formation of four genomic isomers through UL and US sequence inversion (146). The linear DNA rapidly circularises following ligation of the 3’-unpaired nucleotides located at the end of the genome, thereby serving as templates for transcription and replication (147).

The ~70 core genes conserved amongst the herpesvirus family are located in clusters at the heart of the UL region. These are predominantly required for viral replication, while the remaining genes, deemed non-essential for replication, provide accessory functions such as immune evasion and modulating tropism. These non-essential genes are grouped into fifteen multi-gene families and are located at the termini of the unique long and short regions of the viral genome (148-9).

HCMV genes are conventionally named based on their location within the genome and are numbered sequentially. The prefixes ‘pp’, ‘gp’ or ‘p’, refer to phosphoprotein, glycoprotein or proteins that are not known to be phosphorylated or glycosylated respectively, while a descriptor, such as MCP (major capsid protein) may be added at the authors discretion. A lower case letter such as ‘a’ may also be added to a name where a newly discovered gene overlaps with an existing gene (3, 139, 148).

1.4.2 Natural genetic variation between strains

As with many other viruses, it is generally accepted that multiple variants of the HCMV genome exist within the human population (inter-host diversity), potentially as a result of evolutionary selection pressures. Unlike many viruses, hosts have the ability to become infected with multiple strains of HCMV. Strong selective pressure alongside natural selection has the potential

to give rise to further viral gene loss, viral gene expansion, and genetic recombination, resulting in HCMV with greater genetic diversity and fitness (131, 139). Comparative studies have identified a number of genes that display a high degree of variability at the genomic level. These include RL6, RL12, RL13, US9, US28, UL4, UL11, UL18, UL55, UL73 (gN), UL74 (gO), UL115 (gL), UL139, and UL144 (132, 140, 146-48). High-throughput analysis of 101 clinical isolates by Sijmons et al reveal that over 75% of the strains analysed are not genetically intact, but contain disruptive mutations in one or more genes. These mutations can be found in 26 different genes including UL40 and UL111A (149). Genes associated with viral replication are generally wild-type, while proteins located on the virion envelope are highly variable due to their roles in immune evasion or cellular tropism (150-1).

In addition to inter-host variation, samples taken at the same timepoint from the urine and plasma of a number of congenitally infected infants have provided evidence of intra-host variation. Renzette *et al*, demonstrated a ~1.2% variability in the HCMV genome isolated from the plasma and urine of each individual, indicating that dissemination to distal compartments combined with altered environmental conditions may drive the rapid selection of HCMV genomes (139, 149-50).

1.4.3 HCMV strain variability *in vitro*

Since their initial isolation, the HCMV strains AD169, Towne and TB40/F have undergone extensive serial passaging *in vitro*, leading to their classification as laboratory adapted or high passage HCMV strains. Toledo, TR, FX, FIX, TB40/E and Merlin, in contrast, have undergone limited passaging on fibroblasts, and are therefore considered clinical or low passage strains (5). Much of the early work on HCMV was carried out using the high passage strains AD169 and Towne, however, a genome comparative study by Cha *et al* in 1996 revealed that both strains contained an inverted (IR_L) version of the long terminal repeat, (TR_L) in place of the UL/b' region (151-2). This loss of the UL/*b'* region (UL151-UL133) in high passage strains has no detrimental effect on viral replication on fibroblasts, and is therefore hypothesized to play

a role in viral dissemination, virulence or latency *in vivo* (153-4). Within the UL/*b'* region, the UL133-138b region has been extensively studied, with the UL133, UL135, UL136 and 138 ORFs all working in unison to promote latency in $CD34^+$ progenitor cells, while concurrently promoting replication in epithelial cells (153-5). UL138 has also been shown to increase TNFR-1, thereby promoting viral replication and potentially aiding with rescuing the virus from latency (156-7). The UL/*b'* region also consists of genes which have been implicated in immune evasion; UL142 has been demonstrated to encode an MHC class I – like molecule that prevents NK cell mediated killing (158), while UL146 encodes a viral CXCL chemokine, which allows the virus to evade the antiviral activities of the host immune system (159).

Genome wide sequencing of a number of high passage strains, including Towne and AD169 variants, reveal numerous genetic alterations within the HCMV genome as a consequence of serial passaging on fibroblasts, resulting in the loss of cellular tropism, but increased viral replication (139,160). This loss in tropism was later attributed to at least one mutation in the UL128 locus (UL128L, containing UL128, UL130, and UL131A), resulting in viruses that only express the trimeric complex (139, 152, 161-66) (See section 1.6.3.2). Despite their limited propagation on fibroblasts, low passage strains are not immune to genetic re-arrangement. Toledo contains two inverted regions between UL128-UL129 and UL133-UL148a, while FIX and PH lack IRS1 and US1 ORFs (166-68).

Regions of the HCMV genome reproducibly affected by *in vitro* propagation on fibroblasts are the RL13 gene, UL128 locus (UL128L) and in some cases the UL/*b*' region. RL13 is usually the first to mutate, closely followed by the UL128 locus (UL128L), at passages 8-16 and 15-20 respectively (5, 168). Mutations in the UL128L result in the loss of an ability to infect cell types other than fibroblasts, while mutations in either the RL13 and/or UL128L results in viruses with enhanced growth kinetics compared to wild-type virus (151, 160). Mutations within the UL/b', in particular UL140-145, lead to the loss of immune evasion genes (5, 151, 160).

In addition to the mutations observed between laboratory adapted HCMV strains, multiple variants also exist within strains, leading to biological differences not only between, but within stocks (169). Following genomic sequencing of the Towne strain, VR-977, held by the ATCC, Bradley *et al* identified two variants within the strain, subsequently termed varS and varL. The former containing an inverted duplication in place of the U_L/*b'* region, while the latter retained its U_L/*b'* region (139, 170).

As propagation of clinical viruses leads to reproducible mutations within the HCMV genome when cultured *in vitro*, high passage strains generally contain many more mutations compared to their clinical (low passage) counterparts due to environmental selection pressures. Thus, the emergence of mutants is not only inevitable, but rapid (5, 151).

1.5 HCMV life cycle

HCMV infects a broad range of host cell types both *in vivo* and *in vitro*, including fibroblasts, epithelial cells, endothelial cells, smooth muscle cells, neutrophils, macrophages, monocytes, dendritic cells and hepatocytes (1, 2, 47, 136). Unlike other herpesviruses, the replication cycle of HCMV is extremely slow with maximum production of progeny virus observed between 72-96 hours post infection (1). As with all herpesviruses, HCMV undergoes both a lytic and latent life cycle that are characterized by the generation of new virions in the former, and a lack of virion production and limited transcription in the latter. The life cycle of HCMV is summarized in figure 3.

1.5.1 HCMV viral entry, replication and gene expression during *in vivo* infection

gB in conjunction with gM/N, control the adsorption of HCMV onto the host cellular surface via heparin sulfate glycosaminoglycans (GAGs). As one of the core fusion proteins, gB, through its interactions with host cellular receptors including integrins (α2β1, α6β1 and αvβ3), epidermal growth factor receptor

(EGFR) and aminopeptidase (CD13), is essential for virion and host cell receptor binding (93, 171). Viral and cellular fusion is again controlled by gB alongside the gH/gL of the trimeric complex in fibroblasts for direct membrane fusion, or the gH/gL of the pentameric complex where endocytosis is followed by low pH dependent fusion in epithelial and endothelial cells, or pH independent fusion in DCs (137-8, 172-5). The gH/L complex is therefore fundamental for HCMV tropism and is discussed in greater detail in section 1.6.3 (176-7).

Following fusion of the viral envelope with the cellular membrane is the release of nucleocapsids into the cytoplasm. Here the tegument layer is thought to diffuse into the cytoplasm and interact with the host microtubule machinery to promote nucleocapsid translocation to the nucleus. It is the large tegument and binding proteins (UL48 and UL47 products respectively) that initiate viral uncoating and the release of DNA into the nucleus (178). Other tegument proteins have roles in immune evasion or viral replication (179). It is in the nucleus that HCMV genes are expressed in a highly regulated temporal cascade, where immediate early (IE) genes are expressed first, followed by the early (E), delayed early (DE) and late (L) genes (121, 180-1). IE proteins, which are produced 2-4 hours post infection, control subsequent gene expression, and along with the E genes, in particular UL44 and UL54, creates the optimum environment for viral gene expression and synthesis to occur (182). Early gene proteins are crucial for viral genome replication while the L genes, which are expressed at around 48-72 hours, encode the structural proteins required for virion maturation and release (1,183).

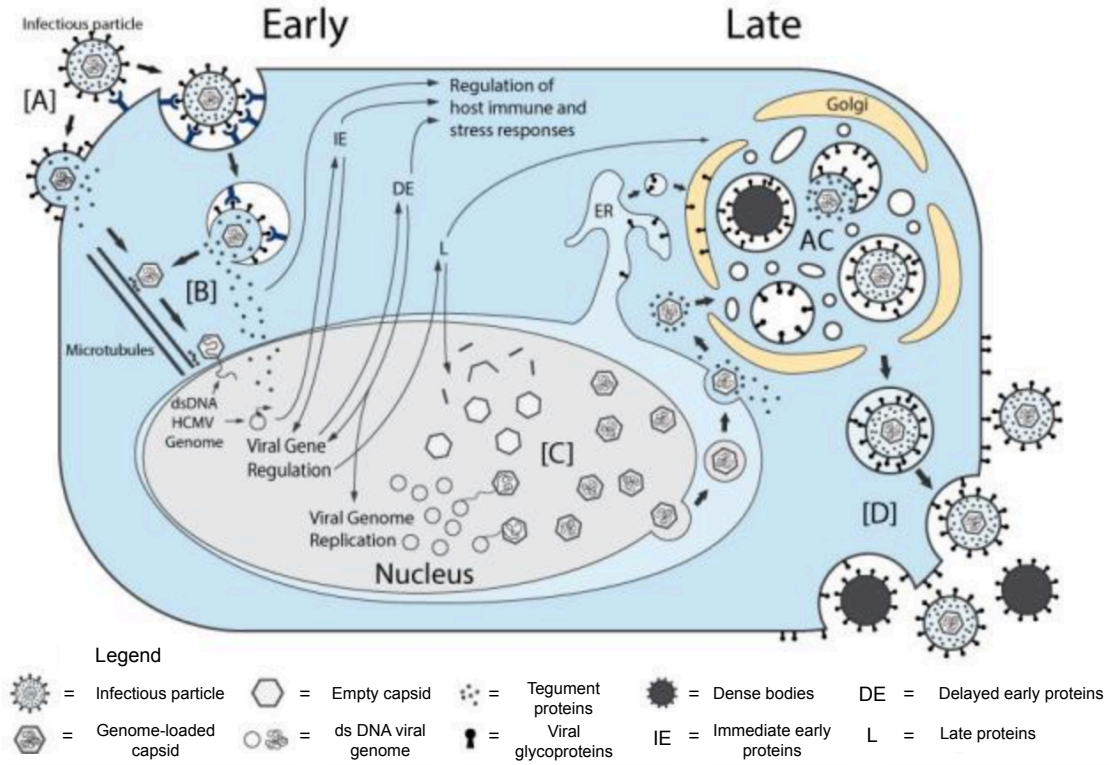

Figure 3. Overview of the HCMV life cycle

A) The virion binds to the host cell surface via specific receptors prior to gB mediated membrane fusion. B) Following entry, proteins are released into the cytoplasm where DNA replication occurs. C) DNA is packaged into capsids, before egress to the cytosol. Here capsids, assimilate tegument proteins before relocating to the viral assembly compartment (vAC), where additional tegument proteins and envelope are acquired D). Acquisition of a secondary envelope leads to the release of infectious particles by exocytosis. Figure reproduced from (184).

1.5.2 HCMV maturation and egress

Following genomic replication and primary tegumentation in the nucleus, viral DNA is cleaved by the terminase complex prior to genome packaging into the capsid. Newly formed capsids are transported from the nucleus to the cytoplasm by the nuclear egress complex (NEC), where nucleocapsids gain secondary tegumentation and envelopment before egress to the extracellular space (1, 185).

Maturation is initiated in the nucleus by the assimilation of tegument proteins by the nucleocapsid, which is done in a highly regulated manner. Assimilation continues during transportation to the viral assembly compartment (VAC) in the cytoplasm, where final HCMV maturation occurs. The VAC is formed during the late stages of viral replication and is composed of viral glycoproteins and tegument proteins -and re-arranged cellular secretory compartments including Golgi and post Golgi compartments and early endosomes (186). Tegument protein ppUL32 provides nucleocapsid stability (187), while the ppUL50-ppUL53 complex regulates egress from the nucleus (188).

Final envelopment and egress relies on the action of multiple viral proteins including pUL71 for envelopment initiation (189), ppUL35 for virion egress (128) and pUL103 for infectious and non-infectious particle release (190). Exocytic trafficking enables the release of mature viral particles from the infected cell (186).

1.5.3 HCMV latency and reactivation

HCMV, like all other herpesviruses, establishes latency within its host and is characterized by a maintenance of the viral genome in the absence of viral replication (191-2). Unlike other viruses in the family, latency occurs in the myeloid lineage, in particular the CD34+ progenitor cells which reside in the bone marrow and the CD14+ cell population that include macrophages and DCs (193-4). The number of latently infected cells is low, with only one in

every ten thousand cells containing viral DNA (195).

Reactivation of latent virus occurs when the IE genes are activated by various physiological and external stimuli including inflammation, stress, drugs and events such as myeloid cell differentiation. The latter has been shown to allow chromatin re-arrangement of the major immediate early promoter (MIEP), thereby prompting the virus to enter the lytic life cycle (196). A competent immune system, through immune surveillance, can generally control the virus preventing it from entering the productive phase of its life cycle. When the host immune system is dysregulated however, lytic infection is initiated, leading to virus associated diseases (197).

To suppress lytic infection and thereby maintain latent infection, the chromatin surrounding the MIEP is placed into a heavily repressive state through chromatin re-modeling (51). Latency is further enhanced by the exclusion of viral activators such as pp71 from the nucleus or up regulation of known latent repressors such as HCMV RNA4.9 (298-200). For HCMV to maintain its latent, inactive state, repressive and activating transcription factors interact with MIEP (200).

The precise interplay between latency and reactivation in HCMV is not yet fully understood, however, understanding this mechanism could prove crucial in the development of novel therapeutic strategies.

1.6 HCMV infection *in vivo*

There are innumerable natural hosts for cytomegalovirus, however only humans are affected by human cytomegalovirus (HCMV), demonstrating the strict species specificity of the virus.

Both the nasal and oral cavities are major sites of HCMV acquisition in individuals. Minimal replication post infection encourages the virus to enter the circulation, and eventually the bone marrow, where latency is established. Viral shedding is at its peak during the first couple of months following initial

infection, however, virions are released sporadically throughout the lifetime of the host, aiding HCMV transmission. Viral shedding is severely restricted following host immune activation (1).

1.6.1 Intra-host HCMV dissemination

Following viral acquisition is primary dissemination, which is thought to predominantly occur in the mucosal tissues located in the pharynx and genital tract (201). Primary cellular targets of HCMV are likely to be epithelial cells where productive replication and viral shedding occurs. This in turn, leads to the release of infectious particles, allowing cell-to-cell dissemination of the virus into other, adjacent cell types including endothelial cells (EC) and fibroblasts. Chemotactic factors released following EC infection, attract neutrophils, natural killer (NK) and other cells of the innate immune system to the site of infection (202).

Following infection, ECs become more permeable, thus increasing their ability to interact with cells from the innate system. Increased surface expression of adhesion molecules including ICAM-1 and VCAM-1 on ECs also enhances adherence between the two cell types (203). Basophils, eosinophils and neutrophils can harbour virus but do not allow lytic infection, and are therefore thought to be important in transporting viral particles to other tissues (201). Due to the ability of innate cells to enter the circulatory system and travel widely within the body, secondary, or systemic infection is thought to be initiated at this point (202).

HCMV can infect the vascular ECs that line the circulatory system, which in turn, infect neighbouring cells that reside in the sub-mucosa (204). A number of infected endothelial cells, termed giant endothelial cells, expand following infection and detach from the blood vessel wall, thus entering the blood stream to infect organs at distal sites (205-7), thereby marking the start of secondary dissemination. See figure 4.

Monocytes, a component of innate immunity also plays a crucial role in viral dissemination and persistence (1, 204). In their naïve state, infected monocytes are unable to support productive replication as immediate early gene expression is blocked. Following viral cell entry, these cells can differentiate, producing macrophages or dendritic cells that are capable of supporting lytic replication (207-9). It is not clear whether the virus has evolved a mechanism to trigger monocyte differentiation or whether HCMV exploits the cellular changes in infected monocytes to its advantage. Monocytes are, none-the-less, essential not only for productive replication, but for dissemination and the establishment of HCMV latency (210).

Work by Greijer *et al,* supports the idea that following secondary dissemination, renal and mammary epithelial cells support lytic infection, before releasing viral particles into their surroundings, allowing infected bodily secretions to infect others (202).

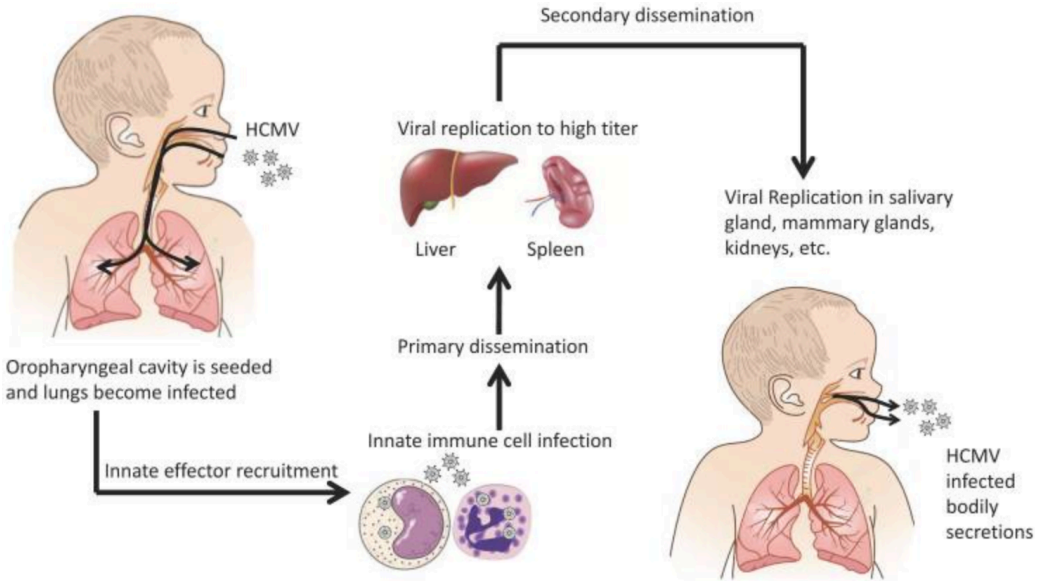

Figure 4. Intra-host dissemination

Intra-host transmission occurs through direct contact with infected bodily fluids, with both the respiratory and gastrointestinal tract major sites of acquisition. Epithelial cells that line the mucosal tissues are the primary cellular targets of HCMV, which subsequently infect other cell types that then enter circulation. Primary dissemination is characterised by the infection of multiple tissues including the liver, kidneys and spleen. Secondary viral dissemination occurs when the virus enters secreting organs such as the mammary gland, saliva and kidneys that shed the virus. Image taken from 211.

1.6.2 Cell-associated versus cell-free dissemination *in vivo*

Based on the independent observations of Lipson *et al* and Spector *et al*, which shows that the majority of virions found in the blood are located within monocytes, lymphocytes, basophils, eosinophils and neutrophils rather than the plasma or serum, it is thought that HCMV dissemination *in vivo* predominantly occurs via cell-associated rather than cell-free mechanisms, presumably in order to avoid attracting the attention of the host immune system (84, 212). Further evidence to support this comes from *in vitro* studies where the decreased ability of HCMV to spread cell-cell is inversely correlated with serial passaging. The loss of this cell-cell dissemination phenotype is due to genetic alternations within the RL13 gene and UL128L (160, 163).

1.6.3 HCMV cell tropism

The breadth of pathologies caused by HCMV *in vivo* can be attributed, at least in part, to the ability of the virus to enter and replicate in a variety of cell types including fibroblasts, epithelial cells, endothelial cells, neurons, smooth muscle cells, stromal cells, dendritic cells, neutrophils, hepatocytes and macrophages (1, 2, 47, 213-4). HCMV cell tropism, defined as the ability of the virus to infect a particular cell type, is heavily dependent on the arrangement of the gH/gL complex, and the precise composition varies depending on the cell type producing the virus (177). On-going *in vitro* studies have revealed the differing mechanisms adopted by the virus to enable entry into the varying aforementioned cell types (see below).

1.6.3.1 Trimeric and pentameric complexes

As previously described in 1.5.1, the envelope glycoprotein B, along with gM/gN, are required for initial viral tethering to the target cell followed by gH/gL mediated cell entry (176-7). The mechanism of entry is dependent on the cell type being infected, with both the trimeric and pentameric complexes playing key roles in viral tropism and entry both *in vivo* and *in vitro.*

HCMV glycoproteins H (pUL75) and L (pUL115) form a disulphide-linked heterodimer (gH/gL) that is highly conserved among the herpesviruses. Cryogenic electron microscopy imaging coupled with recent x-ray crystal structures of the dimer show that the overall structure is an intermediate between the boot-like conformation of HSV-2 and the elongated conformation of EBV (128, 190). gH/gL have been reported to bind cellular receptors immediately prior to gB binding, resulting in gB mediated cell-cell fusion. In contrast, a stable gB-gH/gL complex has been observed in cell-free virions in the absence of receptor binding, thus the precise mechanism(s) governing gB-gH/gL mediated cell entry is unclear (215-17).

In addition to the core fusion machinery described above, HCMV, like other herpesviruses, bind other proteins to modulate viral tropism and entry. HCMV entry into epithelial and endothelial cells is dependent on the UL128L, which encodes the soluble proteins UL128 (15KDa), UL130 (35Kda) and UL131A (18Kda). These proteins simultaneously bind to the core entry glycoproteins, gH/gL to form the pentameric complex (gH/gL/UL128L). This complex is distinct from the trimeric (gH/gL/gO) complex that is necessary for viral entry into fibroblasts (217). See figure 5.

1.6.3.2 Pentameric (gH/gL/UL128L) complex

To understand the pentameric complex assembly, the temporal mechanics of the individual sub-units was investigated by Ryckman *et al*. It was demonstrated that each of the UL128L proteins, when bound sequentially, irrelevant of order, affected the binding capability of the remaining proteins. It was therefore concluded that the UL128L proteins must bind simultaneously onto the gH/gL scaffold for functional complexes to be formed, thus enabling entry into the relevant cell types (173).

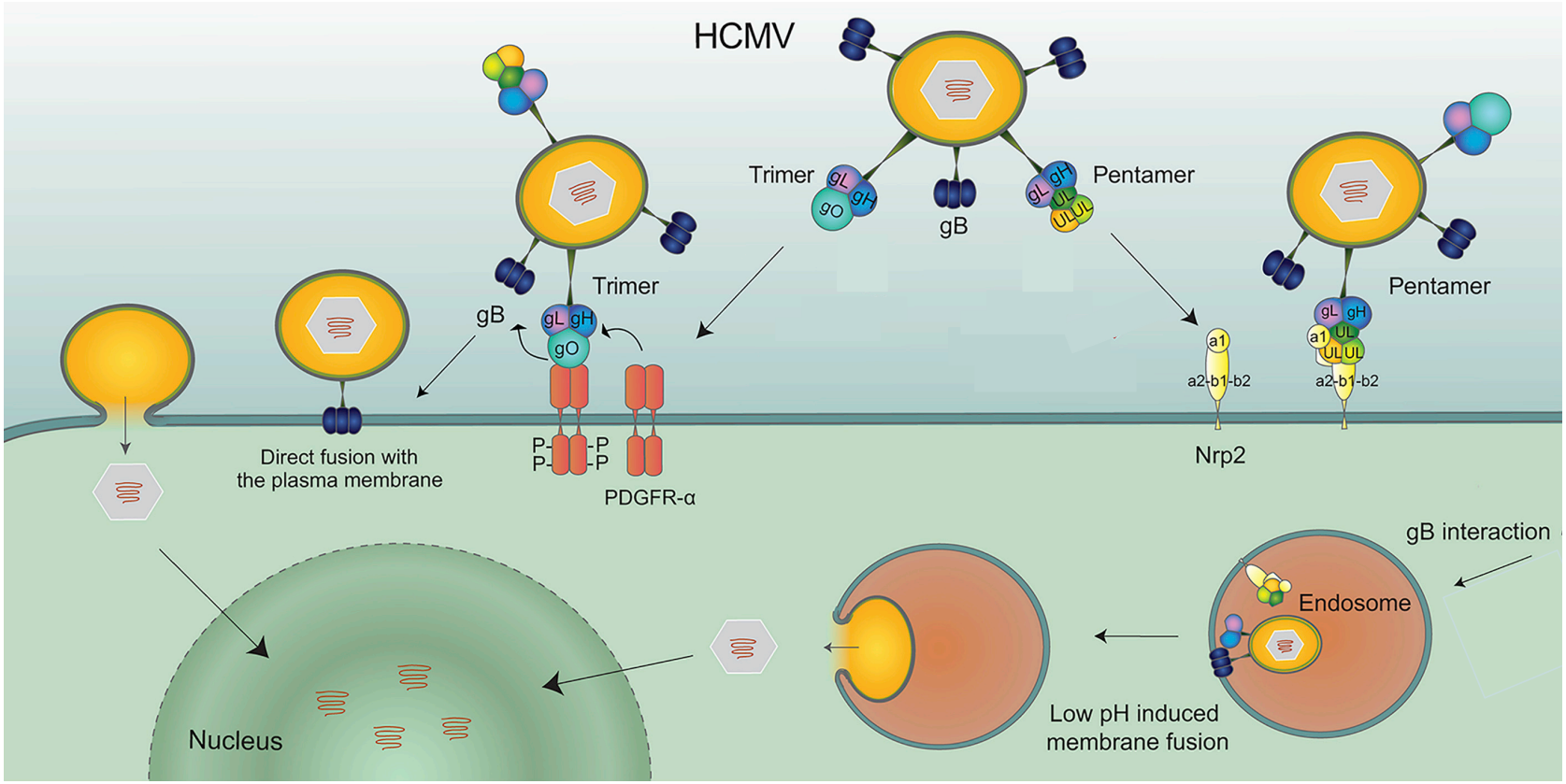

Figure 5. HCMV entry mechanisms; the trimeric and pentameric complexes

The gO sub-unit of the trimeric complex binds the host receptor PDGFRα, promoting gB mediated direct fusion with the plasma membrane of fibroblasts. Receptor-mediated endocytosis of HCMV occurs through pentameric complex and Nrp-2 binding where activation of gB allows the release of viral particles into the cytoplasm in a low pH dependent manner. Image modified from 174.

UL128 and gO have been shown to compete for, and bind gL-Cys144 via a disulfide bond, while UL130 and UL131A are convalently linked to each other, but not to gH/gL. Residues 123 to 162 of UL128 form a flexible linker that extends beyond both UL130 and UL131A to bind its target. It is at this point that the linker performs three helical turns before binding gL (218). Once assembled, the pentameric complex binds the receptor Neuropilin-2 (Nrp-2), allowing viral entry into endothelial cells, epithelial cells, macrophages, and some DCs (174). In addition to identifying the pentameric complex entry receptor, Martinez-Martin *et al*, with the aid of an avidity-based extracellular interaction screen (AVEXIS), identified pentamer interactions with other cellular co-factors including thrombomodulin (THBD), immunoglobulin alpha Fc receptor (FCAR) and leukocyte immunoglobulin-like receptor subfamily B member 3 (LILRB3) with high affinity, while a weak interaction with the complement regulator CD46 (membrane cofactor protein) was also observed. The roles of these other hits have yet to be determined.

It is thought that HCMV entry into epithelial and endothelial cells relies on pentamer/Nrp-2 binding which leads to endocytosis of the virus, where activation of the fusogen, gB, allows the release of viral particles into the cytoplasm in a low pH dependent manner (174). Support for an alternative mode of entry into epithelial and endothelial cells has recently been proposed, where endocytosis may be induced following trimer interaction with an as yet unknown receptor, followed by pentamer/Nrp-2 interaction (219).

1.6.3.3 Trimeric (gH/gL/gO) complex

The gO subunit (~55KDa), encoded by the UL74 gene, undergoes N-linked glycosylation, and there are at least eight genotypes that produce proteins that range between 100-130kDa (222). Within each gO genotype, the amino acid sequences are highly conserved (98-100%), however significant differences (10-30%) are observed between the groups, specifically at the N-terminus where receptor binding prior to cell entry occurs (221). Given its critical role in viral cell entry, this level of variation in the N-terminus between isoforms is surprising.

The precise role of gO in the context of the trimeric complex has been complicated by the existence of multiple genotypes, however, it is now accepted that HCMV entry into fibroblasts is dependent on the gH/gL/gO complex (222). gH/gL/gO has been shown to reside in the virion envelope of WT HCMV (223). Interestingly, the HCMV gO-null strain, TR, was found to release equivalent levels of cell-free virions compared to the WT virus, however, these virions were unable to enter a number of cell types including fibroblasts, epithelial and endothelial cells despite the elevated levels of pentamer present (224). These data combined indicates that cell-free entry into all cell types relies on gH/gL/gO (173, 225).

Building on previous observations by Soroceanu *et al*, where a pentamer deficient virus led to platelet-derived growth factor receptor alpha (PDGFRα) activation in fibroblasts but not epithelial cells, Kabanova *et al* established PDGFRα as the cellular receptor responsible for trimer mediated HCMV cell entry into fibroblasts, with gO identified as the subunit responsible for receptor binding (172, 226). PDGFRα is a known tyrosine kinase receptor present on the cell surface of a variety of cell types such as neurons and fibroblasts, but is importantly absent in epithelial cells.

A number of experiments were conducted by Kabanova *et al*, culminating in the discovery of the mechanism of entry. Trimer immunoprecipitation conducted on biotinylated fibroblasts, coupled with pull-down studies confirmed an interaction between the trimer and PDGFRα, while over-expression of the receptor on epithelial cells allowed the pentamer deficient virus, AD169, to infect this cell type. shRNA knockdown and CRISPR/Cas-9 knockout of PDGFRα provided further evidence of the function of PDGFRα in fibroblasts, with an 80% and 100% reduction, respectively, in the infection of fibroblasts in the presence of pentamer deficient virus, thus establishing the role of PDGFRα in trimer mediated cell entry (172).

Later experiments conducted by Martinez-Martin *et al* using the AVEXIS system re-affirmed PDGFRα as the cellular receptor in fibroblasts necessary for HCMV entry. Additional potential cellular co-factors for the trimeric

complex identified by the screen include transforming growth factor beta receptor type 3 (TGFβRIII) and neuregulin-2 (NRG-2) (174).

The current consensus is that HCMV entry into fibroblasts predominantly, but not exclusively, relies on trimer/PDGFRα binding, followed by a cell membrane/viral envelope fusion event that is orchestrated by gB in a pH independent manner.

1.6.3.4 The importance of the pentameric and trimeric complexes in cell-associated and cell-free spread

Viruses can infect by two routes, with infection starting with cell-free virus, or by direct transfer of virus from an infected cell (cell-cell transfer). These routes are classically distinguished by whether infection is sensitive (cell-free) or resistant (cell-cell) to neutralising antibodies. In addition, a virus spreading predominantly by the cell-free route forms large diffuse plaques, while a virus spreading mainly by the cell-cell route forms tightly localised foci. Primary clinical isolates, along with the low passage strain Merlin, release very low amounts of infectious cell-free virus, and form compact focal plaques, with spread being resistant to neutralising antibodies. They are thus classified as spreading predominantly by the cell-cell route. In contrast, most other strains, including TB40/E, TR and FIX, spread more efficiently via the cell-free route (160, 227-8). This is in part because TB40/E, TR and FIX contain low amounts of the pentamer, but high amounts of the trimer, due to mutations acquired *in vitro.* In comparison, Merlin expresses an abundance of pentamer, but lower amount of trimer. The expression of RL13, which is present in Merlin and other clinical isolates, but mutated in nearly all other passaged strains, also contributes to this cell-associated phenotype.

The function of the trimeric complex has been studied using gO null viruses. Work by Zhang *et al*, Wille *et al* and more recently Schultz *et al* has demonstrated the necessity of the gH/gL/gO for the infectivity of cell-free virions into all cell types, while the presence of the gH/gL/UL128L is also required for cell-free virions to infect monocytes, epithelial and endothelial

cells. The trimeric complex is not necessary for cell-associated epithelial spread (224, 229-30). Schultz *et al* also demonstrated that RL13 expression diminished both cell-free and cell-associated viral spread, indicating that RL13 plays a pivotal role common to both modes of dissemination. Taken together, the route of HCMV spread is determined by RL13 and the pentameric complex, as well as by additional factors (230).

1.6.3.5 Additional host cell surface markers and viral genes implicated in HCMV tropism and entry

By slowing the degradation of gO via the ER-associated degradation (ERAD) pathway, the HCMV protein UL148 has been shown to influence tropism by controlling the ratio of trimer to pentamer in newly generated virions (231-2).

The highly conserved UL116 protein was recently reported to bind gH independently from gL, and is consequently hypothesized to represent an alternative entry mechanism for HCMV (233).

The role of the host receptor, olfactory receptor (OR) 14I1 in HCMV infection of epithelial cells was recently determined in a genome-wide CRISPR/Cas-9 knock out screen. By knocking out the receptor responsible for viral entry, epithelial cells that survived repeated HCMV exposure over several months were sequenced, with both Nrp-2 and OR14I1 shown to be important for productive infection. The authors demonstrated that OR14I1 required the presence of the pentamer for function, but unlike Nrp-2, direct binding between the pentameric complex and OR14I1 has yet to be determined.
The conserved cell surface protein THY-1 (CD90) binds both gB and gH at the commencement of viral infection. The precise role of CD90 is not yet known, but it is thought to play an important role in viral cell entry (234). Both the pentameric complex and gB have been shown to interact with a variety of integrins including αVβ3, α1β1, α3β1, α2β1 and α6β1 for HCMV cell entry into fibroblasts and monocytes (235-7), while CD147 (basigin) assists pentamer mediated entry into epithelial and endothelial cells (238). Other co-receptors implicated in aiding HCMV cell entry include CD151, MHC class I, EGFR,

CD13 (alanyl aminopeptidase) and heparan sulfate proteoglycans (HSPG) (238-41).

1.7 HCMV propagation *in vitro*

Despite the ability of HCMV to infect a plethora of cell types *in vivo*, fibroblasts have traditionally been used to propagate the virus *in vitro*, due to the ease at which these cells become infected at low titres, and the fibroblasts' ability to support superior viral titres compared to all other cell types. It is now known that that the higher HCMV titres achieved are due to *in vitro* associated adaptations by the virus, as a consequence of the loss or modification of viral DNA. Mutations are first observed in the RL13 gene followed by the UL128L (5, 9, 11).

Bacterial artificial chromosome (BAC) technology has been used as a method to stabilize the HCMV genome with both high and low passage strains such as AD169, Towne, Toledo, TB40/E, FIX and TR having been cloned (5). During their creation however, the vector cassette was inserted within the US region, disrupting the immune-regulatory function of the region in viruses derived from these BACs. In addition, the source material for the constructs was no longer available for comparison, meaning that many mutations arising as a result of *in vitro* propagation may not be detected (177). Known genetic alterations within the BACs of clones FIX and TB40-BAC4 include mutations within the UL128L, while the majority of HCMV BACs have been found to contain deletions, frameshift mutations or substitutions within the RL13 ORF, resulting in viruses which no longer behave like their WT counterparts (127, 139).

In order to obtain a wild-type HCMV source to work with *in vitro*, the complete genome of the HCMV strain, Merlin, which was isolated from the urine of a congenitally infected infant, was cloned into a self-excising BAC following minimal passaging (p5) in fibroblasts (228). The generation of this construct led to Merlin being designated the first World Health Organization reference sequence for HCMV (242). Genetic comparison between the Merlin BAC

sequence and the original source material revealed mutations in the UL128 and RL13 genes, either one or both of which were subsequently repaired, resulting in dramatically reduced viral growth on fibroblasts, with the virus preferentially adopting a cell-cell dissemination strategy over cell-free spread. Continued culturing of virus derived form the Merlin-BAC led to the emergence of novel RL13 and UL128L mutants, again resulting in progeny virus with enhanced growth properties (1,5). To prevent selection of these new mutations, Stanton *et al* developed a tetracycline-repression system where both RL13 and UL131A were conditionally suppressed, allowing progeny with a genetically intact virus to be generated. This was achieved by inserting a Tet-operator 19bp upstream of the RL13 gene and two tet-operators upstream of the UL131A, while a HF-Tet repressor cell line was constructed to allow viral growth without the expression of the genes of interest (228). This system permits the generation of a genetically intact virus, however, like all true clinical viruses, cell free viral titres produced by this system are dramatically reduced, making the virus difficult to work with in the laboratory.

1.8 Significance of RL13

RL13 is one of several hypervariable members of the RL11 gene family, which collectively encode a distinctive domain termed RL11D or CR1 (148). RL13 encodes a conserved, highly glycosylated transmembrane protein that rapidly mutates following *in vitro* propagation, yet its conservation *in vivo* suggests that it is essential for survival within the host. It can suppress viral replication in specific cell types, leading to its classification as a temperance gene (131, 139, 160, 228). Fibroblasts cultured with HCMV containing the RL13 gene (+/- UL128L) preferentially adopt a cell-cell dissemination strategy, resulting in very little cell-fee virus (160, 228), potentially as a result of suppressing the function of gO during cell-free spread (243).

Since the realization that viruses that harbor mutations as a consequence of *in vitro* propagation may have lost or acquired pivotal functions, the

importance of working with a genetically defined virus is now evident (5).

1.9 Thesis Aims

In order to exploit the tet-repression system to support the growth of wild-type HCMV in culture, the virus must first be passaged *in vitro* before being BAC cloned, repaired and finally modified so that RL13 and UL128L are tet-repressible. When the virus is cultured in the absence of a tet-repressor however, the virus quickly acquires new RL13 and UL128L mutations rendering the genes non-functional. As RL13 and UL128 are conserved in clinical isolates, this suggests that both genes are essential for the success of the virus *in vivo*. Although the function of the UL128L is known (see section 1.6.3.2), the role of RL13 has yet to be determined.

Due to the highly significant roles these genes are likely to play *in vivo*, it is highly desirable to work with a virus that accurately represents the clinical agent.

The overall aims of the technologies developed in this project are to generate cell lines that will allow the detection or isolation of HCMV from pre-existing laboratory stocks or patient material, without the need for the aforementioned modifications.

Aim 1. Generate a reporter cell line that produces GFP upon infection.

Current methods such as plaque assays for determining successful isolation of HCMV *in vitro* are time-consuming. By generating a novel GFP reporter cell line that fluoresces in the presence of replicating HCMV, confirming isolation of the virus could be reduced from one month down to one week.

Aim 2. Generate shRNA directed against the RL13 and UL128L genes.

By individually suppressing the expression of the UL128L or RL13 genes in culture, the selection pressures driving mutation should be alleviated,

resulting in a high-titre, genetically intact virus being generated directly from clinical isolates.

Aim 3. Generate a UL128 expressing cell line.

Our laboratory has generated over 200 viruses over the past twenty years, none of which contain a wild-type UL128. By generating a UL128 sufficient helper cell line, this will complement the mutated virus stocks already held by the laboratory, resulting in the tropism of the virus being restored to wildtype, without needing to regenerate the mutations on a new viral backbone.

Chapter 2 – Materials and methods

2.1 Reagents

2.1.1 Molecular biology buffers, solutions and components

All buffers, solutions and their components were prepared using double distilled ultra pure grade water (ddH_2O) dispensed from a Barnstead NANOpure® Diamond™ UV unit. All buffers and solutions were used at room temperature unless otherwise stated.

Table 1. Molecular biology buffers, solutions and components

Agarose gel electrophoresis reagents	
Buffer/solution	**Components**
1 x TAE buffer	50X TAE buffer (National Diagnostics, EC-872) diluted 1:50
0.7 or 1% agarose solution	0.7 or 1% Hi-Res standard grade agarose (Geneflow, A4-0700) in 1x TAE buffer. Mixture was heated until fully dissolved
6x DNA loading buffer	30% glycerol (v/v), 0.25% bromophenol blue (w/v) (Sigma, B0126), 0.25% xylene cyanol FF (w/v) (Sigma, X4126)
TE buffer (pH8.0)	10mM Tris, 1mM EDTA
Western blotting reagents	
Lysis buffer (reducing)	25% NuPAGE® LDS (x4) sample buffer (Life Technologies, NP0008), 10% DTT (Fisher, 10674545)
Running buffer	5% 20x BOLT™ MES SDS running buffer (Life Technologies, B0002)
PBS-Tween	0.05% (v/v) Tween 20 (VWR, 8.22184.0500) in DPBS
Stripping buffer	Restore™ stripping buffer (Life Technologies, 21063). Used at 37°C
Transfer buffer	10% (v/v) Novex™ NuPAGE™ transfer buffer (20x) (Life Technologies, NP0006-1), 10% (v/v) methanol
Blocking buffer	5% (w/v) fat-free milk protein in PBS-Tween. Used at 4°C when performing overnight blocking. Used at room

	temperature when used as an antibody diluent
Novex Protein standard	Novex sharp pre-stained protein standard (Life Technologies, LC5800)

2.1.2 Bacterial culture media and antibiotics

All bacterial growth media was subject to sterilization by means of heat treatment prior to use (121°C, 15 minutes, psi 15), and allowed to cool to around 50°C before the addition of antibiotics. All media and supplements were prepared with ddH_2O dispensed from a Barnstead NANOpure® Diamond™ UV unit unless otherwise stated. All buffers and solutions were used at room temperature unless indicated to the contrary.

Table 2. Bacterial culture media and plates

Bacteria growth media and plates	
Luria-Bertani (LB) low salt broth	2% (w/v) LB powder (Melford L1703.0100)
LB agar	15% (w/v) bacteriological agar (VWR 0767.232) in LB agar low salt broth
2% L-arabinose	2% L-arabinose (Sigma, A3256) in LB low broth salt
1% L-arabinose positive selection plates	1% L-arabinose (Sigma, A3256), 25µg/ml kanamycin, 12.5µg/ml chloramphenicol in LB agar
1% L-arabinose negative selection plates	1% L-arabinose (Sigma, A3256), 12.5µg/ml chloramphenicol in LB agar
Negative selection plates	2% (w/v) LB powder (Melford L1703.0100), 12.5µg/ml chloramphenicol
Positive selection plates	2% (w/v) LB powder (Melford L1703.0100), 25µg/ml kanamycin, 12.5µg/ml chloramphenicol

Table 3. Bacterial culture media supplements

Bacterial growth media supplements			
Antibiotic or chemical	**Company and product code**	**Stock concentration and reconstitution media**	**Dilution**
5-Bromo-4-chloro-3-indolyl-β-D-galactopyranoside (X-Gal)	Melford, MB1001	40mg/ml, in dimethyl sulfoxide (DMSO) (Sigma, 276855)	1:500
Ampicillin sodium	Melford, A0104.0025	100mg/ml, in ddH_2O, 0.22 µm filter sterilised	1:1000
Chloramphenicol	Sigma, C0378	12.5mg/ml, in ethanol	1:1000
Isopropyl β-D-1-thiogalactopyranoside (IPTG)	Melford, MB1008	100mM, in ddH_2O	1:500
Kanamycin monosulphate	Melford, K22000-10.0	15mg/ml, in 0.22 µm filter sterilised	1:1000

2.1.3 Tissue culture media

All tissue culture media was pre-warmed to 37°C before use unless otherwise stated. Foetal bovine serum (FBS) source (Sigma, F9665) was batch tested for quality control prior to application.

Table 4. Tissue culture media

General culture media	Supplements
Serum free DMEM	High glucose (4.5ml/L) Dulbecco's Modified Eagles Medium (Sigma, D5796) with no additional supplements
DMEM complete media	High glucose (4.5ml/L) Dulbecco's Modified Eagles Medium (Sigma, D5796), 10% FCS, 1% L-

	Glutamine (200mM stock)
DMEM 20% complete media	High glucose (4.5ml/L) Dulbecco's Modified Eagles Medium (Sigma, D5796), 20% FCS, 1% L-Glutamine (200mM stock)
RPMI complete media	Roswell Park Memorial Institute (RPMI)-1640 medium (Sigma, R0883) with no additional supplements
Dendritic cell (DC) complete media	RPMI complete media supplemented with 1:1000 dilution of ß-mercaptoethanol,100ng/ml each of IL-4 and GM-CSF
DPBS	Dulbecco's Phosphate Buffered Saline (Sigma, D8537)
Freezing media	90% (v/v) FBS, 10% DMSO (Sigma, D2650), 0.22µm filter sterilized. Media used at 4°C

Table 5. Tissue culture growth media supplements

Tissue culture growth media supplements			
Antibiotic	**Company and product code**	**Stock concentration and reconstitution media**	**Dilution**
Geneticin disulfate (G-418)	Melford, G64000	400mg/ml in DPBS, 0.22µm filter sterilised	1:1000
Puromycin dihydrochloride (puromycin)	Insight Bio, SC-108071B	2.5mg/ml in ddH_2O, 0.22µm filter sterilised	1:2500
IL-4	Peprotech, 200-04	100µg/ml in DPBS, 0.22µm filter sterilised	1:1000
GM-CSF	Peprotech, 300-03	100µg/ml in DPBS, 0.22µm filter sterilised	1:1000
ß-mercaptoethanol	Gibco, 21985023	Stock solution supplied	1:1000

Tissue culture growth media supplements were prepared as described, and diluted to working concentration with DC complete media unless otherwise stated.

2.1.4 Experimental media and reagents

Table 6. Plaque assay media

Plaque assay media	
2% avicel	2% Avicel (IMCD UK Limited, 110240AIR25/P-IE) in ddH_2O. Solution mixed thoroughly until homogeneous, then sterilised by heat treatment
2x media	50% (v/v) ddH_2O, 20% (v/v) 10X MEM (Life Technologies, 21430), 20% (v/v) FBS, 6% (v/v) sodium bicarbonate, 7.5% solution (Life Technologies, 25080), 2% Penicillin/streptomycin, 5,000u/ml (Life Technologies, 15070), 1% L-Glutamine, 200mM solution (Life Technologies, 25030)
Avicel overlay media	1:1 volumes of 2% avicel and 2x media

Table 7. Flow cytometry reagents

Flow cytometry reagents	
4% formaldehyde	10% formaldehyde [37 wt. % in H_2O] solution (v/v), (Sigma, 252549), in DPBS
FACS buffer	1 % (v/v) FBS, 2 mM EDTA in DPBS
7-hydroxy-9H(I,3-dichloro-9,9-dimethylacridin-2-one) (DDAO)	CellTrace™ Far Red Cell Proliferation Kit, Life Technologies, C34572. For stock concentration, each lyophilized vial supplied was diluted in 70µl DMSO. Stock diluted 1:2500 in DPBS for working concentration

LIVE/DEAD stain	LIVE/DEAD™ Fixable Aqua Dead Cell Stain Kit, Life Technologies, L34966. Use 1:250 in FACS buffer

Table 8. Immunofluorescence reagents

Immunofluorescence reagents	
Fixing buffer	4% formaldehyde [37 wt. % in H_2O] solution (v/v), (Sigma, 252549), in DPBS
Permeabilisation buffer	0.5% NP-40 in DPBS
4′,6-Diamidino-2-phenyindole (DAPI)	20mg/ml stock (W/V) in in H_2O. Dilute 1:10,000 in in H_2O (Sigma, D9564)
DABCO mounting media	2.5% 1,4-diazabicyclo-[2,2,2]-octane (DABCO) (Sigma, D2522), 90% Glycerol, 7.5%PBS.

2.1.5 Antibodies

Antibodies for flow cytometry (F) were diluted in FACS buffer. Antibodies for western blotting (WB) were diluted in 5% milk/PBS-T. Antibodies for immunofluorescence (IF) were diluted in DPBS.

Table 9. Antibodies

Antibodies			
Antibody	**Clone**	**Company and product code**	**Dilution and use**
CD1a-FITC	HI149	BD biosciences, 555806	1:50, F
CD14 PE-Cyanine7	61D3	e-Bioscience, 9025-0149-120	1:50, F
DC Sign- PE	DCN46	BD biosciences, 551265	1:50, F
Anti-actin		Sigma, A2066	1:2000, WB
Anti UL128		A gift from Dr Daniele Lilleri, Italy	1:250, WB
Anti V5-Tag	SV5-Pk1	Bio-Rad Laboratories Ltd, MCA1360GA	1:5000, WB

Anti mouse HRP (secondary)		Bio-Rad Laboratories Ltd, 170-6516	1:5000, WB
Anti rabbit HRP (secondary)		Bio-Rad Laboratories Ltd, 170-6515	1:5000, WB
Anti V5-Tag		Abcam, ab9116	1:5000, IF
Anti-rabbit AF488 secondary		Life Technologies, A11008	1:500, IF

2.2 Cell culture

Cell culture was performed in a class II microbiological safety cabinet using aseptic technique. All surfaces, consumables and reagents used were wiped with 70% (v/v) industrial methylated spirit (IMS) before and during work to reduce the possibility of contamination. To protect against biological and chemical hazards, appropriate personal protective equipment (PPE) was worn. Cell lines used were periodically tested for mycoplasma contamination.

2.2.1 Established cell lines

Human foetal foreskin fibroblasts, hereto referred to as HF, was kindly provided by Dr Graham Farrar (Centre for Applied Microbiology & Research (CAMR), Salisbury, UK), and immortalised using human telomerase reverse transcriptase by Dr Brian McSharry (Cardiff) to generate HF-Tert cells (244). Transduction of HF-Tert cells with a retrovirus expressing the tetracycline repressor (HF-Tet) was carried out by Dr Richard Stanton (Cardiff) (228). The fibroblast cell line, MG 3468 was a generous gift from Dr Richard Greaves (Imperial College Faculty of Medicine, London, UK). The Human Embryo Kidney (HEK) 293T cell line, which carries a gene encoding the Simian Vacuolating Virus 40 large tumour antigen (SV40TAg) was obtained from the European Collection of Authenticated Cell Cultures (ECACC), 12022001. The HEK 293 phoenix cells, a derivative of the HEK 293T was obtained from the American Type Culture Collection (ATCC®), CRL-3213^{TM}. Retinal Pigmented Epithelial (RPE-1) and Adult Retinal Pigment Epithelial (ARPE-19) cells,

(CRL-4000™ and CRL-2302™ respectively) were also purchased from the ATCC®.

2.2.2 Culturing/harvesting cell lines

Cells were cultured in complete media (DMEM) and maintained at 37°C in an atmosphere containing 5% CO_2. Cell lines were sub-cultured twice a week when approximately 90% confluent. Media was aspirated from the adherent cells and washed twice with DPBS. Cells were treated with 0.05% trypsin/EDTA (Sigma, T3924) to dissociate and disaggregate the monolayer. Flasks were placed at 37°C between 2-4 minutes until the cells became detached. Gentle agitation of the flask aided disassociation. An equal volume of media containing serum was added to the cell suspension to inhibit trypsin activity before the cells were centrifuged at 300 xg for 4 minutes. Pelleted cells were re-suspended in 10mls of fresh complete media and counted or sub-cultured 1/3-1/10 depending on cell type. Harvested cells were re-suspended in an appropriate volume of media depending on future use.

2.2.3 Cell counting

Immediately following re-suspension (section 2.2.2), a 10µl aliquot of cells was added to a bright-line glass hemocytometer (SIGMA, Z359629) by capillary action and counted under white light. Cells crossing the top and left grid lines were counted, while cells intersecting the bottom and right lines were ignored. Viable cells within the four corner grid regions were counted and multiplied by 10^4 before being divided by 4 to calculate the average number of cells per millilitre (ml) of suspension.

2.2.4 Cryopreservation and recovery of cells

Following trypsinisation and centrifugation (section 2.2.2), cells were re-suspended in cold freezing media at a density of $1x10^6$/ml before being aliquoted into 1.5ml cryovials (Greiner, 123280). Cells were placed in a controlled rate (1°C/min) freezing vessel (Nalgene® Mr Frosty, Sigma,

C1562) and placed in an ultra low freezer overnight before being transferred to liquid nitrogen for long term storage.

To recover the cells following liquid nitrogen storage, the cells were thawed rapidly in a 37°C waterbath whilst being gently agitated. Once thawed, the cell suspension was immediately transferred to a 15ml tube and diluted drop-wise with 7mls of complete media (DMEM) to avoid hypotonic shock to the cells. Entire cell suspension was transferred to a T25 flask and monitored.

2.2.5 Generation of dendritic cells (DCs) from whole blood

Permission to approach and obtain whole blood from healthy adult volunteers was granted by the school of medicine research ethics committee (application reference16/52). All blood donations were taken by a trained phlebotomist and recorded in accordance with the Human Tissue (HT) Act 2006.

50mls of heparinized (10i.u/ml) whole blood was taken from healthy adult volunteers, diluted in an identical volume of DPBS and carefully layered onto an equal volume of histopaque® 1077 (Sigma, 10771) solution. Peripheral blood mononuclear cells (PBMCs) were isolated by density gradient centrifugation for 20 minutes, 470 xg with the rotor brake deactivated. The PBMC layer was carefully aspirated from the plasma and histopaque interface and transferred to a clean 50ml tube. The cells were washed twice before being re-suspended in 10mls of fresh DPBS.

To isolate the cells of interest from the PBMCs, CD14+ cells within the mononuclear fraction were magnetically labeled with CD14 human MicroBeads (Miltenyi Biotec, 130-050-201) and loaded onto a MACS® LS column contained within the magnetic field of a MACS separator. In accordance with the protocol, CD14+ cells were retained by the column and eluted to produce an enriched CD14+ monocyte population. To assess the purity of the retained population, the cells were labeled using a CD14-PECy7 antibody and assessed by flow cytometry using an Accuri C6 cytometer, BD (2.5.4)

To differentiate DCs from the enriched population, cells were re-suspended at a density of $2x10^6$ in DC complete media and plated on non-treated tissue culture dishes (Sigma, CLS3738). Cells were maintained at 37ºC in a humidified, 5% CO_2 atmosphere. Culture media was replenished on day 4 with cells phenotyped by flow cytometry on day 7 prior to use. DC differentiation was achieved when cells presented as $CD1a^{high}$, DC-$Sign^{high}$, $CD14^{low}$. See figure 6a-c.

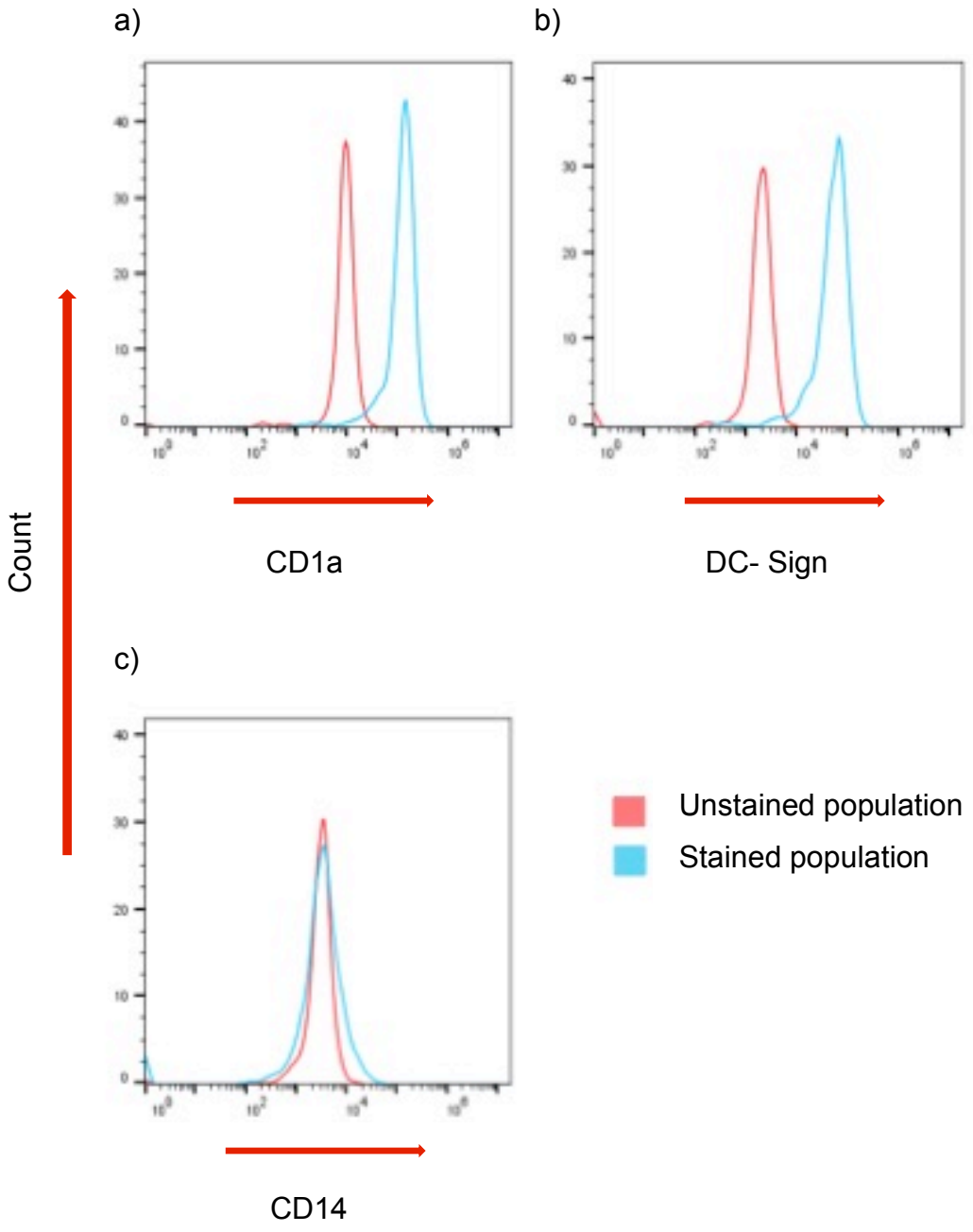

Figure 6a-c. Differentiation profile of CD14+ enruched cell population followign 7 days culture

Phenotypic profile of CD14+ enriched population following 7 days culture in selection media. DC differentiation was achieved when the cells presented as (a) $CD1a^{high}$, (b) $DC\text{-}Sign^{high}$, and (c) $CD14^{low}$.

2.3 HCMV preparation and infection

Generation of viral stocks

The genetic background to the viruses used throughout this study was the HCMV strain Merlin, that originated from bacterial artificial chromosome (BAC) constructed by Stanton et al (228). Briefly, the entire Merlin genome which contained either wild-type RL13 and UL128, or the mutated form of one or both of these genes, were cloned into a self-excising BAC. Both RL13 and UL128L open reading frames (ORF) were placed under tetracycline (tet) conditional control to prevent acquired mutations during *in vitro* culture. Propagation and growth of viruses containing wild-type genes was done in HF-tet cells, which contained the tet-repressor necessary to prevent transcription of the genes of interest. Further BAC manipulation required for this study was performed in a category 1 microbiology laboratory, while growth of live virus and infections were performed within a class II microbiological safety cabinet. The viruses used in chapters 4 and 5 contained a P2A self-cleaving peptide followed by a GFP ORF after UL36, to provide a marker of infection (245-6).

2.3.1 Generation of HCMV viral stocks from bacterial artificial chromosome (BAC) DNA

Fibroblast optimized solutions, supplements and electrical parameters from an AMAXA nucleofector kit were employed to enable the transfer of 2µg of viral BAC DNA directly into the nucleus of HF-Tet cells, according to the manufacturers' instructions. Transfected cells were seeded into a T25 flask and upon initial plaque formation, cells were trypsinised and re-seeded to promote viral spread across the monolayer. Upon full infection of the monolayer, viral supernatant was collected and spun before being used to infect 10 x T150 flasks of HF-Tet cells to generate viral stocks for experimentation.

2.3.2 Generation of viral stocks from existing stocks (or from viral supernatant obtained in 2.3.1)

Ten T150 flasks (150 cm^2, Corning, VWR, 734-1719) of HF-Tet cells were grown to between 80-85% confluency before being infected either with an existing viral stock at a multiplicity of infection (MOI) of 0.03, or $1/10^{th}$ of the supernatant obtained from 2.3.1. Cells were fed twice a week until cytopathic events (CPE) was observed in >90% of the population. Supernatant was removed and stored at -80°C every other day until the monolayer was destroyed. Bleeds were thawed at 37°C before centrifugation at 300 xg for 4 min to remove cellular debris. Pooled supernatant was spun in an Avanti Beckman highspeed centrifuge at 29416 xg for 2 hours at RT. Supernatant was discarded and pellet re-suspended in 8mls of DMEM serum free media using a 19 gauge needle to disperse any aggregates. Suspension was aliquoted in 200µl volumes and frozen at -80°C.

2.3.3 Quantification of viral stocks by plaque assay

Primary HFs were seeded at a density of 2.5 x 10^5 cells per well of a 6 well plate a day prior to infection. The following day, 1 in 1 x 10^4, 10^5 and 10^6 viral stock solutions were prepared and 100µl added to the cells. Plates were placed on a rocker (Stuart See-Saw SSI-4) at 10rpm for 2 hours under normal tissue culture conditions, after which, the inoculum was replaced with avicel overlay media to limit cell-free viral spread. Following 2 weeks incubation at 37ºC at 5% CO_2, the avicel overlay media was removed, monolayer washed and plaque number recorded. Viral titres were calculated and expressed as total plaque forming units per milliliter (PFU/ml^{-1}) using the following equation:

Plaque number x 10 x dilution factor.

2.3.4 Infection of cells with HCMV for experimentation

Target cells were seeded in DMEM serum free (fibroblasts) or complete (epithelial cells) media at 1 x 10^6 cells per T25 flask, 18 hours prior to infection. Number of cells seeded was adjusted according to the culture vessel used. Viral aliquots were thawed quickly at 37°C and cells infected at pre-determined MOI. Cells were placed on a rocking platform at 10rpm (Stuart See-Saw SSI-4) for 2 hours at 37°C/5%CO_2, after which, the inoculum was replaced with fresh SF or complete media. Infections were monitored for evidence of CPE at 18h.p.i and media replaced with DMEM complete media in all cell types used.

2.4 General molecular biology techniques

2.4.1 Polymerase chain reaction (PCR)

Two oligonucleotide sequences, each designed to bind the complementary sequence of either the sense or antisense strand, were used for the amplification of specific nucleic acid fragments. A reaction mixture was prepared using the Expand™ High Fidelity PCR System (Roche, Sigma, 11732650001), and a Biometra T3000 thermocycler allowed amplification of the target sequence. Annealing temperatures and extension times varied depending on the melting temperature of the primers and the length of the desired fragment. All reactions were performed in thin walled PCR tubes (Elkay, THER-05NX). ddH_2O was used in place of a DNA template and served as a negative control.

2.4.2 DNA agarose gel electrophoresis

Plasmid DNA, PCR, restriction enzyme digests and ligation products were separated by agarose gel electrophoresis for visualisation and purification. Agarose concentrations used were 0.7% or 1% (w/v) depending on the size of the DNA fragments of interest. 4µl of Midori Green Advance (Anachem, 95016900) was added to 50mls of molten agarose solution, poured into a

casting gel containing a comb and allowed to solidify. Once solidified, gels were placed in a tank containing 1x TAE buffer. DNA was mixed with 6x DNA loading buffer (table 1) to a final 1x concentration and loaded into a well alongside a molecular marker (HighRanger Plus 100bp DNA ladder, Geneflow, L3-0017). Electrophoresis was performed at 100 volts for 45-60 minutes until the bands were adequately separated. DNA was visualized on a UV transilluminator (Syngene, 2020L) with photographic records taken using a GeneSys xx6 gel doc system.

2.4.3 DNA extraction and purification

Following DNA visualization (above), fragments of interest were excised from the gels and placed in clean 1.5ml microfuge tubes (Fisher, 11558232). Exposure to UV light was kept to a minimum as not to cause unnecessary DNA damage. Geneflow Q-Spin Gel Extraction/PCR purification kit (K1-0040) was used to isolate the DNA according to the manufacturers instructions. Briefly, gel fragments were weighed and binding buffer (100% w/v) added. Mixture was heated for 10 minutes at 55°C to dissolve the agarose before being added to the supplied spin columns. Following centrifugation (13,000 xg), flow through was discarded and the membrane bound DNA was washed twice in an ethanol wash solution to remove contaminants. Pure DNA was collected under low salt conditions by the addition of 30µl of supplied elution buffer. DNA was stored at -20°C until required.

2.4.4 En passant homologous recombination-mediated genetic engineering (recombineering)

En passant recombineering, which relies on a two-step recombination process, was utilized to generate the desired Merlin mutants used in this study. Recombineering was performed as previously described by Tischer et al (247).

Principle

Homologous recombineering employs the E. coli bacterial strain GS1783, a gift from Dr. Gregory Smith, Northwestern University Medical School, Chicago, which contains lambda Red recombination genes. In the first round of recombineering, heat-inducible Red recombination allows insertion of a selectable marker (kanamycin) cassette, which itself contains an I-SceI cleavage site, and flanked by duplicated arms of homology to the target site. L-arabinose induction of the I-SceI enzyme promotes the second round of Red recombination, where seamless excision of the selectable marker and deletion of the gene of interest occurs.

All primers used during en passant recombinering can be found in table ST4. All incubations, unless otherwise started, were performed in a Stuart SI500 shaking incubator (VWR, 444-5503) set at 200rpm, 32°C.

2.4.4.1 First round of recombineering – Cassette insertion

To delete UL141 from a BAC, primers with arms of homology to the target insertion site and the 5' end of the kanamycin/I-SceI cassette were constructed. Following cassette amplification (2.4.1) and DPNI treatment to digest temple DNA, the PCR product was gel purified (2.4.3) and DNA stored at 4°C until required.

GS1783 bacteria containing the BAC of interest were grown overnight as a starter culture in 5ml LB media containing chloramphenicol. 0.5ml of this was used to inoculate 25ml of fresh LB media until an optical density (OD) 600 of between 0.55-65 was reached, equating to the exponential growth phase of the bacterial culture. OD_{600} was measured using a UV spectrophotometer (Pharmicia UltraSpec 3000). Following heat-shock treatment (42°C) to induce the lambda phage genes required for Red recombination, the culture was immediately placed on ice to cease further replication. Transformation competent cells were washed twice by centrifugation for 5 minutes at 3345 xg in cold (<4°C) ddH_2O to eliminate the presence of LB media. The resultant

bacterial pellet was re-suspended in residual water (~400µl) and 25µl of this transferred into 0.5ml pre-chilled tubes.

3µl of the amplified selection cassette was added to the tube before being transferred to pre-cooled cuvettes (Geneflow, E6-0060). Following 5 minutes incubation on ice, the reaction was subject to electroporation at 3.0KV using program EC3 of a MicroPulser™ electroporator (Bio-Rad). Only reactions with a millisecond (ms) value of >5.0 were taken forward. Reactions were allowed to recover in 1ml of LB media for 1 hour. 400ul of this reaction was pelleted and re-suspended in 100ul fresh LB media before being plated on LB agar plates supplemented with 25µg/ml kanamycin and 12.5µg/ml chloramphenicol. Bacteria containing the selectable marker were identified through positive selection on LB agar plates.

Four colonies were selected from the aforementioned plates and a new starter culture initiated. Following overnight incubation, 0.5ml of the starter culture was reserved (at 4ºC) for the second round of recombineering, while the remainder was used for small scale DNA isolation (2.4.6) and screening for insertion of the en-passant cassette by PCR (2.4.1). DNA was visualized on an agarose gel (2.4.2) and products that ran at the expected molecular weight were selected for the next round of manipulation.

2.4.4.2 Second round of recombineering – Resolving en passant cassette.

10µl of the saved starter culture from the first round was added to 1ml LB media supplemented with chloramphenicol, and incubated at 32ºC for 2 hours. The starter culture was diluted 1:1 with 2% L-arabinose and incubated for 1 hour before being transferred to a 42°C waterbath for 30 minutes to induce the lambda phage genes required for the second round of Red recombination. Following this, they were returned to the shaking incubator for 2 hours, then plated onto 1% L-arabinose selection plates supplemented with chloramphenicol for negative bacterial selection. Colonies were allowed to form overnight at 32°C in a bacterial oven.

2.4.4.3 Determining resolved colonies.

Ten bacterial colonies were picked using a sterile loop from the negative selection plates above, and re-plated onto plates containing chloramphenicol or chloramphenicol plus kanamycin. Bacteria where the cassette had been successfully resolved would be sensitive to kanamycin, and would therefore only grow in the absence of the antibiotic, allowing easy identification of correct clones.

Four kanamycin sensitive clones were selected for small scale DNA isolation with 0.5ml of the starter culture added to glycerol (15% v/v) to form bacterial glycerol stocks for future preservation and subsequent large scale DNA isolation suitable for transfection. DNA was purified from 4.5ml overnight culture, the modified region PCR amplified (2.4.1) and run on an agarose gel to confirm loss of the selection cassette (2.4.2). DNA of the correct molecular weight were sequenced to confirm deletion of the UL141 gene of interest.

2.4.5 Generation and storage of transformed E. Coli HST08 strain cells

Transformation of E. coli HST08 strain cells with plasmid DNA was performed using Stellar™ Competent Cell kit (Clontech - Protocol PT5055-2) as per the manufacturer's specifications, with untransformed bacteria used as a comparator. Briefly, cells were thawed on ice and agitated to ensure even distribution. A 50µl aliquot was transferred to a pre-chilled 15ml tube along with 5ng of the DNA of interest and placed on ice for 30 minutes. Immediately following heat-shock treatment (45 seconds, 42°C), cells were placed on ice for a further 2 minutes before the addition of pre-warmed (37°C) SOC media (supplied with kit). Cells were allowed to recover at 37°C for 1 hour on a rotating platform before overnight incubation on LB agar plates containing ampicillin. Colonies were observed where uptake of DNA occurred. The shRNA vector preparations in chapter 4 were performed by Miss Ourania Kolliniatiin. All other vector isolations were performed by me.

To generate bacterial stocks for downstream applications, single colonies were picked and incubated in 5mls LB broth containing ampicillin overnight. Glycerol stocks were prepared by adding 150μl sterile glycerol to 350μl of the overnight culture and stored at -80°C.

2.4.6 Small scale DNA isolation (mini preparation)

For the isolation of molecular biology grade DNA, QIAprep Spin Miniprep Kit (Qiagen, 27016) was used as described by the manufacturer. Following overnight growth of the bacterial culture of interest, pelleted cells (300 xg, 4 minutes, 4°C) were re-suspended (250μl buffer P1), lysed by alkaline conditions (250μl buffer P2), and neutralised (350μl buffer N3) prior to flocculate clearance. Cell suspension containing the DNA of interest was bound to a silica membrane by centrifugation (17,000 xg, 10 minutes), washed in supplied buffers and eluted into a fresh tube by the addition of 50μl ddH_2O. DNA was stored at -20°C until required.

2.4.7 Large scale DNA isolation (maxi preparation)

To perform large scale DNA isolation for transfection, glycerol stocks of transformed bacteria containing the gene of interest were plated on LB agar plates containing an appropriate antibiotic. Following overnight incubation at 32°C, single colonies were inoculated into 5mls of LB broth (+ antibiotic), and incubated for 6 hours at 32°C in a shacking incubator (200rpm). Cultures were transferred to 250ml volumes of LB broth (+antibiotic) and incubated for 18 hours in a 32°C shacking incubator (200rpm) in preparation for large (maxi) scale DNA extraction.

Maxi preparations were performed using NucleoBond® BAC 100 (Macherey-Nagel, 740579) according to the manufacturers protocol for low-copy number plasmid purification. Briefly, bacteria were pelleted at 6000 xg for 15 minutes at 4°C before being lysed by a modified alkaline/SDS lysis procedure. Following potassium acetate neutralization, a flocculate containing unwanted

DNA formed while the DNA of interest was retained in solution. Plasmids of interest were captured, washed and eluted from an equilibrated nucleobond column using reagents that were supplied with the kit. To eliminate contaminants from the eluted DNA, the plasmid was precipitated by the addition of isopropanol before being washed in 70% (v/v) ethanol. Following centrifugation at 15000 xg for 10 minutes at RT, the final pellets were air dried and reconstituted in 100µl of ddH_2O.

2.4.8 Calculating DNA concentration

Nucleic acid concentration was determined using a NanoDrop® 100 spectrophotometer. The instrument was initiated by the addition of 2µl of ddH_2O onto the analyser, followed by 2µl of the reference sample, which was used to 'blank' the machine. DNA concentration was calculated by measuring the absorbance of the sample of interest at 280nm. DNA purity was determined by the 260/280 absorbance ratio, where readings between 1.7-2 were deemed good quality. Samples were stored at 4°C (short term) or -20°C (long term) until required.

2.4.9 Restriction digest

For UL128 retroviral construction, both the pMXs-IP retroviral vector DNA and UL128 insert generated by PCR (2.4.1) were subject to BamHI and XhoI double restriction digest to ensure the ends of each construct were compatible for annealing to occur. Reactions were set up as outlined in table 10. Reactions were performed at 37ºC for 18 hours.

Table 10. Restriction enzyme reactions - individual construct digests

	pMXs-IP vector (µl)	UL128 insert (µl)
10 x buffer 3.1 (NEB)	6	3
BamHI	1	1
XhoI	1	1
ddH_2O	2	5
Construct	50	30
Total volume	60	40

Following transformation of Stellar™ Competent Cells with the ligated retroviral construct (2.4.5), starter cultures were grown and DNA extracted. To confirm UL128 uptake by the retroviral vector, BamHI and XhoI restriction digest was performed (Table 11) at 37ºC for 1 hour, with DNA vizualised using gel electrophoresis. Digested and undigested banding patterns were compared to determine ligation success.

Table 11. Restriction enzyme reactions - ligated construct digests

	Ligated construct (µl)
10 x buffer 3.1 (NEB)	1
BamHI	0.5
XhoI	0.5
ddH_2O	6
Construct	2
Total volume	10

2.4.10 Dephosphorylation.

To prevent the pMXs-IP vector from re-circularizing, the gene carrier was subject to dephosphorylation to remove the 5’ phosphate usually required to form a phosphodiester bond with another DNA fragment. The reaction was set

up with 60µl of sample DNA, 7µl antarctic phosphatase reaction buffer (x10) (NEB, M0289), 1µl antarctic enzyme (NEB, M0289) and 2µl ddH_2O. Following 15 minutes incubation at 37ºC, inactivation of the reaction was achieved by heating the sample (65ºC) for 5 minutes. UL128 and pMXs-IP constructs were subsequently purified (2.4.3) to remove contaminants before ligation.

2.4.11 Ligation

To ligate the vector and UL128 gene construct, T4 DNA ligase (NEB, M0202) was used to catalyze the formation of the phosphodiester bond between the 3' hydroxyl and 5' phosphate groups of the different sources of DNA. The reaction was performed at 16°C, overnight. An insert:vector molarity ratio of 3:1 was used and calculated using the following formula:

$$\frac{\text{Kb of insert}}{\text{Kb of vector}} \times \text{ng of vector}$$

In addition to the sample of interest, two negative control reactions were performed in parallel, one lacking the insert, the other lacking the T4 enzyme.

To verify the ligation process, all reactions were run on an agarose gel (2.4.2) and visualized with UV illumination.

2.4.12 Insertion of UL128 into pCR™4-TOPO® TA vector

Due to initial difficulties encountered during direct cloning of UL128 into the pMXs-IP retroviral vector, the gene of interest was cloned into a pCR™4-TOPO® TA vector (Life Technologies, K459540).

Incorporation of the insert into the pCR™4-TOPO® TA vector relies on the ability of adenosine (A) and thymine (T) to form strong associations through hydrogen bonding. As the vector is supplied containing a T extension, a complimentary 3' A overhang was added to the UL128 construct post amplification by the addition of 1 unit of Taq polymerase, and heated to 72ºC

for 10 minutes. Following UL128 gel purification (2.4.3) and insert/vector ligation (as 2.4.11 but using ligation reagents (salt, topo vector) supplied by the manufacturer), the competent E. coli bacterial strain, DH5 alpha (DH5α), was transformed using sodium/magnesium chloride and heat-shock method as per the manufacturers' instructions. A *LacZα-ccdB* gene in the E. coli permitted easy identification of transformed bacteria through blue-white screening on ampicillin-containing LB agar plates supplemented with 5-bromo-4-chloro-indolyl-β- D-galactopyranoside (x-gal, 80μg/ml). Growth of white colonies indicated successful uptake of the vector into the bacteria. Four colonies were selected and small-scale DNA isolation performed (2.4.6). As EcoRI restriction sites flanked the UL128 insertion site, isolated DNA was subject to EcoRI restriction enzyme digest, allowing easy extraction of the gene of interest post transformation. Following DNA sequencing (2.4.12), correct sequences containing the gene of interest plus the EcoRI site were further digested (2.4.9) with BamHI and XhoI restriction enzymes to release the UL128 insert required to ligate with the pMXs-IP retroviral vector.

2.4.13 Sequencing DNA

To confirm UL128 insertion into target vectors, deletion of the UL141 sequence from a BAC or to check that modified DNA regions were free from errors, DNA fragments to be sequenced were obtained by PCR (2.4.1), gel purified (2.4.3) and commercially sequenced using a Mix2Seq kit (Eurofins Genomics). Each reaction consisted of 2μl of either the forward or reverse primer (10μM) and 15μl of the DNA of interest (10ng/ul) as per the manufacturers protocol. Sequence analysis was carried out using CLC main workbench version 7.9.1, where sequences generated were compared to the reference sequence Merlin.

2.4.14 Transfection and co-transfection

2.4.14.1 Co-transfection with Effectene® Transfection Reagent

Co-transfection of HEK 293T cells was achieved using the Effectene® Transfection Reagent protocol (Qiagen, 301425). To improve user safety when working with lentiviruses, the genes necessary for viral packaging and transduction were absent from the vector and added prior to transfection. DNA for the pRSV-REV (248), pMDLg (249) and pMD2G (250) packaging plasmids which transport RNA from the nucleus (251), organise virion structure (252), and aid viral fusion to the envelope (253) respectively, were kindly provided by Didier Trono. Briefly, target cells were seeded on Corning® CellBIND® 25cm^2 flasks (Fisher, 10194302) at a density of 5.0 x 10^5 the day preceding infection. 2.0μg of total DNA was combined with DNA condensation buffer and enhancer solution to promote the formation of condensed effectene® –DNA complexes. Following incubation with effectene® transfection reagent, the mixture was directly added, drop-wise, into pre-prepared flasks and briefly placed on a slow moving rocker to ensure an even distribution of complexes. 72 hours following cell-DNA complex incubation (under normal growth conditions), supernatant containing the viral transgene was collected, spun (300 xg, 4 minutes), 0.45μm sterile filtered and either used immediately or stored at -80ºC until required for transduction.

2.4.14.2 Transfection with Effectene® Transfection Reagent

Transfection of HEK 293 phoenix cells with a retroviral vector using Effectene® Transfection Reagent was performed as outlined in 2.4.11.1, with the exception of the requirement for helper plasmids. As the envelope gene for determining the tropism of the retroviral vector was provided by the packaging cell line, no helper plasmids were necessary. As the vector lacked a reporter gene, transfection efficiency was determined by transfecting a GFP expressing plasmid into the packaging cell line.

2.4.14.3 Co-transfection with GeneJuice®

For lentiviral DNA co-transfection of HEK 293T cells, GeneJuice® reagent (Merck, 70967) was used. In brief, room temperature GeneJuice was added to serum free DMEM (1:33) and incubated at RT for 5 minutes. 150µl of this mixture was added to 1.91µg total DNA per reaction, and incubated at ambient temperature for 30 minutes to allow transfection complexes to form. For the reasons stated in 2.4.11.1, the genes required for viral packaging and transduction were absent from the vector and therefore added prior to transfection. Complexes were added drop-wise to HEK 293T cells that had been seeded at 1.0 x 10^6 per T25cm^2 flask the previous day. Following 72 hours incubation, supernatant containing the lentivirus of interest was harvested and spun (600 xg, 15 minutes) to remove cellular debris, 0.45µm sterile filtered and either used immediately or stored at -80ºC until required for transduction of the target cells.

To estimate transfection efficiency, target cells were co-transfected with a GFP DNA control that were visualized and assessed under a fluorescent microscope. Green cells indicated successful integration of the DNA into the host cell.

2.4.15 Transduction

2.4.15.1 Direct transduction of lentiviral vectors

Live lentivirus was placed directly onto target cells seeded in DMEM complete media the day prior to infection at a density of 1.0 x 10^6 per T25cm^2 flask.

2.4.15.2 Transduction with RetroNectin® reagent

To improve transduction efficiency through enhancement of viral particle and target cell co-localization, RetroNectin® (TaKaRa Bio Inc, T100A/B) reagent was used according to the manufacturers instructions. Briefly, lentivirus was spun onto RetroNectin® coated (20µg/ml) dishes at 1639 xg for 2 hours at RT. Following supernatant removal, target cells were seeded at 4.1 x 10^5 and

maintained at 37°C in an atmosphere containing 5% CO_2. After 24 hours, appropriate selection medium was added to the wells.

Transduction efficiency was monitored, where possible, with fluorescently labelled (GFP or mCherry) viruses under a fluorescent microscope at 72 hours. In all cases, following growth selection media, dying cells detached from the plate, allowing for easy identification of transformed clones.

2.5 Functional and analytical assays

Unless otherwise stated, all dilutions and infections were carried out in DMEM serum free media with all infections performed in triplicate.

2.5.1 Plaque assay for determining HCMV genetic background

Glycoproteins H and L form the foundation on which the trimer and pentamer complexes are formed (see 1.6.3.1). As there is a finite amount of gH-gL present in HCMV, in wild-type virus, both gO and the UL128L compete for these complexes. Merlin gO is less efficient at competing for gH/gL than UL128L, resulting in small plaque formation when incubated on fibroblasts. In contrast, a virus lacking the UL128L is incapable of forming the pentamer, leaving gO free to bind all gH-gL present, resulting in the formation of larger plaques on fibroblasts compared to wild-type virus.

To exploit plaque size formation as an indicator of UL128L HCMV genetic status, plaque assays were preformed as described in 2.3.3 with the following adjustments. MG 3468 or HF-Tert cells lacking or carrying the transgene of interest (UL128) were seeded at the stated density and infected at 60, 120 and 240 plaque forming units (PFUs). Following avicel overlay media removal, plaques were imaged (Leica DMi8 Inverted microscope) and analysed using Image J software (Fiji).

2.5.2 Adherent and non-adherent co-culture assay

Co-cultures were performed using adherent epithelial (RPE-1, ARPE-19) or non-adherent dendritic cell (DC) targets. All viruses used contained a UL36-P2A-GFP fusion, allowing infection to be tracked by flow cytometry (2.5.4). Washes were performed by centrifugation using DPBS. All samples were performed in triplicate.

Control and/or UL128 transduced fibroblast cells were infected with HCMV at an MOI of 10 (2.3.4), and incubated for 72 hours at 37°C in an atmosphere containing 5% CO_2. Fibroblasts were harvested, washed and stained with DDAO for 15 minutes (37ºC) before repeated washing to remove unbound stain. Stained cells were added to previously (epithelial cells) or freshly (DC's) plated target cells at a ratio of 3:1 (donor:target). Co-cultures were harvested 24 hours post incubation, with supernatant also retained for processing during DC co-culture. Cells were washed and stained with LIVE/DEAD™ aqua fixable dye to distinguish dead from live cell populations. Samples were washed thoroughly and fixed in 4% formaldehyde solution before being analyzed by an Attune NxT flow cytometer (Life Technologies).

2.5.3 Western blotting sample preparation and protein analysis

Cell samples were washed twice in DPBS before total protein was extracted using reducing sample buffer (25% NuPAGE LDS sample buffer, 10%DTT, 65% ddH2O). Cell scrapers (Greiner Bio-One, 541 070) were used to ensure sample dissociation from the flask before collection. Proteins were diluted with 6X loading buffer and boiled at 100ºC for 5 minutes to ensure sample denaturation. A pre-cast BOLT bis-tris gradient (4-12%) gel (Thermofisher, NW04125BOX) was loaded with 30µl of boiled sample and 10µl of pre-stained protein standard, and subjected to electrophoresis at 150V for 1 hour using BOLT MES running buffer. Proteins were transferred onto a methanol activated Hybond® P, 0.45µm, PVDF membrane (Sigma, GE10600023) for 2 hours at 10V in transfer buffer (50mls NuPAGE transfer buffer (x20), 50mls methanol, 40mls ddH2O). The membrane was dried prior to incubation with

UL128, V5 or actin primary antibody diluted in blocking buffer at varying concentrations (Table 9). Membrane was washed in PBS-T (3 x 10 minute washes) to wash off unbound antibody, and incubated with an appropriate HRP secondary antibody for 45 minutes. Membrane was visualized by chemiluminescence using Supersignal West Pico (Pierce). Signal was detected using a GeneSys xx6 gel doc system.

2.5.4 Flow cytometry

Flow cytometry was performed using an Accuri C6 (BD) or Attune NxT (Life Technologies) flow cytometer. Cell suspensions were spun prior to all washing procedures at 300 xg for 4 minutes. All incubations were performed on ice in dark conditions.

2.5.4.1 Sample preparation and staining

Working on ice, harvested cells (2.2.2) were placed in a 96V bottom plate (Thermo Scientific™, 612V96) and washed twice in cold FACS buffer. Cells were stained with LIVE/DEAD aqua dye or appropriate antibody (Table 9) for 30 minutes. Following repeated washes in FACS buffer, cells were fixed in 4% formaldehyde solution for 20 minutes and washed twice in FACS buffer. Final cell pellets were re-suspended in 150µl DPBS before being analyzed by flow cytometry.

2.5.4.2 Compensation

Fluorophore compensation was performed to eliminate the possibility of readings being recorded by a second channel/detector, thereby generating a double positive sample. Compensation control samples included unstained donor and target cells, DDAO stained fibroblasts, LIVE/DEAD stained fibroblasts and GFP infected fibroblasts. Samples were processed as in 2.5.4.1. To exclude dead cell readings from the analysed data, a dead cell population was generated by heating 5 x 10^5 cells to 80ºC for 10 minutes before incubation in an ice bath. Once cooled, the cells were added to an

equivalent number of untreated (live) cells and stained as in 2.5.4.1. Compensation was performed using both the Attune NxT software and FlowJoV10.

2.5.4.3 Data acquisition

Events were acquired using forward (FSC) and side scatter area (SSC), with doublets excluded by changes in refractive index. When used, a LIVE/DEAD gating strategy was applied to the single cell population, with cells heavily stained by the dye (dead) excluded from further analysis. Percentage of infected cells using the Accuri C6 cytometer was determined by gating on GFP+ cells. Percentage of target fluorescent cells during co-culture assay was measured by gating on DDAO-/GFP+ cells.

2.5.4.4 Data analysis

Co-culture assay compensation was preformed using Attune NxT software. All data was analysed using FlowJoV10 software.

2.5.5 Immunofluorescence staining

All treatments were conducted at room temperature unless otherwise stated. Three washes were performed after each treatment using DPBS.
4×10^3 parental or UL128 transduced fibroblasts were seeded onto black 96 well plates (Ibidi, Thistle Scientific, IB-89626) 18-24 hours prior to staining. Cells were fixed with 4% formaldehyde solution for 15 minutes before incubation with permeabilisation buffer for 20 minutes. Cells were incubated with primary (V5-tag) then secondary (anti rabbit AF488) antibody (Table 9) for 30 minutes at 37ºC. To stop the fluorophores fading during imaging, DABCO mounting media was added to the cells and incubated for 1 hour in a darkened environment. Immunofluorescence was detected using a Zeiss axio observer microscope.

2.5.6 Single cell cloning

To obtain single cell clones from heterogeneous UL54 and UL112/3 transduced cell populations, single cell cloning was performed as described below. Parental HF-Tert cells were harvested (2.2.2), re-suspended in DMEM complete media and gamma irradiated at 6,000 Gy. Cells were seeded at 1 x 10^4 cells/well of a 96-well plate. The following day, transduced cells were harvested (2.2.2), counted and diluted to 100 cells per 10ml of DMEM 20% complete media. Cell counts were verified using an Accuri C6 cytometer. Using a multichannel pipette, 100µl of the diluted cells were pipetted into each well of the prepared 96 well plates. To confirm that the irradiated fibroblasts were unable to proliferate, a negative control plate was set up to monitor cell growth. Plates were fed twice a week in DMEM 20% complete media until the appearance of micro-colonies. Cells were trypsinized and re-seeded into a 96 well plate, allowing non-proliferating cells to be eliminated. Clones were expanded by plating into progressively larger plates until a sufficient number of cells could be harvested for experimentation.

2.6 Microscopy

2.6.1 Leica microscope for immunofluorescence

A DMi8 Leica fluorescent microscope was used to monitor and record GFP or mCherry fluorescence and brightfield images during plaque assays (2.3.3, 2.5.1) and viral infections (2.3.4). Images were saved as Tiff files before being analyzed using ImageJ (Fuji) software. Plaque size area was determined manually with plaque size areas calculated using ImajeJ software (Analyze➔ Measure). Plaque sizes were calculated as pixels^2.

2.6.2 Zeiss Microscope for Immunofluorescence

A Zeiss (Axio Observer) microscope was used for determining the localization and expression levels of the V5 tag in the UL128 transduced cell lines generated in chapter 5. Exposure times were determined manually for each

fluorophore/dye used using Zeiss in-built exposure software. Images were saved as Tiff files with composite images generated using ImageJ (Fuji) software.

2.7 Statistical analyses of functional assays

GraphPad Prism 6 software (GraphPad Software, Inc., CA, USA) was used for all statistical analyses of functional assays. Statistical significance was determined using two-way ANOVA with Tukey's multiple comparison test or two-tailed unpaired T test. Differences were considered significant if the probability (P) value was ≤0.05. Significance was displayed in figures as follows; ns, *; P≤0.05, **; P≤0.01, ***; P≤0.001, ****, P≤0.0001. Data from a minimum of three independent experiments were analyzed in all cases. Bar graphs represent the mean of a minimum of three experiments (each in triplicate) with error bars representing the standard deviation of the mean.

Chapter 3 - Results

Generation of an indicator cell line for HCMV detection based on enhanced green fluorescent protein

3.1 Introduction

In collaboration with the Wales Kidney Research Unit (WKRU), our group is contributing to understanding of HCMV disease in renal transplant recipients by examining HCMV genotype in relation to disease outcome. To achieve this, HCMV is isolated from the urine of patients undergoing productive infection prior to, and post transplantation. Isolated virus is then sequenced and/or cultured for future use. Viral titres from clinical isolates are often low however, making it necessary to culture the virus for several (4-5) weeks in order to determine whether HCMV has been successfully isolated.

In order to expedite the detection process, indicator cell lines that rely on HCMV induced expression of a reporter gene, driven by viral promoters were developed.

3.2 Promoter rationale and design

The expression of early (E) HCMV genes relies on the viral immediate-early 1 (IE-1) and 2 (IE-2) transcription regulators working in partnership with host transcription factors (1, 3 254). Luganini *et al* (255) exploited the IE-2 dependent activation of the UL54 and UL112/3 early gene promoters to generate reporter assays where enhanced green fluorescence protein (eGFP) gene expression was driven by either the UL54 or UL112/3 promoter, demonstrating the presence of replicating HCMV in the assay. However, their work exploited plasmid integration into the glioblastoma U373-MG cell line. HCMV does not replicate efficiently in this line, making it unsuitable for isolation of primary clinical isolates. We therefore attempted to recapitulate their results using identical promoters to drive eGFP expression in fibroblasts (HF-Tert). Plasmids do not integrate into these cells at measurable levels, therefore a lentiviral based delivery system was utilised.

The UL54 and UL112/3 promoter sequences were chosen based on their strong activation upon HCMV infection (256), transactivation following IE2 expression (257), lack of basal activity in uninfected cells (258) and proven ability in Luganini's cell-based assay to generate a rapid and specific method for detecting replicating HCMV *in vitro* (255). The primer sequences adopted by Luganini *et al* to amplify the promoters of interest were designed against the HCMV strain, AD169. The AD169 and Merlin genomes, both obtained from the National Center for Biotechnology Information (NCBI) GenBank nucleotide database, NC001347 and GU179001 respectively, were aligned using CLC main workbench version 7.9.1. The promers were located on the AD169 sequence, and the homologus region on Merlin used. The genome located between, and including each paired primer was obtained and used as the specific promoter sequence in the lentiviral vector of choice (Appendix: Tables ST1, ST2).

3.3 Generation of a lentiviral expression vector

A mammalian HIV based lentiviral expression vector (Vector Builder) was selected as the means of attaining gene delivery into target cells based on its ability to permanently incorporate its genes into host DNA in both dividing and non–dividing cells *in vitro* (259-60), resulting in long-term expression of the gene of interest (261). Viral UL54 or UL112/3 promoters were chosen to drive eGFP expression in HF-Tert cells to allow early detection of replicating virus by fluorescence and flow cytometry. To permit selection of stable expressing clones after transduction, a neomycin resistance gene was inserted into the vector. An ampicillin resistance gene was included for plasmid maintenance in E. coli (Figure 7). Plasmids were shipped as E. coli bacterial glycerol stocks.

Transformed bacteria containing the packaging or expression plasmids of interest were grown in preparation for large (maxi) scale DNA isolation.

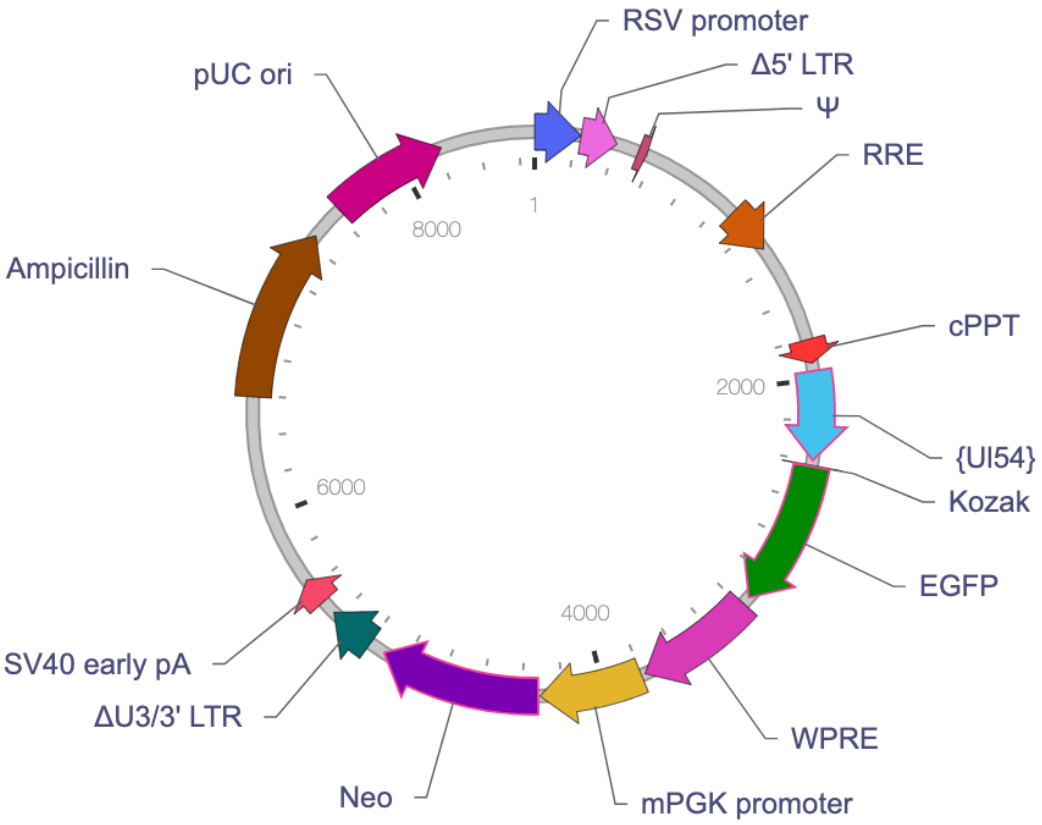

Figure 7. Plasmid map of the lenti-UL54-eGFP lentiviral vector backbone

Schematic of the lenti-UL54-eGFP viral vector plasmid, highlighting location of key genes; UL54 promoter, neomycin and ampicillin resistance genes and eGFP open reading frame. The lenti-UL112/3 vector contained an identical lentiviral template

3.4 Production and validation of lentiviruses

To produce lentiviral particles, the 293T cell line was subject to simultaneous transfection with three packaging plasmids and a single lentiviral expression vector (see 2.4.14.3). Transfection efficiency was evaluated by transfecting a GFP expressing plasmid in place of the lentiviral vector into the cell line. 60% transfection efficiency was observed at 72h.p.i. (data not shown), validating transfection.

To establish the desired cell lines, lentiviral transduction into target HF-Tert cells using retronectin® reagent was performed (see 2.4.15.2). Cells were continually cultured in neomycin selection media until all non-transduced cells were eliminated. Surviving cell populations were expanded, inferring successful uptake of the viral vector by the HF-Tert cell line. UL54 and UL112/3 transduced cells are hereto known as HF-UL54-eGFP and HF-UL112/3-eGFP respectively.

3.5 Transduced HF-Tert cell lines display strong autofluorescence

Cellular autofluorescence, an ever-present issue when imaging cells and tissues, is often assumed to be negligible in comparison to the signal of interest. To test this, uninfected parental control (HF-Tert) and transduced (HF-UL54-eGFP or HF-UL112/3-eGFP) cells were observed under a fluorescence microscope. It can be seen from figure 8a that transduced HF-Tert cells exhibit patchy areas of background fluorescence compared to the parental cell line. The non-uniform signal could be due to the random insertion of the lentiviral vector into the transduced cell lines, resulting in a heterogeneous population, in which some express eGFP constitutively. Quantitative analysis by flow cytometry (Figures 8b and c) confirms the presence of background fluorescence, as indicated by a shift in the detectable peak between the control and each of the transduced cell lines.

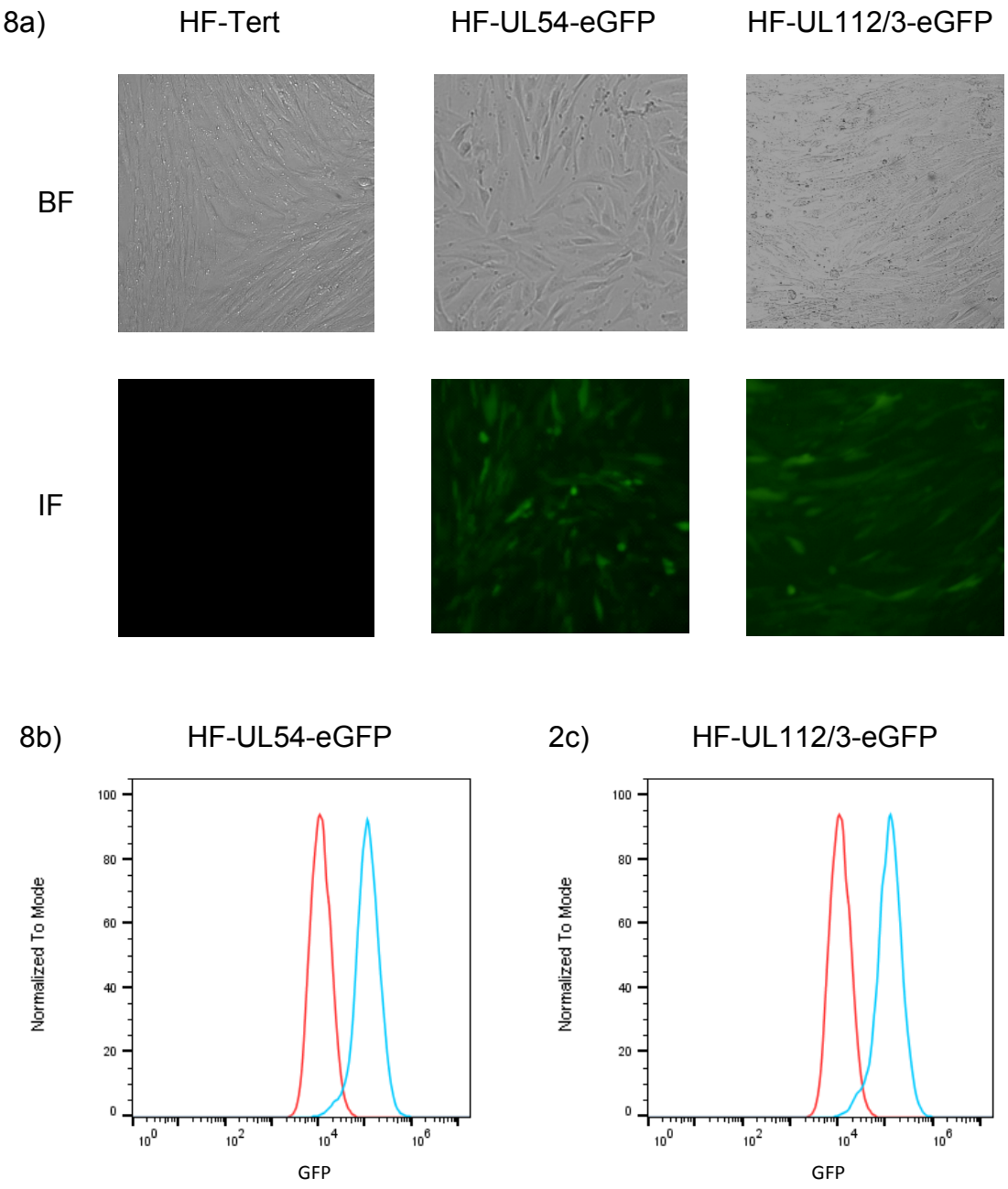

Figure 8a-c. Comparison of background fluorescence between parental control and transduced cell lines

8a) Fluorescence (IF) and bright-field (BF) images of parental (HF-Tert) and transduced (HF-UL54-eGFP or HF-UL112/3-eGFP) cell lines.
8b-c) Quantification of cellular fluorescence by flow cytometry. Red peak denotes the HF-Tert parental cell line. Blue peak signifies b) HF-UL54-eGFP or c) HF-UL112/3-eGFP.

3.6 Transduced U373-MG cell line displays strong background fluorescence

The glioblastoma cell line, U373-MG, utilized by Luganini *et al* to generate a cell-based HCMV reporter assay, had previously shown undetectable basal fluorescence levels by fluorescence following transfection of their plasmid construct. To determine whether the cell type of choice influenced background fluorescence levels, the U373-MG cell line, obtained from Cardiff Universities' repository, was transduced with either UL54 or UL112/3 lentivirus using retronectin® reagent (see 2.4.15.2). Following neomycin antibiotic selection, all non-transduced cells were eliminated, leaving behind adherent transduced cells for expansion. UL54 and UL112/3 transduced cells are hereto known as U373-UL54-eGFP and U373-UL112/3-eGFP respectively.

The background fluorescence levels of uninfected transduced and parental U373-MG cells were monitored using a fluorescence microscope and quantified by flow cytometry. As with the HF-Tert transduced cell lines, figures 9a-c reveal that uninfected transduced U373-MG cells also display fluorescence compared to the parental cell line. This fluorescence was weaker than in the HF-Tert cell line, indicating that the choice of cell line can influence the level of background fluorescence observed to some extent.

3.7 eGFP expression kinetics by fluorescence microscopy and quantification by flow cytometry

Despite the high level of background fluorescence observed in the HF-Tert and U373-MG transduced cell lines, to determine whether the intensity of the fluorescent signal produced through HCMV induced eGFP signalling was

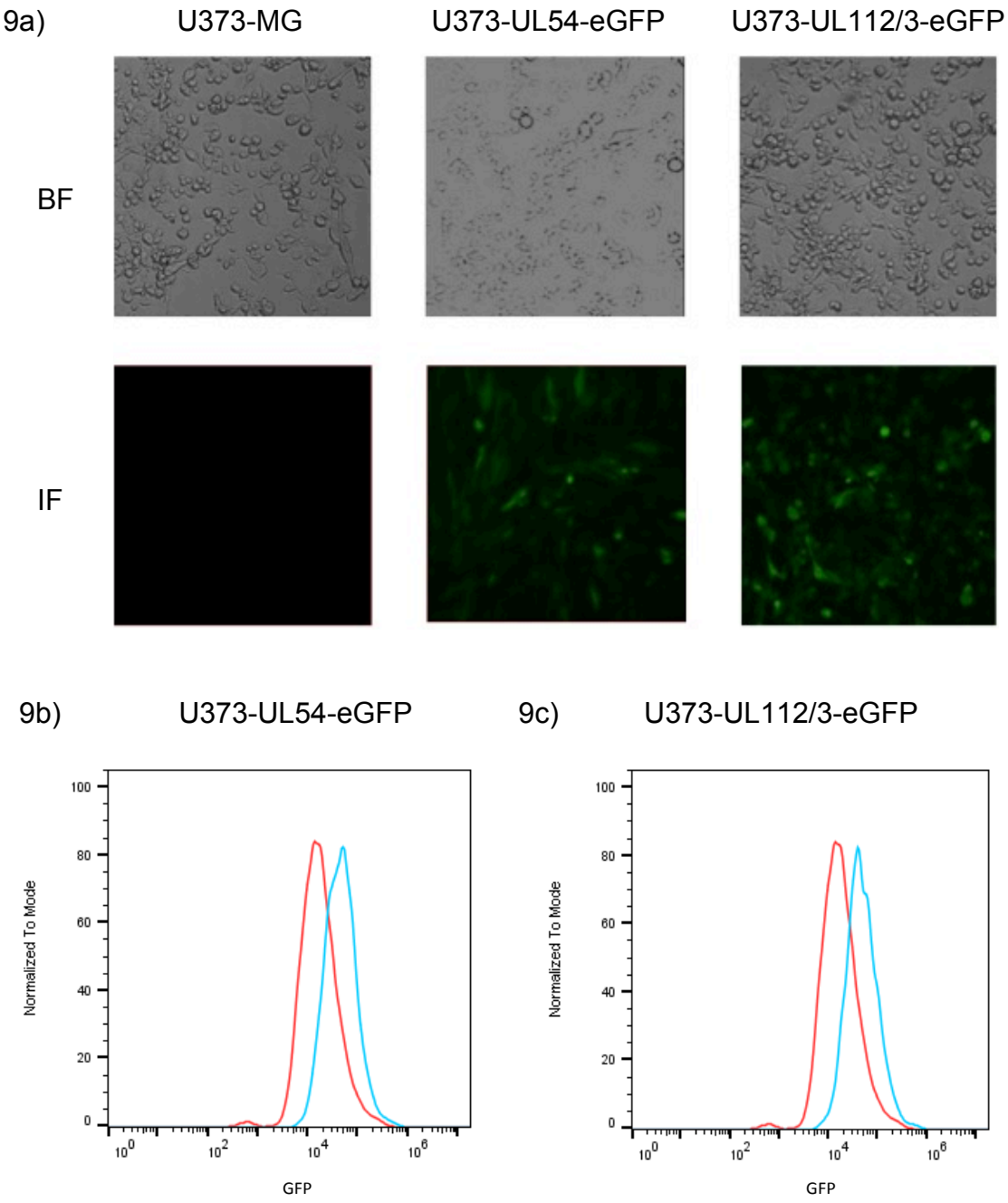

Figure 9a-c. Comparison of autofluorescence between parental control and transduced U373-MG cell lines

9a) Fluorescence (IF) and bright-field (BF) images of parental (U373-MG) and transduced (U373-UL54-eGFP or U373-UL112/3-eGFP) cell lines.
9b-c) Quantification of cellular autofluorescence by flow cytometry. Red peak denotes the U373-MG parental cell line. Blue peak signifies b) U373-UL54-eGFP or c) U373-UL112/3-eGFP.

sufficiently greater than background fluorescence, thus allowing detection of replicating virus, parental and transformed HF-Tert/U373-MG cell lines were each seeded onto a 24 well plate and infected with the HCMV strain Merlin (see 2.3.4) at varying MOIs (0.1, 0.5, 1, 5, and 10). To ensure that non-replicating HCMV could not induce eGFP expression, irradiated HCMV at an MOI of 10 was used as a control. Uninfected parental (HF-Tert or U373-MG) and transduced (HF-Tert-UL54-eGFP, HF-Tert-UL112/3-eGFP, U373-UL54-eGFP or U373-UL112/3-eGFP) cell lines were used to establish zero and background fluorescence levels respectively. Based on the expression profile of both UL54 and UL112/3 promoters, eGFP expression would not be detectable until 24h.p.i, with an increase in eGFP intensity expected at 48 and 72h.p.i (262). To observe fluorescent cells, culture media was replaced with DPBS and visualized at 24 hour intervals (24, 48, 72, 96h.p.i), before being harvested (see 2.5.4.1) and analysed on an Acurri C6 flow cytometer (see 2.5.4.3) (Figures 10-14).

Imaging by fluorescence (Figures 10-13) failed to detect a difference in fluorescence intensity between the infected and mock-infected transduced cell populations at any time point or MOI used. This was not due to a lack of replicating virus, as bright-field images taken in parallel to the fluorescent images showed an increase in cytopathic effects (cell roundedness) with dose and time. Analysis by flow cytometry (Figure 14) also failed to distinguish infected from mock-infected transduced cell populations, as all histogram plots for the first 72h.p.i overlapped. While this observation was also true for both UL54 cell lines at 96h.p.i, a slight shift in the histogram peaks were observed in the HF-Tert-UL112/3-eGFP and U373-UL112/3-eGFP cell lines at this same time point. This shift was extremely weak, thereby rendering the cell lines ineffective.

Mock-infected and infected HF-Tert/U373-MG control cell lines gave no detectable fluorescence or eGFP reading at all MOIs and time points used (Figures 15a-b), therefore the background fluorescence observed in the transduced cell lines must be due to the presence of the lentiviral vector.

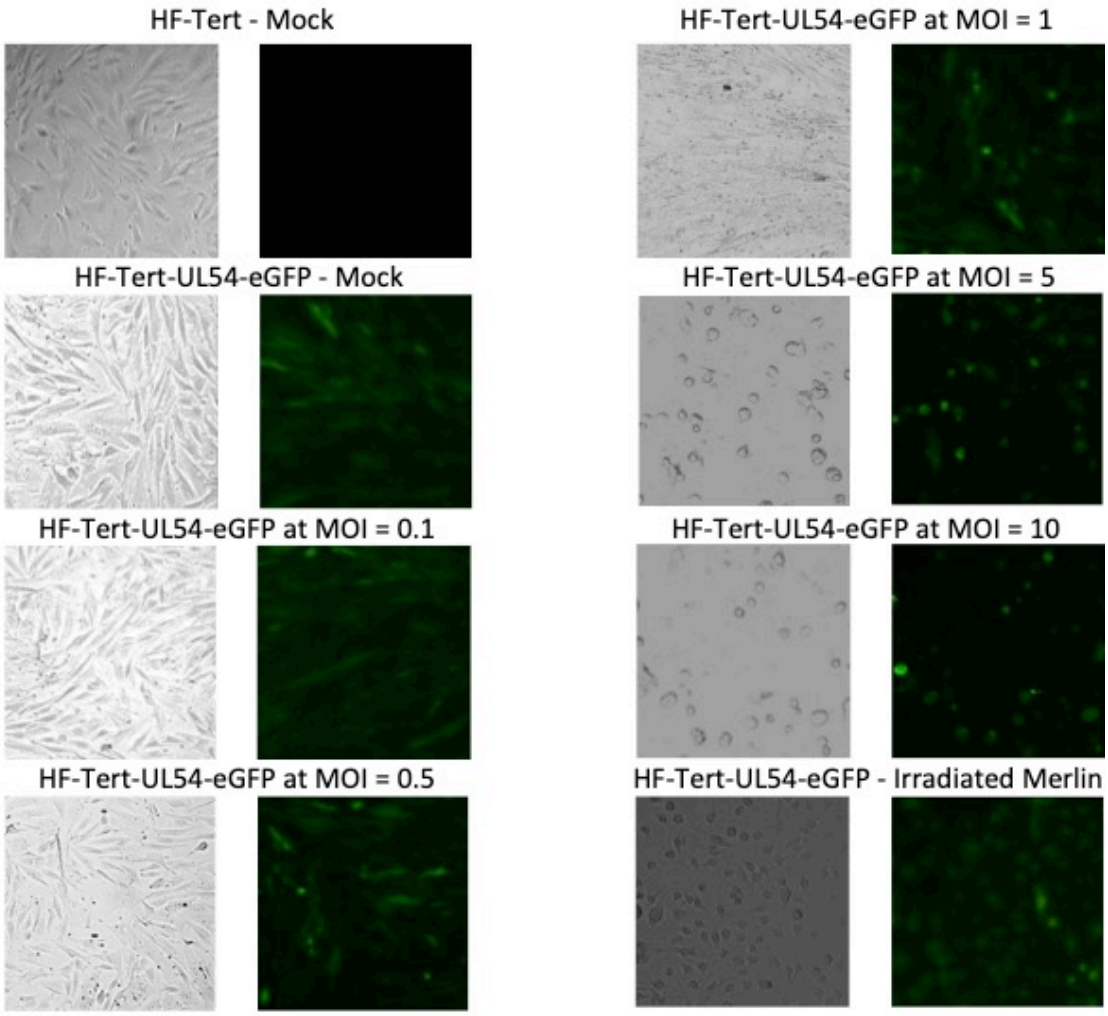

Figure 10. HCMV infection does not induce eGFP expression in HF-Tert-UL54-eGFP cells

HF-Tert or HF-Tert-UL54-eGFP cells were mock-infected or infected with Merlin at various MOIs (0.1, 0.5, 1, 5, 10). Irradiated virus at an MOI of 10 served as an eGFP induction control. Representative fluorescence and bright-field images shown at 72 h.p.i

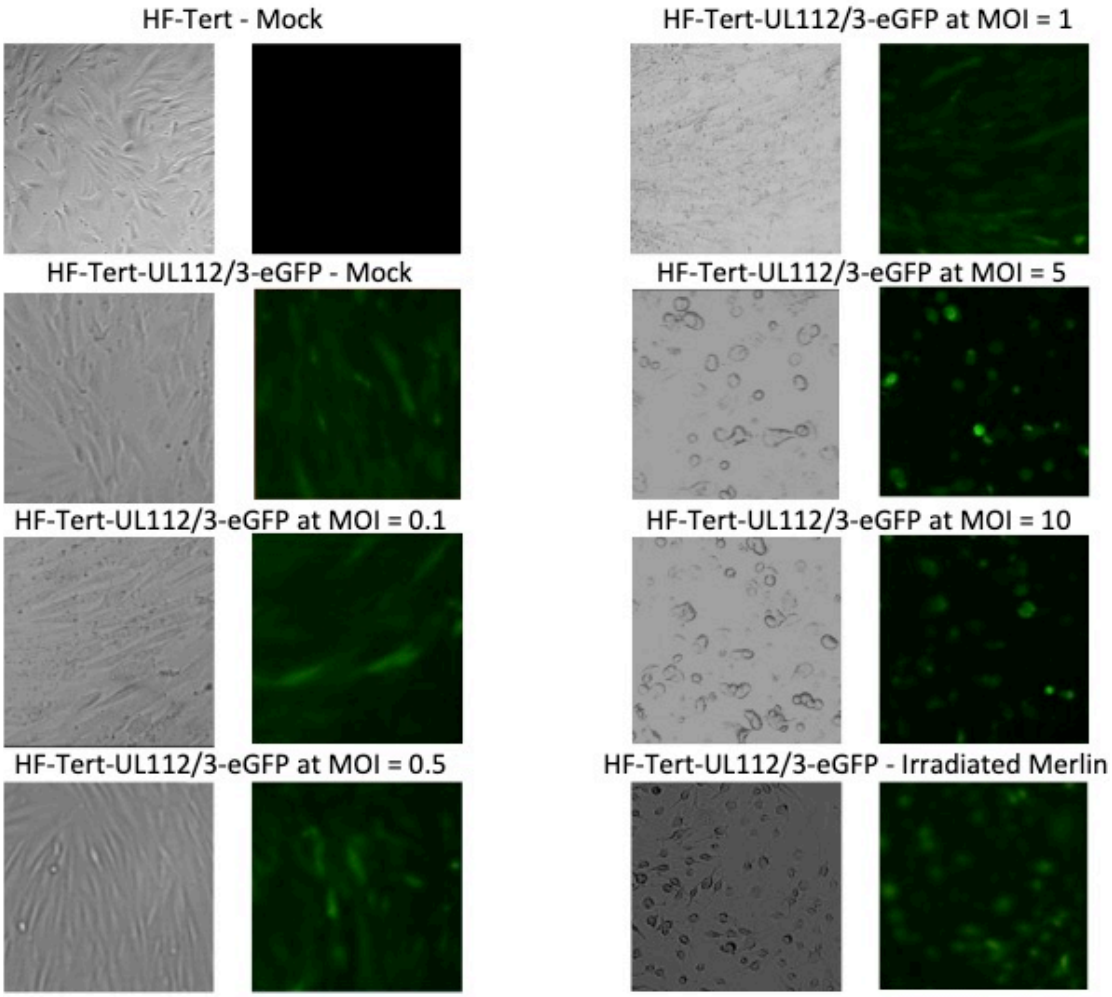

Figure 11. HCMV infection does not induce eGFP expression in HF-Tert-UL112/3-eGFP cells

HF-Tert or HF-Tert-UL112/3-eGFP cells were mock-infected or infected with Merlin at various MOIs (0.1, 0.5, 1, 5, 10). Irradiated virus at an MOI of 10 served as an eGFP induction control. Representative fluorescence and bright-field images shown at 72 h.p.i.

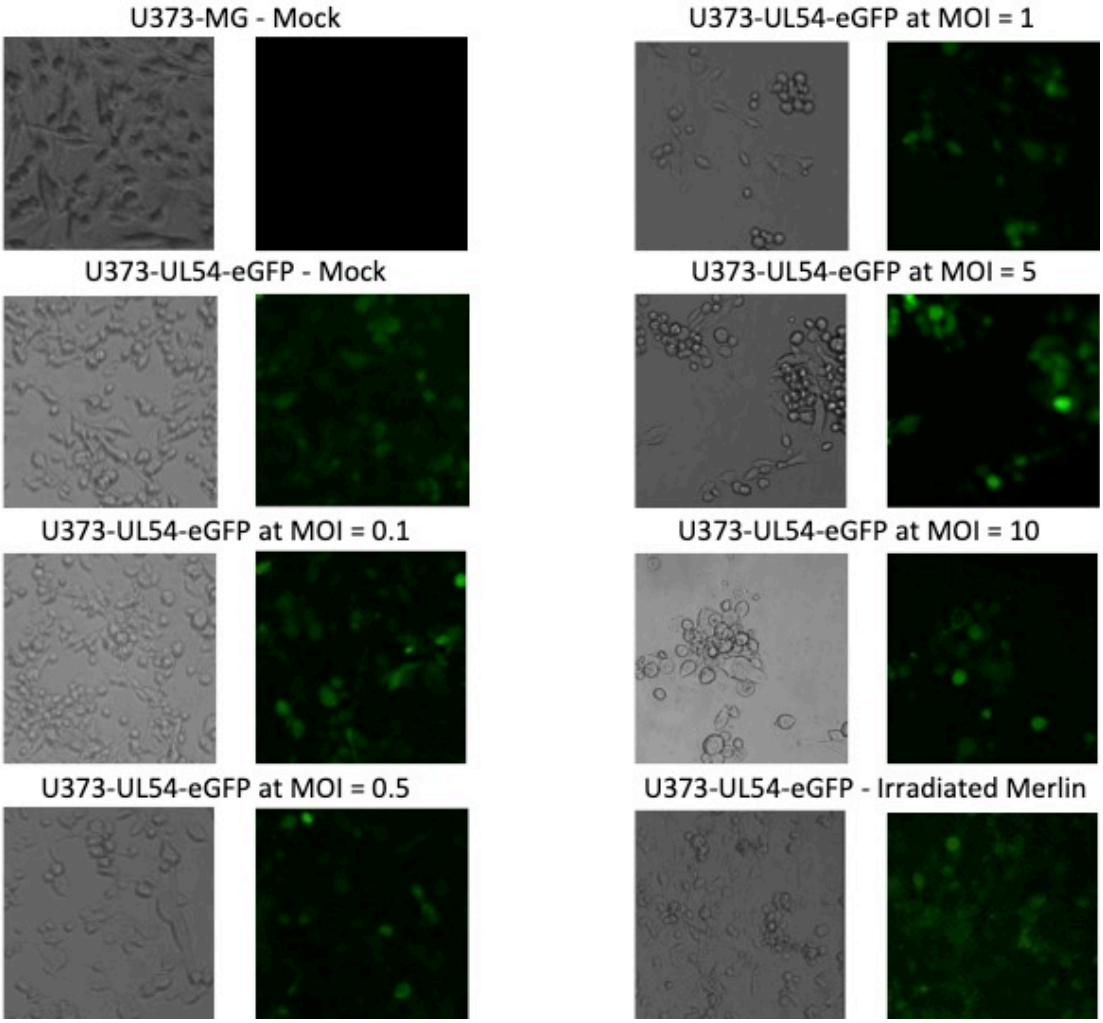

Figure 12. HCMV infection does not induce eGFP expression in U373-UL54-eGFP cells

U373-MG or U373-UL54-eGFP cells were mock-infected or infected with Merlin at various MOIs (0.1, 0.5, 1, 5, 10). Irradiated virus at an MOI of 10 served as an eGFP induction control. Representative fluorescence and bright-field images shown at 72 h.p.i .

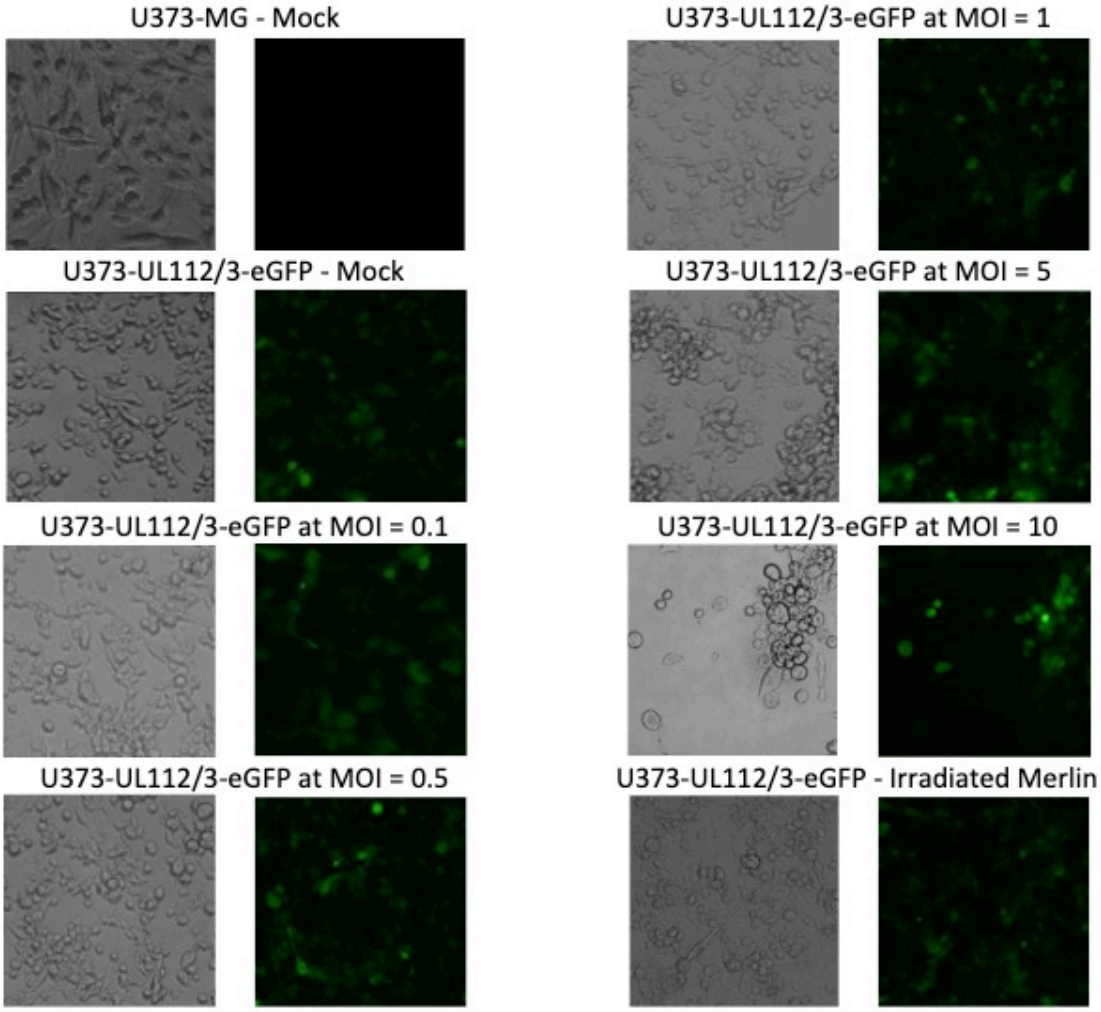

Figure 13. HCMV infection does not induce eGFP expression in U373-UL112/3-eGFP cells

U373-MG or U373-UL112/3-eGFP cells were mock-infected or infected with Merlin at various MOIs (0.1, 0.5, 1, 5, 10). Irradiated virus at an MOI of 10 served as an eGFP induction control. Representative fluorescence and bright-field images shown at 72 h.p.i .

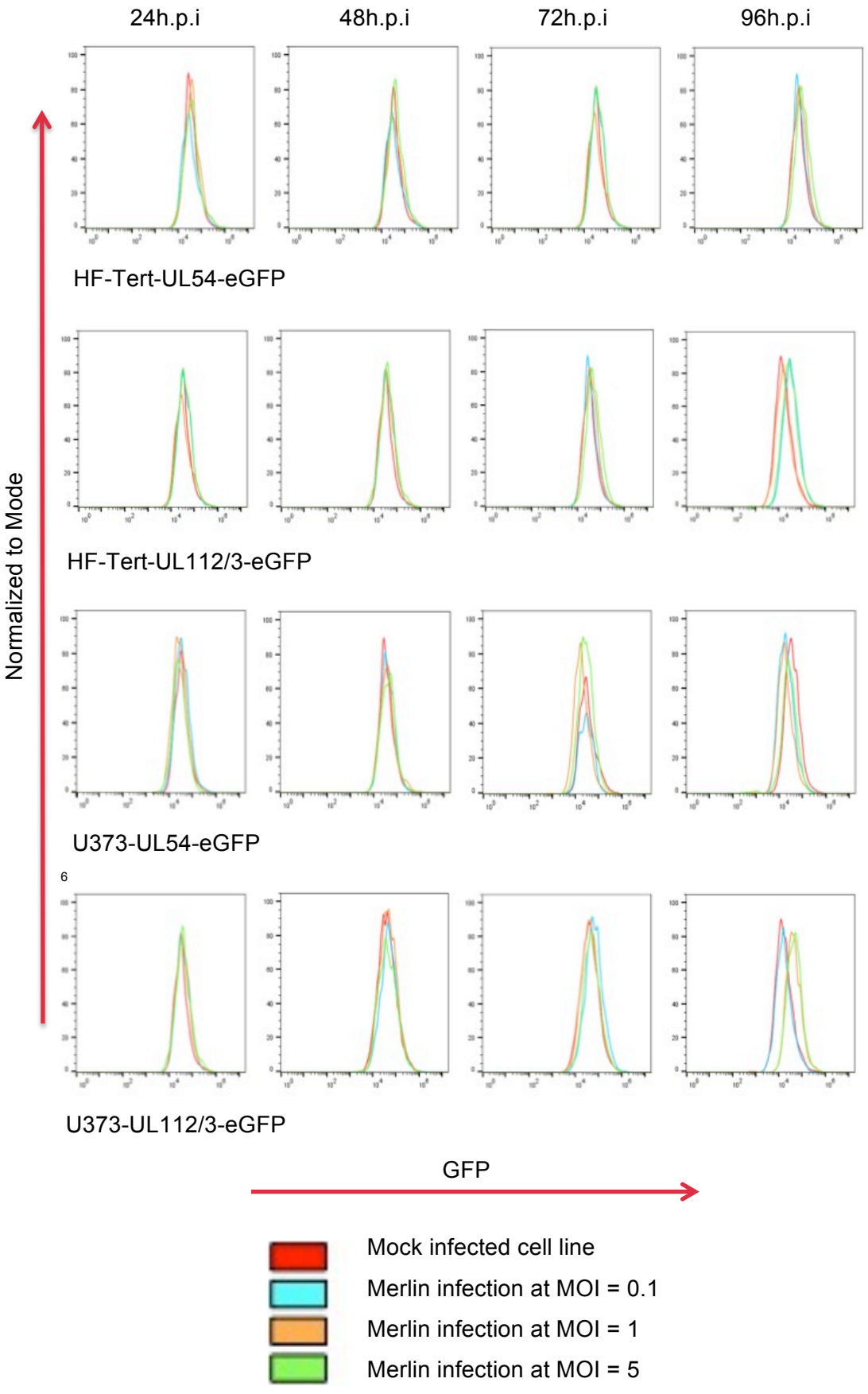
24h.p.i
48h.p.i
72h.p.i
96h.p.i
HF-Tert-UL54-eGFP
HF-Tert-UL112/3-eGFP
U373-UL54-eGFP
U373-UL112/3-eGFP
Normalized to Mode
GFP
Mock infected cell line
Merlin infection at MOI = 0.1
Merlin infection at MOI = 1
Merlin infection at MOI = 5

Figure 14. HCMV infection does not induce eGFP expression in HF-Tert or U373-MG transduced cell lines

Time course of Merlin infection of HF-Tert-UL54-eGFP, HF-Tert-UL112/3, U373-UL54-eGFP or U373-UL112/3-eGFP cell lines conducted in parallel to the fluorescent images, figures. Cells were grown on a 24 well plate and either mock-infected or infected with Merlin at an MOI of 0.1, 0.5, 1, 5 or 10. Data set for mock-infected, MOI = 0.1, 1 and 5 shown.

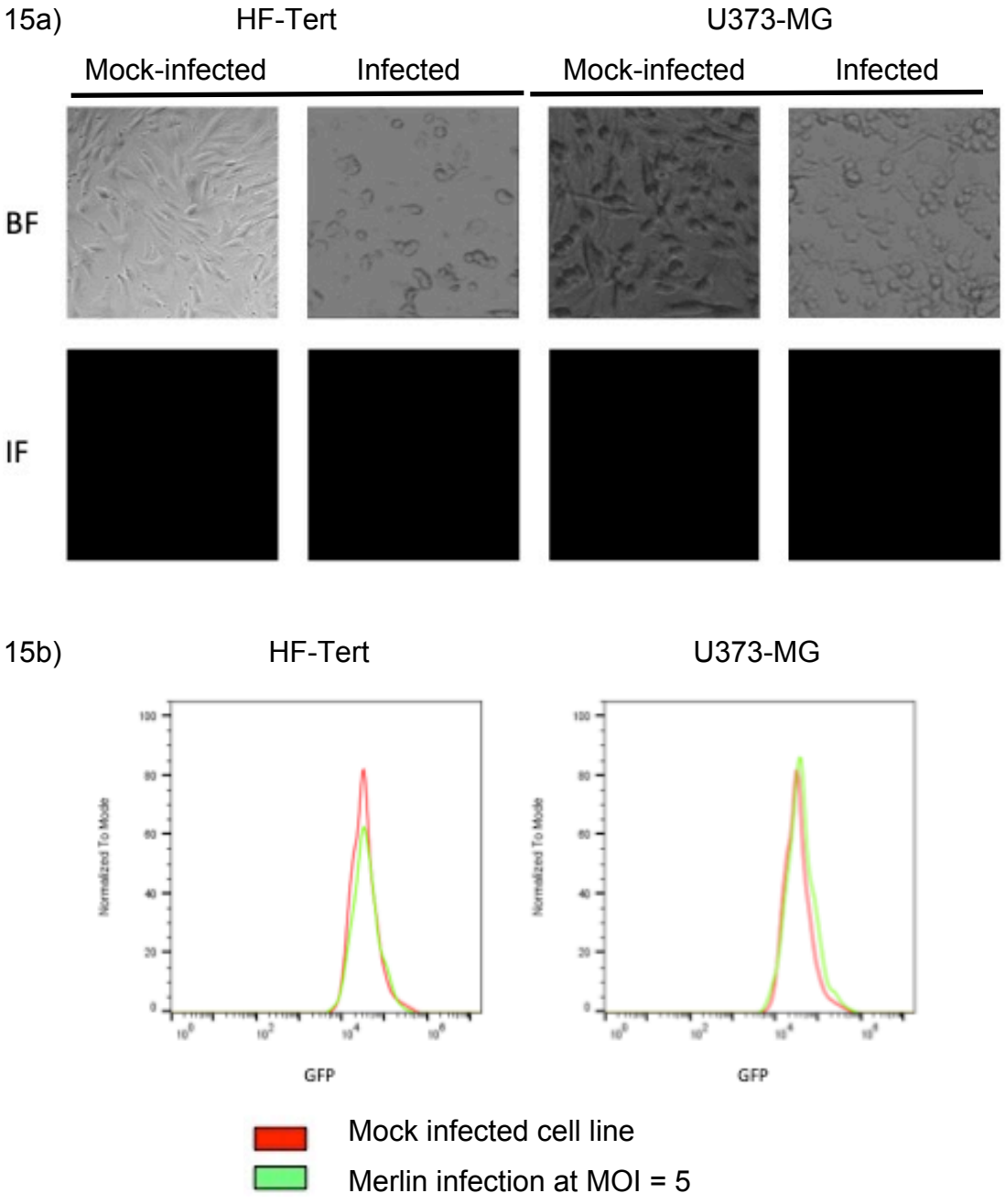

Figure 15a-b. HCMV infection does not alter background fluorescence in parental cells

HF-Tert or U373-MG cells were mock-infected or infected with Merlin at an MOI of 5. a) Representative fluorescence and bright-field images shown at 72h.p.i. b) FACS plots comparing fluorescence between mock-infected and Merlin infected HF-Tert or U373-MG cells at 72h.p.i.

3.8 Transduced single cell clones display strong autofluorescence

It was notable in Luganini *et al* that single cell cloning was carried out after selection, to generate the cell lines that worked. This may indicate that the site of integration of the eGFP cassette affects basal or induced levels of expression. The heterogeneous HF-Tert-UL54-eGFP and HF-Tert-UL112/3-eGFP cell lines were therefore subjected to single cell cloning (see 2.5.6) to identify clones with a lower background fluorescence, which might offer a better background/signal ratio.

All HF-Tert-UL54-eGFP and HF-Tert-UL112/3-eGFP single cell clones generated (24 and 29 respectively) were subject to visualization by fluorescence prior to acquisition by flow cytometery (data not shown). For each cell line generated, 5 clones displaying the lowest levels of background fluorescence were selected for further investigation.

3.9 eGFP expression kinetics of single cell clones by fluorescence microscopy and quantification by flow cytometry

To ascertain in the first instance, whether the magnitude of eGFP signal achieved through HCMV induced expression of a reporter gene was greater than the background fluorescence observed in each of the transduced single cell clones, a small-scale version of the experiment conducted in section 3.7 was performed. HF-Tert-UL54-eGFP or HF-Tert-UL112/3-eGFP single cell clones were seeded on a 24 well plate and infected with wild-type HCMV (see 2.3.4) at an MOI of 5. An MOI of 5 was chosen, as this dose had proved sufficient to infect the entire monolayer previously. Mock-infected control (HF-Tert) and transduced (HF-Tert-UL54-eGFP or HF-Tert-UL112/3-eGFP) single cell clones cells were used to set zero and background fluorescence levels

respectively. Live cells were visualized at 24 hour intervals (24, 48, 72 and 96h.p.i), before being processed (see 2.5.4.1) prior to acquisition on an Acurri C6 flow cytometer (see 2.5.4.3) (Figures 16-19).

Figures 16-19 demonstrate that at an MOI of 5, only one of the lines containing the UL54 promoter demonstrated HCMV-dependent induction of eGFP, however this was very weak. In contrast, most of the UL112/3 promoter containing clones showed HCMV-dependent induction, however the shift in signal was again relatively poor. The lack of HCMV induced eGFP signal was not due to the absence of replicating virus, as viral induced characteristic changes in cell morphology were observed in the bright field images taken in parallel to the fluorescent pictures. As previously, no basal fluorescence or eGFP signal was evident in either infected or mock-infected control (HF-Tert) cell lines, therefore the origin of the fluorescence observed in the transduced cell line must be due to the presence of the lentiviral vector.

A double histogram peak was observed in both the mock-infected and infected HF-Tert-UL112/3-eGFP clone E. This is likely due to more than one population being cultured. In either case however, the level of eGFP induction in both cell populations was poor.

As viral titres from clinical isolates are considerably lower than the titres used in the aforementioned single cell assay, it is unlikely that these cell lines are sensitive enough to identify eGFP expressing cells for detecting infectious HCMV particles.

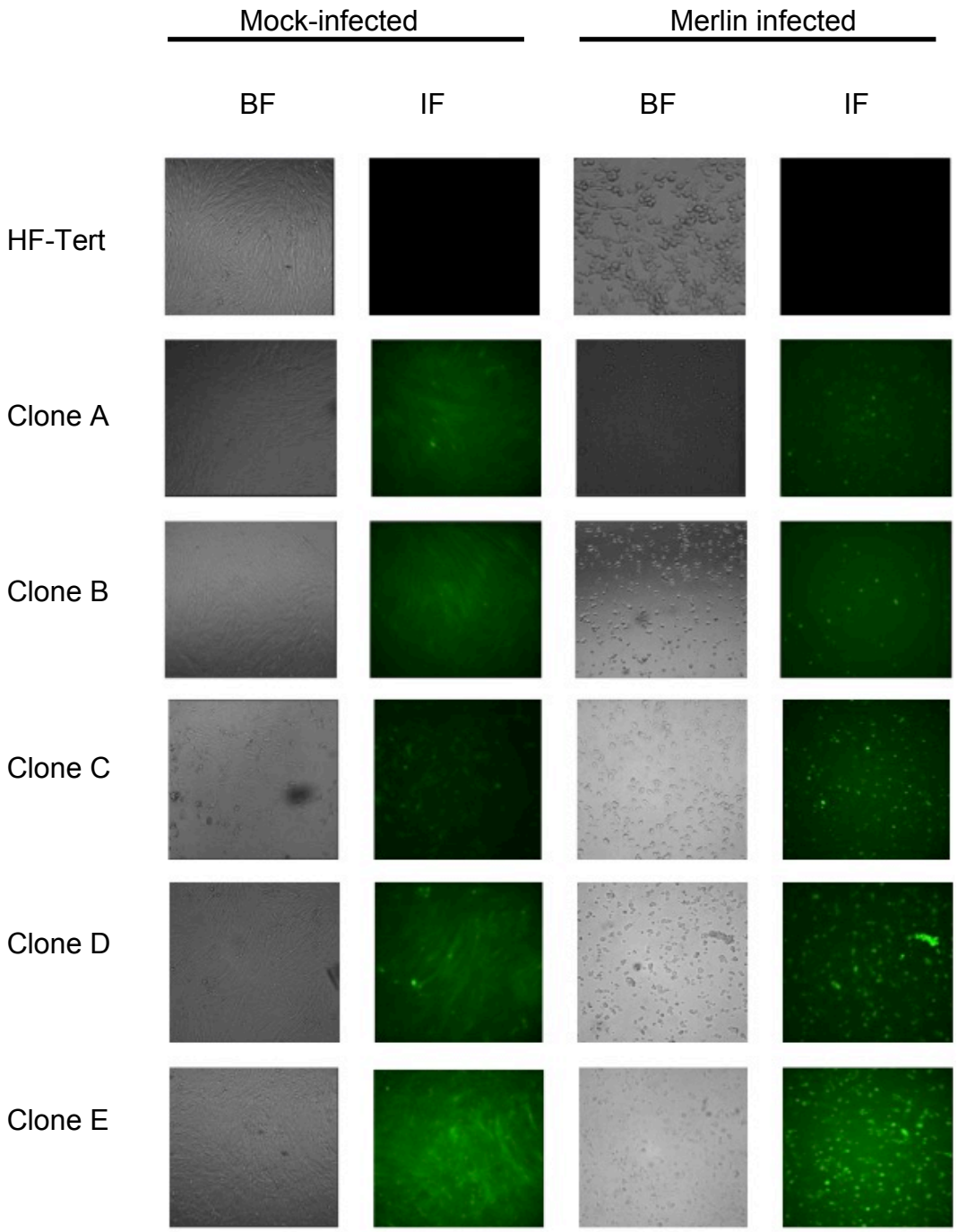

Figure 16. HCMV infection does not induce eGFP expression in HF-Tert-UL54-eGFP single cell clones

HF-Tert or HF-Tert-UL54-eGFP clones (A – E) were mock-infected or infected with Merlin at an MOI of 5. Representative fluorescence and bright-field images shown at 72 h.p.i

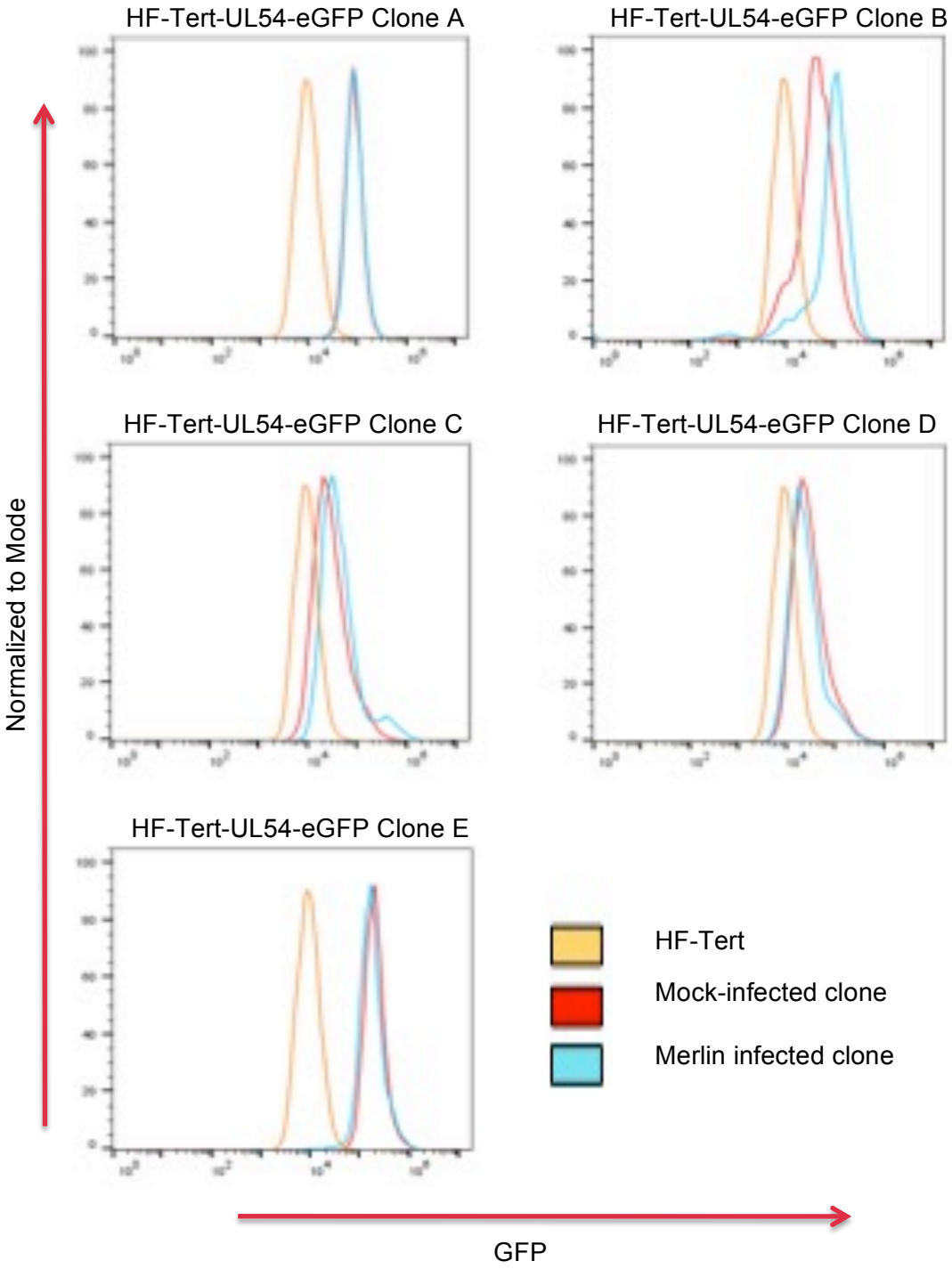

Figure 17. HCMV infection does not induce eGFP expression in HF-Tert-UL112/3-eGFP cell clones

Infection of HF-Tert or HF-Tert-UL112/3 single cell clones conducted in parallel to the immunofluorescent images in figure 16. Cells were grown on a 24 well plate and either mock-infected or infected with Merlin at an MOI of 5. Data analysed in Flow Jo.

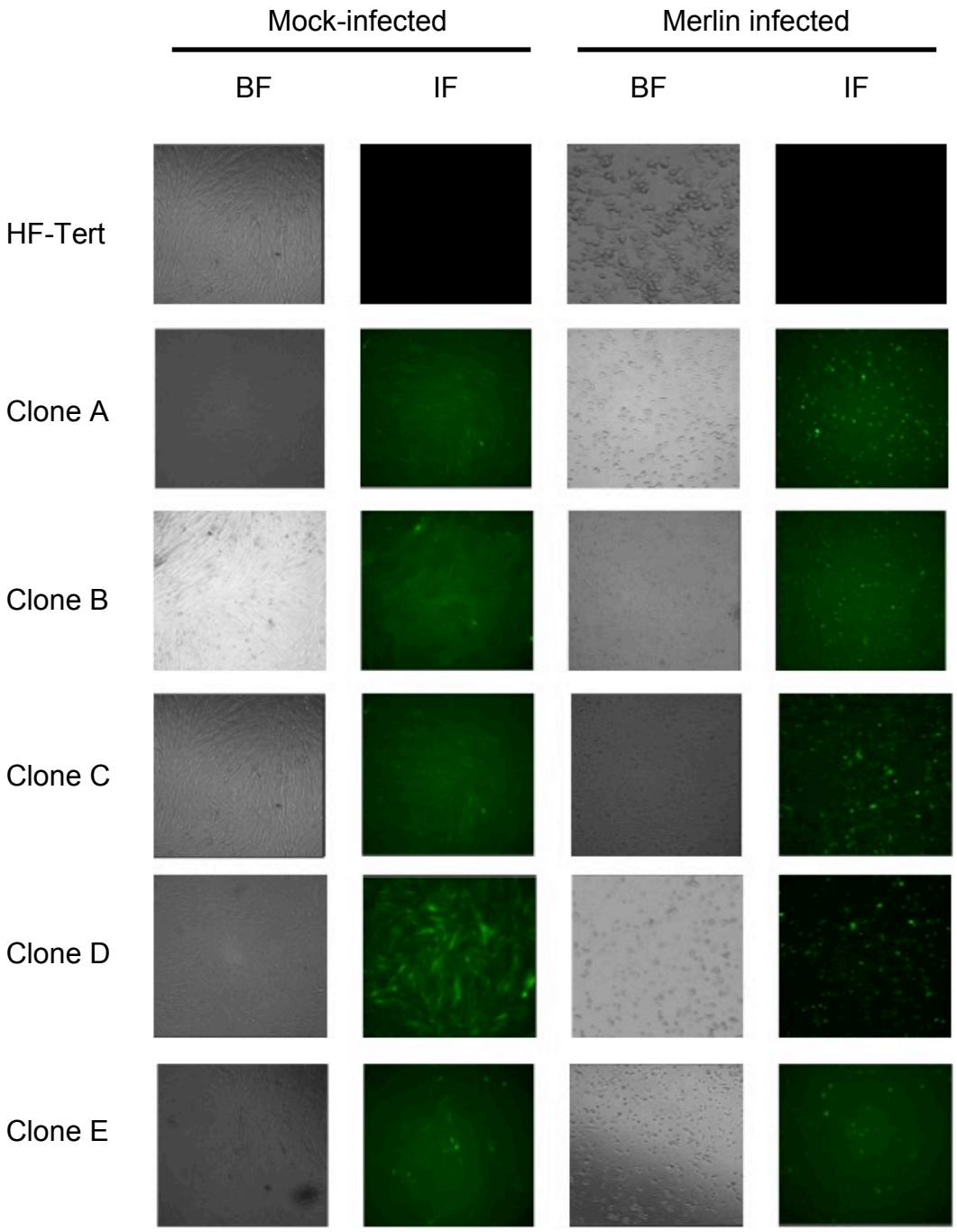

Figure 18. HCMV infection does not induce eGFP expression in HF-Tert-UL112/3-eGFP signle cell clones

HF-Tert or HF-Tert-UL112/3-eGFP clones (A – E) were mock-infected or infected with Merlin at an MOI of 5. Representative fluorescence and bright-field images shown at 72 h.p.i

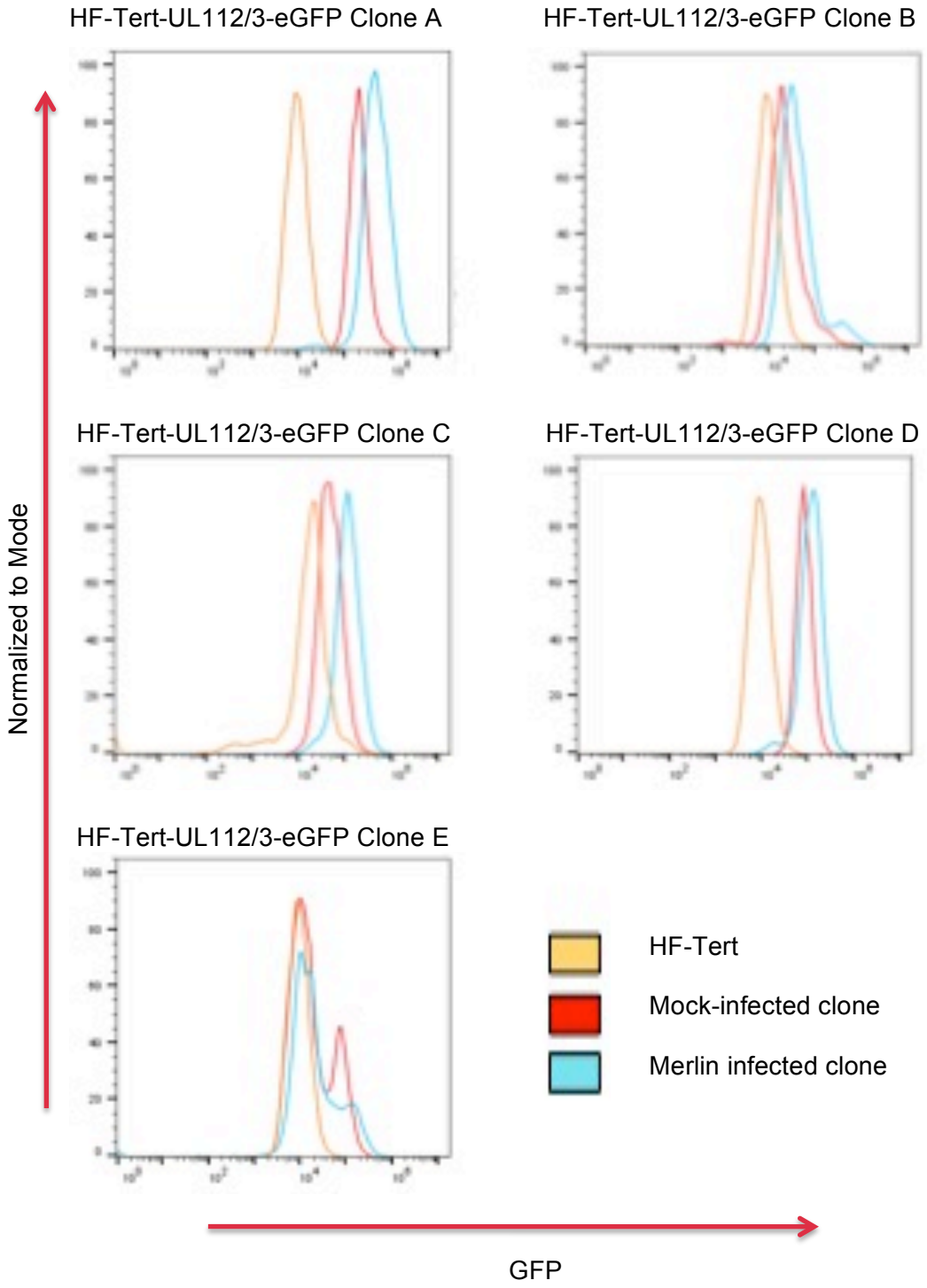

Figure 19. HCMV infection does not induce eGFP expression in HF-Tert-UL112/3-eGFP single cell clones

Infection of HF-Tert or HF-Tert-UL112/3 single cell clones conducted in parallel to the immunofluorescent images in figure 18. Cells were grown on a 24 well plate and either mock-infected or infected with Merlin at an MOI of 5.

3.10 Chapter discussion

Cell based indicator assays for the detection of viruses, in particular herpes simplex virus (HSV) or human immunodeficiency viruses (HIV), which depend on the expression of viral trans-activators to induce early viral promoters to drive luciferase or fluorescent gene expression is not new (262-7). Only a small number of reporter assays have been developed for HCMV detection however (255, 268-9), with only one developed using eGFP as a marker and none have been developed using human fibroblasts for viral propagation.

The temporal expression of HCMV genes can be broadly divided into immediate-early (IE), early (E) and late phases (1), with work by Meier *et al* highlighting the pivotal role of IE2 in triggering the transcription of viral E and L genes (254). The importance of IE2 function in HCMV replication led Luganini *et al* to develop two reporter assays using the HCMV permissive cell line, U373-MG (255). The 5' regulatory region of the early UL54 promoter that encodes viral DNA polymerase (270-1) and the very early UL112/3 gene that is essential in viral DNA replication (272) were used to drive eGFP expression in the transformed cell lines, signifying the presence of replicating HCMV in the assay.

The objective of this chapter was to generate two reporter cell lines adopting the rationale and promoter sequences utilized by Luganini *et al* (255) into the HF-Tert fibroblast cell line, for the rapid detection of clinically isolated HCMV from the urine of renal transplant patients. This aim was not achieved in this chapter as confirmed by fluorescence microscopy and flow cytometry (Figures 16-19).

In contrast to the Luganini paper, where establishment of a reporter cell line was generated by transfection, lentiviral transduction was adopted in this chapter so as to generate indicator cell lines with a long lasting, constant level of eGFP expression due to permanent integration into the host genome.

In keeping with the Luganini paper, an eGFP reporter gene was used for HCMV detection due to its ease of use and superior signal intensity compared to standard GFP (273-4). Fluorescent genes are also easily monitored in living cells by fluorescence microscopy, unlike alternative indicator genes such as the firefly luciferase or chloramphenicol acetyltransferase reporter genes that require processing and fixation before evaluation (273, 275). Despite extensive use in cell reporter assays, a well characterized disadvantage of using GFP and the enhanced (eGFP) version of the reporter gene is the potential for background fluorescence (276-7). All cells have basal levels of background fluorescence, however, larger cells and those with additional genetic material generally have greater levels of fluorescence due to the increased number of fluorescent compounds within the cell. GFP/eGFP fluorescence also overlaps with autofluorescence, making it potentially difficult to separate the two signals.

With this in mind, the background fluorescence of transduced and un-transduced HF-Tert cell populations (prior to single cell cloning) was compared using fluorescence microscopy and flow cytometry (Figures 8a-c). Transduced cells displayed high background fluorescence when compared to the untransduced cell line. As both the HF-Tert-UL54-eGFP and HF-Tert-UL112/3-eGFP cell lines displayed similar patterns and intensity in background fluorescence, it was deemed probable that the undesired fluorescence was due to leaky expression of eGFP from the presence of the lentiviral vector in both cell lines. Evidence to support this hypothesis is given in figure 9a-c, where insertion of the lentiviral vector into the glioblastoma cell line, U373-MG, also resulted in background fluorescence in transduced cells when compared to untransduced controls. The unusually high levels of basal fluorescence observed in the transduced cell lines was not due to known problematic biochemical factors such as NAD1/NADP1 (278-80), elastin, collagen (280-1) or media related components, including flavin molecules (280, 282), as infected and mock-infected HF-Tert/U373-MG control cells did not show background fluorescence under the same experimental conditions.

Previous reporter based assays using the UL54 or UL112/3 promoter to drive eGFP expression in U373-MG (255) or mink lung cells (269), demonstrated no basal fluorescence or background expression from the promoters in uninfected cells following single cell cloning, suggesting that clones with low background fluorescence could be isolated. It should be noted however, that gene transfer into these aforementioned cell lines was achieved by plasmid transfection rather than transduction. It is possible, therefore, that the method of gene delivery adopted in this chapter may have contributed to the high levels of basal fluorescence observed. Random integration of plasmid fragments occurs with transfection, while the entire lentiviral vector is incorporated during transduction. Gene transfer by transfection may have led to an incomplete promoter sequence being incorporated, resulting in lower basal fluorescence levels. Alternatively, the lentiviral vector utilized may not have contained a fully silenced promoter in its LTR region, resulting in an additional active promoter, independent of the UL54 or UL112/3 promoters. It is also important to note that in 2012, as a result of short tandem repeat-PCR profiling, the U373-MG (ATCC HTB-17) utilized by Luganini *et al* was shown to contain differing genetic properties to the U373-MG deposited by the original laboratory. A publication by Ishii *et al* (283) in 1999 raised questions as to the genetic properties of this cell line, but it wasn't until much later that the authenticity of the U373-MG was proven to be incorrect. It is not known whether the cell line used by either myself or Luganini *et al* is the original U373-MG cell line, now termed U373-MG (Uppsala), or the U-251 glioblastoma cell line which was also called 'U373-MG' in error, by ECCAC (284).

As the transduced cell lines generated were heterogeneous, consisting of various cells with differing background fluorescence and variable levels of eGFP expression following HCMV infection (Figures 10-14), in keeping with the Luganini paper, single cell cloning was performed, with those displaying the lowest background fluorescence retained for further study.

Unless induction of eGFP was high following infection, the fluorescent signal from the reporter gene would be lost due to the basal level of fluorescence.

Following HCMV infection, only one of the transduced UL54 single cell clones displayed eGFP at levels exceeding background fluorescence. Several of the UL112/3 single cell clones (particularly HF-Tert-UL112/3-eGFP Clones A and C) were capable of inducing eGFP expression, however levels were too weak to be reliable for identification of infected cells (Figures 16-19). The fluorescence spectra, which spans a wide wavelength range, including most of the visible spectra (285), overlaps the emission wavelength of eGFP, leading to difficulties in detecting or visualizing the signal. Given that HF-Terts exhibit high levels of background fluorescence, in future, the use of bright red fluorescence proteins (mCherry, mScarlet) or infrared fluorescent proteins may help to improve the background/signal ratio (286).

The lack of enhanced fluorescent signal in the infected transduced cell lines is likely due to low eGFP expression. The activation of each promoter could have been assessed by co-transfection with a plasmid expressing HCMV IE2, thereby providing a known activation and signal control. A correlation would be expected between infection mediated and IE2 mediated activation. As the strength of the fluorescent signal directly correlates with promoter activity, future construct design could incorporate multiple copies of the promoter into the lentiviral vectors, to enhance eGFP signal.

Taken together, these cell-based assays have not proved a reliable, robust or reproducible tool for measuring the presence of infectious HCMV particles in this chapter.

Chapter 4 - Results

Production of shRNA silenced cell lines directed against RL13 and UL128L

4.1 Introduction

When clinical HCMV is isolated and grown in fibroblasts in the laboratory, the wild-type virus rapidly acquires genetic alterations in the RL13 and UL128L genes, enhancing its growth properties. As a solution to this problem, bacterial artificial chromosome (BAC) technology has been used to clone and repair the HCMV genome so that it resembles wild-type virus, resulting in stable genomes to work with in the short term. Long term culturing, however, sees the emergence of new RL13 and UL128L mutants, resulting in progeny virus with improved growth kinetics (160-1). To prevent these new mutations, Stanton *et al* introduced a tetracycline-repression system into the BAC, where expression of both RL13 and UL131A is conditionally supressed, allowing genetically intact virus to be passaged *in vitro* (228). However, this technology can only be applied once a genome has been BAC cloned.

The objective of this chapter was to generate a system independent of the BAC, allowing *in vitro* growth of clinical viruses without risk of mutation. To achieve this, fibroblasts capable of supressing the expression of RL13/UL128L, akin to the BAC system, but infectable by any CMV's, was generated via RNA interference (RNAi), using targeted short hairpin ribonucleic acid (shRNA).

4.2. Short hairpin RNA (shRNA) design and conservation of the target sequence across HCMV strains.

shRNA construction is complicated by the fact that predictive computational algorithms which exist for siRNA design rarely apply to shRNA composition. Despite this, it has been observed that successful target sequences lack A or T nucleotide repeats >3bp (287), have a GC content between 35-55% (288-90), are between 19-29bp (288), have an A or G starting nucleotide and contain a loop region between 3-9nt in length (291). Based on these observations, three shRNAs directed against Merlin RL13 and two against

each of the Merlin UL128L genes were devised using the Invivogen siRNA Wizard^{TM}. Nucleotide sequences for target genes were obtained from the National Center for Biotechnology Information (NCBI) BLASTN 2.4.0+ nucleotide database and 21bp sequences selected from HCMV strain Merlin (GenBank: GU179001.1) (Table 12). As a known hypervariable gene (228), the C-terminal cytosolic domain and the relatively conserved region of the transmembrane domain of RL13 (292) was targeted for shRNA construction, while all other targets were selected due to their location on the transcript, the GC% content of the selected sequence and the lack of A or T nucleotide repeats over 3 base pairs (bp). A scrambled shRNA construct was also included as a control. shRNA design was performed by Dr Virginia-Maria Vlachava.

The knockdown cell lines generated were intended to support propagation of a wide range of patient derived HCMVs *in vitro*, therefore to investigate how conserved the target sequences were across known HCMV strains, the RL13, UL128, UL130 and UL131A sequence of all known HCMV strains were obtained from the NCBI BLASTN 2.4.0+ nucleotide database and aligned using CLC main workbench version 7.9.1 (Figure 20a-i, Table 14). Analysis of the target sequences confirmed that control shRNA lacked homology with Merlin, the virus strain with which subsequent experiments were going to be performed. Interestingly, two of the RL13-targets (shRL13-a and –c) were found to lack homology with the Merlin sequence, although they were shown to be present in the RL13 gene from other HCMV strains. The RL13-a and -c sequences were found to be present in 35 and 15 respectively of all 123 NCBI listed RL13 HCMV sequences.

Further sequence alignment of the RL13-a and -c constructs against HCMV strain Merlin (Table 13) revealed a double (shRL13-a) and single (shRL13-c) mis-match at the terminal end of the designed sequences. Several RNAi studies (293-96) have demonstrated that sequence mis-match at the terminal nucleotides of si/shRNA has little effect on construct binding to the intended sequence, leading to degradation of the gene of interest. Mis-matches found at the center of the sequence however, lead to an impairment in binding

ability, with no degradation of the gene of interest detected. Based on these observations, both shRL13-a and -c were considered to be potential constructs for achieving RL13 gene knockdown in HCMV strain Merlin.

All other target sequences within the RL13 and UL128L transcripts were present in Merlin.

Additional analysis of the shRL13 constructs revealed that target sequences were completely conserved in only 28.45%, 5.7% and 12.2% (RL13-a, -b and –c respectively) of all known HCMV strains. These conservation rates were extremely low, but unsurprising given that RL13 is a known hypervariable gene (228). Conversely, all UL128L targets exhibited high sequence conservation rates across all strains: 97.7% (UL128a), 98.4% (UL128-b), 90% (Ul130-a), 80% (UL130-b), 99% (UL131A-a), 100% (UL131A-b). Given that the aim of generating an engineered cell line was to support the propagation of wild-type HCMV in culture, high target conservation rates across all strains was considered extremely important.

Table 12. shRNA target sequence for RL13, UL128, UL130 and UL131A

Plasmid ID	New plasmid ID	Sequence	Percentage G/C content
pLV-Puro-U6>{ shRL13 597-617}	shRL13-a	TAAGACCTCTCTCACTATATA	33.3
pLV-Puro-U6>{ shRL13 890-910transm}	shRL13-b	TGGCACTCATAGCGCTATATA	42.86
pLV-Puro-U6>{ shRL13 18-38}	shRL13-c	GGTTATGTGGACGATACTAAT	38.1
pLV-mCherry:T2A:Puro-U6>{shUL128 117-136}	shUL128-a	GCCGGAACGCTGTTACGATTT	52.3
pLV-EGFP:T2A:Puro-U6>{shUL128 441-460}	shUL128-b	TCAGTACCTGGAGAGCGTTAA	47.62
pLV-mCherry:T2A:Puro-U6>{shUL130 11-31}	shUL130-a	TTCTGCTTCGTCACCACTTTC	47.62
pLV-mCherry:T2A:Puro-U6>{shUL130 419-439}	shUL130-b	GCGTGGAAGACGCCAAGATTT	52.3
pLV-mCherry:T2A:Puro-U6>{shUL131A 257-277}	shUL131A-a	CGTTGCTCATCAGCGACTTTA	47.62
pLV-mCherry:T2A:Puro-U6>{shUL131A 87-107}	shUL131A-b	TTATTACCGAGTACCGCATTA	38.1
pLV-Puro-U6>{shcont}	shcont	GCCTAAGTATCGCCTAATTTA	38.1

Sequences showing <100% match to the HCMV strain Merlin are coloured in red. Sequences constructed by Dr Dr Virginia-Maria Vlachava.

20a)

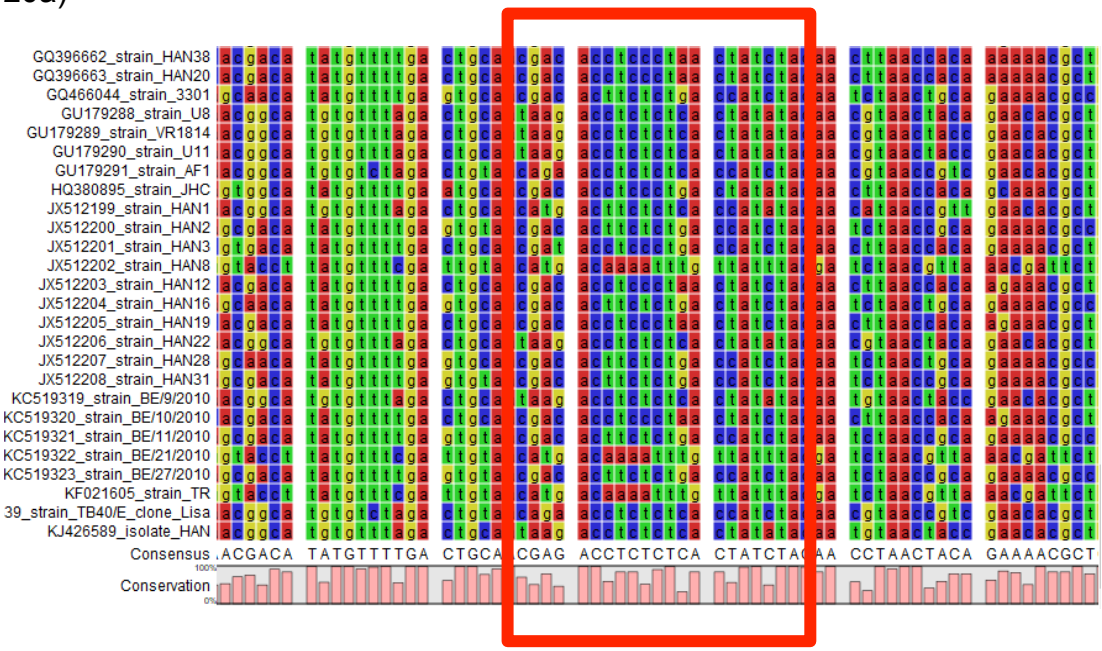
GQ396662_strain_HAN38
GQ396663_strain_HAN20
GQ466044_strain_3301
GU179288_strain_U8
GU179289_strain_VR1814
GU179290_strain_U11
GU179291_strain_AF1
HQ380895_strain_JHC
JX512199_strain_HAN1
JX512200_strain_HAN2
JX512201_strain_HAN3
JX512202_strain_HAN8
JX512203_strain_HAN12
JX512204_strain_HAN16
JX512205_strain_HAN19
JX512206_strain_HAN22
JX512207_strain_HAN28
JX512208_strain_HAN31
KC519319_strain_BE/9/2010
KC519320_strain_BE/10/2010
KC519321_strain_BE/11/2010
KC519322_strain_BE/21/2010
KC519323_strain_BE/27/2010
KF021605_strain_TR
39_strain_TB40/E_clone_Lisa
KJ426589_isolate_HAN
Consensus
ACGACA TATGTTTTGA CTGCA CGAG ACCTCTCTCA CTATCTAC AA CCTAACTACA GAAAACGCT
Conservation

b)

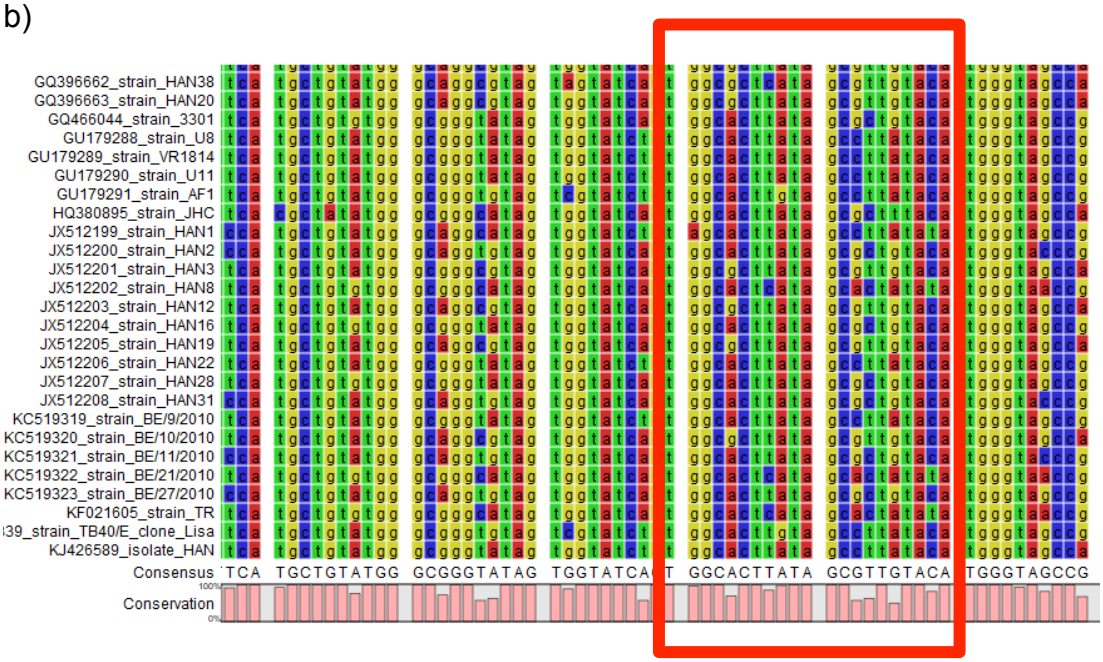
GQ396662_strain_HAN38
GQ396663_strain_HAN20
GQ466044_strain_3301
GU179288_strain_U8
GU179289_strain_VR1814
GU179290_strain_U11
GU179291_strain_AF1
HQ380895_strain_JHC
JX512199_strain_HAN1
JX512200_strain_HAN2
JX512201_strain_HAN3
JX512202_strain_HAN8
JX512203_strain_HAN12
JX512204_strain_HAN16
JX512205_strain_HAN19
JX512206_strain_HAN22
JX512207_strain_HAN28
JX512208_strain_HAN31
KC519319_strain_BE/9/2010
KC519320_strain_BE/10/2010
KC519321_strain_BE/11/2010
KC519322_strain_BE/21/2010
KC519323_strain_BE/27/2010
KF021605_strain_TR
39_strain_TB40/E_clone_Lisa
KJ426589_isolate_HAN
Consensus
TCA TGCTGTATGG GCGGGTATAG TGGTATCA T GGCACTTATA GCGTTGTACA TGGGTAGCCG
Conservation

c)

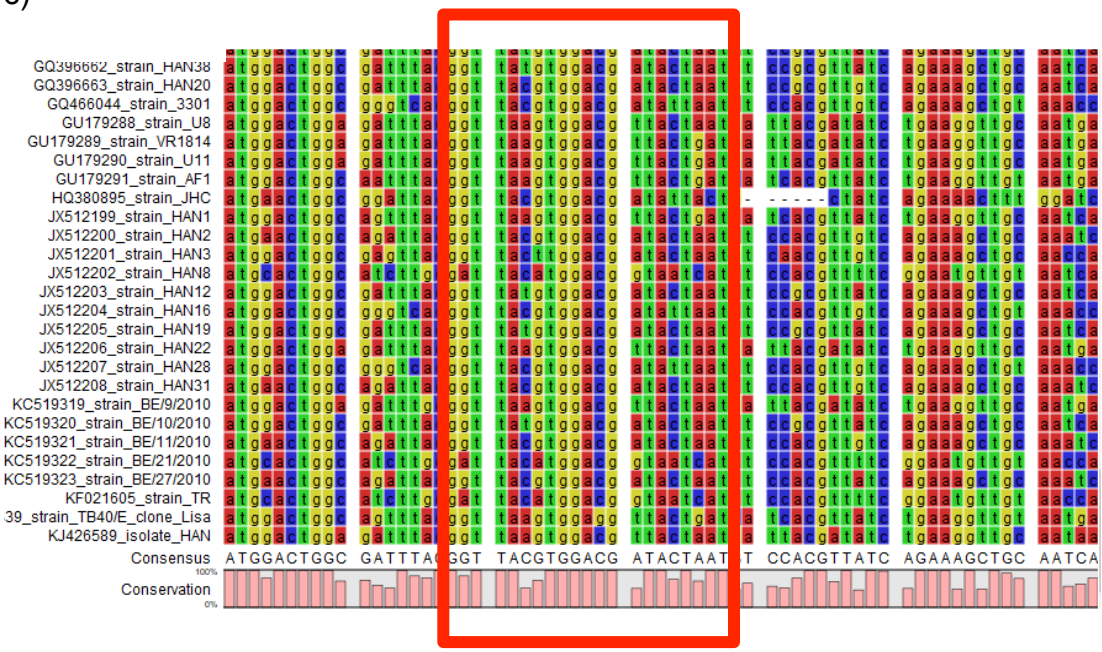
GQ396662_strain_HAN38
GQ396663_strain_HAN20
GQ466044_strain_3301
GU179288_strain_U8
GU179289_strain_VR1814
GU179290_strain_U11
GU179291_strain_AF1
HQ380895_strain_JHC
JX512199_strain_HAN1
JX512200_strain_HAN2
JX512201_strain_HAN3
JX512202_strain_HAN8
JX512203_strain_HAN12
JX512204_strain_HAN16
JX512205_strain_HAN19
JX512206_strain_HAN22
JX512207_strain_HAN28
JX512208_strain_HAN31
KC519319_strain_BE/9/2010
KC519320_strain_BE/10/2010
KC519321_strain_BE/11/2010
KC519322_strain_BE/21/2010
KC519323_strain_BE/27/2010
KF021605_strain_TR
39_strain_TB40/E_clone_Lisa
KJ426589_isolate_HAN
Consensus
ATGGACTGGC GATTTAGGT TACGTGGACG ATACTAATT CCACGTTATC AGAAAGCTGC AATCA
100%
Conservation
0%

d)

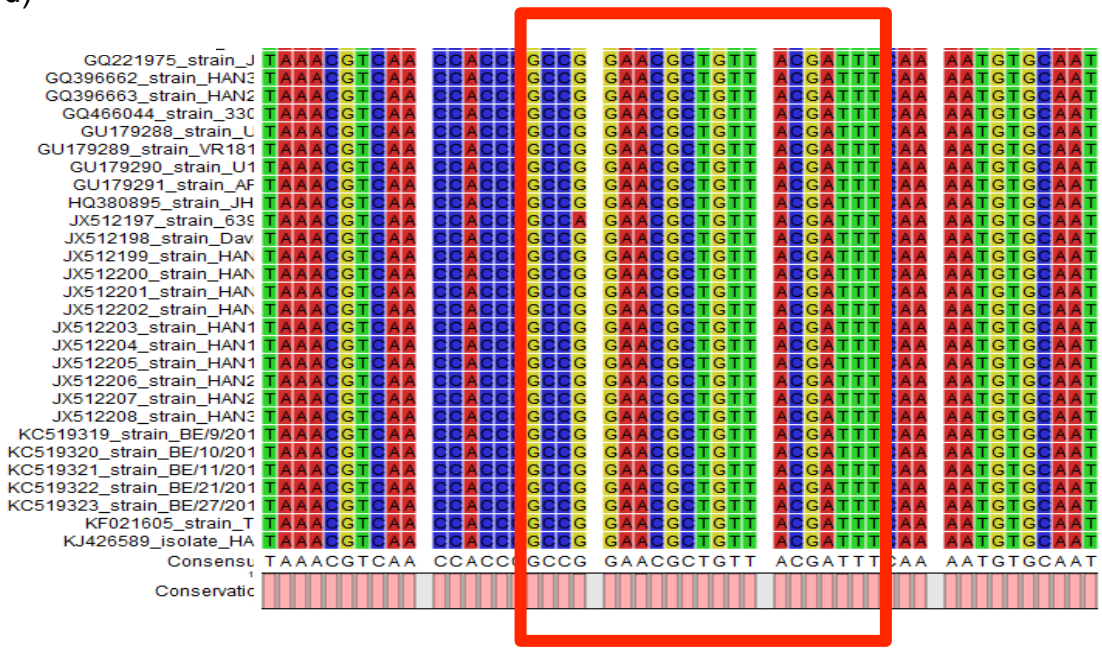
GQ221975_strain_J
GQ396662_strain_HAN3
GQ396663_strain_HAN2
GQ466044_strain_330
GU179288_strain_U
GU179289_strain_VR181
GU179290_strain_U1
GU179291_strain_AF
HQ380895_strain_JH
JX512197_strain_63
JX512198_strain_Dav
JX512199_strain_HAN
JX512200_strain_HAN
JX512201_strain_HAN
JX512202_strain_HAN
JX512203_strain_HAN1
JX512204_strain_HAN1
JX512205_strain_HAN1
JX512206_strain_HAN2
JX512207_strain_HAN2
JX512208_strain_HAN3
KC519319_strain_BE/9/201
KC519320_strain_BE/10/201
KC519321_strain_BE/11/201
KC519322_strain_BE/21/201
KC519323_strain_BE/27/201
KF021605_strain_T
KJ426589_isolate_HA
Consensu
TAAACGTCAA CCACCGCCG GAACGCTGTT ACGATTTCAA AATGTGCAAT
Conservatic

e)

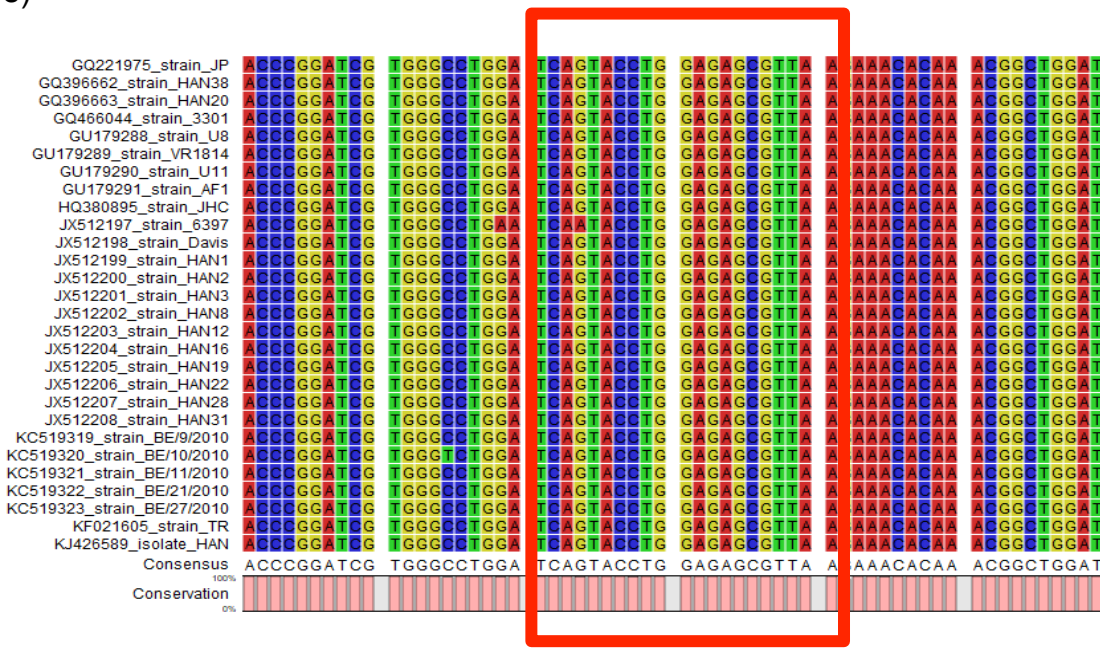
GQ221975_strain_JP
GQ396662_strain_HAN38
GQ396663_strain_HAN20
GQ466044_strain_3301
GU179288_strain_U8
GU179289_strain_VR1814
GU179290_strain_U11
GU179291_strain_AF1
HQ380895_strain_JHC
JX512197_strain_6397
JX512198_strain_Davis
JX512199_strain_HAN1
JX512200_strain_HAN2
JX512201_strain_HAN3
JX512202_strain_HAN8
JX512203_strain_HAN12
JX512204_strain_HAN16
JX512205_strain_HAN19
JX512206_strain_HAN22
JX512207_strain_HAN28
JX512208_strain_HAN31
KC519319_strain_BE/9/2010
KC519320_strain_BE/10/2010
KC519321_strain_BE/11/2010
KC519322_strain_BE/21/2010
KC519323_strain_BE/27/2010
KF021605_strain_TR
KJ426589_isolate_HAN
Consensus
ACCCGGATCG TGGGCCTGGA TCAGTACCTG GAGAGCGTTA A AAACACAA ACGGCTGGAT
100%
Conservation
0%

f)

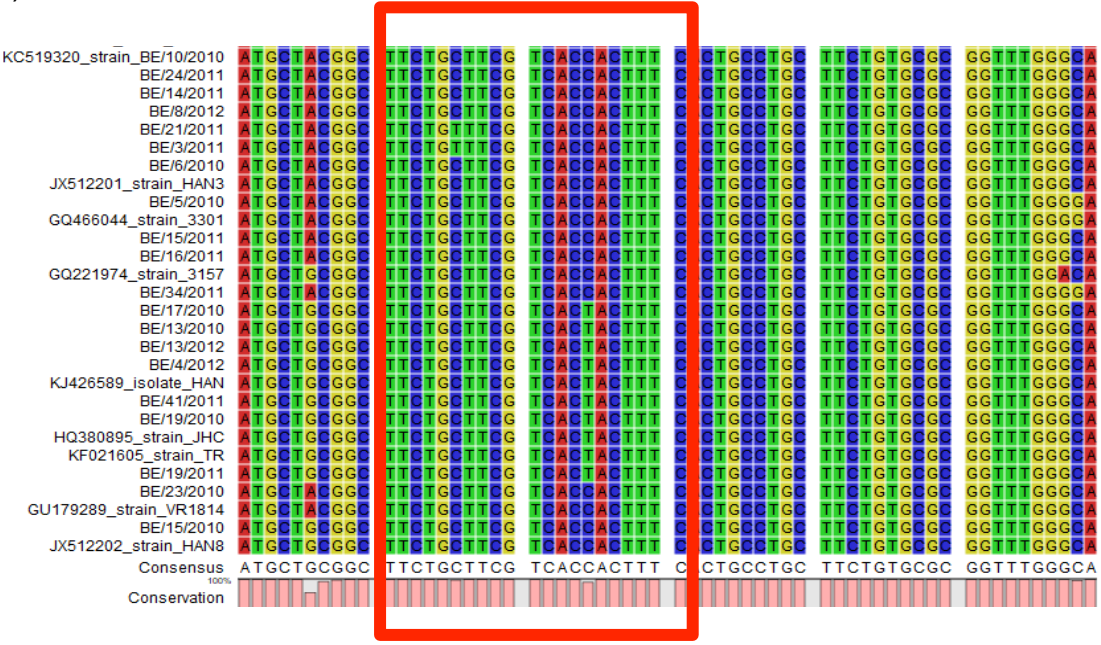
KC519320_strain_BE/10/2010
BE/24/2011
BE/14/2011
BE/8/2012
BE/21/2011
BE/3/2011
BE/6/2010
JX512201_strain_HAN3
BE/5/2010
GQ466044_strain_3301
BE/15/2011
BE/16/2011
GQ221974_strain_3157
BE/34/2011
BE/17/2010
BE/13/2010
BE/13/2012
BE/4/2012
KJ426589_isolate_HAN
BE/41/2011
BE/19/2010
HQ380895_strain_JHC
KF021605_strain_TR
BE/19/2011
BE/23/2010
GU179289_strain_VR1814
BE/15/2010
JX512202_strain_HAN8
Consensus
ATGCTGCGGC TTCTGCTTCG TCACCACTTT C CTGCCTGC TTCTGTGCGC GGTTTGGGCA
100%
Conservation

g)

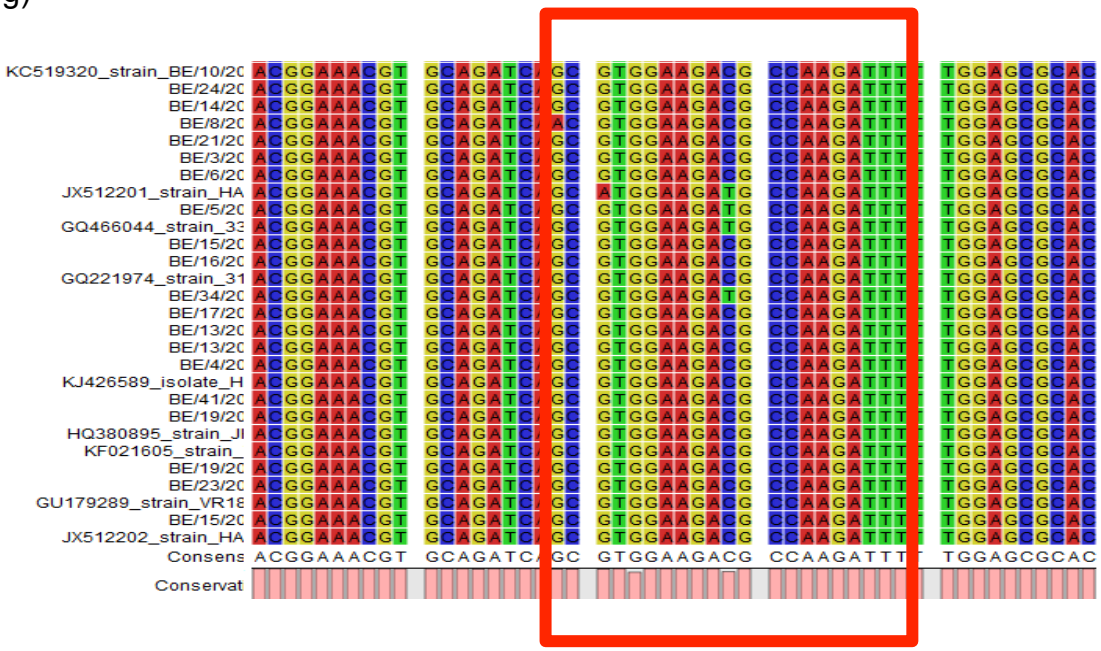
KC519320_strain_BE/10/20
BE/24/20
BE/14/20
BE/8/20
BE/21/20
BE/3/20
BE/6/20
JX512201_strain_HA
BE/5/20
GQ466044_strain_33
BE/15/20
BE/16/20
GQ221974_strain_31
BE/34/20
BE/17/20
BE/13/20
BE/13/20
BE/4/20
KJ426589_isolate_H
BE/41/20
BE/19/20
HQ380895_strain_JI
KF021605_strain_
BE/19/20
BE/23/20
GU179289_strain_VR18
BE/15/20
JX512202_strain_HA
Consens
ACGGAAACGT GCAGATC GC GTGGAAGACG CCAAGATTTT TGGAGCGCAC
Conservat

h)

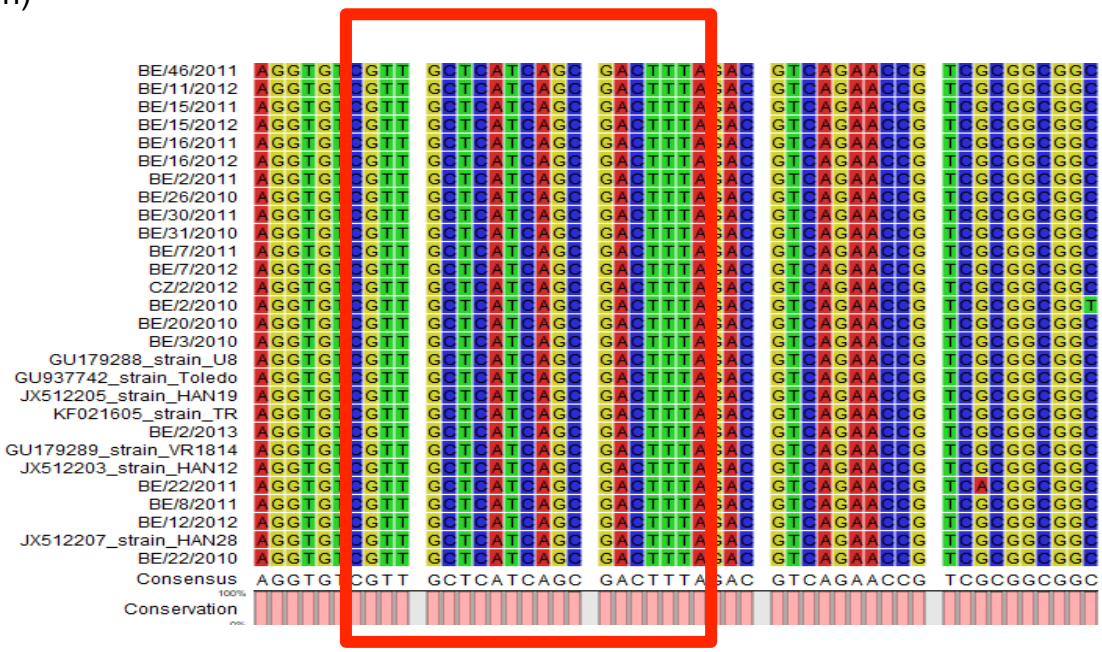
BE/46/2011
BE/11/2012
BE/15/2011
BE/15/2012
BE/16/2011
BE/16/2012
BE/2/2011
BE/26/2010
BE/30/2011
BE/31/2010
BE/7/2011
BE/7/2012
CZ/2/2012
BE/2/2010
BE/20/2010
BE/3/2010
GU179288_strain_U8
GU937742_strain_Toledo
JX512205_strain_HAN19
KF021605_strain_TR
BE/2/2013
GU179289_strain_VR1814
JX512203_strain_HAN12
BE/22/2011
BE/8/2011
BE/12/2012
JX512207_strain_HAN28
BE/22/2010
Consensus
AGGTGTCGTT GCTCATCAGC GACTTTAGAC GTCAGAACCG TCGCGGCGGC
Conservation

i)

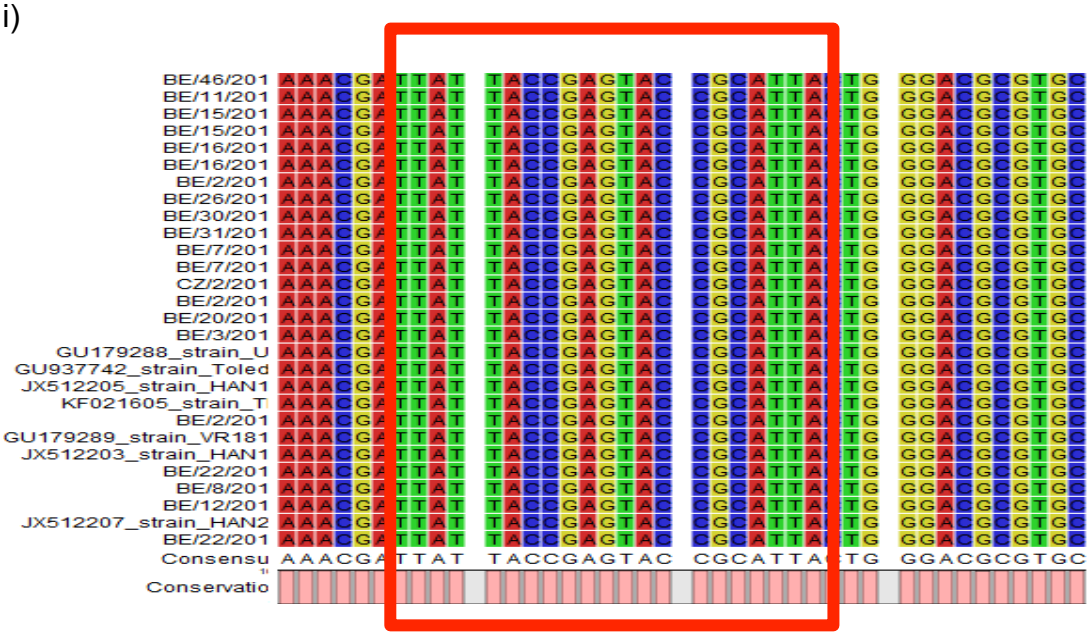

Figure 20 a-i. Sequence alignment of Merlin source RL13/UL128L with other known HCMV strains

RL13 and UL128L shRNA Merlin targets were aligned to known strains of HCMV to test for sequence conservation. Target sequence for shRL13-a (a), shRL13-b (b), shRL13-c (c), shUL128-a (d), shUL128-b (e), shUL130-a (f), shUL130-b (g), shUL131A-a (h) and shUL131A-b (i) are shown. Data set highlighted (red box) refers to RL13/UL128L target sequence of HCMV. Due to size of the database, partial results only shown. Sequence alignment performed in CLC Main Workbench version 7.9.1.

Table 13. Sequence alignment of target source RL13-a and -c with HCMV strain Merlin

shRL13-a	T	A	A	G	A	C	C	T	C	T	C	T	C	A	C	T	A	T	A	T	A
Merlin	C	A	T	G	A	C	C	T	C	T	C	T	C	A	C	T	A	T	A	T	A

shRL13-c	G	G	T	T	A	T	G	T	G	G	A	C	G	A	T	A	C	T	A	A	T
Merlin	G	A	T	T	A	T	G	T	G	G	A	C	G	A	T	A	C	T	A	A	T

Red denotes sequence mis-match with the intended target sequence

Table 14. Sequence alignment of target source RL13 and UL128L with other knwn HCMV strains

shRL13-a	T	A	A	G	A	C	C	T	C	T	C	T	C	A	C	T	A	T	A	T	A
conservation	72	52	80	48	100	100	61	85	85	53	92	100	33	85	85	58	98	100	51	100	100

shRL13-b	T	G	G	C	A	C	T	C	A	T	A	G	C	G	C	T	A	T	A	T	A
conservation	100	97	100	100	70	100	100	75	98	100	100	100	100	59	63	100	51	100	100	82	100

shRL13-c	G	G	T	T	A	T	G	T	G	G	A	C	G	A	T	A	C	T	A	A	T
conservation	100	85	100	100	100	53	72	100	100	100	100	100	99	52	100	100	76	100	72	99	100

shUL128-a	G	C	C	G	G	A	A	C	G	C	T	G	T	T	A	C	G	A	T	T	T
conservation	100	100	100	99	100	100	99	100	100	100	100	100	100	100	100	100	100	100	99	100	100

shUL128-b	T	C	A	G	T	A	C	C	T	G	G	A	G	A	G	C	G	T	T	A	A
conservation	100	100	100	99	100	100	100	99	100	100	100	100	100	100	100	100	100	100	100	100	100

shUL130-a	T	T	C	T	G	C	T	T	C	G	T	C	A	C	C	A	C	T	T	T	C
conservation	100	100	100	100	100	98	100	100	100	100	99	100	100	100	92	100	100	100	100	100	100

shUL130-b	G	C	G	T	G	G	A	A	G	A	C	G	C	C	A	A	G	A	T	T	T
conservation	99	99	99	100	90	100	100	100	100	100	91	100	100	100	100	100	100	100	100	100	100

shUL131A-a	C	G	T	T	G	C	T	C	A	T	C	A	G	C	G	A	C	T	T	T	A
conservation	100	100	100	100	100	100	100	100	100	100	100	100	100	99	100	100	100	100	100	100	100

shUL131A-b	T	T	A	T	T	A	C	C	G	A	G	T	A	C	C	G	C	A	T	T	A
conservation	100	100	100	100	100	100	100	100	100	100	100	100	100	100	100	100	100	100	100	100	100

shcont	G	C	C	T	A	A	G	T	A	T	C	G	C	C	T	A	A	T	T	T	A

No sequence alignment found with any known strain of HCMV from the NCBI database.

RL13 and UL128L shRNA targets were aligned to known strains of HCMV to test for sequence conservation. Where sequence conservation is <100% for a given base in the genome, box is highlighted in blue. Values denote percentage sequence conservation across 123 HCMV strains. Sequence alignment performed in CLC Main Workbench version 7.9.1

4.3 Generation of a lentiviral expression vector

Using the 'design vector' feature on the Vector Builder website, a mammalian lentiviral expression vector was selected as the vehicle for shRNA gene delivery based on its ability to transduce a plethora of cell types and permanently integrate its genes into host DNA in both dividing and non–dividing cells *in vitro* (259-60). This should result in long-term knockdown of the gene of interest (261).

To a HIV based lentiviral vector template (Vector Builder), the human RNA polymerase III U6 promoter, which had previously been demonstrated to drive high-level expression of shRNA in cells (297-8) was chosen to drive the expression of the shRNA construct of interest. Two complementary sequences of 21 nucleotides separated by a loop structure complete with a terminal sequence were also inserted into the vector backbone for each construct. An ampicillin resistance gene was included for plasmid maintenance in E. coli. To permit selection of stable expressing clones after transduction, a puromycin resistance gene was inserted into the vector. In order to create a cell line capable of suppressing the expression of both RL13 and any one of the UL128L genes, the UL128L vectors contained a GFP or mCherry fluorescent protein for future selection by cell sorting (Figures 21-22). Fibroblasts would initially be transduced with shRL13, selected for by the addition of puromycin, before transduction with a UL128L vector. Cell sorting by mCherry would isolate RL13 and UL128L transformed clones. This new cell line would be able to propagate a fully wild-type virus in the laboratory. Plasmids were stored as E. coli bacterial glycerol stocks.

Transformed bacteria containing the packaging or shRNA plasmids of interest were grown in preparation for large (maxi) scale DNA isolation.

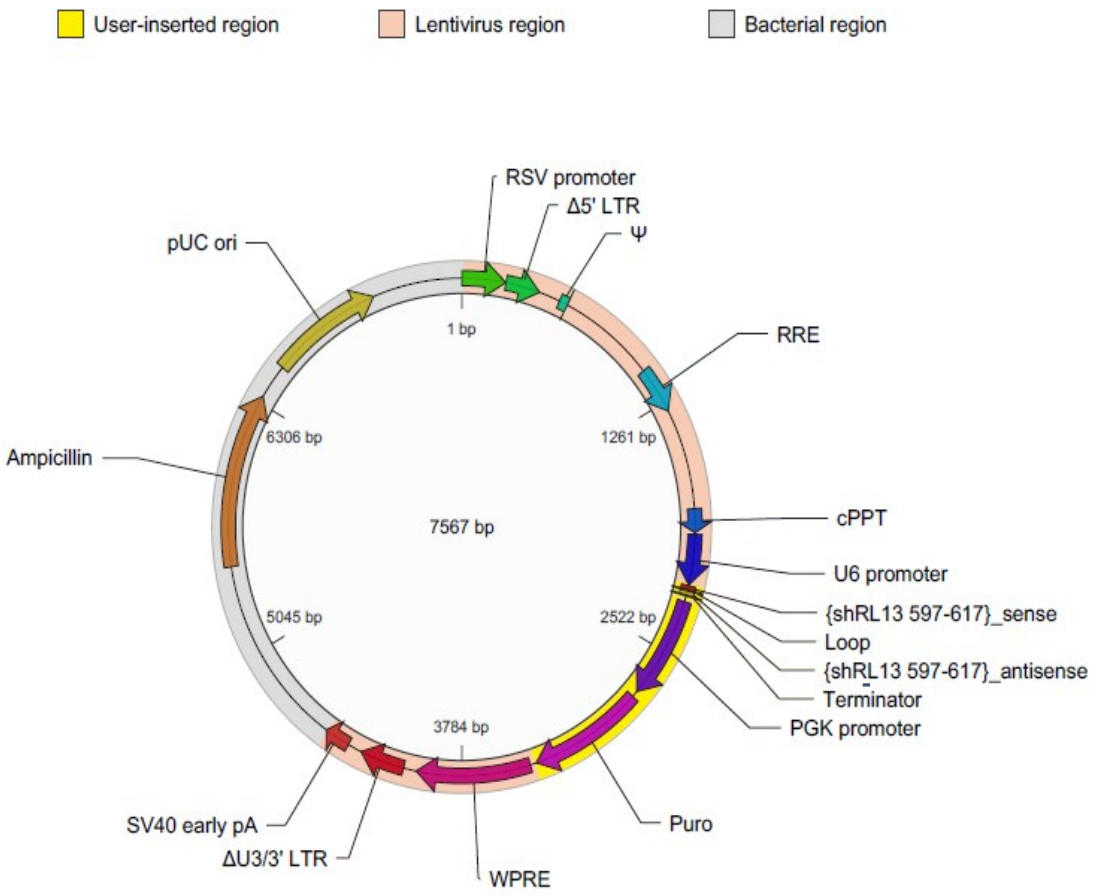

Figure 21. Plasmid map of the shRL13-a lentiviral vector backbone

Map of the shRL13-a viral vector plasmid highlighting location of key genes; sense and anti-sense strands of the shRL13-a gene, puromycin and ampicillin resistance genes and U6 promoter. All RL13 shRNA vectors had the same lentiviral template.

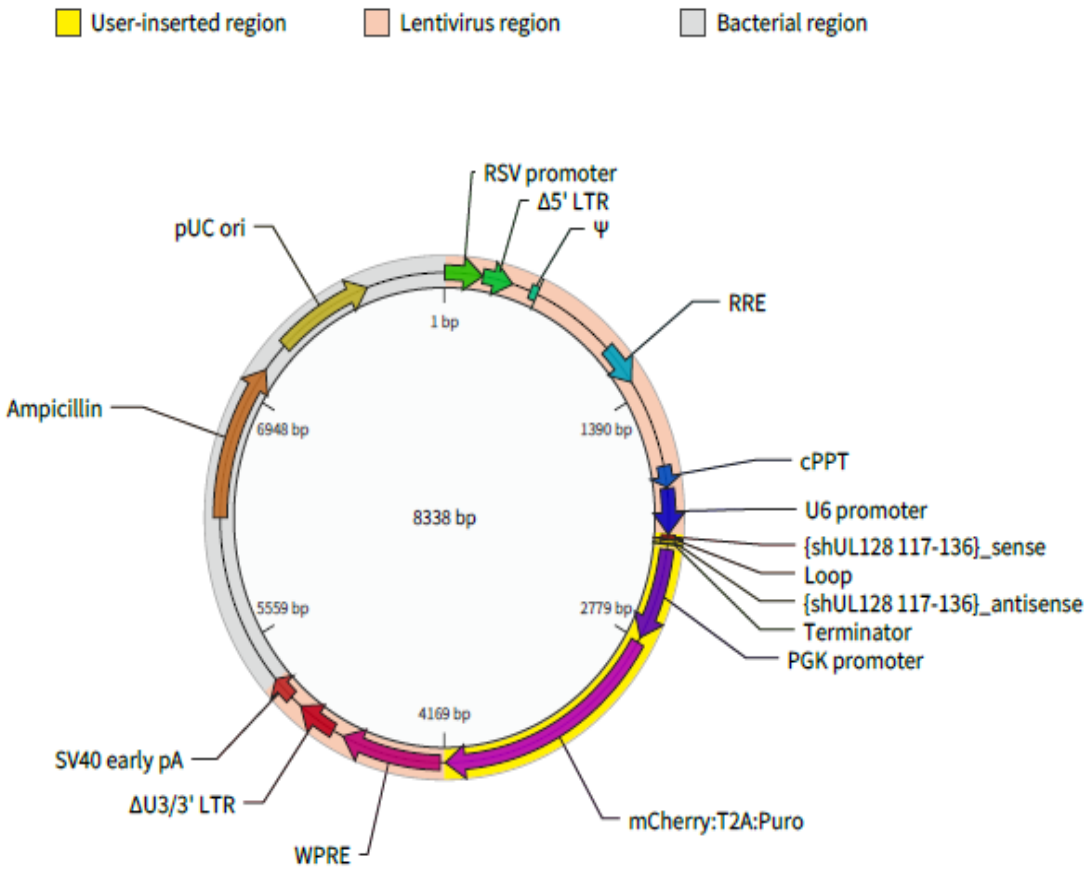

Figure 22. Plasmid map of the shUL128-a lentiviral vector backbone

Map of the shUL128-a viral vector plasmid highlighting location of key genes; sense and anti-sense strands of the shUL128-a gene, puromycin and ampicillin resistance genes and U6 promoter. UL128-a also contained an mCherry tag driven by the PGK promoter. All UL130 and UL131A vectors had the same lentiviral template.

UL128–b contained an eGFP tag in place of an mCherry.

Table 15. DNA concentration of shRNA and packaging plasmids from maxi preparation

Plasmid I.D	Concentration ng/μl
shRL13-a	240.0
shRL13-b	740.1
shRL13-c	196.8
shUL128-a	228.9
shUL128-b	1267.6
shUL130-a	982.59
shUL130-b	269.4
shUL131-a	189.3
shUL131-b	371.7
Shcont	368.8
pRSV-REV	373.76
pMDLg	268.86
pMD2G	576.0

The pRSV-REV packaging plasmid expresses HIV-1 REV under the transcriptional control of the rous sarcoma virus (RSV) U3 promoter. pRSV-REV binds to the REV responsive element (RRE) for efficient RNA export from the nucleus. pmDLg contains the gag and pol genes which provide the main structural proteins and reverse transcriptase respectively. pMD2G encodes vesicular stomatitis virus glycoprotein (VSV-G) that coats the viral envelope and expands the tropism of the vector (299).

4.4 Production and validation of lentiviruses

The cell line 293T, was subjected to co-transfection with three packaging plasmids and a single shRNA vector. To measure transfection efficiency, fluorescent images of 293T cells were taken at 72 hours post infection. Where fluorescently tagged lentivirus had been successfully transfected into the packaging line, green (GFP) or red (mCherry) cells could be observed depending on the tag used. Between 20-40% transfection efficiency was observed across all fluorescently tagged constructs at 72h.p.i. (data not shown). No RL13 lentiviruses contained a fluorescent marker, therefore transfection efficiency could not be determined.

The MG 3468 fibroblast cell line was transduced with un-tagged (shRL13a-c), GFP (UL128-b) or mCherry (UL128-a, UL130-a, b, UL131-a, b) tagged fluorescent lentivirus using retronectin® reagent, which had been shown by Hanernberg *et al* (300) to significantly improve gene transfer into target cells through enhanced co-localization of viral particles and target cells. Following puromycin selection, dying cells detached from the plates, allowing for easy identification of transformed cells. Fluorescent microscopy images of the tagged lentiviral vectors confirmed uptake of the lentivirus into the cells (Figure 23).

Expansion of surviving cell populations in puromycin selection media resulted in all non-transformed cells being eliminated. Incorporation of the viral vector was therefore shown to be successful in all MG 3468 fibroblast cell lines.

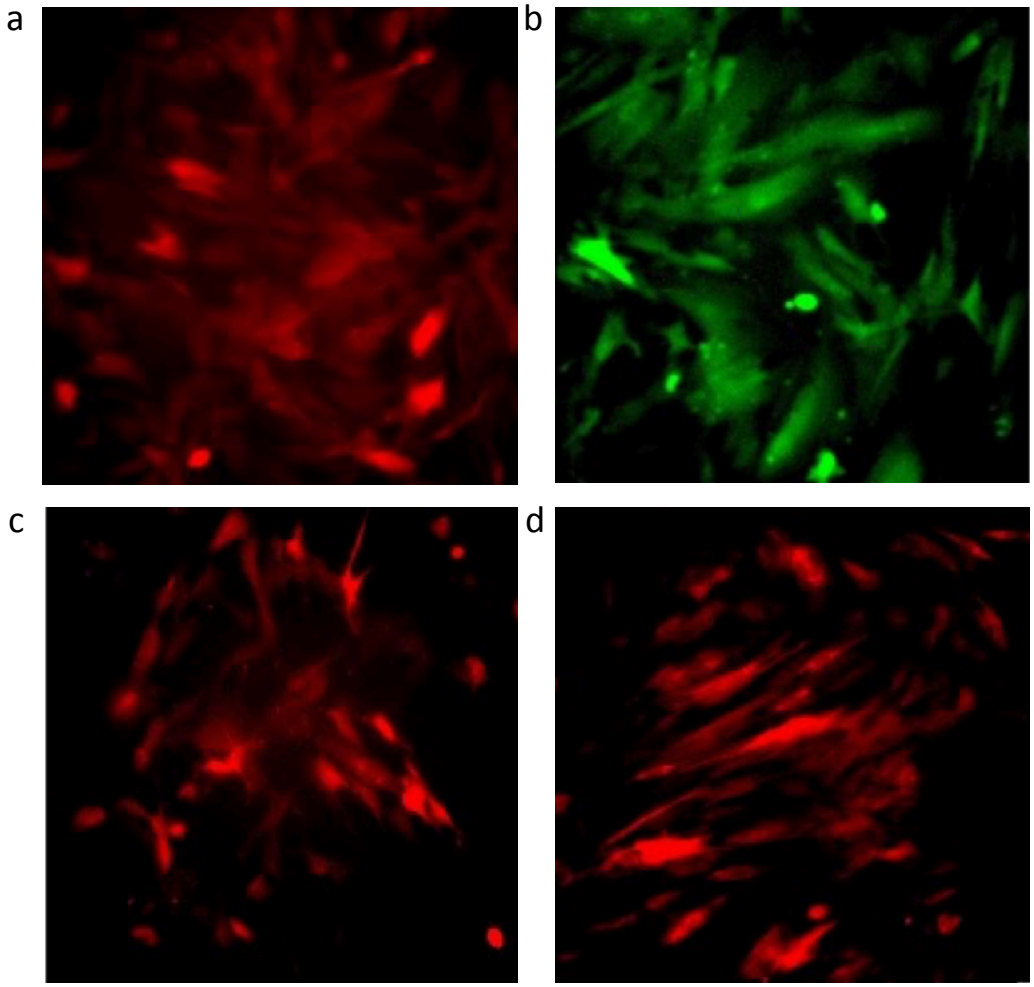

Figure 23. Fluorescent images indicating transduction of lentivirus into target fibroblast cells

eGFP or mCherry expression in MG 3468 fibroblast line following transduction of a) shUL128-a b) shUL128-b c) shUL130-b or d) shUL131-a vectors at 72 h.p.i. Representative images selected. No RL13 lentiviruses contained a fluorescent marker therefore transduction success could not be measured by fluorescent microscopy with these constructs.

4.5 shRNA directed against RL13 and UL128L genes did not suppress the expression of the genes of interest

The phenotype of the virus in the presence of wild-type RL13 and UL128L genes in HCMV vary dramatically to their mutated (Δ) counterparts. The presence of wild-type genes results in small viral plaques while RL13 and UL128L mutants form considerably larger plaques following 14 days culture (5, 160, 228). Interestingly, viruses with either RL13 or one of the UL128L genes repressed produce plaques that are larger than the wild-type, but smaller than the double mutant over the same time course. To therefore distinguish the effects of RL13 suppression from UL128L expression and vice versa, all experiments were performed with viruses lacking the gene not being tested. i.e for all shRL13 constructs, a ΔUL128 Merlin viral background was used. Conversely, for all UL128L constructs, ΔRL13 Merlin viruses were employed. Plaque assay was used to determine the efficacy of shRNA knockdown.

To test the shRL13 constructs, ΔUL128 viruses containing or lacking the RL13 gene were allowed to form plaques on transduced MG 3468 cells (Figure 24). Similarly, ΔRL13 viruses containing or lacking the UL128 gene were permitted to form plaques on transduced MG 3468 cells (Figure 25). Plaques were measured at 14 d.p.i. If the shRNA constructs directed against RL13 or UL128L reduce gene expression, the resulting plaque sizes should be equivalent to that seen with no RL13/UL128 genes present.

Representative images of ΔUL128 HCMV viral plaque formation, in the presence (+) or absence (Δ) of RL13 on the shRL13 engineered cell lines is given in figure 24, with quantification of multiple plaques given in figure 26.

Figures 24 and 26 taken together clearly demonstrate that in the control cell line (shcont), when the RL13 gene was expressed in the assay, plaque sizes

were significantly reduced compared to the system lacking RL13. In contrast, no increase in plaque size was observed when RL13 intact virus was grown on fibroblasts containing the shRNA directed against RL13, indicating that the shRNA constructs did not suppress the expression of RL13 sufficiently to alter the small-plaque phenotype of the virus.

Example images of ΔRL13 HCMV viral plaque establishment, with (+) or without (Δ) UL128 on cell lines containing shUL128L constructs is given in figure 25, with quantification of multiple plaques given in figures 27a and 7b.

Figures 26, 27a and b also show that the control cell line (shcont), in the presence of UL128, exhibited reduced plaque size formation compared to the experiment lacking UL128. No enhancement in plaque size was seen when UL128 intact virus was propagated on fibroblasts containing the shRNA constructs targeting UL128, UL130 or UL131A. As previously demonstrated with the RL13 constructs, the shUL128L compositions did not restrict the expression of these genes adequately to increase the small-plaque phenotype of HCMV. The only data set to show non-significance (ns) was the shUL128-b cell line. In figure 27a, the plaque sizes formed in the shUL128-b control cells were markedly reduced compared to that of the other control samples, thus rather than inhibiting UL128 expression specifically, this line non-specifically inhibited all virus growth.

The only data set not to be included in figure 27a is the UL131-b cell line as technical difficulties were encountered during transduction. Initial gene transfer using retronectin resulted in no transduced cells being generated. Subsequent attempts at transduction with retronectin however, proved successful, albeit at low efficiency rates (data not shown). Once established, the UL131-b cell line demonstrated reduced growth kinetics compared to its counterparts *in vitro*, resulting in plaque assay experiments being performed in parallel with the shcont cell line at a later time point. A possible reason for the reduced growth kinetics observed in this cell line may be due to off target effects of the lentiviral vector itself.

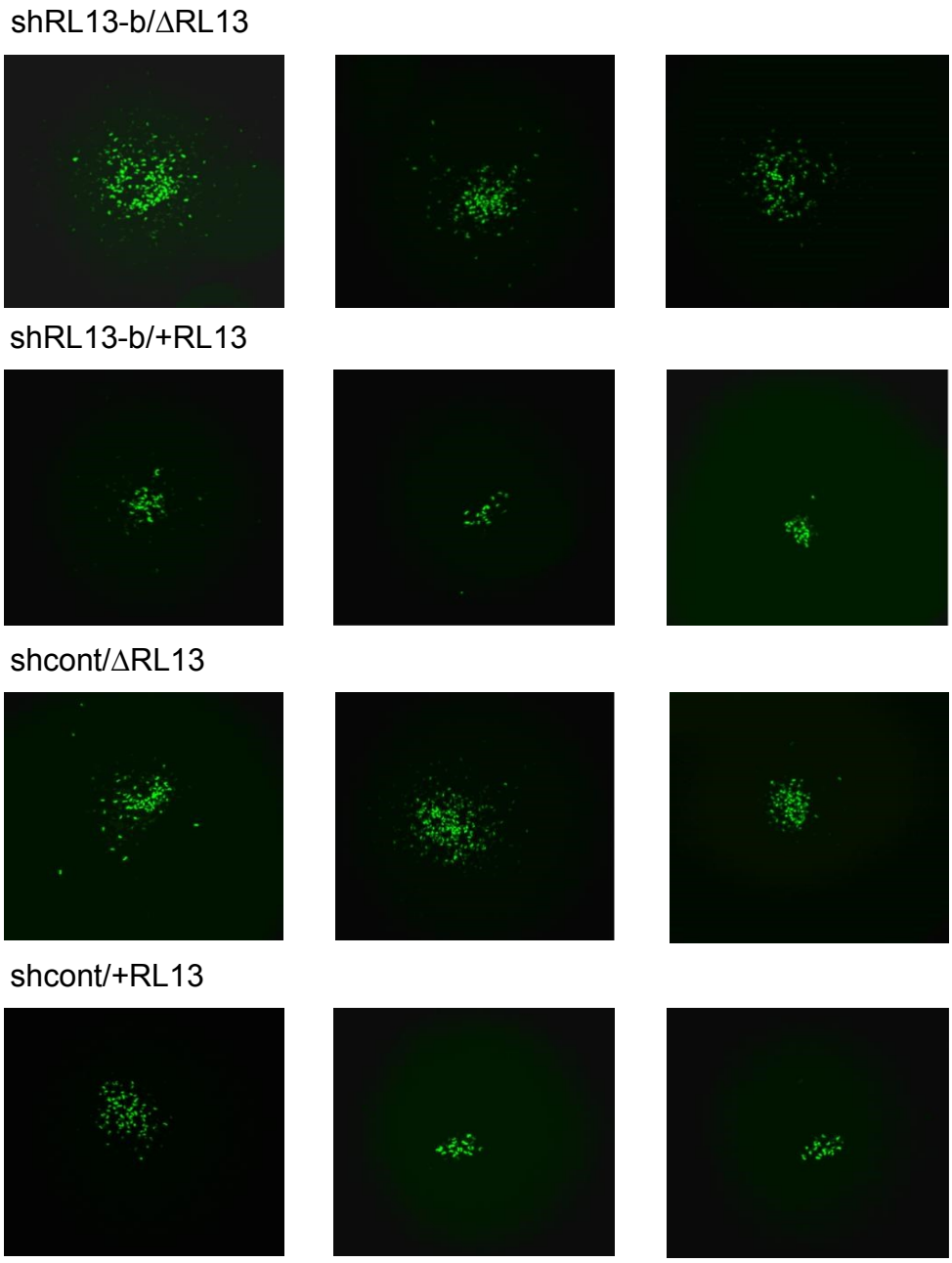

Figure 24. Comparison of plaque size formation on MG 3468 fibroblasts infected with ΔUL128 HCMV containing (+) or lacking (Δ) RL13

shRL13-b/ΔRL13) shRL13-b transduced fibroblasts infected with double mutant (ΔUL128/ ΔRL13) HCMV. shRL13-b/+RL13) shRL13-b transduced fibroblasts infected with ΔUL128/+RL13 HCMV. shcont/ΔRL13) shcont transduced fibroblasts infected with double mutant (ΔUL128/ΔRL13) HCMV. shcont transduced fibroblasts infected with ΔUL128/+RL13 HCMV.

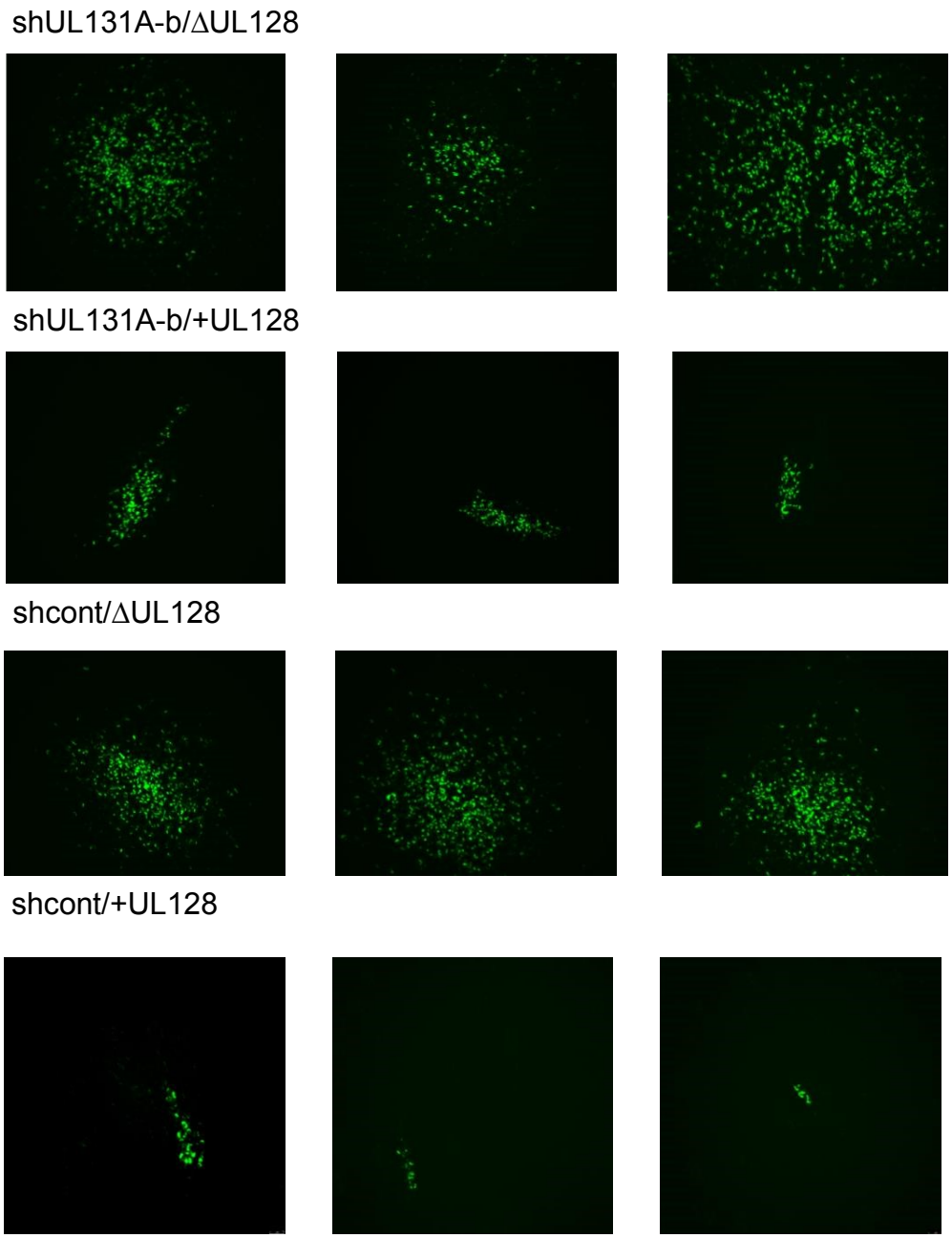

Figure 25. Comparison of plaque size formation on MG 3468 fibroblasts infected with ΔRL13 HCMV containing (+) or lacking (Δ) UL128

shUL131A-b/ΔUL128) shUL131A-b transduced fibroblasts infected with double mutant (ΔRL13/ ΔUL128) HCMV. shUL131A-b/+UL128) shUL131A-b transduced fibroblasts infected with ΔURL13/+UL128 HCMV. shcont/ΔUL128) shcont transduced fibroblasts infected with double mutant (ΔRL13/ ΔUL128) HCMV. shcont/+UL128) shcont transduced fibroblasts infected with ΔRL13/+UL128 HCMV.

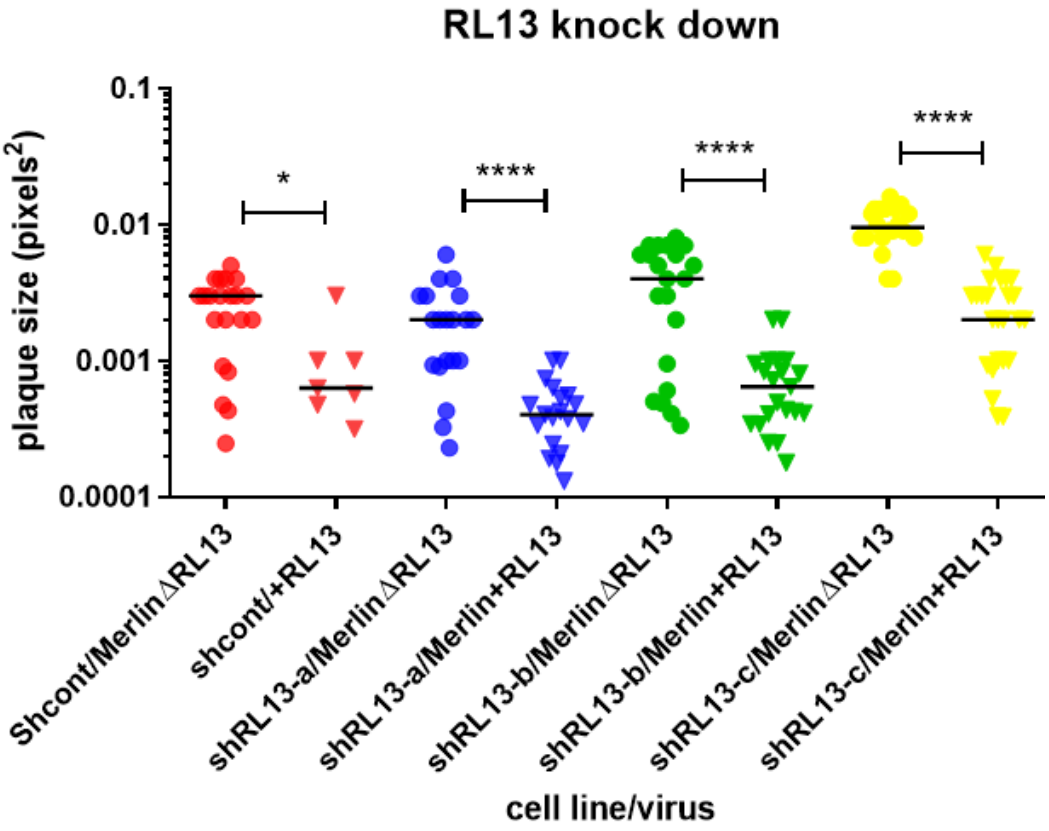

Figure 26. shRNA constructs do not suppress the expression of the RL13 genes

Three shRNA constructs (designated shRL13-a, -b and -c respectively) were generated in fibroblasts, each targeting different regions of the RL13 gene. A shRNA scrambled control (shcont) was also included. Cells were infected with either ΔRL13 or +RL13 virus, and plaque sizes measured 14 days post infection. Each data point represents a single measurement. Representative data from three independent experiments. Statistics performed with two-tailed unpaired T test.
ns, P≤0.05: **, P≤0.01: ***, P≤0.001: ****, P≤0.0001

27a)

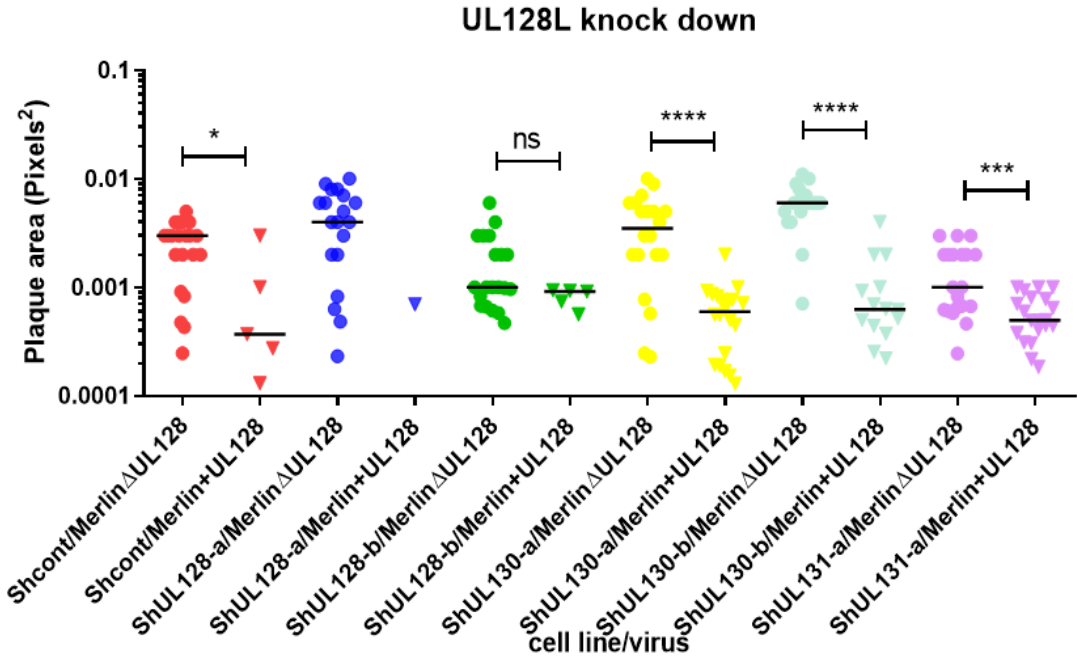
UL128L knock down
Plaque area (Pixels²)
0.1
0.01
0.001
0.0001
*
ns
****
****
***
Shcont/MerlinΔUL128
Shcont/Merlin+UL128
ShUL128-a/MerlinΔUL128
ShUL128-a/Merlin+UL128
ShUL128-b/MerlinΔUL128
ShUL128-b/Merlin+UL128
ShUL130-a/MerlinΔUL128
ShUL130-a/Merlin+UL128
ShUL130-b/MerlinΔUL128
ShUL130-b/Merlin+UL128
ShUL131-a/MerlinΔUL128
ShUL131-a/Merlin+UL128
cell line/virus

27b)

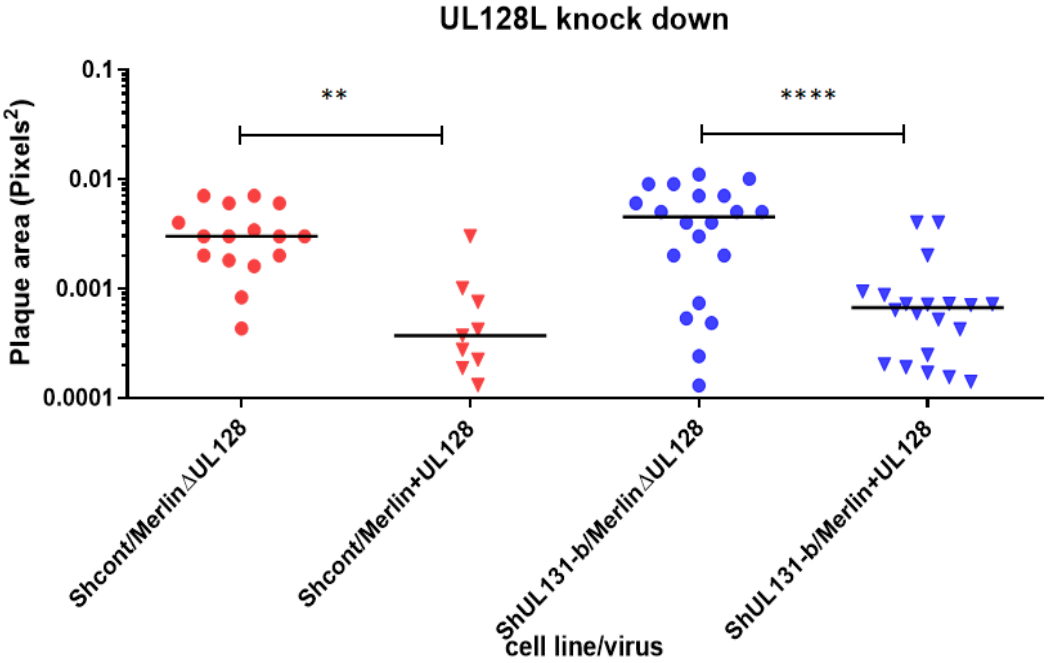
UL128L knock down
Plaque area (Pixels²)
0.1
0.01
0.001
0.0001
**
****
Shcont/MerlinΔUL128
Shcont/Merlin+UL128
ShUL131-b/MerlinΔUL128
ShUL131-b/Merlin+UL128
cell line/virus

Figure 27a and b. shRNA constructs do not suppress the expression of the UL128L genes

Six shRNA constructs (designated shUL128-a, –b, shUL130-a, -b, and shUL131-a, -b) were generated in fibroblasts, each targeting different regions of the UL128L genes. A shRNA scrambled control (shcont) was also included. ΔUL128 or +UL128 virus was incubated with the cells and plaque sizes measured 14 days post infection. Each data point represents a single measurement.
Representative data from three independent experiments. Statistics performed with two-tailed unpaired T test.
ns, P≥0.05, *, P≤0.05: **, P≤0.01: ***, P≤0.001: ****, P≤0.0001

4.6 Chapter discussion

RNAi is a naturally conserved biological process in eukaryotes that can be triggered by the introduction of small interfering (si) or short hairpin (sh) RNA into host cells. Since its discovery in 1998 by Fire *at al* (301), RNA interference (RNAi) has been widely used by researchers to successfully suppress the expression of genes targeted through their sequence by the addition of exogenous dsRNA in plants (302), insects (303-4) and cultured mammalian cells (305-6).

shRNA was the RNAi method of choice adopted in this chapter, as it can be incorporated into a lentiviral vector, which stably integrate into the host genome, resulting in long-term knockdown of the target gene (307).

shRNA-mediated knockdown is initiated by the polymerase III enzyme DICER, which recognizes and cleaves long exogenous dsRNA into 21-23nt siRNA fragments. Uptake of DICER and siRNA into the RNA-induced silencing complex (RISC), results in degradation of the siRNA passenger strand. The complex is then primed to bind to target mRNA, which is cleaved and degraded, resulting in gene knockdown (308-9).

The aim of shRNA constructs to affect the growth phenotype of wild-type HCMV by impairing the expression of viral RL13 and UL128L genes *in vitro* through RNAi was not achieved in this chapter as confirmed by plaque assay (Figures 25, 26a, 26b). This may have been because the level of knockdown was insufficient to mitigate the effects of the viral proteins - to determine whether any degree of knockdown was achieved, quantitative reverse transcriptase polymerase chain reaction (RT-QPCR) could have been performed to investigate transcript levels, or western blot could have been performed to investigate protein levels. However, although this would inform on the reasons for failure, it would not have altered the ultimate outcome.

Three shRNA directed against RL13 and two against each of the UL128L genes, UL128, UL130 and UL131A, were constructed and tested during this

project. Analysis of the shRNA target sequences revealed that shRL13-a and shRL13-c did not align with the HCMV sequence strain Merlin (Table 13) although both existed in the RL13 genes of alternate HCMV strains including strains VR1814 (GU179290) and Han22 (JX512206) for RL13-a, or strains Han12 (JX512203) and JP (GQ221975) for RL13-c (Figures 20a, 1c). shRL13-a was found to contain two sequence mis-matches at nucleotide bases 1 and 3, while shRL13-c contained a single miss-match at nucleotide base 2 when compared to the Merlin RL13 gene. Based on RNAi analyses by Elbashir (310), Jackson (311), Amarzguioui (312) and others, these terminal sequence mis-matches were unlikely to impede shRNA binding to its target sequence and consequently, the decision was taken to use the HCMV strain Merlin to measure shRNA knockdown efficiency in all cell types.

Due to the lack of change in the small-plaque phenotype of the virus following 14 days culture, future knockdown studies with the shRL13-a and -c should be performed with one of the alternative HCMV strains recognized by these constructs as well as strain Merlin to fully eliminate the possibility that sequence mis-match had any impact on virus phenotype. Alternatively, the RL13 sequence from one of those strains could be incorporated into Merlin.

CLC main sequence analysis of the shRL13 constructs revealed that up to 94.3% of all known RL13 HCMV sequences did not align with their target shRNA. As a known hypervariable gene (5), this low level of recognition between the strains for the target sequences selected was unsurprising. At variance with the shRL13 constructs, all UL128L targets exhibited high (80-100%) target sequence recognition rates across all the known strains, consistent with previous analysis by Baldanti *et al* (313).

All viruses used in this assay contained a GFP marker for easy plaque identification. An oversight in vector design therefore was the insertion of an eGFP marker in place of mCherry into the shUL128-b vector backbone. Despite this error, data suggests that the intensities between the two competing GFP signals was sufficient to differentiate plaques (Appendix: Figure S1). What this image highlights, however, is the low eGFP expression

of the transduced cells. Fluorescent images taken of the other lines post transduction (Figure 22) also demonstrated that only a small proportion of the cells in each image strongly express their tag, indicating the heterogeneous GFP expression levels of the cell population. It is important to note that eGFP/mCherry signal does not directly correlate to the levels of shRNA expression in the cells, as the eGFP/mCherry signal was driven by a different (PGK) promoter. However this does imply that single-cell cloning may provide a way to isolate clones expressing the shRNA at higher levels, and may therefore be more effective.

All shRNA used in this chapter were designed using InvivoGen's siRNA Wizard^{TM}, which selects shRNA sequences that match criteria proposed by analysis of RNAi which have the best expression rate in psiRNA vectors. The psiRNA vector however, was not the vector supplied by Vector Builder and differs to the lentiviral backbone used by having a 7SK rather than a U6 promoter. The efficiency of the U6 promoter has been shown to be comparable to the efficiency of the 7SK promoter however (314-5), and is therefore unlikely to have contributed to poor shRNA expression rates in the cell lines generated, resulting in the inability of the cell to generate sufficient gene knockdown to affect the viral small plaque-size phenotype.

Another possible reason for the inability of shRNA to ablate gene expression may be due to viral induced effects on the infected cell. During infection, the virus may overwhelm the cell by generating viral mRNA at exceptionally high levels, from multiple genomes. This differs from host genes, which may be expressed at lower levels from a single genome. Under such conditions, the shRNA may be unable to effectively silence the expression of the gene of interest. There are, however, examples where shRNA has proved successful in targeting and knocking down the expression of specific viral genes, including the rev, gag and vif sequences of HIV-1 (316) and the VP2, VP3 and VP4 sequences of foot and mouth disease (317). The effects of viral knockdown on the cells could be determined by qPCR. This point could also be addressed by generating a positive control for the shRNA vector, using a targeting sequence that is known to efficiently knock down the expression of a

host gene. As the pLV-puro-U6 vector backbone has not been shown to be effective in viral gene knockdown in fibroblasts, a positive control was not included in this study. The vector has, however efficiently knocked down the expression of FOXA2 in bone marrow-derived mesenchymal stem cells (318) and Jun expression in the breast cancer cell line MCF-7 (319). It would also be possible to investigate knockdown efficiency by expressing RL13/UL128 from a lentiviral vector, such that expression levels were more similar to a cellular gene.

It is possible that the selected target site sequences led to the failure of this objective. Over the years, much controversy has surrounded the development of guidelines for the creation of potent siRNA sequences and whether these rules can be applied to shRNA sequences. Despite this, numerous academic and commercial si/shRNA sources are widely available, each with predictive algorithms broadly following similar guiding principles. These include sequences generally 21 nucleotides in length with a GC content between 30-55% (288-90), a lack of >4 single nucleotide repeats (320), a loop region between 3-9 nucleotides in length (291), sequences with thermodynamic asymmetry (289-90), base preferences at specific positions (321-4), mRNA secondary formation (325-6), and the specificity of the target site itself (327-9). Studies by Schwarz *et al* has also highlighted the importance of GC arrangement within the sequence, with particular emphasis on the 3' end of the antisense strand containing a higher GC content than the 5' end (290).

Taken together, these guidelines could have the potential to give rise to high potency shRNA with low off-target effects, however, empirical data has demonstrated that even when these rules are applied to shRNA design, knockdown efficacy can be highly variable (330-1). The variability of gene knockdown efficiency is likely due to our limited understanding of the RNAi process, resulting in incomplete predictive algorithms.

Chapter 5 - Results

Generation of a UL128 expressing fibroblast cell line

5.1 Introduction

Over the past 20 or so years, our laboratory has generated a library of over 200 cytomegaloviruses, each genetically manipulated to contain or lack different combinations of genes to aid our investigation into HCMV pathogenesis. The genetic background to the majority of these viruses are based on the sequence of strain Merlin at passage 3, which contains a C to T nucleotide substitution in gene UL128, leading to a premature truncation of the gene. Given the role of UL128 in promoting infection of multiple cell types, this virus is restricted to infection of fibroblasts (332).

The objective of this chapter was to generate a UL128 expressing cell line capable of *trans*-complementing our existing UL128 deficient viral stocks. UL128 gene transfer into fibroblasts was performed using a retroviral-based vector.

5.2. pMXs-IRES-Puro (pMXs-IP) retroviral vector

The pMXs-IP retroviral vector (Figure 28), was chosen due to its proven ability to successfully generate HFFF-tet cells by our group in 2010 (228). Inherent features of the vector that were exploited during this study included long terminal repeats (LTRs) to promote and terminate gene transcription and a puromycin resistance gene linked to the transgene via an IRES, for the selection of stable UL128 expressing cells following transduction.

Two unique restriction sites, XhoI and BamHI, within the multiple cloning site (MCS) region of the vector were selected as regions to incorporate the UL128 gene. These sites were chosen based on their relative location to each other and restriction digest buffer compatibility.

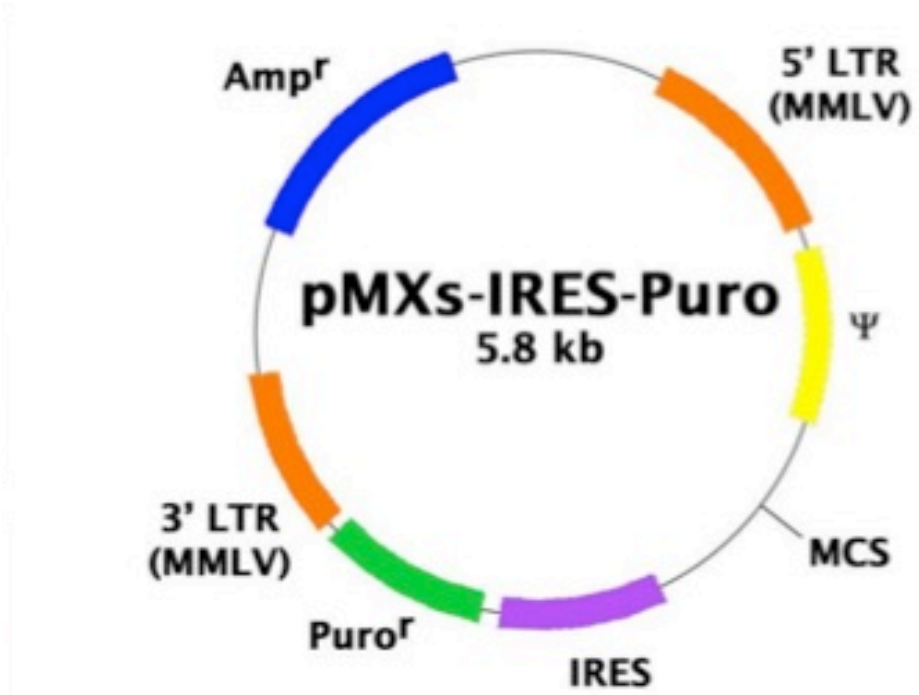

Figure 28. Schematic representation of the pMXs-IP retroviral vector backbone

Schematic of the pMXs-IP retroviral vector plasmid highlighting location of key genes; puromycin and ampicillin resistance genes, packaging signal (Ψ), long terminal repeats (LTRs), internal ribosome entry site (IRES) and multiple cloning site (MCS). Image taken from the Cell Biolabs Inc product data sheet (RTV-014).

5.3 UL128 sequence construction

Primers suitable for amplifying the entire UL128 gene from Merlin were designed using CLC main workbench version 7.9.1. (See Appendix: Table ST3). Each primer also included sequences corresponding to an appropriate restriction site (XhoI/BamHI), an additional four base pairs to improve restriction enzyme digestion efficiency, and in the case of the forward primer, a kozak sequence to promote efficient translation.

Genetically intact UL128 DNA from the HCMV strain Merlin, was provided by Dr Carmen Bedford, for use as a DNA template.

5.4 Generation of a UL128 retroviral vector

Direct cloning of PCR amplified UL128 into pMXs-IP was unsuccessful, therefore the PCR product was TOPO-cloned into a pCR™4-TOPO® TA vector, before being subcloned into pMXs-IP. Cloning was confirmed by agarose gel electrophoresis (Figure 29) and DNA sequencing.

5.5 Production and validation of retroviruses

To allow production of the retroviral vector in the absence of a replication-competent virus, the helper-free virus packaging cell line, 293 phoenix cells, was subject to transfection with the UL128 retroviral vector. As the vector lacked a reporter gene, transfection efficiency was determined by transfecting a GFP expressing plasmid in place of the UL128 vector into the cell line. Fluorescent images of 293 phoenix cells were taken at 72 h.p.i. Where GFP had been successfully inserted into the packaging line, green cells could be observed. 50% transfection efficiency was observed at 72h.p.i. (data not shown), validating the technique.

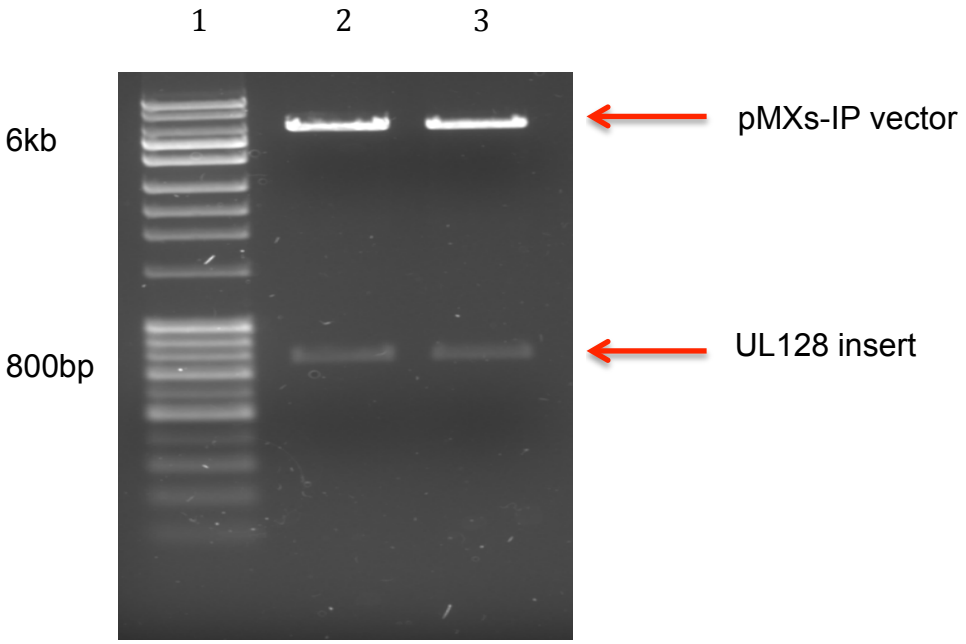

Figure 29. Agarose gel electrophoresis confirms UL128 and pMXs-IP presence in the transformed E. coli colonies

Agarose gel electrophoresis of two transformed E. coli clones following small-scale production and purification. Clones were subject to BamHI and XhoI double digest to confirm vector uptake (lanes 2 and 3). DNA bands corresponding to the insert (752Kb) and vector (5.8Kb) are clearly visible. Molecular weight standards are shown in lane 1.

Retrovirus mediated gene transduction into two fibroblast cell lines, MG 3468 and HF-Tert, was performed using retronectin® reagent, as previously described (section 2.5.15.2). Following puromycin antibiotic selection, non-transduced cells detached from the plates, leaving behind adherent transduced cells, which should contain the retroviral vector.

5.6 Retrovirus mediated UL128 gene transfer into fibroblasts did not generate a UL128 expressing cell line.

The phenotype of HCMV varies dramatically depending on the RL13 and UL128 status of the virus. The presence of both wild-type genes gives rise to small viral plaque formation following 14 days culture on fibroblasts. In contrast, viruses harboring defective and therefore non-functional RL13 and UL128 genes over the same time course, form considerably larger plaques (5, 160). Viruses containing a single mutant (WT RL13 and ΔUL128 or vice versa) produce viral plaques that are larger than the wild-type, but smaller than the double mutant phenotype. All viruses used in this chapter therefore lacked RL13 so that any difference in plaque size observed between the parental and transduced cell line would be solely due to UL128 expression. Plaque size was used as a measure of UL128 expression in the MG 3468 and HF-Tert cell lines.

To test the cell lines generated, viruses containing or lacking UL128 were allowed to form plaques on parental and transduced cell lines (Figure 30, 32). Plaques were measured at 14 d.p.i. In the presence of UL128, whether expressed from the virus or the transduced cell line, plaque size should be significantly reduced when compared with a system lacking the gene.

Representative images of HCMV plaque formation on parental and transduced fibroblasts in the presence (+) or absence (Δ) of viral UL128 is given in figures 30 (MG 3468) and 32 (HF-Tert), with quantification of multiple plaques given in figures 31 (MG 3468) and 33 (HF-Tert).

Figures 30 and 32 show that in the presence of viral UL128, plaque size formation in the parental (blue) and transduced (red) cell lines are greatly reduced compared to the parental control in the absence of a viral UL128. Plaque size formation on the transduced fibroblasts in the absence of viral UL128, however, is equivalent to that seen in the control cells in the absence of the gene of interest, indicating that UL128 was either absent or poorly expressed in the transduced cell lines.

As both MG 3468 and HF-Tert transduced cells survived continuous culturing in the presence of puromycin antibiotic selection, retroviral integration was likely successful. This did not, however, confirm that the gene of interest was being expressed. To determine UL128 expression levels in the cells of interest, cell lysates from transduced and parental fibroblasts were generated, with UL128 protein level measured using SDS-PAGE followed by western blotting (Figure 34). To provide a positive control for the western blotting, HF-Tert cells were infected with wild-type Merlin at an MOI of 5, with protein expression levels measured at 24hr intervals between 48 and 168 hours. Figure 34 shows that HCMV infected HF-Tert cells express UL128 at detectable levels from 96 hours post infection, with a decrease in signal observed over time. Figure 34 also demonstrates the lack of UL128 protein expression in the transduced cell populations, as UL128 was only observed in the positive control samples.

Having been unsuccessful in generating a functional UL128 helper cell line using the pMXs-IP retroviral vector, I was fortunate to obtain a lentiviral vector (pHAGE) containing a V5-tagged UL128 (Lenti-V5-UL128) from our collaborator, Dr Michael Weekes (Cambridge University), a construct which was made in parallel to my work.

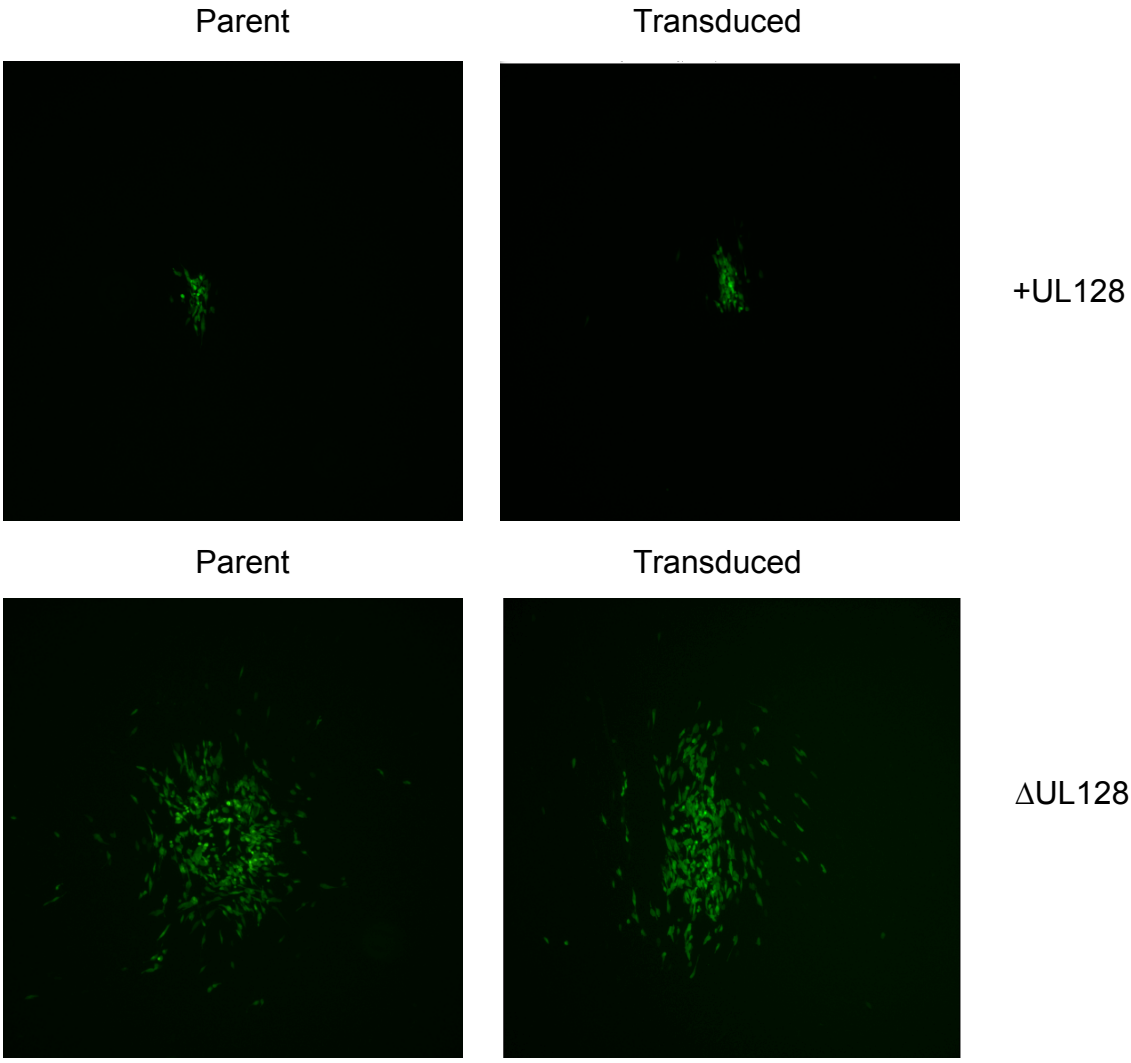

Figure 30. Comparison of plaque size formation on parental and UL128 tranduced MG 3468 fibroblasts infected with HCMV containing (+) or lacking (Δ) UL128

Representative fluorescence images of parental and transduced MG 3468 cells infected with or without HCMV containing UL128 at 14 days post infection.

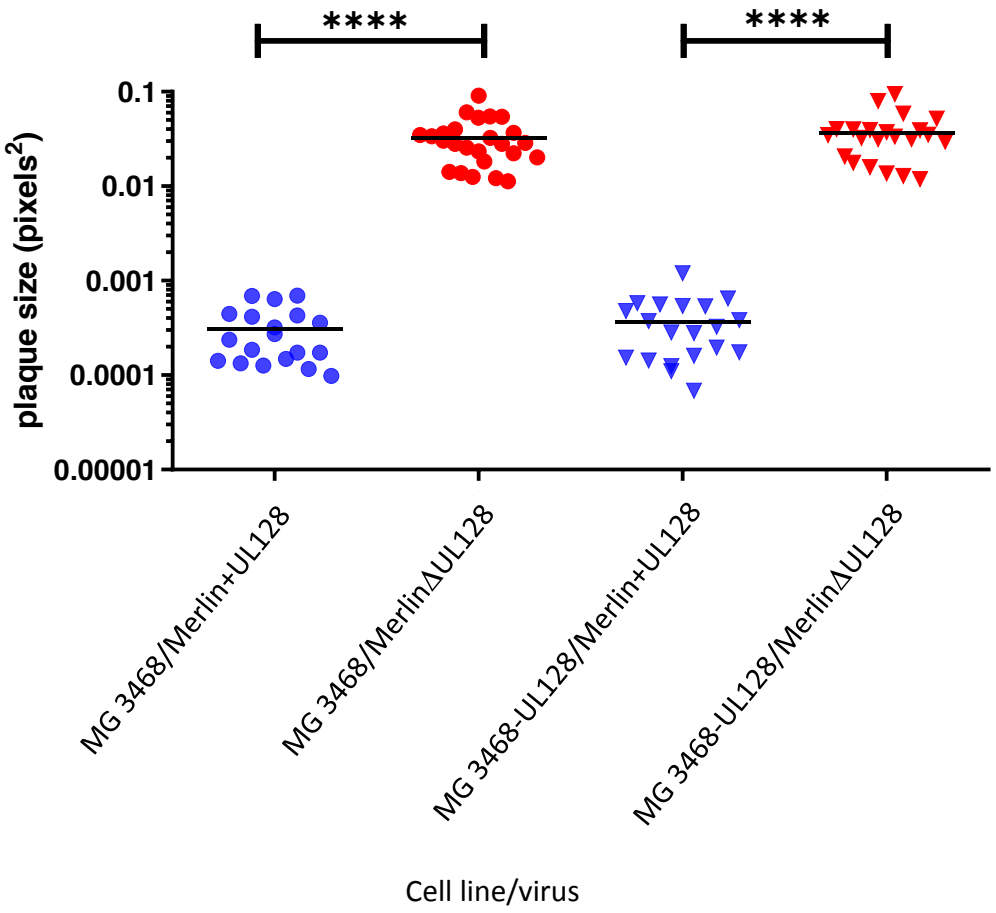

Figure 31. UL128 transduced MG 3468 fibroblasts do not *trans*-complement ΔUL128 HCMV

Parental (circle) and transduced (triangle) cells were infected with either +UL128 (blue) or ΔUL128 (red) HCMV. Plaque sizes were measured 14 days post infection. Each data point represents a single measurement. Representative data from three independent experiments. Statistics performed with two-tailed unpaired T test.
ns, P≤0.05: **, P≤0.01: ***, P≤0.001: ****, P≤0.0001

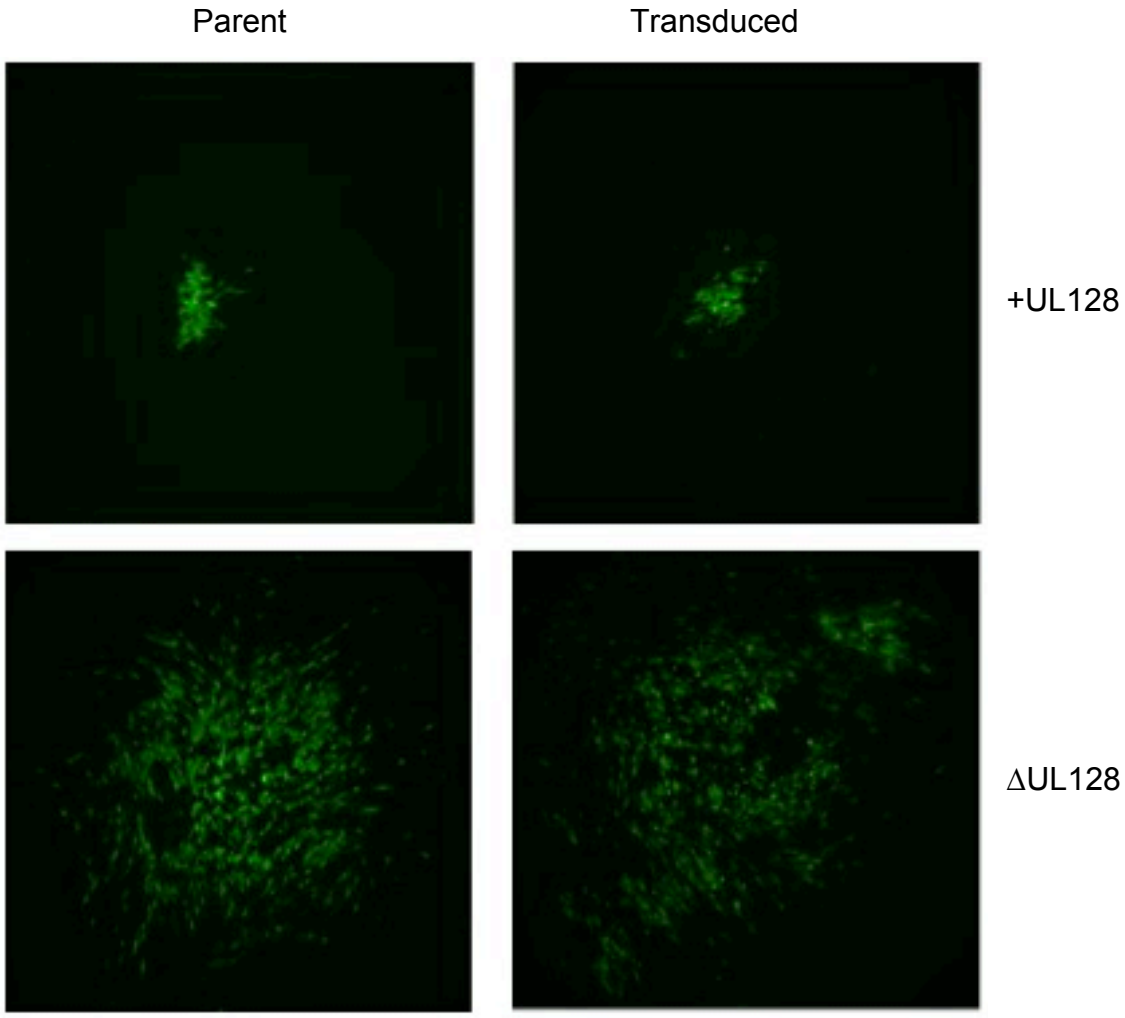

Figure 32. Comparison of plaque size formation on parental and UL128 transduced HF-Tert fibroblasts infected with HCMV containing (+) or lacking (Δ) UL128

Representative fluorescence images of parental and transduced HF-Tert cells infected with or without HCMV containing UL128 at 14 days post infection.

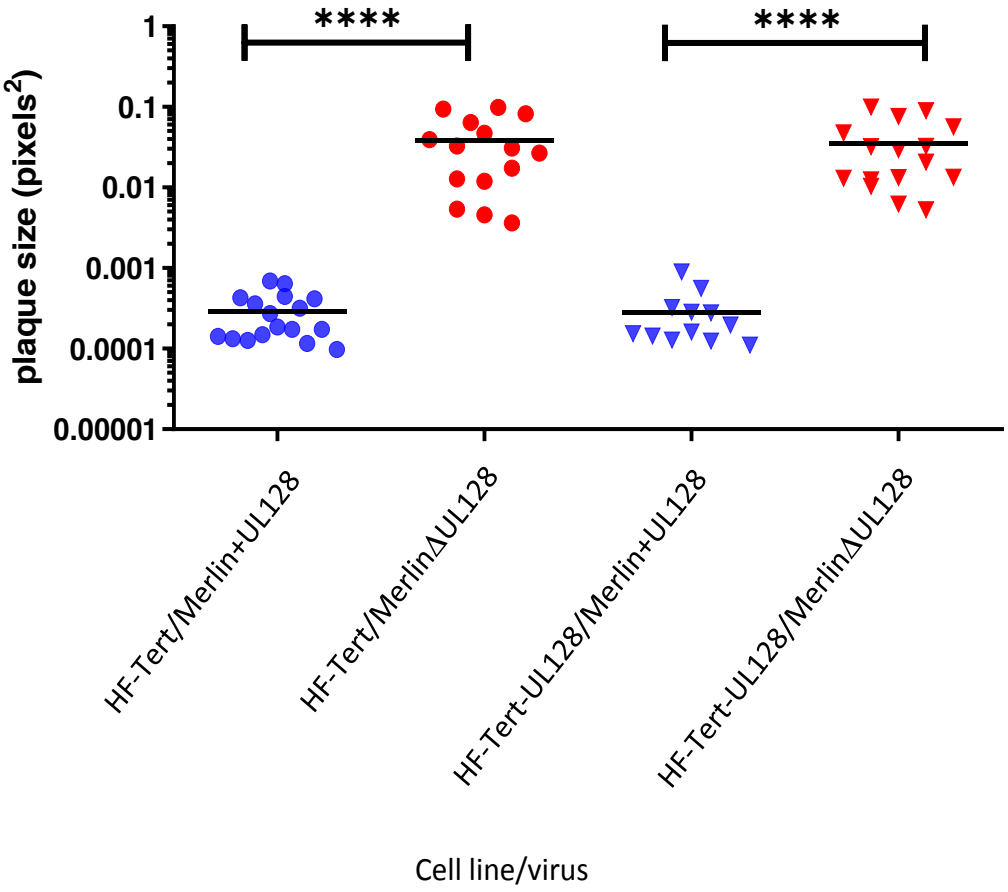

Figure 33. UL128 transduced HF-Tert fibroblasts do not *trans*-complement ΔUL128 HCMV

Parental (circle) and transduced (triangle) cells were infected with either +UL128 (blue) or ΔUL128 (red) HCMV. Plaque sizes were measured 14 days post infection. Each data point represents a single measurement. Representative data from three independent experiments. Statistics performed with two-tailed unpaired T test.
ns, P≤0.05: **, P≤0.01: ***, P≤0.001: ****, P≤0.0001

Figure 34. Immunoblot showing UL128 expression

Lanes: 1-6. Time-course of HF-Tert cells infected with wild-type Merlin at an MOI of 5. A; transduced MG 3468 cells, B; MG 3468 cells, C; transduced HF-Tert cells, D; HF-Tert cells. Actin served as a loading control. All samples were prepared in reducing sample buffer.

5.7 V5-tagged UL128 lentiviral vector

The lentiviral construct (Lenti-V5-UL128) obtained from the Weekes laboratory was confirmed to contain full length UL128 that matched the Uniprot annotation for the HCMV Merlin strain.

Hereditary features of the pHAGE vector that were exploited during the procedure included the wood chuck hepatitis virus post-transcriptional regulatory unit (WPRE) and central polypurine tract (cPPT) promoters which had previously been demonstrated to increase gene expression levels in transduced cells (333), a spleen focus-forming virus (SFFV) promoter shown to drive high expression of the transgene of interest (334) and a puromycin resistance gene for the selection of stable UL128 expressing cells after transduction.

Lenti-V5-UL128 DNA was shipped as an absorbed construct on filter paper, and following recovery in ddH_2O, was subject to transformation. Single colonies were selected and grown in preparation for large-scale (maxi) preparation.

5.8 Production and validation of lentiviruses

To produce lentiviral particles, the human cell line, 293T, was subject to polyamine-based transfection (see 2.4.14.1) with the V5-tagged UL128 lentiviral vector. As the vector lacked a reporter gene, transfection efficiency was measured by transfecting a GFP expressing plasmid as a vector substitute into the packaging cell line. 70% transfection efficiency was observed at 72h.p.i. (data not shown), validating transfection.

UL128 lentiviral gene transfer into target MG 3468 and HF-Tert cells using retronectin® reagent was performed as formerly described (see 2.5.15.2). Cells cultured in media containing puromycin promoted the elimination of non-transduced cells. Expansion of surviving cell populations in selection media

signified successful lentiviral integration by the MG 3468 and HF-Tert fibroblast cell lines.

5.9 Lentiviral mediated UL128 gene transfer into fibroblasts generates a UL128 expressing cell line.

Owing to a lack of commercially available immunofluorescent UL128 antibodies, an immunofluorescent antibody directed against V5 was used to determine UL128 expression in the HF-Tert and MG 3468 fibroblast cell lines (Figure 35). Figure 35 indicates that the V5 staining pattern was reminiscent of the endoplasmic reticulum (ER).

To confirm UL128 expression, cell lysates from transduced and parental fibroblasts were produced, and UL128 protein levels measured using SDS-PAGE followed by western blot. Figure 36 confirms UL128 expression in both transformed cell lines.

As before (see 5.6), a plaque assay was performed to assess UL128 function in MG 3468 and HF-Tert cell lines (Figures 37 and 39 respectively). The assay was performed using RL13 null (Δ) viruses to eliminate the undesired influence of the gene on the experiment. Viruses containing or excluding UL128 were permitted to form plaques on parental and transduced MG 3468 or HF-Tert fibroblasts (Figures 37 and 39 respectively). Plaques were measured at 14 d.p.i (Figures 38 and 40). In the presence of UL128, obtained either from the virus or the transduced cell line, resultant plaque size should be significantly reduced when compared with a system lacking the gene.

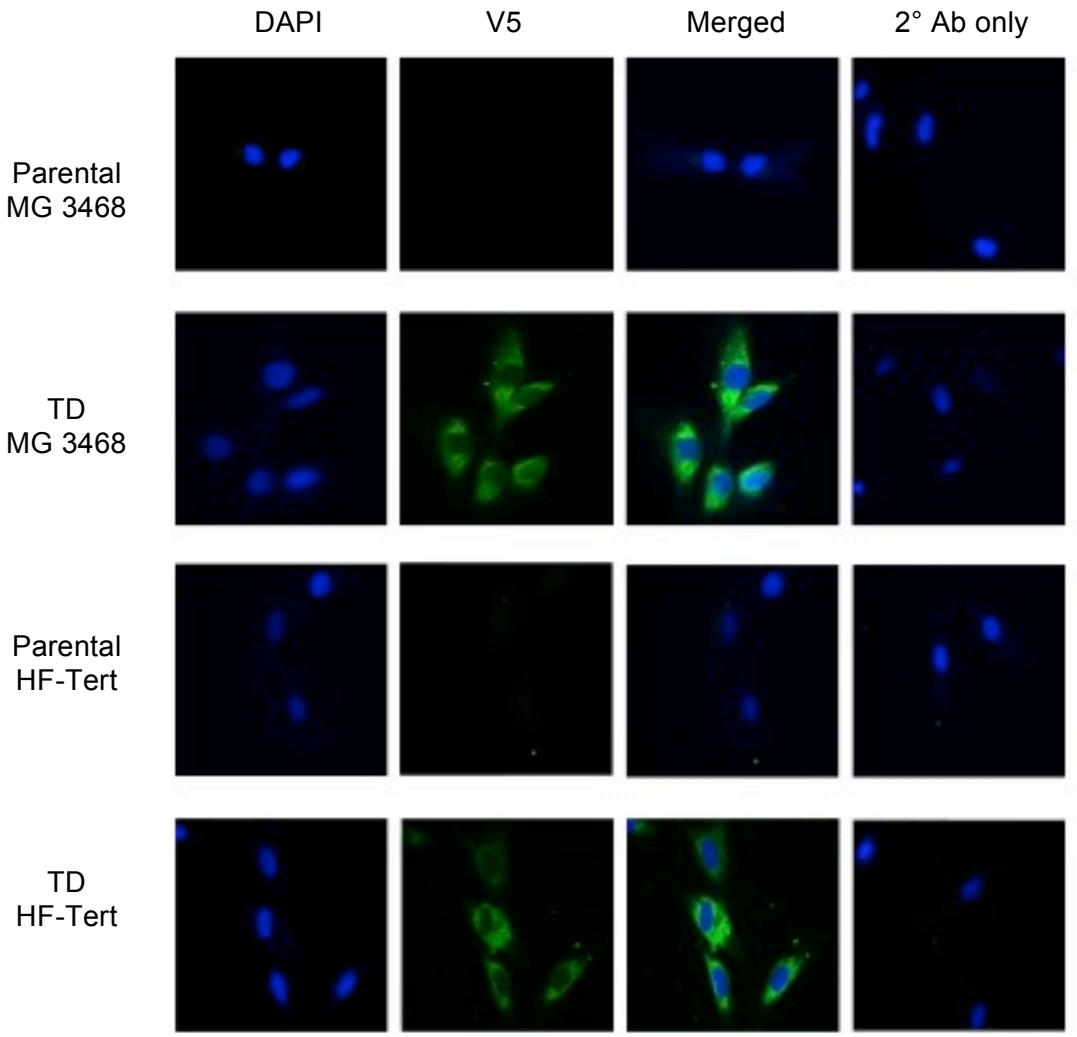

Figure 35. Immunofluorescent staining of parental and transduced (TD) MG 3468 or HF-Tert cells using Zeiss Axio Observer Z1 microscope

Immunofluorescent staining of V5 in parental and transduced MG 3468 or HF-Tert cells. Cells were labelled with a V5-specific monoclonal antibody, followed by Alex Fluor 488 secondary antibody (green). Nuclei were counterstained with 4–6-diamidino-2-phenylindole (DAPI) (blue). Representative images are shown.

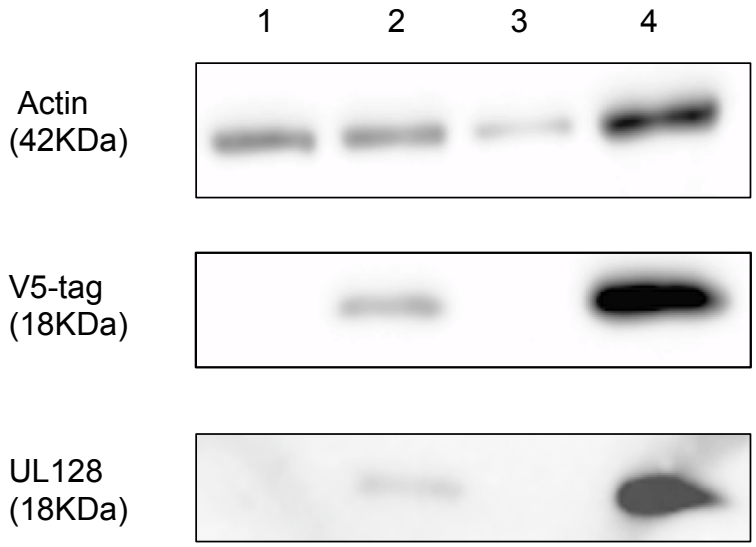

Figure 36. Immunoblot showing UL128 and V5 expression

Lane 1; MG 3468 cells, 2; Transduced MG 3468 cells, 3; HF-Tert cells. 4; Transduced HF-Tert cells. Actin served as a loading control. All samples were prepared in reducing sample buffer.

Representative images of HCMV plaque formation on parental and transduced fibroblasts in the presence (+) or absence (Δ) of viral UL128 is given in figures 37 (MG 3468) and 39 (HF-Tert), with quantification of multiple plaques given in figures 38 (MG 3468) and 40 (HF-Tert).

Plaque size in the transduced cells in the absence of viral UL128 was equivalent to that seen in both the parental and transduced cell lines in the presence of viral UL128, demonstrating both successful expression, and functional effects of the gene of interest in the transduced cell lines.

5.10 Fibroblasts containing lenti-V5-UL128 *trans*-complement UL128 deficient virus

In addition to affecting plaque size (see previous chapter), the loss of UL128 in a proportion of our Merlin derived HCMV stocks impacts their ability to infect a natural range of host cell types *in vitro,* including endothelial and epithelial cells, dendritic cells and macrophages (5, 228). To determine whether the lenti-V5-UL128 transduced fibroblasts were capable of *trans*-complementing the tropism of the UL128 deficient viral stocks held by the laboratory, a functional assay was performed. Since expression of UL128 also restricts release of cell-free virus, but promotes cell-cell transfer, virus infection was measured by co-culture. Co-cultures were performed using adherent epithelial (RPE-1, ARPE-19) or non-adherent dendritic cell (DC) targets to reflect the differing cell types the virus would naturally encounter during infection.

The exact role of RL13 in HCMV has yet to be determined, but as the presence of either RL13 or UL128 changes the viral plaque phenotype of the virus and results in a cell-to-cell rather than a cell-free disseminating strategy (228), co-culture experiments were performed with RL13 null (Δ) viruses to exclude the unwanted influence of the gene on the experiment. All viruses

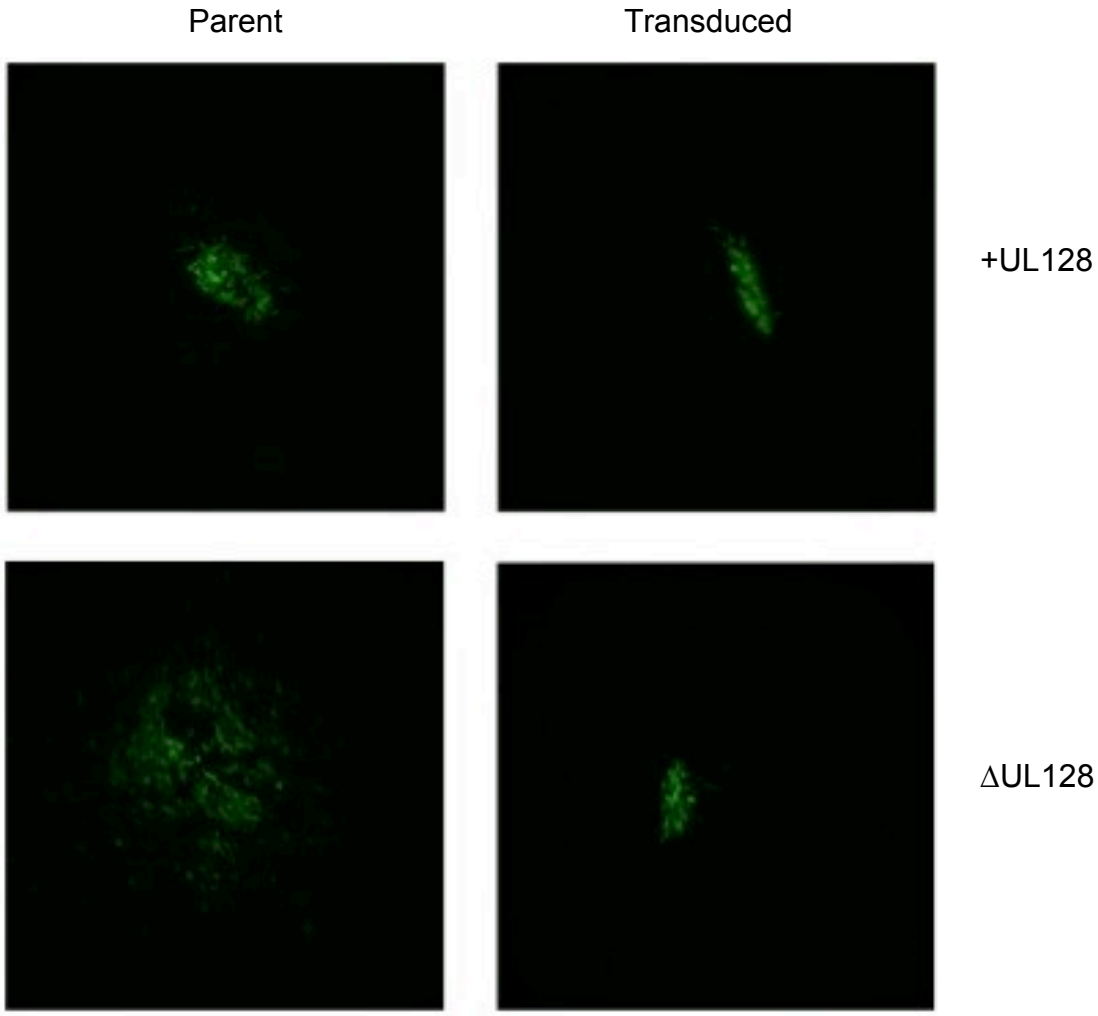

Figure 37. Comparsion of HCMV plaque size formation on parental (MG 3468) and UL128 transduced (MG 3468-UL128) fibroblasts infected with HCMV containing (+) or lacking (Δ) UL128

Representative fluorescence images of parental (MG 3468) and transduced MG 3468-UL128) cells infected with or without HCMV containing UL128 at 14 days post infection.

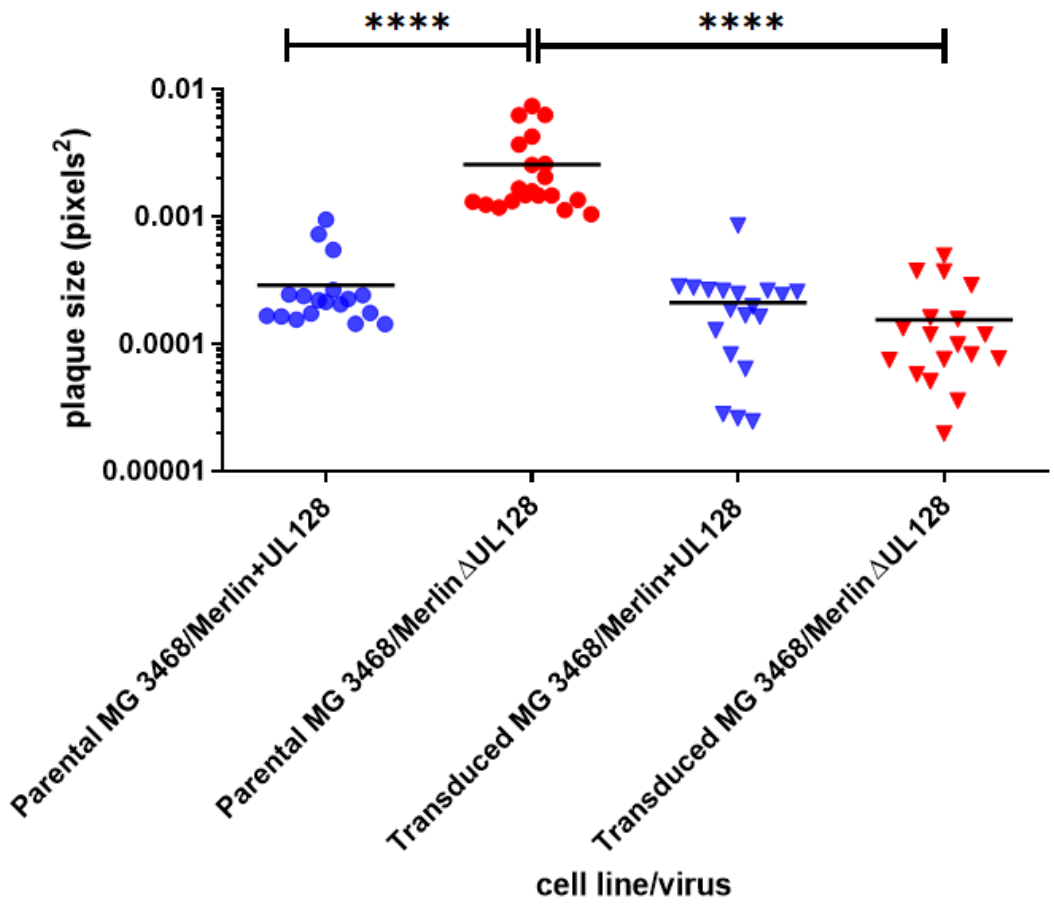

Figure 38. Transduced MG 3468 fibroblasts give rise to small plaque phenotype in the absence of viral UL128

Parental (MG 3468) or UL128 transduced (MG 3468-UL128) fibroblasts were infected with either +UL128 or ΔUL128 virus, and plaque sizes measured 14 days post infection. Each data point represents a single measurement. Representative data from three independent experiments. Statistics performed with two-tailed unpaired T test.
ns, P≤0.05: **, P≤0.01: ***, P≤0.001: ****, P≤0.0001

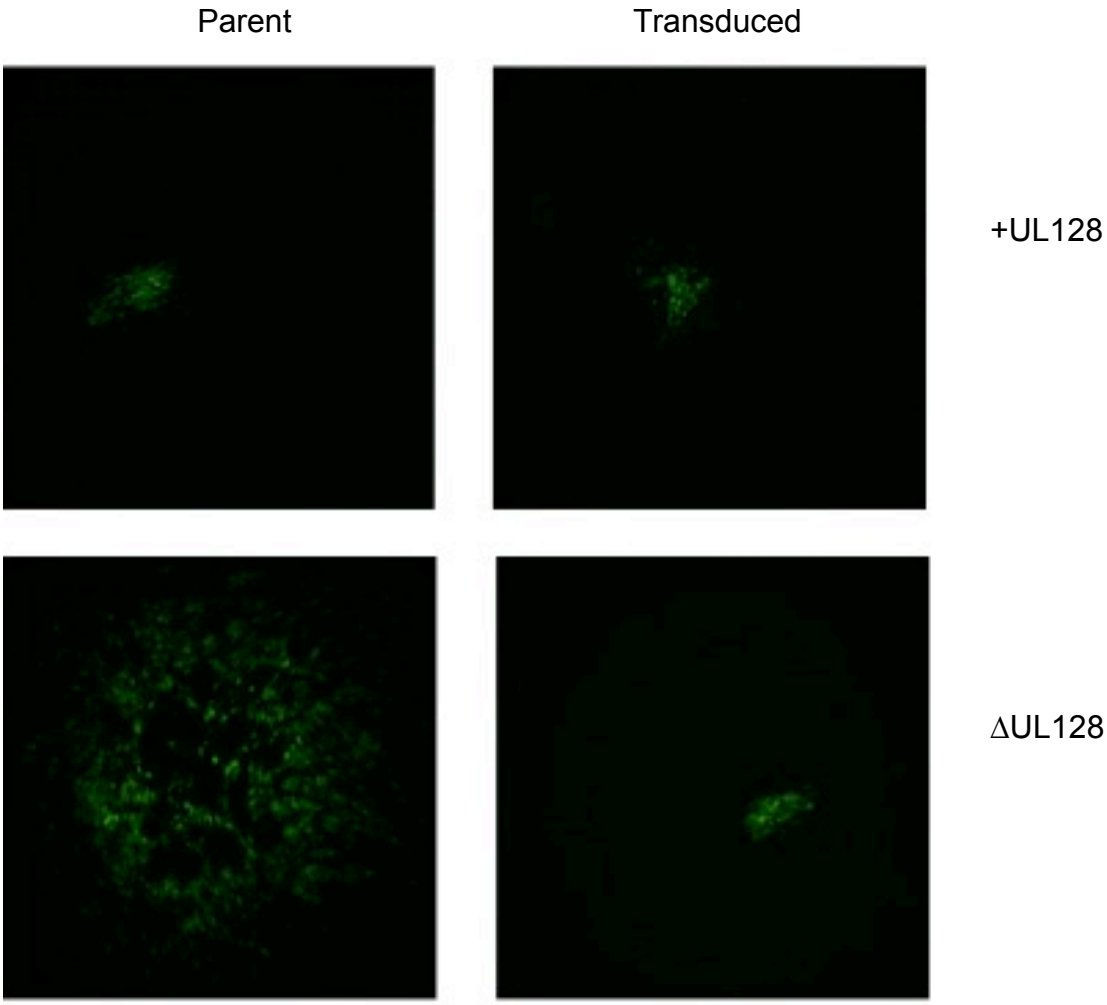

Figure 39. Comparison of plaque size formation on parental (HF-Tert) and UL128 transduced (HF-Tert-UL128) fibroblasts infected with HCMV containing (+) or lacking (Δ) UL128

Representative fluorescence images of parental (HF-Tert) and transduced (HF-Tert-UL128) cells infected with or without HCMV containing UL128 at 14 days post infection.

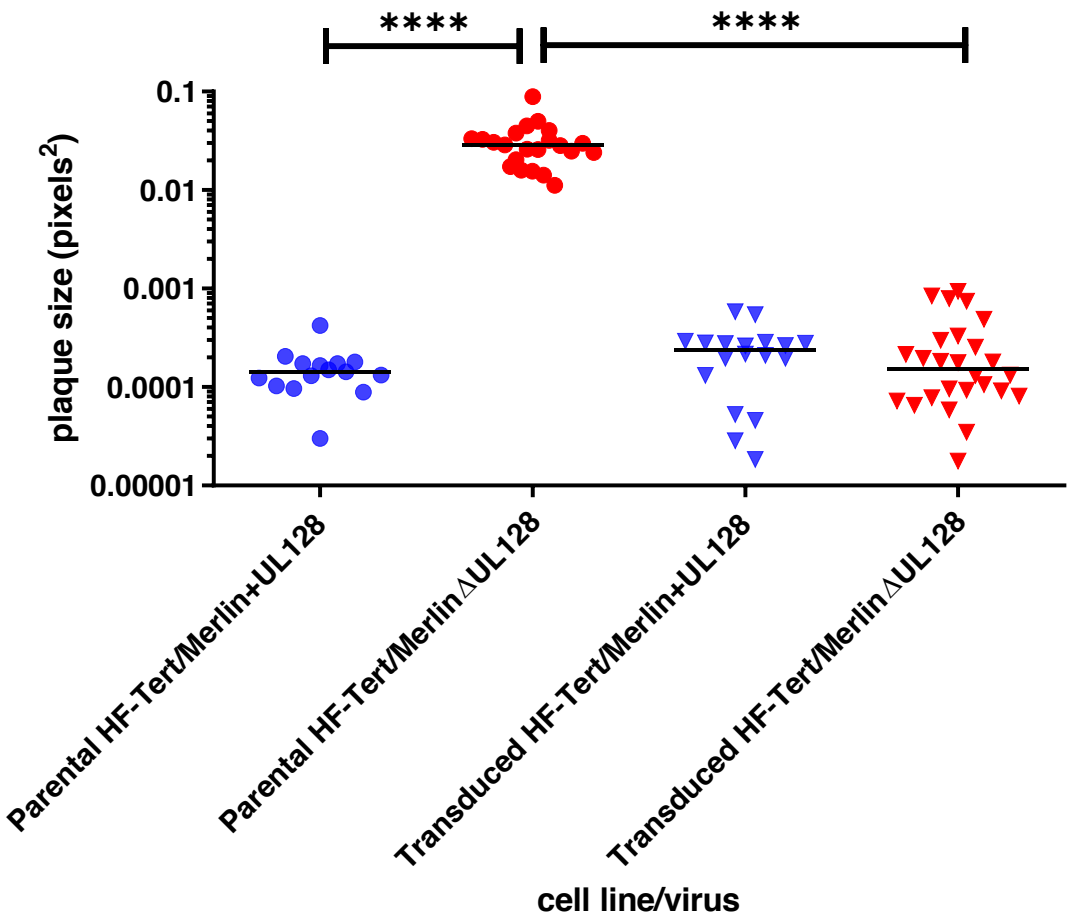

Figure 40. Transduced HF-Tert fibroblasts give rise to small plaque phenotype in the absence of viral UL128

Parental (HF-Tert) or UL128 (HF-Tert-UL128) transduced fibroblasts were infected with either +UL128 or ΔUL128 virus, and plaque sizes measured 14 days post infection. Each data point represents a single measurement. Representative data from three independent experiments. Statistics performed with two-tailed unpaired T test.
ns, P≤0.05: **, P≤0.01: ***, P≤0.001: ****, P≤0.0001

used contained a UL36-P2A-GFP fusion, allowing infection to be tracked by flow cytometry. Fibroblasts were DDAO stained prior to co-culture to distinguish previously infected from newly infected 'target' cells.

+ or Δ UL128 HCMV infected parental and transduced MG 3468 or HF-Tert cells were co-cultured 3:1 with either uninfected ARPE-19, RPE-1 or DCs. Cells were harvested 24 hours post co-incubation and the percentage infection rate of the target cells determined.

As expected, co-culture of parental ΔUL128 HCMV infected fibroblasts with DCs resulted in no DC infection, confirming the role of UL128 in DC viral entry (Figures 41a and b). However, approximately 20% of the DC population contained a GFP signal following co-culture with ΔUL128 virus that was transferred from UL128 expressing fibroblasts, demonstrating that both the transduced MG 3468 and HF-Tert cell lines were capable of *trans*-complementing the UL128 deficient viruses held by the laboratory. Importantly, the level of DC infection achieved through *trans*-complementation (i.e. using virus lacking functional UL128) was equivalent to that seen with virus expressing functional UL128, proving the infection efficiency of the transduced cell lines.

Rather surprisingly however, co-culture of the infected parental cell lines with ARPE-19 or RPE-1 cells (Figures 42a and b) resulted in infection of epithelial cells even in the absence of functional UL128 (i.e. when both virus and cells lacked UL128), which contradicts current dogma on viral cell entry into epithelial cells (see 1.6.3.1-4). Only minor differences were observed in infection efficiency of the two viruses, and these effects were inconsistent between the cell lines used. The strain TB40 has been widely used in these studies, and contains a mutation in UL141 that impacts expression. In contrast, Merlin expresses functional UL141. In ongoing work (not shown), we have found that UL141 is a component of the virion envelope. We therefore investigated whether the presence of UL141 could explain the differing results between the literature, and our data.

41a)

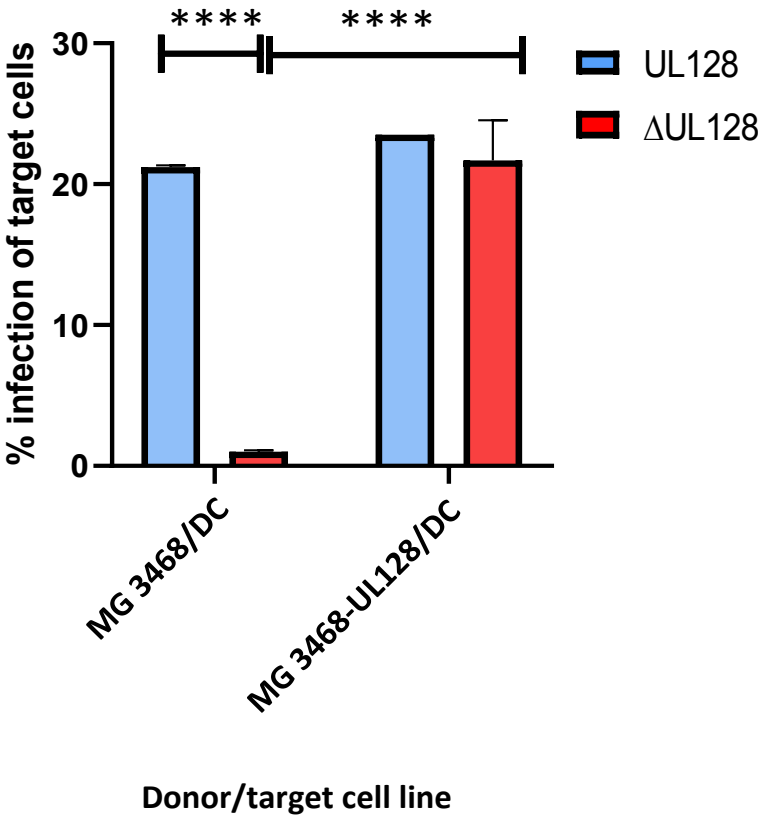
****
****
30
20
10
0
% infection of target cells
UL128
ΔUL128
MG 3468/DC
MG 3468-UL128/DC
Donor/target cell line

41b)

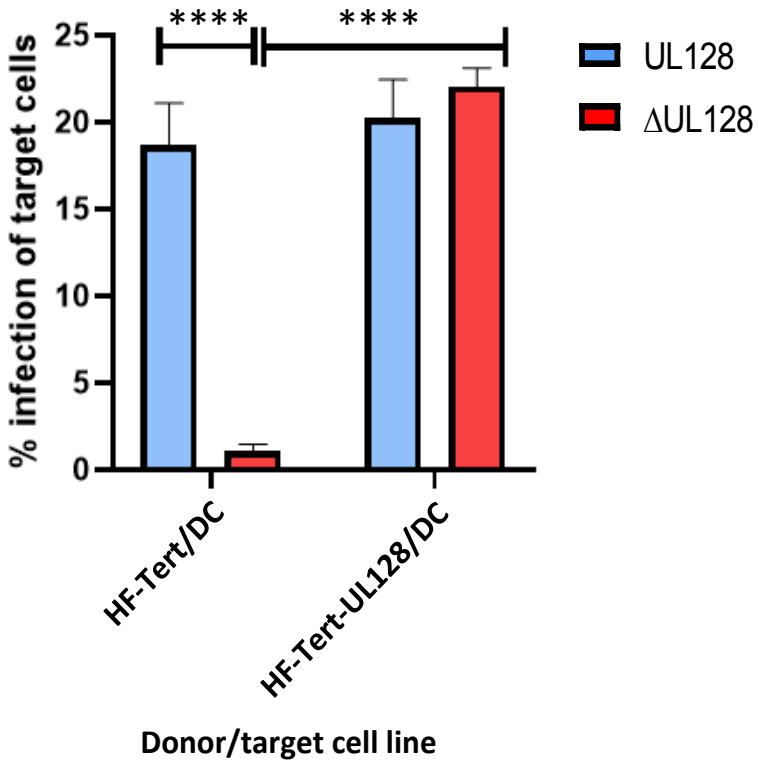
****
****
25
20
15
10
5
0
% infection of target cells
UL128
ΔUL128
HF-Tert/DC
HF-Tert-UL128/DC
Donor/target cell line

Figure 41. Transduced MG 3468 and HF-Tert cell lines are capable of *trans*-complementing UL128 deficient HCMV in DCs

Parental or UL128 transduced MG 3468 (a) or HF-Tert (b) cells were infected with either +UL128 or ΔUL128 GFP virus at an MOI of 10 for 72 hours. Fibroblasts were DDAO stained prior to co-culture with DCs. Cells were harvested 24 hours post co-culture and the percentage infection of target cells determined by flow cytometry. Cells were gated on LIVE/DEAD stain, followed by DDAO stain and GFP signal.
Representative data from five independent experiments. Statistics performed with two-way ANOVA with Tukey's multiple comparison test.
ns, P≤0.05: **, P≤0.01: ***, P≤0.001: ****, P≤0.0001

42a)

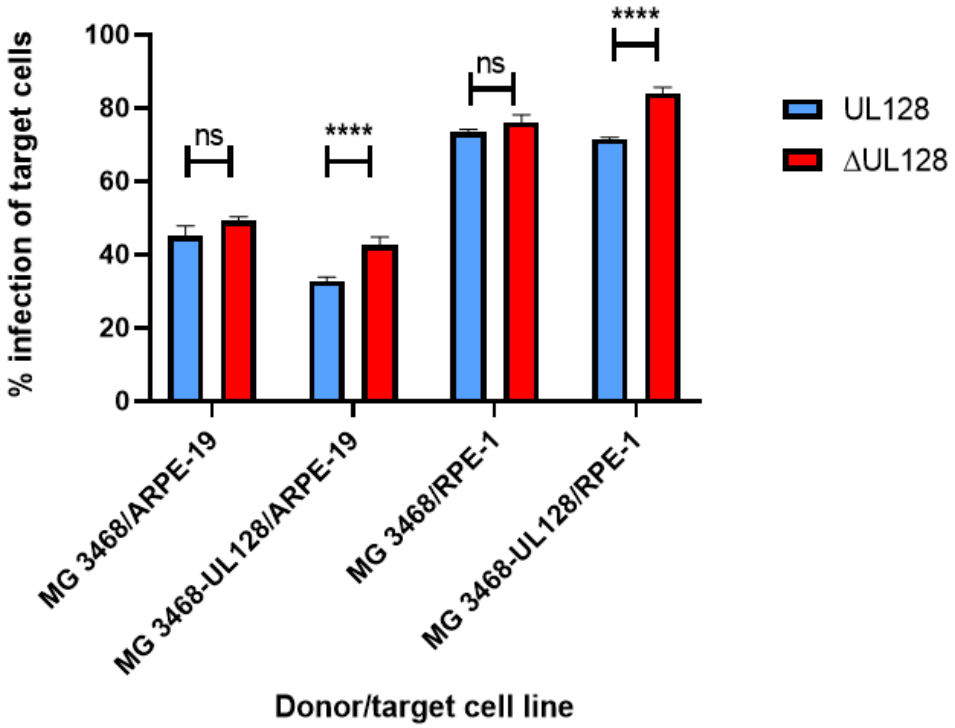
% infection of target cells
100
80
60
40
20
0
ns
****
ns
****
UL128
ΔUL128
MG 3468/ARPE-19
MG 3468-UL128/ARPE-19
MG 3468/RPE-1
MG 3468-UL128/RPE-1
Donor/target cell line

42b)

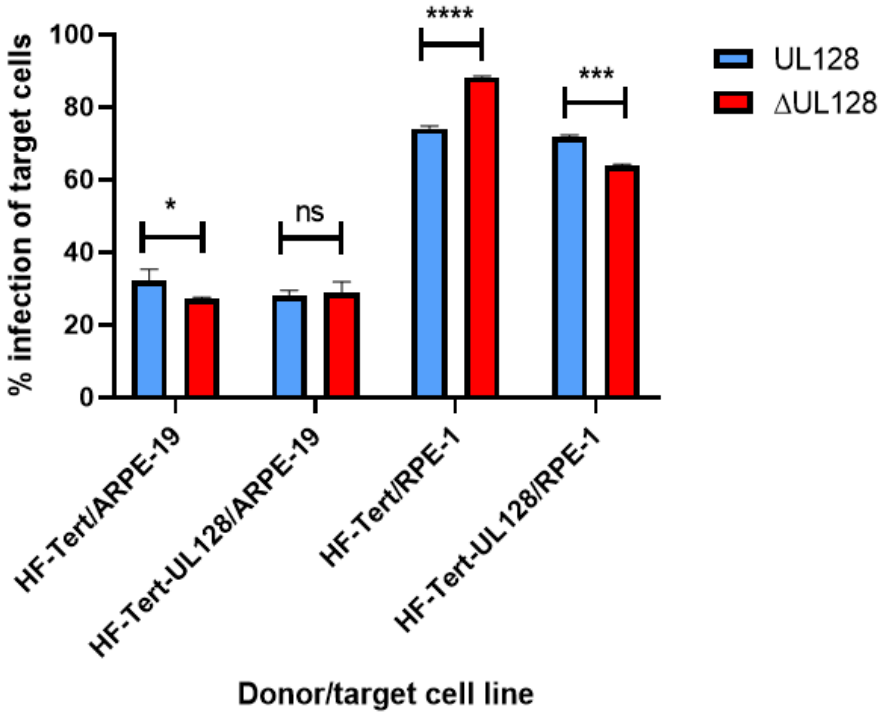
% infection of target cells
100
80
60
40
20
0
*
ns
****
***
UL128
ΔUL128
HF-Tert/ARPE-19
HF-Tert-UL128/ARPE-19
HF-Tert/RPE-1
HF-Tert-UL128/RPE-1
Donor/target cell line

Figure 42. Transduced MG 3468 and HF-Tert cell lines are not required for *trans*-complementation of UL128 deficient HCMV in epithelial cells.

Parental or UL128 transduced MG 3468 (a) or HF-Tert (b) cells were infected with either +UL128 or ΔUL128 GFP virus at an MOI of 10 for 72 hours. Fibroblasts were DDAO stained prior to co-culture with ARPE-19 or RPE-1. Cells were harvested 24 hours post co-culture and the percentage infection of target cells determined by flow cytometry. Cells were gated on LIVE/DEAD stain, followed by DDAO stain and GFP signal.
Representative data from five independent experiments. Statistics performed with two-way ANOVA with Tukey's multiple comparison test.
ns, P≤0.05: **, P≤0.01: ***, P≤0.001: ****, P≤0.0001

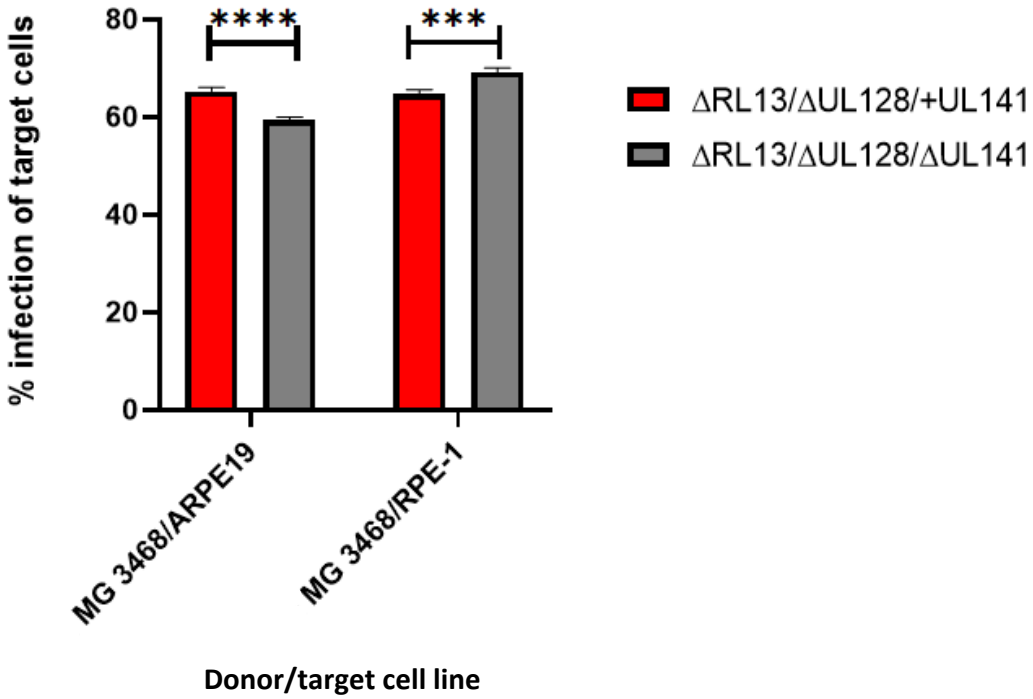

Figure 43. UL141 is not required for epithelial cell entry in the absence of viral UL128

MG 3468 cells were infected with either double (ΔRL13/ΔUL128/+UL141) or triple (ΔRL13/ΔUL128/ΔUL141) mutant GFP virus at an MOI of 10 for 72 hours. Fibroblasts were DDAO stained prior to co-culture with ARPE-19 or RPE-1. Cells were harvested 24 hours post co-culture and the percentage infection of target cells determined by flow cytometry. Cells were gated on LIVE/DEAD stain, followed by DDAO stain and GFP signal. Representative data from three independent experiments. Statistics performed with two-way ANOVA with Tukey's multiple comparison test. ns, P≤0.05: **, P≤0.01: ***, P≤0.001: ****, P≤0.0001

UL141 was deleted from the ΔRL13/ΔUL128 virus (see 2.4.4) using en passant mutagenesis (247), and tested against the parental virus (ΔRL13/ΔUL128/+UL141) in a co-culture assay. Only minor differences were observed in infection efficiency of the two viruses, and these effects were inconsistent between the two cell lines. We therefore concluded that UL141 does not promote epithelial cell entry in the absence of UL128 (Figure 43).

In addition to using a different strain (TB40) to our work, previous work has used cell-free virus, rather than virus transfer by co-culture. To enable a direct comparison with the literature, ARPE-19 and RPE-1 cells were incubated with cell-free virus containing or lacking UL128. Fluorescent images taken 14 d.p.i (Figure 44) clearly show that even in the absence of functioning UL128, both ARPE-19 and RPE-1 cells become infected. However, quantification by flow cytometry (Figures 45 a and b) revealed that in the presence of UL128, a much greater number of RPE-1 cells were infected at 24 h.p.i in comparison to virus lacking UL128. The same was also true in ARPE-19 cells, although the overall level of infectivity was slightly lower.

The difference in infectivity between RPE1 and ARPE19 is likely because serum free media was used to infect the RPE-1/HF-Tert cell lines, while complete media was used for the ARPE-19/HFFFs, and thus the uninfected ARPE19 may have proliferated more, thus reducing the percentage of infected cells. Nevertheless, the important point is that, in agreement with the literature, the pentamer is important for the efficiency of cell-free infection of epithelial cells. The lack of a requirement for pentamer in previous experiments was due to the cell-cell method of infection.

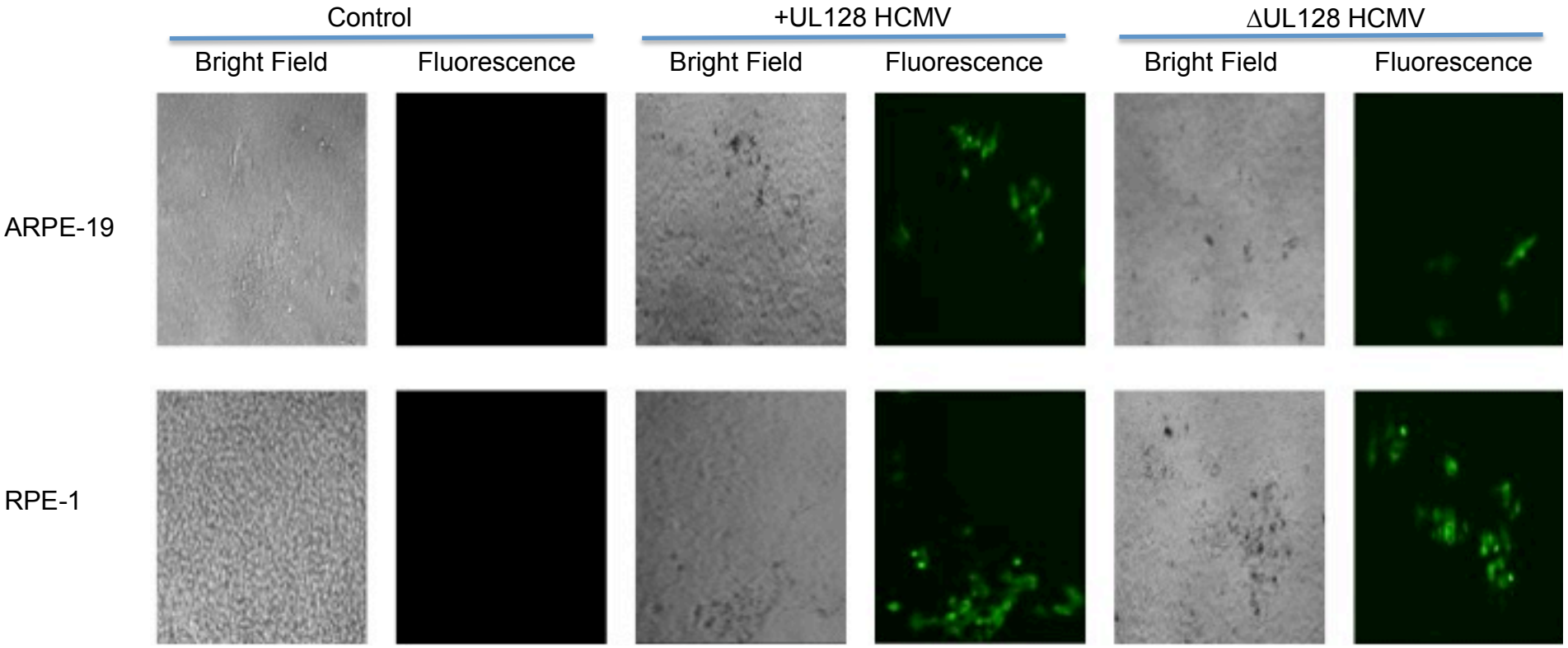

Figure 44. Fluorescent and bright field images of ARPE-19 and RPE-1 cells directly infected with (+) or without (Δ) UL128 IE2-P2A-GFP HCMV

Representative images of ARPE-19 and RPE-1 cells infected with or without HCMV containing UL128 at 14 days post infection.

45a

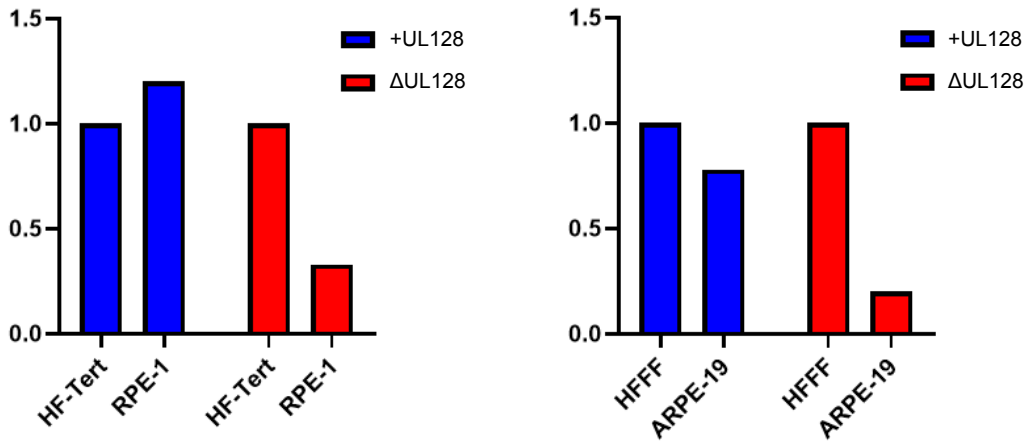

45b

HF-Tert	RPE-1
1	1.2

HFFF	ARPE-19
1	0.78

Figure 45. Level of cell-free HCMV infection in epithelial cells in relation to fibroblast controls

Cells infected with HCMV at an MOI of 1 containing (+) or lacking (Δ) UL128. Cells were harvested 24 hours post infection with the levels of infection in control and target cells determined by flow cytometry.
a) Levels of infection in epithelial cells normalized to fibroblast controls. b) Levels of infection in epithelial cells (with HCMV +UL128), are quoted as a ratio relative to fibroblast controls.

5.11 Chapter discussion

The use of *trans*-complementation to restore a lost phenotype or characteristic is not new. Influenza A, human immunodeficiency virus (HIV) and HCMV viral studies have all shown that viruses lacking functional wild-type genes can have their function re-instated by the introduction of exogenous DNA into the host cell line (161, 335-7). Viral tropism (161, 335-6) and replication (337) have previously been rescued by this technology in these viruses.

The rationale for transducing fibroblasts rather than epithelial or dendritic cells directly was due to the inability of HCMV lacking the pentamer (i.e. the majority of our existing viruses) to infect all cell types apart from fibroblasts. UL128, UL130 and UL131A are all required to bind simultaneously to gH/gL in order for a functional pentameric complex to form (175). The objective of this chapter therefore, was to generate a UL128 expressing fibroblast cell line capable of *trans*-complementing the UL128 mutated viruses held by our laboratory, thus allowing their transfer to additional cell types. This aim was achieved as confirmed by DC co-culture assay (Figures 41a, b).

In keeping with the Hahn paper (161), a retroviral based gene carrier was initially chosen to transduce UL128 into the MG 3468 and HF-Tert fibroblast cell lines. The pMXs-IP retroviral vector was chosen due to its proven ability to transfect and transduce fibroblasts by our laboratory (228).

The data presented in figures 30-34 clearly demonstrate that the transduced cell lines did not *trans*-complement the mutated virus used in the plaque assay, as large viral plaques (resembling virus lacking UL128) were observed. Due to a lack of commercial UL128 antibodies, further examination of UL128 expression levels by more sensitive methodologies such as immunofluorescence was not possible. To determine whether any degree of expression was achieved, reverse-transcriptase quantitative polymerase chain reaction (RT-QPCR) could

be performed. The choice of promoter to drive expression of the gene of interest is critical and the retroviral LTR used to drive the transgene of interest in this vector may have been too weak, contributing to low levels of gene expression in the fibroblasts.

Having been unsuccessful in generating a functional UL128 cell line using the pMXs-IP retroviral vector, I was fortunate to receive a pHAGE lentiviral vector containing a V5-tagged UL128 (Lenti-V5-UL128) from our collaborator, Dr Michael Weekes (Cambridge University) that utilized the SFFV promoter to drive expression of the transgene of interest. Having confirmed lentiviral transduction into MG 3468 and HF-Tert cells through immunofluorescence (Figure 35) and western blotting (Figure 36), plaque assay validated the function of the transgene of interest (Figures 37-40).

To elucidate whether the lenti-V5-UL128 transduced fibroblasts were capable of *trans*-complementing the ΔUL128 viral stocks held by the laboratory, a co-culture assay was performed. Co-cultures consisted of adherent epithelial (RPE-1, ARPE-19) or non-adherent dendritic cell (DC) targets to mirror the contrasting cell types the virus would naturally encounter during infection, and that are dependent on a functioning pentameric complex.

DCs are professional antigen presenting cells (APCs) found in peripheral tissues that are actively recruited to sites of mucosal inflammation such as the inner lining of the nose, lungs, stomach and intestine (338-9). They are believed to be one of the first cells of the immune system to come into contact with HCMV during infection (340). It is worth noting that the DCs used in this study were peripheral blood monocyte derived, and as such, resemble inflammatory or TNFα- and iNOS-producing (Tip) DCs (243-4). These are a DC sub-population ordinarily produced during human infection and inflammation, and are a sub-type that is likely encountered by the virus *in vivo*. Monocyte derived DCs (moDCs), following 7 days culture with GM-CSF and IL-4, are widely used in research (343-

4) and gives rise to a large populationof uniform, well characterized cells (345-7). Inflammatory DCs can be identified by a variety of cell expression markers, including CCR2, DC-SIGN (CD209), CD64 and Ly6C in a variety of settings (347). For the purpose of testing the restoration of HCMV tropism, the moDCs isolated in the laboratory were deemed suitable target cells to infect as they displayed the characteristic DC phenotype; CD14 low, CDa1 low, DC-SIGN high (see Figure 6). Importantly for this work, moDCs are fully permissive to HCMV infection (340), making them an ideal DC sub-population to work with *in vitro*.

Trans-complementation of UL128 restored viral tropism for DCs, with infection levels equivalent to that seen when UL128 is expressed from the viral genome, highlighting the efficiency of the process (Figures 41a, b).

In contrast to the freshly isolated DCs, ARPE-19 and RPE-1 are established cell lines that can be sub-cultured for prolonged periods of time. Both are extensively used in research as they have well defined, uniform cell characteristics, although this uniformity may be due to a loss of features as a result of prolonged culturing *in vitro* (348). They have been shown to express some RPE phenotypes found *in vivo*, including RPE-65 (ARPE-19) (349) and cellular retinaldehyde-binding protein (CRALBP) on their cell surfaces (349-51). The precise characteristics of the cell, however, depend on the duration and exact manner that the cells are maintained in culture. (350-1). Nevertheless, APRE-19 and RPE-1 cells were deemed appropriate epithelial cell viral targets to test the recovery of HCMV tropism in ∆UL128 HCMV, due to their well characterized use in the literature.

Surprisingly, epithelial co-culture assays revealed that both target cell types tested were permissive to HCMV infection following co-culture with ∆UL128 HCMV infected fibroblasts (Figure 42a, b). This was an unexpected result given that several groups have demonstrated the necessity of the UL128L in forming the pentameric entry complex required for epithelial cell infection (161, 175, 353-5). A possible reason for successful cell-associated viral entry in the absence of

a functioning pentamer may be due to an as yet undiscovered entry mechanism/complex. Given indirect evidence previously generated by our laboratory, we investigated whether UL141 promoted such an entry mechanism. However co-culture assays revealed that UL141 was not required for epithelial cell entry in the absence of UL128 in the target cells (Figure 43).

Alternatively, an alteration in epithelial cell characteristics as a result of the culturing methods utilized, or the use of cell-cell infection, may have resulted in differences from the literature. This was addressed by directly comparing cell-cell and cell-free infection using viruses lacking or containing UL128 (Figures 42, 44 and 45). Cell-free infection recapitulated previous literature (i.e. UL128 was important for infection of epithelial cells), while cell-cell infection did not (i.e. UL128 was not important for infection). Thus cell-cell infection may have different requirements for entry, and potentially may be able to enter via a novel epithelial specific entry complex. Alternatively, entry may still be mediated by the gH/gL/gO complex binding to PDGFRα, as PDGFRα is present on ARPE-19 cells, albeit at very low levels (356). The presence of PDGFRα on RPE-1 cells has yet to be determined, but it is possible that the higher rates of infection observed in these cells may equate to higher PDGFRα expression levels on the RPE-1 cell surface. If this is the case, it appears that virus spread by co-culture is much less dependent on high levels of PDGFRα, since cell-free entry of ΔUL128 virus into ARPE-19 and RPE-1 was relatively poor, yet this same virus infected both RPE-1 and ARPE19 very efficiently during co-culture experiments.

Over the past two decades, our laboratory has generated over 200 cytomegaloviruses based on the strain Merlin. Like nearly all other laboratory-adapted strains, our isolates lack UL128 as a result of *in vitro* passaging on fibroblasts, resulting in a loss of tropism for multiple cell types. Interrogation of HCMV infection is therefore limited to this cell type.

Having successfully generated two UL128 expressing fibroblast cell lines capable of *trans*-complementing our ΔUL128 deficient viral library (figures 40a, b), our

existing viral stocks can infect these cells, rescuing the ability of the virus to infect its natural range of host cell types including DCs, endothelial and epithelial cells for a single cycle. This technology will therefore dramatically increase the group's ability to interrogate HCMV pathogenesis in a variety of cell types, using our existing viruses.

The objective of generating a UL128 expressing cell line capable of *trans*-complementing our existing UL128 deficient viral stocks was achieved in this chapter.

Chapter 6 – General discussion

Human cytomegalovirus is an important human pathogen that presents a major health risk to immunocompromised individuals and neonates. Each year, over a thousand babies are born with lifelong disability as a result of congenital HCMV infection in the UK, costing the NHS, social services and educational services over £300m per annum (357). Antivirals for the control of the virus in immunologically weakened individuals exist, but their effectiveness are limited by toxicity and drug resistance. It is their toxicity that prevents their use in congenital HCMV infections, leaving neonates with no protection against the virus. New, less harmful antivirals are therefore required. Despite its inclusion as a high priority target for vaccine development by the U.S Institute of Medicine in 2000 (358), no licenced vaccine currently exists, although a number of candidates are currently under investigation.

To evaluate the effectiveness of emerging therapeutics, it is desirable to work with a genetically intact virus *in vitro* that resembles the agent found *in vivo.*

What is a genetically intact cytomegalovirus?

'Genetically intact' or 'wild-type' are terms given to viruses that occur naturally within a population and are free from *in vitro* acquired mutations. Circulating HCMV can develop mutations as a result of sustained therapeutic use, but these viruses do not seem to transmit efficiently between individuals, are therefore may not be considered wild-type. In contrast, circulating strains do not necessarily contain the complete complement of viral genes, with up to 77% of strains containing a mutation that disrupts at least one viral gene (149, 359) – since these are circulating and transmitting between people, they may be termed 'wild-type' despite containing mutations. In addition, large-scale sequence analysis by Renzette *et al,* Sijmons *et al,* and more recently*,* Suárez *et al,* has revealed high levels of inter and intra-host genetic diversity within circulating HCMV (149-50, 359), potentially due to evolutionary selection pressures and natural selection (see 1.4.2) (139, 361-2), or superinfection and within host recombination (359-

61). Essential genes, such as those associated with replication are broadly conserved, while those associated with cellular tropism or viral escape from antibody neutralisation, are highly variable (149-50). HCMV should therefore be regarded as a heterogeneous population of related genomes.

The work presented in this thesis has focused on generating cell lines that enable our laboratory to work with a HCMV genotype that resembles one example of a clinical agent, expressing the complete repertoire of viral genes, free from *in vitro* acquired mutations.

Mutations rapidly arise in the HCMV RL13 and UL128L gene regions following *in vitro* propagation, leading to enhanced viral growth kinetics and altered cellular tropism respectively. Our *in vitro* studies have previously relied on a combination of HCMV BAC, the genome of which has been repaired to match the original clinical sequence, and a tetracycline repressor system to suppress the RL13/UL128L mutations. This system can not be used directly with primary clinical isolates however. Recent attempts at culturing wild-type virus by the addition of CMV-hyperimmuneglobin (HIG) to tissue culture medium allowed Ourahmane *et al* to serially passage (13-22 passages) HCMV in fibroblasts without mutations to the RL13 or UL128L (363). Although effective, the viral titres produced by this system are too low to be used routinely *in vitro*.

Attempts at recovering primary clinical HCMV in the laboratory is itself problematic, again due to the low viral titres recovered, making it necessary to culture the virus for several weeks in order to determine whether the virus has been successfully isolated. Prolonged culturing contributes to the emergence of genetic mutations however.

To evaluate the recovery of clinical isolates from clinical material, two cell based reporter assays were generated using the HF-Tert cell line, in which the eGFP reporter gene was placed under the control of two inducible HCMV E promoters,

UL54 and UL112/3. Neither the UL54 or UL112/3 indicator cell lines initially generated were able to induce eGFP expression following HCMV infection, however, following single cell cloning, a single UL54 and several UL112/3 clonal populations were capable of expressing eGFP, albeit at levels that were too weak to be reliable. As the strength of the reporter signal directly correlates with promoter activity, to increase the strength of the eGFP signal, future construct design could incorporate multiple copies of the promoter into the UL54 or UL112/3 lentiviral vectors.

Had these new cell based assays proven reliable tools for measuring the presence of replicating HCMV, their specificity, reproducibility and sensitivity to HCMV infection would have been assessed further. To assess whether the reporter cells lines were capable of detecting infectious HCMV from different sources, a number of laboratory-adapted and clinical HCMV isolates would be tested. To demonstrate that eGFP expression could only be triggered by replicating HCMV, the specificity and reproducibility of the assay would be assessed by infection with a number of other common viruses such as influenza A, adenovirus type 5 and human alphaherpesviruses 1 and 2 (HSV-1, HSV-2). To test the sensitivity of the assay, the upper and lower detection limits of the assay would need to be established by infecting the cells with a range of pre-determined MOIs.

Both Hitt *et al and* Gueret *et al* have successfully used reporter cells to determine the titre of adenoviruses by flow cytometry (364-5). To exploit eGFP quantification by flow cytometry to determine HCMV titre, validated UL54 or UL112/3 driven reporter lines could be used to determine the viral titres of new HCMV viral preparations, allowing rapid quantification of previously unknown viral titres in lieu of the traditional plaque assay. In order to accurately calculate HCMV titre, the assay parameters would need to ensure that one green fluorescent cell is equivalent to one infectious particle. Infection of cells with a low MOI would therefore be required to avoid multiple particles infecting a single cell.

In addition to the intended purpose of the assay, validated cell lines could also be used to identify and develop novel inhibitors of HCMV that interfere with IE-2 or earlier expressing proteins.

The second aim of this work was to produce a number of cell lines expressing shRNA targeting the conserved regions of viral RL13, UL128, UL130 or UI131A to suppress protein expression during infection, resulting in a virus with a mutant phenotype capable of generating higher viral titres than WT virus. The data presented in this study suggests that all shRNA constructs generated failed to suppress the expression of either RL13 or UL128L genes as evaluated by plaque assay. As previously noted in the chapter discussion, this may be due to a combination of inadequate shRNA computational algorithms along with poor shRNA design, or that shRNA expression levels were inadequate to overcome high levels of transcription from multiple viral genomes in a cell.

During this study, the efficiency of singe shRNA constructs was investigated. Based on previous RNAi studies by Jackson *et al* (366), pooled shRNAs targeting the RL13 or UL128L genes may prove more effective in future investigations.

In order to support the propagation of a fully wild-type virus in the laboratory, the creation of a cell line capable of suppressing the expression of both the RL13 and any one of the UL128L genes is required. To achieve this, each of the shRNA constructs designed should contain a unique selection marker for future selection. A number of drug resistance markers such as puromycin, neomycin, hygromycin and blasticidin, plus a variety of fluorophores may be utilized to achieve this. Furthermore, each could be individually assessed for their efficacy at knocking down expression levels of a single genetic copy of the target gene (e.g. in a lentivirus), before testing combinations against intact virus.

As a known hypervariable gene, it is unsurprising that up to 94.3% of all known RL13 gene sequences failed to align with their target shRNA, as assessed by CLC main. Future shRNA design should therefore place emphasis on both the prevalence of the target sequence across all known HCMV strains and how much the target sequence itself is conserved across these strains. Given the variation in RL13, it may never be possible to design a single shRNA that targets all possible strains, however multiple shRNA targeting different RL13 sequences could be incorporated into a single expression construct, providing a potential solution to this problem.

In future, many more target sequences need to be constructed and tested, taking into account sequence conservation and strain variability. Despite improvements in shRNA predictive algorithms, the only way to test the efficacy of these constructs is through experimentation.

Our laboratory has amassed more than 200 cytomegaloviruses over the past two decades, the majority of which are on the background of the HCMV strain, Merlin. This clinical isolate is known to contain a C to T nucleotide substitution in gene UL128, rendering the gene non-functional. Given the importance of UL128 in promoting infection of multiple cell types, our viruses are currently limited to infection of fibroblasts only.

To aid understanding of the biological and genetic mechanisms governing disease in all cell types, the final objective in this thesis was to generate a UL128 expressing cell line capable of *trans*-complementing our existing UL128 deficient viral stocks. This aim was achieved as confirmed by DC co-culture assay.

Previous studies have reported that HCMV infection in epithelial cells is dependent on UL128 for the formation of the pentameric entry complex (section 1.6.3.2), however, co-culture assays performed with this cell type, in this thesis,

demonstrated that HCMV dissemination occurs independently of UL128, as UL128 null viruses efficiently infected both RPE-1 and ARPE-19 cell lines.

It is widely recognized that TB40/E, extensively used in tropism studies, contains multiple variants within the strain, and unlike many other laboratory-adapted strains, has retained its diverse tropism, by containing both pentameric and trimeric rich variants (139, 367-9). It is also known to contain a mutant copy of the UL141 ORF, impeding expression of this gene (367). UL141, highly conserved in clinical isolates, is known to inhibit cell surface expression of CD155 (369), CD112 (in conjunction with other viral glycoproteins) (370), and tumor necrosis factor-related apoptosis-inducing ligand death (TRAIL) receptors 1 and 2 (371), demonstrating it's importance as an immune evasion gene. pUL141 has also been shown to interact with the human protein CUGBP Elav-like family member 5 (CEL5) to regulate viral replication (372). In contrast to TB40/E, Merlin expresses a functional UL141 that has been shown to reside on the virion envelope (Stanton, unpublished), and as such, has the potential to modulate tropism. It was therefore tempting to investigate the role of UL141 in HCMV epithelial cell entry, in the absence of UL128.

The co-culture assays performed in chapter 5 revealed that there was no evidence that UL141 expression facilitated viral entry into epithelial cells in the absence of a functioning pentamer, suggesting that viral entry into this cell type relies on an alternative, and as yet, undetermined mechanism.

HCMV, like other enveloped viruses, can spread by either cell-free or by direct cell-cell contact (see 1.6.3.4). *In vivo* viral dissemination predominantly occurs through cell-associated mechanisms, potentially as a means of avoiding host neutralizing antibodies. Despite this phenotype *in vivo*, *in vitro* tropism studies are predominantly performed using highly passaged, cell-free strains as a result of adaptive mutations to RL13 and UL128L. Cell-free adapted virions consequently contain low amounts of the pentamer, and an abundance of trimer,

while non-adapted cell-associated virus contains an abundance of the pentamer, but diminished amounts of the trimer. The mechanistic differences between both modes of dissemination remain unclear, however. As the functional (co-culture) assays performed in this thesis relied on cell-cell rather than cell-free HCMV transmission, in keeping with the published work, the requirement of a functional pentameric complex, in the context of cell-free infection of epithelial cells was investigated. In contrast to the cell-cell data, UL128 was shown to be important for the efficiency of epithelial cell entry during cell-free infection, supporting the idea of a mechanistic difference between cell-free and cell-associated modes of infection. Whether this novel cell-associated mechanism is restricted to epithelial cells is currently unknown, therefore future work should firstly examine the importance of UL128 during cell-cell spread into other pentamer dependent cell types, before evaluating viral transfer efficiency of the UL128 transduced cell lines generated.

In recent years, the cellular receptors for the trimeric (gH/gL/gO) and pentameric (gH/gL/UL128L) viral entry complexes have been identified; PDGFRα and neuropilin-2 (Nrp-2) respectively (172, 174). PDGFRα, highly expressed on fibroblasts, is expressed at significantly lower levels in epithelial cells, while Nrp-2, is expressed at similar levels in both cell types (174). Studies with trimer-only HCMV revealed that viral entry was abolished in PDGFRα knockout fibroblasts, while wild-type HCMV (i.e virus containing both the trimer and pentameric complexes), were capable of entering PDGFRα knockout fibroblasts, albeit at reduced levels compared with the parental cell line. The authors concluded that this low level of infectivity was likely due to Nrp-2/pentamer binding on fibroblasts (174). With this in mind, as very low levels of PDGFRα are known to be expressed on ARPE-19 cells (356), it is possible, that trimer/PDGFRα binding may offer an alternative viral entry mechanism into epithelial cells in the absence of a functional pentamer. In support of this hypothesis, PDGFRα blocking studies performed by *Naing et al* on human extravillous placental trophoblasts, which naturally express PDGFRα, prevented HCMV entry of gH/gL/UL128L deficient,

but not sufficient strains, while expression of the receptor in naturally deficient villous trophoblasts allowed viral entry for pentamer deficient but not pentamer positive viral strains (373). To test whether PDGFRα/trimer binding promotes HCMV cell entry in epithelial cells in the absence of the pentamer, the infection rates of wild-type and trimer-only virus into PDGFRα knockout epithelial cells would need to be compared. There are a number of conflicting reports on PDGFRα expression levels on RPE-1 cells, therefore future work should establish PDGFRα receptor levels on this cell type by western blot analysis of membrane fractions or flow cytometry.

Should epithelial cell Nrp-2 knockout studies fail to identify PDGFRα/trimer as the alternative entry mechanism in pentamer deficient viruses, it is tempting to speculate, given the recent discovery that pUL116 binds gH independently of gL (233), that this heterodimer, of current unknown function, may serve this purpose. To test this hypothesis, a new RL13/UL128/UL116 triple mutant virus would need to be generated, and co-culture assays performed.

In the event that gH/UL116 does not aid viral entry into epithelial cells, due to its universal role in herpesvirus cell fusion and entry, the glycoproteins H and L (gH/gL) warrant further investigation. A pull-down assay, a method designed to identify a physical interaction between two or more proteins, could be performed using the gH/gL heterodimer as the ‘bait’. Any proteins found to be in association with the dimer, may be involved in viral cell entry.

The two UL128 transduced fibroblasts generated during this study are capable of *trans*-complementing our ∆UL128 viral library for a single cycle only, transforming the group’s ability to investigate HCMV pathogenesis in all cell types. In order to support long-term propagation of WT HCMV in endothelial cells or monocytes following co-culture with transduced fibroblasts, lentiviral mediated UL128 gene transfer of endothelial cells/monocytes would support this. Due to the necessity of the pentameric complex for viral entry into the aforementioned cell types, further mutations to the UL128L can be avoided. The transduced fibroblasts

themselves have the potential to support long term culture of WT virus, however, as these cells require the trimer for viral cell entry, the emergence of new UL128L mutants is inevitable.

Concluding remarks.

Research into human cytomegalovirus should involve the use of a strain that accurately represents the clinical agent as closely as possible. Although the repaired Merlin BAC, used throughout this, and many other studies may be representative of the clinical agent, it must be recognised that other genetically distinct, but related HCMV strains exist *in vivo*, each with a potential to display altered pathogenesis. The limitations of using a single isolate to represent the biology and pathology of all other HCMV strains must therefore be taken into consideration when interpreting experimental data.

As a result of our collaboration with the Wales Kidney Research Unit, our laboratory has unique access to primary HCMV samples, which if isolated and grown in cell lines that repair or prevent adaptive mutations to the RL13 and UL128L genes, enable us to evaluate the effectiveness of emerging therapeutics against multiple wild-type viruses, in all cell types. Although the mutations affecting the RL13 and UL128L have been the main focus of this study, it's important to note that other gene mutations eventually emerge following prolonged culturing, putting into question, the integrity of the viral strain being studied. Frequent evaluation of the genome by next generation sequencing is therefore necessary.

Technologies developed in this thesis allow the tropism of UL128 deficient isolates to be restored, while providing a platform for the development of future reporter and gene silencing cell lines. This work will aid understanding of HCMV biology, including the mechanisms underlying cell-associated and cell-free spread.

Chapter 7 - Appendix

S.1 Primer sequences used in this project

Table ST1. UL54 sequence primers for lentiviral construction

UL54 forward	AGTGATAAGCTTGAATTCAACTCGTACAAGCAG
UL54 reverse	AGTCATGGATCCTCAGACGACGGTGGTCCC

Table ST2. UL112/3 sequence primers for lentiviral construction

UL112/3 forward	ACTGATAAGCTTCCGCACAGAGGTAACAAC
UL112/3 reverse	AGTGATGGATCCGTG GAGCGAGTGC

Table ST3. UL128 sequence primers for insertion into retrovirus

UL128 forward	GGCCGGATCCGCCACCATGAGTCCCAAAGATCTGACG
UL128 forward	GGCCCTCGAGTCACTGCAGCATATAGCCCA
Sequencing primer	AGTAGACGGCATCGCAGCTT

Table ST4. UL141 amplificaion primers for en passant cassette

UL141 forward	ACGGTGAAAATACTCCAAAATCCCAAAAATGCCGCGATTCC CCGAGTGGCCCAGGGAGAGATGATTCTTTTCTTCCCTTTAG GGATAACAGGGTAATGGC
UL141 reverse	TAATATAGAGTATACAATAGTGACGTGGGATCCTCACGTAGA ATCAAGACCTAGGAGCGGGTTAGGGATTGGCTACCGGCGC TCCG AGTGGCCCAGGGA
Sequencing primer	CGCGACGGCGAGGGAGAGGC

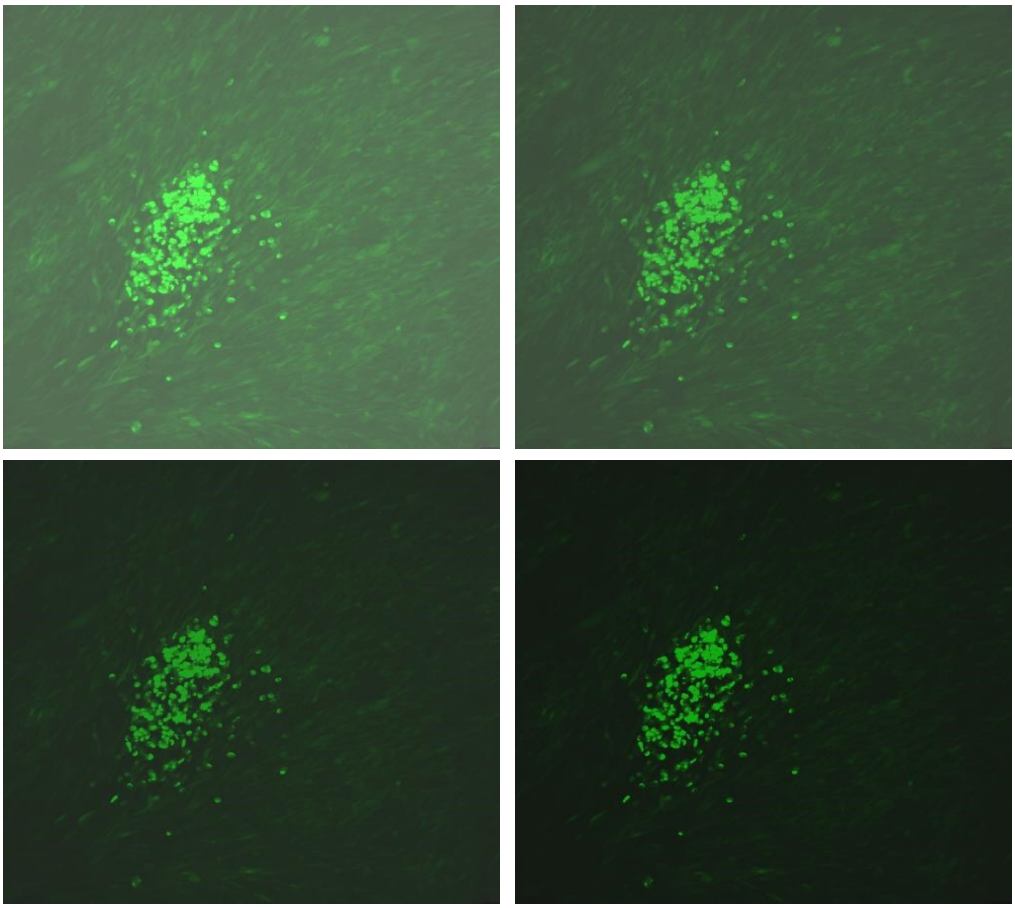

Figure S1. Contrast between GFP expression in MG 3468 fibroblast cells following transduction and puromycin selection with GFP expressing viral plaques

The contrast between GFP transduced cells and GFP expressing viral plaques was investigated in a plaque assay. UL128-b shRNA contains eGFP. Virus contains GFP-tag. When comparing the brightness of the transduced cells with the GFP tagged virus, cellular levels of eGFP were greatly reduced compared to that of the virus. The contrast aided viral plaque identification, but confirmed the low expression levels of the eGFP and therefore shRNA expression in the cell.

Chapter 8 - References

1. Mocarski SM, Shenk T, Griffiths PD, Pass FP. Cytomegaloviruses. Fields Virology. 6th ed. Philadelphia: Lippincott Williams & Wilkins; 2013:1960-2014.

2. Boeckh M, Geballe AP. Cytomegalovirus: pathogen, paradigm, and puzzle. J Clin Invest. 2011:121(5):1673-80.

3. Landolfo S, Gariglio M, Gribaudo G, Lembo D. The human cytomegalovirus. Pharmacology and Therapeutics. 2003:98:269-297.

4. Kaminski H, Fishman JA. The Biology of Cytomegalovirus: Implications for Transplantation. American Journal of Transplantation. 2016:16:2254-2269.

5. Wilkinson GWG, Davison AJ, Tomasec P, Fielding CA, Aicheler RA, Murrell I, Seirafian S, Wang ECY, Weekes M, Lehner PJ, Wilkie GS, Stanton RJ. Human cytomegalovirus: taking the strain. Med Microbiol Immunol. 2015: 204:273–284.

6. Leung AKC, Sauve RS, Davies HD. Congenital cytomegalovirus infection. Journal of the National Medical Association. 2003:95(3):213-218.

7. cmvaction.org.uk

8. Cannon MJ, Davis KF. Washing our hands of the congenital cymomegalovirus disease epidemic. BMC Public Health. 2005:5:70.

9. MacLachlan NJ, Dubovi EJ (Eds). Fenner's Veterinary, Virology. Fourth Edition. Chapter 9 – *Herpesvirales.* Academic Press. 2011:179-201.

10. Crough T, Khanna R. Immunobiology of human cytomegalovirus: from bench to bedside. Clin Microbiol Rev. 22. United States. 2009:76-98, Table of Contents.

11. Roizmann B, Desrosiers RC, Fleckenstein B, Lopez C, Minson AC, Studdert MJ. The family Herpesviridae: an update. The Herpesvirus Study Group of the International Committee on Taxonomy of Viruses. Arch Virol. 1992:123(3-4):425-49.

12. Murphy E, Shenk T. Human cytomegalovirus genome. Curr Top Microbiol Immunol. 2008:325:1-19.

13. Fleischmann WR Jr. Viral Genetics. In: Baron S, editor. Medical Microbiology. 4th edition. Galveston (TX): University of Texas Medical Branch at Galveston; 1996. Chapter 43.

14. https://talk.ictvonline.org/taxonomy/

15. Andrä CJ (ed) Verhandlungen des naturhistorischen Vereines der preussischen Rheinlande und Westfalens. Achtunddreissigter Jahrgang. Vierte Folge: 8. Jahrgang, Max Cohen & Sohn, Bonn. 1881:161–162.

16. Jesionek A, Kiolemenoglou B. Uber einen befund von protozoenartigen gebilden in den organen eines heriditarluetischen fotus. Munch. Med. Wochenschr. 1904:51:1905–1907.

17. Lowenstein C. Uber protozoenartigen gebilden in den organen von dindern. Žentralbl. Allg. Pathol. 1907:18:513–518.

18. Goodpasture EW, Talbot FB. Concerning the nature of “proteozoan-like” cells in certain lesions of infancy. Am. J. Dis. Child. 1921:21:415–421.

19. Lipschutz B. Untersuchungen uber die atiologie der krankheiten der herpesgruppe (herpes zoster, herpes genitalis, herpes febrilis). Arch. Derm. Syph. (Berl.). 1921:136:428–482.

20. Von Glahn WC, Pappenheimer AM. Intranuclear Inclusions in Visceral Disease. Am J Pathol. 1925:1(5):445-663.

21. Cole R, Kuttner AG. A filtrable virus present in the submaxillary glands of guinea pigs. J. Exp. Med. 1926:44:855–873.

22. Wyatt JP, Saxton J. Generalized cytomegalic inclusion disease. J Pediatr. 1950:36(3):271-94, illust.

23. Minder W. Die Aetiologie der Cytomegalia infantum. Schweizer Med Wochenschr. 1953:83:1180-2.

24. Smith, MG. Propagation of salivary gland virus of the mouse in tissue cultures. Proceedings of the Society for Experimental Biology and Medicine. 1953:86:435-40.

25. Smith MG. Propagation in Tissue Cultures of a Cytopathogenic Virus from Human Salivary Gland Virus (Sgv) Disease. Proceedings of the Society for Experimental Biology and Medicine. 1956:92(2):424-30.

26. Ho M. The history of cytomegalovirus and its diseases. Med Microbiol Immunol. 2008:197(2):65-73.

27. Rowe WP, Hartley JW, Waterman S, Turner HC, Huebner RJ. Cytopathogenic agent resembling human salivary gland virus recovered from tissue cultures of human adenoids. Proceedings of the Society for Experimental Biology and Medicine. 1956:92(2):418-24.

28. Weller TH, Macauley JC, Craig JM, Wirth P. Isolation of intranuclear inclusion producing agents from infants with illnesses resembling cytomegalic inclusion disease. Proceedings of the Society for Experimental Biology and Medicine. 1957:94(1):4-12.

29. Zuhair, M, Smit GSA, Wallis G, Jabbar F, Smith, C, Devleesschauwer, B, Griffiths P. Estimation of the worldwide seroprevalence of cytomegalovirus: A systematic review and meta-analysis. Rev. Med. Virol. 2019:29:e2034.

30. Abu-Madi MA, Behnke JM, Dabritz HA. Toxoplasma gondii seropositivity and co-infection with TORCH pathogens in high-risk patients from Qatar. Am J Trop Med Hyg. 2010:82(4):626–33.

31. Spano L, Gatti J, Nascimento JP, Leite J. Prevalence of human cytomegalovirus infection in pregnant and non-pregnant women. J Infect. 2004:48(3):213–20.

32. Pembrey L, Raynor P, Griffiths P, et al. Seroprevalence of cytomegalovirus, Epstein Barr virus and varicella zoster virus among pregnant women in Bradford: a cohort study. PloS One. 2013:8(11):e81881.

33. Enders G, Daiminger A, Lindemann L, et al. Cytomegalovirus (CMV) seroprevalence in pregnant women, bone marrow donors and adolescents in Germany, 1996–2010. Med Microbiol Immunol. 2012:201(3):303–09.

34. Staras SA, Dollard SC, Radford KW, Flanders WD, Pass RF, Cannon MJ. Seroprevalence of cytomegalovirus infection in the United States, 1988-1994. Clin Infect Dis. 2006:43:1143-51.

35. Cannon MJ, Schmid DS, Hyde TB. Review of cytomegalovirus seroprevalence and demographic characteristics associated with infection. Rev Med Virol. 2010:20(4):202-13.

36. Arisalo J, Ilonen J, Vainionpaa R, Volanen I, Kaitosaari T, Simell O. Development of antibodies against cytomegalovirus, varicella-zoster virus and herpes simplex virus in Finland during the first eight years of life: a prospective study. Scand J Infect Dis. 2003:35:750-3.

37. De Ory F, Ramirez R, Garcia Comas L, Leon P, Sagues MJ, Sanz JC. Is there a change in cytomegalovirus seroepidemiology in Spain? Eur J Epidemiol. 2004:19:85-9.

38. Dowd JB, Aiello AE, Alley DE. Socioeconomic disparities in the seroprevalence of cytomegalovirus infection in the US population: NHANES III. Epidemiol Infect. 2009:137:58-65.

39. Lopo S, Vinagre E, Palminha P, Paixao MT, Nogueira P, Freitas MG. Seroprevalence to cytomegalovirus in the Portuguese population, 2002- 2003. Euro Surveill, 2011:16(25):19896.

40. Staras SA, Flanders WD, Dollard SC, Pass RF, McGowan JE, Cannon MJ. Cytomegalovirus seroprevalence and childhood sources of infection: A population-based study among pre-adolescents in the United States. J Clin Virol, 2008:43:266-71.

41. Vyse AJ, Hesketh LM, Pebody RG. The burden of infection with cytomegalovirus in England and Wales: how many women are infected in pregnancy? Epidemiol Infect. 2009:137:526-33.

42. Hassan J, O'Neill D, Honari B, De Gascun C, Connell J, Keogan M, , Hickey D. Cytomegalovirus Infection in Ireland: Seroprevalence, HLA Class I Alleles, and Implications. Medicine (Baltimore). 2016:95:e2735.

43. Futohi F, Saber A, Nemati E, Einollahi B, Rostami Z. Human Leukocyte Antigen Alleles and Cytomegalovirus Infection After Renal Transplantation. Nephrourol Mon. 2015:7:e31635.

44. Choo SY. The HLA system: genetics, immunology, clinical testing, and clinical implications. Yonsei medical journal. 2007:48(1):11–23.

45. Sia IG, Patel R. New strategies for prevention and therapy of cytomegalovirus infection and disease in solid-organ transplant recipients. Clin Microbiol Rev. 2000:13(1):83-121. Table of contents.

46. De Jong MD, Galasso GJ, Gazzard B, Griffiths PD, Jabs DA, Kern ER, Spector SA. Summary of the II international symposium on cytomegalovirus. Antiviral Res. 1998:39:141–162.

47. Cannon MJ, Hyde TB, Schmid DS. Review of cytomegalovirus shedding in bodily fluids and relevance to congenital cytomegalovirus infection. Rev. Med. Virol. 2011:21:240–255.

48. Mayer BT, Krantz EM, Swan D, Ferrenberg J, Simmons K, Selke S, Huang ML, Casper C, Corey L, Wald A, Schiffer JT, Gantt S. Transient oral human cytomegalovirus infections indicate inefficient viral spread from very few initially infected cells. J. Virol. 2017:91(12):e00380-17.

49. Pultoo A, Jankee H, Meetoo G, Pyndiah MN, Khittoo G. Detection of cytomegalovirus in urine of hearing-impaired and mentally retarded children by PCR and cell culture. J Commun Dis. 2000:32(2):101-108.

50. Krishna BA, Poole EL, Jackson SE, Smit MJ, Wills MR, Sinclair JH. Latencyassociated expression of human cytomegalovirus US28 attenuates cell signaling pathways to maintain latent infection. mBio 2017:8:e01754-17.

51. Reeves MB. Chromatin-mediated regulation of cytomegalovirus gene expression. Virus Res. 2011:157(2):134-43.

52. Biron CA, Byron KS, Sullivan JL. Severe herpesvirus infections in an adolescent without natural killer cells. N Engl J Med. 1989:320:1731–1735.

53. Orange JS. Human natural killer cell deficiencies and susceptibility to infection. Microbes Infect. 2002:4:1545–1558.

54. Hurt C, Tammaro D. Diagnostic evaluation of mononucleosis-like illnesses. Am J Med. 2007:120 (10):911.e1-8.

55. Caposio, P, Orloff SL, Streblow DN. The role of cytomegalovirus in angiogenesis. Virus Res. 2010:157:204–211.

56. Lawlor G, Moss AC. Cytomegalovirus in inflammatory bowel disease: Pathogen or innocent bystander? Inflamm. Bowel Dis. 2010:16:1620–1627.

57. Nauclér CS, Geisler J, Vetvik K. The emerging role of human cytomegalovirus infection in human carcinogenesis: A review of current evidence and potential therapeutic implications. Oncotarget. 2019:10:4333–4347.

58. Geisler J, Touma J, Rahbar A, Söderberg-Naucler C, Vetvik K. A Review of the Potential Role of Human Cytomegalovirus (HCMV) Infections in Breast Cancer Carcinogenesis and Abnormal Immunity. Cancers. 2019:11: 1842.

59. Manicklal S, Emery V, Lazzarotto T, Boppana SB, Gupta RK. The “Silent” Global Burden of Congenital Cytomegalovirus. Clin. Microbiol. Rev. 2013:26:86–102.

60. Pass RF, Stagno S, Myers GJ, Alford CA. Outcome of symptomatic congenital CMV infection: results of long-term longitudinal follow-up. Pediatrics. 198:66:758–762.

61. Stagno S, Reynolds DW, Amos CS, et al. Auditory and visual defects resulting from symptomatic and subclinical congenital cytomegaloviral and toxoplasma infections. Pediatrics. 1977:59:669–678.

62. Williamson WD, Desmond MM, Fevers N, Taber LH, Catlin FI, Weaver TGI. Symptomatic congenital cytomegalovirus: disorders of language, learning and hearing Am. J. Dis. Child. 1982:136902–905.

63. Kenneson A, Cannon MJ. Review and meta-analysis of the epidemiology of congenital cytomegalovirus (CMV) infection. *Rev Med Virol* 2007:17:253–276.

64. Dollard SC, Grosse SD, Ross DS. New estimates of the prevalence of neurological and sensory sequelae and mortality associated with congenital cytomegalovirus infection. *Rev Med Virol* 2007:17:355–363.

65. Stagno S, Pass RF, Cloud G, Britt WJ, Henderson RE, Walton PD, et al. Primary cytomegalovirus infection in pregnancy. Incidence, transmission to fetus, and clinical outcome. Jama. 1986:256(14):1904-8.

66. https://www.cdc.gov/cmv/clinical/congenital-cmv.html#:~:text=A%20pregnant%20woman%20can%20pass,70%25%20in%20the%20third%20trimester

67. Reynolds DW, Stagno S, Hosty TS, et al. Maternal cytomegalovirus excretion and perinatal infection. N Engl J Med. 1973:289:1–5.

68. Stagno S, Reynolds DW, Pass RF, Alford CA. Breast milk and the risk of cytomegalovirus infection. N Engl J Med. 1980:302:1073–6.

69. Hotsubo T, Nagata N, Shimada M, et al. Detection of human cytomegalovirus DNA in breast milk by means of polymerase chain reaction. Microbiol Immunol. 1994:38:809–11.

70. Vochem M, Hamprecht K, Jahn G, Speer CP. Transmission of cytomegalovirus to preterm infants through breast milk. Pediatr Infect Dis J. 1998:17:53–8.

71. Myers JD, Spencer HC Jr, Watts JC, et al. Cytomegalovirus pneumonia after human marrow transplantation. Ann. Int. Med. 1975:82:181–188.

72. Ho M. Virus infections after transplantation in man. Arch. Virol. 1977:55:1–24.

73. Rubin RH, Russell PS, Levin M, Cohen C. From the National Institutes of Health. Summary of a workshop on cytomegalovirus infections during organ transplantation. J. Infect. Dis. 1979:139:728–734.

74. Rubin RH, Colvin RB. Cytomegalovirus infection in renal transplantation, clinicl importance and control. In Williams GM, Burdick JFF, Solez K (eds) Kidney transplant rejection: diagnosis and treatment. Dekker, New York. 1986:283–304.

75. Rubin RH. Impact of cytomegalovirus infection on organ transplant recipients Rev. Infect. Dis. 1990:12:S754–S766.

76. Azevedo LS, Pierrotti LC, Abdala E, Costa SF, Strabelli TM, Campos SV, Ramos JF, Latif AZ, Litvinov N, Maluf NZ, Caiaffa Filho HH, Pannuti CS, Lopes MH, Santos VA, Linardi Cda C, Yasuda MA, Marques HH. Cytomegalovirus infection in transplant recipients. Clinics (Sao Paulo). 2015:70(7):515-23.

77. Simon DM, Levin S. Infectious complications of solid organ transplantations. Infect Dis Clin of North Am. 2001:15(2):521–49.

78. Humar A, Snydman D. The AST Infectious Diseases Community of Practice: Cytomegalovirus in solid organ transplant recipients. Am J Transplant. 2009:9(Suppl 4):S78–6.

79. Legendre C, Pascual M. Improving outcomes for solid-organ transplant recipients at risk from cytomegalovirus infection: late-onset disease and indirect consequences. Clin Infect Dis. 2008:46(5):732–40.

80. https://www.medicinenet.com/cytomegalovirus_cmv/article.htm

81. Gandhi MK, Khanna R. Human cytomegalovirus: clinical aspects, immune regulation, and emerging treatments. The Lancet infectious diseases. 2004:4:725-738.

82. Selik RM, Chu SY, Ward JW. Trends in infectious diseases and cancers among persons dying of HIV infection in the United States from 1987 to 1992. Ann. Intern. Med. 1996:123:933–936.

83. Klatt EC, Shibata D. Cytomegalovirus infection in the acquired immunodeficiency syndrome. Clinical and autopsy findings. Arch. Pathol. Lab. Med. 1988:112:540–544.

84. Spector SA, Hsia K, Crager M, Pilcher M, Cabral S, Stempien MJ. Cytomegalovirus (CMV) DNA load is an independent predictor of CMV disease and survival in advanced AIDS. J. Virol. 1999:73:7027–7030.

85. Griffiths PD. CMV as a cofactor enhancing progression of AIDS. J Clin Virol. 2006:35(4):489-92.

86. Kempen JH, Jabs DA, Wilson LA, Dunn JP, West SK, Tonascia J. Mortality risk for patients with cytomegalovirus retinitis and acquired immune deficiency syndrome. Clin Infect Dis. 2003:37(10):1365-73.

87. Majumder S, Mandal SK, Bandyopadhyay D, Chowdhury SR, Chakraborty PP, Mitra K. Multiorgan involvement due to cytomegalovirus in AIDS. Braz J Infect Dis. 2007:11:176-8.

88. Hodson EM, Jones CA, Webster AC, Strippoli GF, Barclay PG, Kable K, Vimalachandra D. Craig JC. Antiviral medications to prevent cytomegalovirus disease and early death in recipients of solid-organ transplants: a systematic review of randomised controlled trials. The Lancet. 2005:365(9477):2105–2115.

89. Littler E, Stuart AD,.Chee MS. Human cytomegalovirus ul97 open reading frame encodes a protein that phosphorylates the antiviral nucleoside analogue ganciclovir, Nature. 1992:9(358(6382)):160–2.

90. Sullivan V, Talarico CL, Stanat SC, Davis M, Coen DM, Biron KK. A protein kinase homologue controls phosphorylation of ganciclovir in human cytomegalovirus-infected cells. Nature. 1992;358(6382):162-4.

91. Chou S. Antiviral drug resistance in human cytomegalovirus. Transpl Infect Dis. 1999:1(2):105-114.

92. Tan BH. Cytomegalovirus Treatment. Curr Treat Options Infect Dis. 2014:6(3):256-270.

93. Feire, AL, Koss H, Compton T. Cellular integrins function as entry receptors for human cytomegalovirus via a highly conserved disintegrin-like domain. Proc Natl Acad Sci. U S A. 2004:101(43):15470-5.

94. Ljungman P, Deliliers GL, Platzbecker U, Matthes-Martin S, Bacigalupo A, Einsele H, Ullmann J, Musso M, Trenschel R Ribaud P, Bornhäuser M, Cesaro S, Crooks B Dekker A, Gratecos N, Klingebiel T, Tagliaferri E, Ullmann AJ, Wacker P, Cordonnier C: for the Infectious Diseases Working Party of the European Group for Blood and Marrow Transplantation. Cidofovir for cytomegalovirus infection and disease in allogeneic stem cell transplant recipients. Blood 2001:97(2):388–392.

95. Verkaik NJ, Hoek RAS, van Bergeijk H, van Hal PThW, Schipper MEI, Pas SD, Beersma MFC, Boucher CAB, Jedema I, Falkenburg F, Hoogsteden HC , van den Blink B, Murk JL. Leflunomide as part of the treatment for multidrug-resistant cytomegalovirus disease after lung transplantation: case report and review of the literature. Transpl Infect Dis. 2013:15:E243-9.

96. Gokarn A, Toshniwal A, Pathak A, Arora S, Bonda A, Punatar S, Nayak L, Dwivedi P, Bhat V, Biswas S, Kelkar R, Kannan S, Khattry N. Use of Leflunomide for Treatment of Cytomegalovirus Infection in Recipients of Allogeneic Stem Cell Transplant. Biol Blood Marrow Transplant. 2019:25(9):1832-1836.

97. Ligat G, Cazal R, Hantz S, Alain S. The human cytomegalovirus terminase complex as an antiviral target: a close-up view. FEMS Microbiology Reviews. 2018:42:2:137–145.

98. Biron KK, Harvey RJ, Chamberlain SC, et al. Potent and selective inhibition of human cytomegalovirus replication by 1263W94, a benzimidazole L-riboside with a unique mode of action. Antimicrob Agents Chemother. 2002:46:2365-2372.

99. Krosky PM, Baek MC, Coen DM. The human cytomegalovirus UL97 protein kinase, an antiviral drug target, is required at the stage of nuclear egress. J Virol 2003:77:905-914.

100. Frange P, Leruez-Ville M. Maribavir, brincidofovir and letermovir: efficacy and safety of new antiviral drugs for treating cytomegalovirus infections. Med Mal Infect 2018:48(8):495-502.

101. Marty FM, Boeckh M. Maribavir and human cytomegalovirus—what happened in the clinical trials and why might the drug have failed? Curr Opin Virol 2011:1:555–62.

102. Institute of Medicine Division of Health Promotion and Disease Prevention. Vaccines for the21st century: a tool for decisionmaking. IOM Committee to Study National Priorities for Vaccine Development. National Academies Press,Washington, DC. 2000.

103. Elek SD, Stern H. Development of a vaccine against mental retardation cased by cytomegalovirus infection in utero. Lancet. 1974:1:1–15.

104. Neff BJ, Weibel RE, Buynak EB, Allen AA, Hillman MR, Clinical and laboratory studies of live cytomegalovirus vaccine Ad-169 Proc. Soc. Exp. Biol. Med. 1997:16032–37.

105. Jacobson MA, Sinclair E, Bredt B, et al. Safety and immunogenicity of Towne cytomegalovirus vaccine with or without adjuvant recombinant interleukin-12. Vaccine. 2006:24:5311–5319.

106. Pass RF, Duliege AM, Sekulovich R, Percell S, Britt W, Burke RLA. Subunit cytomegalovirus vaccine based on recombinant envelope glycoprotein B and a new adjuvant. J. Infect. Dis. 1999:180:970–975.

107. Plotkin SA. Vaccination against cytomegalovirus. Arch. Virol. Supplementum. 2001:121–134.

108. Pass RF, Burke RL. Development of cytomegalovirus vaccines: prospects for prevention of congenital CMV infection. Semin. Pediatric. Infect. Dis. 2002:13:196–204.

109. Pass RF, Zhang C, Evans A, Simpson T, Andrews W, Huang ML, et al. Vaccine prevention of maternal cytomegalovirus infection. N Engl J Med. 2009:360(12):1191-9.

110. Bernstein DI, Munoz FM, Callahan ST, Rupp R, Wootton SH, Edwards KM, et al. Safety and efficacy of a cytomegalovirus glycoprotein B (gB) vaccine in adolescent girls: A randomized clinical trial. Vaccine. 2016:34(3):313-9.

111. Anderholm KM, Bierle CJ, Schleiss MR. Cytomegalovirus Vaccines: Current Status and Future Prospects. Drugs. 2016:76(17):1625-1645.

112. Fu TM, An Z, Wang D. Progress on pursuit of human cytomegalovirus vaccines for prevention of congenital infection and disease. Vaccine. 2014:32(22):2525-33.

113. Wloch MK, Smith LR, Boutsaboualoy S, Reyes L, Han C, Kehler J, et al. Safety and immunogenicity of a bivalent cytomegalovirus DNA vaccine in healthy adult subjects. J Infect Dis. 2008:197(12):1634–42.

114. Kharfan-Dabaja MA, Boeckh M, Wilck MB, Langston AA, Chu AH, Wloch MK, et al. A novel therapeutic cytomegalovirus DNA vaccine in allogeneic haemopoietic stem-cell transplantation: a randomised, double-blind, placebo-controlled, phase 2 trial. Lancet Infect Dis. 2012:12(4):290–9.

115. Valentine, H. Cytomegalovirus infection and allograft injury. Curr Opinion Org Trans. 2001:6:290–294.

116. Valentine H, Luikart H, Doyle R, Theodore J, Hunt S, Oyer P, et al. Impact of cytomegalovirus hyperimmune globulin on outcome after cardiothoracic transplantation. Transplantation. 2001:72(10):1647–1652.

117. Nigro G, Adler SP, La Torre R, Best AM. Passive immunization during pregnancy for congenital cytomegalovirus infection. New England Journal of Medicine. 2005:353(13):1350–1362.

118. Nigro G, Adler SP, Parruti G, Anceschi MM, Coclite E, Pezone I, Di Renzo GC. Immunoglobulin therapy of fetal cytomegalovirus infection occurring in the first half of pregnancy—a case-control study of the outcome in children. Journal of Infectious Diseases. 2012:205(2):215–227.

119. Brito LA, Chan M, Shaw CA, Hekele A, Carsillo T, Schaefer M, et al. A cationic nanoemulsion for the delivery of next-generation RNA vaccines. Mol Ther. 2014:22(12):2118–29.

120. Schottstedt V, Blümel J, Burger R, Drosten C, Gröner A, Gürtler L, Heiden M, Hildebrandt M, Jansen B, Montag-Lessing T, Offergeld R, Pauli G, Seitz R,

Schlenkrich U, Strobel J, Willkommen H, von König CH. Human Cytomegalovirus (HCMV) - Revised. Transfus Med Hemother. 2010;37(6):365-375.

121. Mocarski Jr E. Betaherpes viral genes and their functions. In: Arvin A, Campadelli-Fiume G, Mocarski E, Moore PS, Roizman B, Whitley R, et al., editors. Human Herpesviruses: Biology, Therapy, and Immunoprophylaxis. Cambridge: Cambridge University Press. 2007.

122. Newcomb WW, Cockrell SK, Homa FL, Brown JC. Polarized DNA ejection from the herpesvirus capsid. J Mol Biol. 2009:392(4):885-94.

123. Gibson W, Bogner E. Morphogenesis of the cytomegalovirus virion and subviral particles. In: Reddehase M, editor. Cytomegaloviruses. 2013:230-47.

124. Bresnahan WA, Shenk T. A subset of viral transcripts packaged within human cytomegalovirus particles. Science. 2000:288(5475):2373–2376.

125. Irmiere A, Gibson W. Isolation and characterization of a noninfectious virion-like particle released from cells infected with human strains of cytomegalovirus. Virology. 1983:130(1):118- 33.

126. Gibson W. Structure and assembly of the virion. Intervirology. 1996:39:389–400.

127. Bechtel, JT, Shenk T. Human cytomegalovirus UL47 tegument protein functions after entry and before immediate-early gene expression. J. Virol. 2002:76:1043-1050.

128. Schierling K, Buser C, Mertens T, Winkler M. Human cytomegalovirus tegument protein ppUL35 is important for viral replication and particle formation. J. Virol. 2005:79:3084-3096.

129. Baldick CJ, Marchini A, Patterson CE, Shenk T. Human cytomegalovirus tegument protein pp71 (ppUL82) enhances the infectivity of viral DNA and accelerates the infectious cycle. J. Virol. 1997:71:4400-4408.

130. Winkler M, Rice SA, Stamminger T. UL69 of human cytomegalovirus, an open reading frame with homology to ICP27 of herpes simplex virus, encodes a transactivator of gene expression. J. Virol 1994:68:3943-3954.

131. Hayashi ML, Blankenship C, Shenk T. Human cytomegalovirus UL69 protein is required for efficient accumulation of infected cells in the G1 phase of the cell cycle. Proc. Natl. Acad. Sci. USA. 2000:97:2692-2696.

132. Scalzo AA, Corbett AJ, Rawlinson WD, Scott GM, Gli Esposti MA. The interplay between host and viral factors in shaping the outcome of cytomegalovirus infection. Immunol. Cell Biol. 2007:85:46-54.

133. Eickmann M, Gicklhorn D, Radsak, K. Glycoprotein trafficking in virion morphogenesis.In: ReddehaseMJ (ed) Cytomegalovirus molecular biology and immunology. Caister Academic Press, Norfolk, UK. 2006:245-264.

134. Gibson W. Structure and formation of the cytomegalovirus virion. Current topics in microbiology and immunology. 2008:325:187–204.

135. Bankier AT, Beck S, Bohni R, Brown CM, Cerny R, MS, Hutchison CA, Kouzarides T, Martignetti JA, Preddie E, et al. The DNA sequence of the human cytomegalovirus genome. DNA Seq. 1991:2:1–12.

136. Vanarsdall AL, Johnson DC. Human cytomegalovirus entry into cells. Curr Opin Virol. 2012:2(1):37-42.

137. Vanarsdall AL, Chase MC, Johnson DC. Human cytomegalovirus glycoprotein gO complexes with gH/gL, promoting interference with viral entry into human fibroblasts but not entry into epithelial cells. J Virol. 2011:85(22):11638-45.

138. Vanarsdall AL, Ryckman BJ, Chase MC, Johnson DC. Human cytomegalovirus glycoproteins gB and gH/gL mediate epithelial cell–cell fusion when expressed either in cis or in trans. J Virol. 2008:82:11837–11850.

139. Dolan A, Cunningham C, Hector RD, Hassan-Walker AF, Lee L, Addison C, Dargan DJ, McGeoch DJ, Gatherer D, Emery VC, Griffiths PD, Sinzger C, McSharry BP, Wilkinson GWG, Davison AJ. Genetic content of wild-type human cytomegalovirus. J Gen Virol. 2004:85(Pt 5):1301-1312.

140. Stern-Ginossar N, Weisburd B, Michalski A, Le VTK, Hein MY, Huang SX, Ma M, Shen B, Qian SB, Hengel H, et al. Decoding human cytomegalovirus. Science. 2012:338(6110):1088–1093.

141. Stark TJ, Arnold JD, Spector DH, Yeo GW. High-resolution profiling and analysis of viral and host small rnas during human cytomegalovirus infection. Journal of virology. 2012:86(1):226–235.

142. Gatherer D, Seirafian S, Cunningham C, Holton M, Dargan DJ, Baluchova K, Hector RD, Galbraith J, Herzyk P, Wilkinson GW, et al. High-resolution human cytomegalovirus transcriptome. Proceedings of the National Academy of Sciences. 2011:108(49):19755–19760.

143. Ji Z. RibORF: Identifying Genome-Wide Translated Open Reading Frames Using Ribosome Profiling. Curr Protoc Mol Biol. 2018:124(1):e67.

144. Kemble GW, Mocarski ES. A host cell protein binds to a highly conserved sequence element (pac-2) within the cytomegalovirus a sequence. J Virol. 1989:63(11):4715-28.

145. Wang JB, McVoy MA. A 128-Base-Pair Sequence Containing the pac1 and a Presumed Cryptic pac2 Sequence Includes cis Elements Sufficient To Mediate Efficient Genome Maturation of Human Cytomegalovirus. Journal of Virology. 2011:85:(9):4432-4439.

146. Davison A. Chapter 2 : Comparative analysis of the genomes. Human Herpesviruses: Biology, Therapy, and Immunoprophylaxis. Cambridge: Cambridge University Press; 2007.

147. Tamashiro JC, Spector DH. Terminal structure and heterogeneity in human cytomegalovirus strain AD169. J Virol. 1986:59(3):591-604.

148. Chee MS, Bankier AT, Beck S, Bohni R, Brown CM, Cerny R, et al. Analysis of the protein- coding content of the sequence of human cytomegalovirus strain AD169. Curr Top Microbiol Immunol. 1990:154:125-69.

149. Sijmons S, Thys K, Mbong Ngwese M, Van Damme E, Dvorak J, Van Loock M, Li G, Tachezy R, Busson L, Aerssens J, Van Ranst M, Maes P. High-throughput analysis of human cytomegalovirus genome diversity highlights the widespread occurrence of gene-disrupting mutations and pervasive recombination. J Virol . 2015:89:7673-7695.

150. Renzette N, Gibson L, Bhattacharjee B, Fisher D, Schleiss MR, Jensen JD, Kowalik TF. Rapid intrahost evolution of human cytomegalovirus is shaped by demography and positive selection. PLoS Genet. 2013:9:e1003735.

151. Plotkin SA, Furukawa T, Zygraich N, Huygelen C. Candidate cytomegalovirus strain for human vaccination. Infect Immun. 1975:12(3):521-7.

152. Cha TA, Tom E, Kemble GW, Duke GM, Mocarski ES, Spaete RR. Human cytomegalovirus clinical isolates carry at least 19 genes not found in laboratory strains. J Virol. 1996:70(1):78-83.

153. Goodrum F, Reeves M, Sinclair J, High K, Shenk T. Human cytomegalovirus sequences expressed in latently infected individuals promote a latent infection in vitro. Blood. 2007:110: 937–945.

154. Grainger L, Cicchini L, Rak M, Petrucelli A, Fitzgerald KD, Semler BL, et al. Stress-inducible alternative translation initiation of human cytomegalovirus latency protein pUL138. J Virol. 2010:84: 9472–9486.

155. Umashankar M, Petrucelli A, Cicchini L, Caposio P, Kreklywich CN, Rak M, et al. A novel human cytomegalovirus locus modulates cell type-specific outcomes of infection. PLoS Pathog. 2011:7:e1002444.

156. Montag C, Wagner JA, Gruska I, Vetter B, Wiebusch L, Hagemeier C. The latency-associated UL138 gene product of human cytomegalovirus sensitizes cells to tumor necrosis factor alpha (TNF-alpha) signaling by upregulating TNF-alpha receptor 1 cell surface expression. J Virol. 2011:85: 11409–11421.

157. Le VT, Trilling M, Hengel H. The cytomegaloviral protein pUL138 acts as potentiator of tumor necrosis factor (TNF) receptor 1 surface density to enhance ULb'-encoded modulation of TNF-α signaling. J Virol. 2011:85: 13260–13270.

158. Wills MR, Ashiru O, Reeves MB, Okecha G, Trowsdale J, Tomasec P, et al. Human cytomegalovirus encodes an MHC class I-like molecule (UL142) that functions to inhibit NK cell lysis. J Immunol. 2005:175(11):7457-65.

159. Penfold ME, Dairaghi DJ, Duke GM, Saederup N, Mocarski ES, Kemble GW, et al. Cytomegalovirus Sequential mutations associated with adaptation of human cytomegalovirus. Proc Natl Acad Sci U S A. 1999:96(17):9839-44.

160. Dargan DJ, Douglas E, Cunningham C, Jamieson F, Stanton RJ, Baluchova K, et al. Sequential mutations associated with adaptation of human cytomegalovirus to growth in cell culture. J Gen Virol. 2010:91(Pt 6):1535-46.

161. Hahn G, Revello MG, Patrone M, Percivalle E, Campanini G, Sarasini A, Wagner M, Gallina A, Milanesi G, Koszinowski U, Baldanti F, Gerna G. Human cytomegalovirus UL131-128 genes are indispensable for virus growth in endothelial cells and virus transfer to leukocytes. J Virol. 2004:78:10023–10033.

162. Waldman WJ, Roberts WH, Davis DH, Williams MV, Sedmak DD, Stephens RE. Preservation of natural endothelial cytopathogenicity of cytomegalovirus by propagation in endothelial cells. Arch Virol. 1991:117:143-64.

163. Sinzger C, Schmidt K, Knapp J, Kahl M, Beck R, Waldman J, et al. Modification of human cytomegalovirus tropism through propagation in vitro is associated with changes in the viral genome. J Gen Virol. 1999:80(Pt 11):2867-77.

164. Sinzger C, Knapp J, Plachter B, Schmidt K, Jahn G. Quantification of replication of clinical cytomegalovirus isolates in cultured endothelial cells and fibroblasts by a focus expansion assay. J Virol Methods. 1997:63(1-2):103-12.

165. MacCormac LP, Grundy JE. Two clinical isolates and the Toledo strain of cytomegalovirus contain endothelial cell tropic variants that are not present in the AD169, Towne, or Davis strains. J Med Virol. 1999:57(3):298-307.

166. Prichard MN, Penfold ME, Duke GM, Spaete RR, Kemble GW. A review of genetic differences between limited and extensively passaged human cytomegalovirus strains. Rev Med Virol. 2001:11(3):191-200.

167. Hahn G, Khan H, Baldanti F, Koszinowski UH, Revello MG, Gerna G. The human cytomegalovirus ribonucleotide reductase homolog UL45 is dispensable for growth in endothelial cells, as determined by a BAC-cloned clinical isolate of human cytomegalovirus with preserved wild-type characteristics. J Virol. 2002:76(18):9551-5.

168. Murphy E, Yu D, Grimwood J, Schmutz J, Dickson M, Jarvis MA, Hahn G, Nelson JA, Myers RM, Shenk TE. Coding potential of laboratory and clinical strains of human cytomegalovirus. Proc Natl Acad Sci U S A. 2003:100:14976–14981.

169. Brown JM, Kaneshima H, Mocarski ES. Dramatic interstrain differences in the replication of human cytomegalovirus in SCID-hu mice. J Infect Dis. 1995:171(6):1599-603.

170. Hahn G, Rose D, Wagner M, Rhiel S, McVoy MA. Cloning of the genomes of human cytomegalovirus strains Toledo, TownevarRIT3, and Towne long as BACs and site-directed mutagenesis using a PCR-based technique. Virology. 2003:307(1):164-77.

171. Soderberg C, Giugni TD, Zaia JA, Larsson S, Wahlberg JM, Moller E. CD13 (human aminopeptidase N) mediates human cytomegalovirus infection. J. Virol. 1993:67:6576–6585.

172. Kabanova A, Marcandalli J, Zhou T, Bianchi S, Baxa U, Tsybovsky Y, et al. Platelet-derived growth factor-alpha receptor is the cellular receptor for human cytomegalovirus gHgLgO trimer. Nat Microbiol. 2016:1(8):16082.

173. Ryckman BJ, Chase MC, Johnson DC. HCMV gH/gL/UL128-131 interferes with virus entry into epithelial cells: evidence for cell type-specific receptors. Proc Natl Acad Sci U S A. 2008:105(37):14118-23.

174. Martinez-Martin N, Marcandalli J, Huang CS, Arthur CP, Perotti M, Foglierini M, et al. An Unbiased Screen for Human Cytomegalovirus Identifies Neuropilin-2 as a Central Viral Receptor. Cell. 2018:174(5):1158-71.e19.

175. Ryckman BJ, Rainish BL, Chase MC, Borton JA, Nelson JA, Jarvis MA, et al. Characterization of the human cytomegalovirus gH/gL/UL128-131 complex that mediates entry into epithelial and endothelial cells. J Virol. 2008:82(1):60-70.

176. Murrell I, Tomasec P, Wilkie GS, Dargan DJ, Davison AJ, Stanton RJ. Impact of sequence variation in the UL128 locus on production of human cytomegalovirus in fibroblast and epithelial cells. J Virol. 2013:87(19):10489-500.

177. Scrivano L, Sinzger C, Nitschko H, Koszinowski UH, Adler B. HCMV spread and cell tropism are determined by distinct virus populations. PLoS Pathog. 2011:7:e1001256.

178. Dohner K, Sodeik B. The role of the cytoskeleton during viral infection. Curr Top Microbiol Immunol. 2005:285:67-108.

179. Kalejta RF. Tegument proteins of human cytomegalovirus. Microbiol Mol Biol Rev. 2008:72(2):249-265.

180. Torres L, Tang Q. Immediate-Early (IE) gene regulation of cytomegalovirus: IE1- and pp71-mediated viral strategies against cellular defenses. Virol Sin. 2014:29(6):343-52.

181. Mocarski ES, Pass RF. Human Cytomegalovirus: General Features. In: Mahy BWJ, Van Regenmortel MHV (eds.). Encyclopedia of Virology. Third ed. Oxford: Oxford Academic Press. 2008.

182. Fehr AR, Dong Y. Human Cytomegalovirus Early Protein pUL21a Promotes Efficient Viral DNA Synthesis and the Late Accumulation of Immediate-Early Transcripts. Journal of Virology. 2010:85(2)663-674.

183. White EA, Spector DH. Early viral gene expression and function. Human Herpesviruses: Biology, Therapy, and Immunoprophylaxis. Human Herpesviruses: Biology, Therapy, and Immunoprophylaxis. 2007. Chapter 18.

184. Jean Beltran PM, Cristea IM. The life cycle and pathogenesis of human cytomegalovirus infection: lessons from proteomics. Expert Rev Proteomics. 2014:11(6):697-711.

185. Schmolke S, Kern HF, Drescher P, Jahn G, Plachter B. The dominant phosphoprotein pp65 (UL83) of human cytomegalovirus is dispensable for growth in cell culture. J. Virol. 1995:69:5959–5968.

186. Das S, Vasanji A, Pellett PE. Three-dimensional structure of the human cytomegalovirus cytoplasmic virion assembly complex includes a reoriented secretory apparatus. J. Virol. 2007:81:11861–11869.

187. Baxter MK, Gibson W. Cytomegalovirus basic phosphoprotein (pUL32) binds to capsids in vitro through its amino one-third. *J. Virol.2001:*75:6865–6873.

188. Milbradt J, Auerochs S, Marschall M. Cytomegaloviral proteins pUL50 and pUL53 are associated with the nuclear lamina and interact with cellular protein kinase C. *J. Gen. Virol. 2007:*88:2642–2650.

189. Schauflinger M, Fischer D, Schreiber A, Chevillotte M, Walther P, Mertens T, et al. The tegument protein UL71 of human cytomegalovirus is involved in late envelopment and affects multivesicular bodies. J Virol. 2011:85(8):3821-32.

190. Ahlqvist J, Mocarski E. Cytomegalovirus UL103 controls virion and dense body egress. J Virol. 2011:85(10):5125-35.

191. Zhuravskaya T, Maciejewski JP, Netski DM, Bruening E, Macintosh FR, St. Jeor S. Spread of human cytomegalovirus (HCMV) after infection of human hematopoietic progenitor cells: model of HCMV latency. Blood. *1997:*90:2482–2491.

192. Kondo K, Kaneshima H, Mocarski ES. Human cytomegalovirus latent infection of granulocyte-macrophage progenitors. *Proc Natl Acad Sci U S A. 1994:*91:11879–11883.

193. Taylor-Wiedeman J, Sissons JG, Borysiewicz LK, Sinclair JH. Monocytes are a major site of persistence of human cytomegalovirus in peripheral blood mononuclear cells. J. Gen. Virol. 1991:72(Pt 9), 2059–2064.

194. Bolovan-Fritts CA, Mocarski E.S, Wiedeman JA. Peripheral blood CD14(+) cells from healthy subjects carry a circular conformation of latent cytomegalovirus genome. Blood. 1999:93, 394–398.

195. Slobedman B, Mocarski ES. Quantitative analysis of latent human cytomegalovirus. J Virol. 1999:73:4806-12.

196. Reeves MB, Sinclair JH. Circulating dendritic cells isolated from healthy seropositive donors are sites of human cytomegalovirus reactivation in vivo. J Virol. 2013:87(19):10660-7.

197. Sinclair J, Sissons P. Latency and reactivation of human cytomegalovirus. J Gen Virol. 2006:87(Pt 7):1763-79.

198. Noriega VM, Haye KK, Kraus TA, Kowalsky SR, Ge Y, Moran TM, Tortorella D. Human cytomegalovirus modulates monocyte-mediated innate immune responses during short-term experimental latency in vitro. J Virol. 2014:88:9391-405.

199. Wright E, Bain M, Teague L, Murphy J, Sinclair J. Ets-2 repressor factor recruits histone deacetylase to silence human cytomegalovirus immediate-early gene expression in non-permissive cells. Journal of General Virology. 2005:86, 535-544.

200. Rossetto CC, Tarrant-Elorza M, Pari GS. Cis and trans acting factors involved in human cytomegalovirus experimental and natural latent infection of CD14 (+) monocytes and CD34 (+) cells. PLoS Pathog. 2013:9:e1003366.

201. Sinzger C, Jahn G. Human cytomegalovirus cell tropism and pathogenesis. Intervirology. 1996:39(5-6):302-19.

202. Jackson JW, Sparer T. There Is Always Another Way! Cytomegalovirus' Multifaceted Dissemination Schemes. Viruses. 2018:10(7):383.

203. Bentz GL, Jarquin-Pardo M, Chan G, Smith MS, Sinzger C, Yurochko AD. Human cytomegalovirus (hcmv) infection of endothelial cells promotes naive monocyte extravasation and transfer of productive virus to enhance hematogenous dissemination of hcmv. J. Virol. 2006:80:11539–11555.

204. Britt W. Virus entry into host, establishment of infection, spread in host, mechanisms of tissue damage. In: Arvin A, Campadelli-Fiume G, Mocarski E, Moore PS, Roizman B, Whitley R, Yamanishi K, editors. Human Herpesviruses: Biology, Therapy, and Immunoprophylaxis. Cambridge: Cambridge University Press; 2007. Chapter 41.

205. Grefte A, van der Giessen M, van Son W, The TH. Circulating cytomegalovirus (CMV)- infected endothelial cells in patients with an active CMV infection. J Infect Dis. 1993:167(2):270-7.

206. Sweet C. The pathogenicity of cytomegalovirus. FEMS Microbiol Rev. 1999:23(4):457-82.

207. Taylor-Wiedeman J, Sissons P, Sinclair J. Induction of endogenous human cytomegalovirus gene-expression after differentiation of monocytes from healthy carriers. J. Virol. 1994:68:1597–1604.

208. Gerna G, Percivalle E, Baldanti F, Sozzani S, Lanzarini P, Genini E, Lilleri D, Revello MG. Human cytomegalovirus replicates abortively in polymorphonuclear leukocytes after transfer from infected endothelial cells via transient microfusion events. J Virol 2000:74:5629–5638.

209. Rice GP, Schrier RD, Oldstone MB. Cytomegalovirus infects human lymphocytes and monocytes: virus expression is restricted to immediate-early gene products. Proc Natl Acad Sci U S A. 1984:81:6134–6138.

210. Goodrum FD, Jordan CT, High K, Shenk T. Human cytomegalovirus gene expression during infection of primary hematopoietic progenitor cells: A model for latency. Proc. Natl. Acad. Sci. USA. 2002:99:16255–16260.

211. Astrid E, Greijer Chantal, Dekkers AJ, Middeldorp JM. Human Cytomegalovirus Virions Differentially Incorporate Viral and Host Cell RNA during the Assembly Process. Journal of Virology. 2000:74:(19):9078-9082.

212. Lipson SM, Shepp DH, Match ME, Axelrod FB, Whitbread JA. Cytomegalovirus infectivity in whole blood following leukocyte reduction by filtration. Am. J. Clin. Pathol. 2001:116:52–55.

213. Mandell GL, Bennett JE, Dolin R (editors). Principles and Practice of Infectious Diseases. 4th ed. New York: Churchill Livingstone. 1995.

214. Van der Meer JTM, Drew WL, Bowden RA, Galasso GJ, Griffiths PD, Jabs DA, Katlama C, Spector SA, Whitley RJ. Summary of the international consensus symposium on advances in the diagnosis, treatment and prophylaxis of cytomegalovirus infection. Antiviral Res. 1996:32:119–140.

215. Wille PT, Wisner TW, Ryckman B, Johnson DC. Human cytomegalovirus (HCMV) glycoprotein gB promotes virus entry in trans acting as the viral fusion protein rather than as a receptor-binding protein. MBio. 2013:4:e00332–13.

216 Vanarsdall AL, Howard PW, Wisner TW, Johnson DC. Human cytomegalovirus gH/gL forms a stable complex with the fusion protein gB in virions. PLoS Pathog. 2016:12:e1005564.

217. Zhou M, Yu Q, Wechsler A, Ryckman BJ. Comparative analysis of gO isoforms reveals that strains of human cytomegalovirus differ in the ratio of gH/gL/gO and gH/gL/UL128-131 in the virion envelope. J Virol. 2013:87:9680–9690.

218. Chandramouli S, Malito E, Nguyen T, Luisi K, Donnarumma D, Xing Y, Norais N, Yu D, Carfi A. Structural basis for potent antibody-mediated neutralization of human cytomegalovirus. Sci Immunol. 2017:30;2(12).

219. Liu J, Jardetzky TS, Chin AL, Johnson DC, Vanarsdall AL. The human cytomegalovirus trimer and pentamer promote sequential steps in entry into epithelial and endothelial cells at cell surfaces and endosomes. J. Virol. 2018:92:e01336-18.

220. Rasmussen L, Geissler A, Cowan C, Chase A, Winters M. The genes encoding the gCIII complex of human cytomegalovirus exist in highly diverse combinations in clinical isolates. J Virol. 2002:76(21):10841-8.

221. Foglierini M, Marcandalli J, Perez L. HCMV Envelope Glycoprotein Diversty Demystified. Front. Microbiol. 2019:10:1005.

222. Ciferri C, Chandramouli S, Donnarumma D, Nikitin PA, Cianfrocco MA, Gerrein R, Feire AL, Barnett SW, Lilja AE, Rappuoli R, Norais N, Settembre EC, Carfi A. Structural and biochemical studies of HCMV gH/gL/gO and Pentamer reveal mutually exclusive cell entry complexes. Proc Natl Acad Sci U S A. 2015:10;112(6):1767-72.

223. Compton T, Nepomuceno RR, Nowlin DM. Human cytomegalovirus penetrates host cells by pH-independent fusion at the cell surface. Virology. 1992:191(1):387–395.

224. Wille P, Knoche A, Nelson J, Jarvis M, Johnson D. A human cytomegalovirus gO-null mutant fails to incorporate gH/gL into the virion envelope and is unable to enter fibroblasts and epithelial and endothelial cells. J. Virol. 2010:84:2585–2596.

225. Wu Y, Prager A, Boos S, Resch M, Brizic I, Mach M, Wildner S, Scrivano L, Adler B. Human cytomegalovirus glycoprotein complex gH/gL/gO uses PDGFR-alpha as a key for entry. PLoS Pathog. 2017:13:e1006281.

226. Soroceanu L, Akhavan A, Cobbs CS. Platelet-derived growth factor-alpha receptor activation is required for human cytomegalovirus infection. Nature. 2008:455:391–395.

227. Nguyen CC, Kamil JP. Pathogen at the Gates: Human Cytomegalovirus Entry and Cell Tropism. Viruses. 2018:10(12):704.

228. Stanton RJ, Baluchova K, Dargan DJ, et al. Reconstruction of the complete human cytomegalovirus genome in a BAC reveals RL13 to be a potent inhibitor of replication. J Clin Invest. 2010:120(9):3191-3208.

229. Zhang L, Zhou M, Stanton RJ, Kamil J, Ryckman BJ. Expression Levels of Glycoprotein O (gO) Vary between Strains of Human Cytomegalovirus, Influencing the Assembly of gH/gL Complexes and Virion Infectivity. Journal of Virology. 2018:92:(15):e00606-18.

230. Schultz EP, Lanchy JM, Day LZ, Yu Q, Peterson C, Preece J, Ryckman BJ. Specialization for Cell-Free or Cell-to-Cell Spread of BAC-Cloned Human Cytomegalovirus Strains Is Determined by Factors beyond the UL128-131 and RL13 Loci. Journal of Virology. 2020:94:(13):e00034-20.

231. Li G, Nguyen CC, Ryckman BJ, Britt WJ, Kamil JP. A viral regulator of glycoprotein complexes contributes to human cytomegalovirus cell tropism. Proc Natl Acad Sci U S A. 2015:112(14):4471-6.

232. Nguyen CC, Siddiquey MNA, Zhang H, Li G, Kamil JP. Human Cytomegalovirus Tropism Modulator UL148 Interacts with SEL1L, a Cellular Factor That Governs Endoplasmic Reticulum-Associated Degradation of the Viral Envelope Glycoprotein gO. J Virol. 2018:29:92(18):e00688-18.

233. Caló S, Cortese M, Ciferri C, Bruno L, Gerrein R, Benucci B, Monda G, Gentile M, Kessler T, Uematsu Y, Maione D, Lilja AE, Carfí A, Merola M. The Human Cytomegalovirus UL116 Gene Encodes an Envelope Glycoprotein Forming a Complex with gH Independently from gL. Journal of Virology Apr 2016:90:(10):4926-4938.

234. Li Q, Wilkie AR, Weller M, Liu X, Cohen JI. THY-1 cell surface antigen (CD90) has an important role in the initial stage of human cytomegalovirus infection. PLoS Pathog. 2015:11:e1004999.

235. Feire AL, Roy RM, Manley K, Compton T. The glycoprotein B disintegrin-like domain binds beta 1 integrin to mediate cytomegalovirus entry. J. Virol. 2010:84:10026–10037.

236. Wang X, Huang DY, Huong SM, Huang ES. Integrin alphavbeta3 is a coreceptor for human cytomegalovirus. Nat Med. 2005:11:515–521.

237. Campadelli-Fiume G, Collins-McMillen D, Gianni T, Yurochko AD. Integrins as herpesvirus receptors and mediators of the host signalosome. Annu Rev Virol. 2016:3:215–236.

238. Vanarsdall AL, Pritchard SR, Wisner TW, Liu J, Jardetzky TS, Johnson DC. CD147 Promotes Entry of Pentamer-Expressing Human Cytomegalovirus into Epithelial and Endothelial Cells. mBio. 2018:9:(3):e00781-18.

239. Wang X, Huong SM, Chiu ML, Raab-Traub N, Huang ES. Epidermal growth factor receptor is a cellular receptor for humam cytomegalovirus. Nature. 2003:424:456–461.

240. Hochdorfer D, Florin L, Sinzger C, Lieber D. Tetraspanin CD151 promotes Initial Events in Human Cytomegalovirus Infection. J. Virol. 2016:90:6430–6442.

241. Grundy JE, McKeating JA, Ward PJ, Sanderson AR, Griffiths PD. Beta 2 microglobulin enhances the infectivity of cytomegalovirus and when bound to the virus enables class I HLA molecules to be used as a virus receptor. Pt 3J. Gen. Virol. 1987:68:793–803.

242. Fryer J, Heath AB, Anderson R, Minor PD, The Collaborative Study Group. Collaborative study to evaluate the proposed 1st [first] WHO international standard for human cytomegalovirus (HCMV) for nucleic acid amplification (NAT)-based assays. 2010.

243. Laib Sampaio K, Stegmann C, Brizic I, Adler B, Stanton RJ, Sinzger C. The contribution of pUL74 to growth of human cytomegalovirus is masked in the presence of RL13 and UL128 expression. J. Gen. Virol. 2016:97:1917-27.

244. McSharry BP, Jones CJ, Skinner JW, Kipling D, Wilkinson GW. Human telomerase reverse transcriptase-immortalized MRC-5 and HCA2 human fibroblasts are fully permissive for human cytomegalovirus. Journal of general virology. 2001:82:855-863.

245. Kim JH, Lee SR, Li LH, Park HJ, Park JH, Lee KY, et al. High cleavage efficiency of a 2A peptide derived from porcine teschovirus-1 in human cell lines, zebrafish and mice. PLoS One. 2011:6(4):e18556.

246 Trichas G, Begbie J, Srinivas S. Use of the viral 2A peptide for bicistronic expression in transgenic mice. BMC biology. 2008:6:40.

247. Tischer BK, Smith GA, Osterrieder N. En passant mutagenesis: a two step markerless red recombination system. Methods Mol Biol. 2010:634:421-430.

248. Addgene plasmid # 12253 : http://n2t.net/addgene:12553 : RRID:Addgene_12253.

249. Addgene plasmid # 12251 : http://n2t.net/addgene:125531 : RRID:Addgene_12251.

250. Addgene plasmid # 12259 : http://n2t.net/addgene:12559 : RRID:Addgene_12259.

251. Li M, Husic N, Lin Y, Snider BJ. Production of Lentiviral Vectors for Transducing Cells from the Central Nervous System. J Vis Exp. 2012:(63):4031.

252. Dull T, Zufferey R, Kelly M, Mandel RJ, Nguyen M, Trono D, Naldini L. A third-generation lentivirus vector with a conditional packaging system. J Virol. 1998:72(11):8463-71.

253. Otahal A, Fuchs R, Al-Allaf FA, Blaas D. Release of vesicular stomatitis virus spike protein G-pseudotyped lentivirus from the host cell is impaired upon low-density lipoprotein receptor overexpression. J Virol. 2015:89:11723–11726.

254. Meier JL, Stinski MF. Major immediate–early enhancer and its gene products. In Cytomegalovirus Molecular Biology and Immunology, ed. Norfolk, UK: Caister Academic Press. 2006:151–166.

255. Luganini A, Caposio P, Mondini M, Landolfo,S, Gribaudo G. New cell-based indicator assays for the detection of human cytomegalovirus infection and

screening of inhibitors of viral immediate-early 2 protein activity. Journal of applied microbiology. 2008:1791-1801.

256. Schwartz R, Sommer MH, Scully A, Spector DH. Site-specific binding of the human cytomegalovirus IE2 86-kilodalton protein to an early gene promoter. J. Virol. 1994:68:5613–5622.

257. Wu J, O'Neill J, Barbosa MS. Transcription factor Sp1 mediates cell-specific trns-activation of the human cytomegalovirus DNA polymerase gene promoter by immediate-early protein IE86 in glioblastoma U373MG cells. J. Virol. 1998:72:236–244.

258. Asmar J, Wiebusch L, Truss M, Hagemeier C. The putative zinc finger of the human cytomega- lovirus IE2 86-kilodalton protein is dispensable for DNA binding and autorepression, thereby demarcating a concise core domain in the C-terminus of the protein. J Virol. 2004:78:11853–11864.

259. Bukrinsky MI, Haggerty S, Dempsey MP, Sharova N, Adzhubel A, Spitz L, Lewis P, Goldfarb D, Emerman M, Stevenson M. A nuclear localization signal within HIV-1 matrix protein that governs infection of non-dividing cells. Nature. 1993:365:666–669.

260. Gallay P, Chin D, Hope T J, Trono D. HIV-1 infection of nondividing cells mediated through the recognition of integrase by the import/karyopherin pathway. Proc Natl Acad Sci USA. 1997:94:9825–9830.

261. Naldini L, Blömer U, Gallay P, Ory D, Mulligan R, Gage FH, Verma IM, Trono D. In vivo gene delivery and stable transduction of non-dividing cells by a lentiviral vector. Science. 1996:272(5259):263-7.

262. Weekes MP, Tomasec P, Huttlin EL, Fielding CA, Nusinow D, Stanton RJ, Wang ECY, Aicheler R, Murrell I, Wilkinson GWG, Lehner PJ, Gygi SP. Quantitative Temporal Viromics: An Approach to Investigate Host-Pathogen Interaction Cell 2014:157:1460–1472.

263. Tebas P, Stabell EC, Olivo PD. Antiviral susceptibility testing with a cell line which expresses beta-galactosidase after infection with herpes simplex virus. Antimicrob Agents Chemother. 1995:39:1287–1291.

264. Tebas P, Scholl D, Jollick J, McHarg K, Arens M, Olivo PD. A rapid assay to screen for drug-resistant herpes simplex virus. J Infect Dis. 1998:177:217–220.

265. Patel N, Kauffmann L, Baniewicz G, Forman M, Evans M, Scholl D. Confirmation of low-titer, herpes simplex virus-positive specimen results by the enzyme- linked virus-inducible system (ELVIS) using PCR and

repeat testing. J Clin Microbiol. 1999:37:3986–3989.

266. Roos JW, Maughan MF, Liao Z, Hildreth JE, Clements JE. LuSIV cells: a reporter cell line for the detection and quantitation of a single cycle of HIV and SIV replication. Virology. 2000:273:307–315.

267. Kung SH, Wang YC, Lin CH, Kuo RL, Liu WT. Rapid diagnosis and quantification of herpes simplex virus with a green fluorescent protein reporter system. J Virol Methods. 2000:90:205–212.

268. Wu J, O'Neill J, Barbosa MS. Late temporal gene expression from the human cytomegalovirus pp28US (UL99) promoter when integrated into the host cell chromosome. Journal of General Virology. 2001:82:1147–1155.

269. Liu WT, Sun JR, Lin CH, Kuo RL, Kung SH. An indicator cell assay for detection of human cytomegalovirus based on enhanced green fluorescent protein. Journal of Virological Methods. 2001:96:85–92.

270. Kerry, JA, Priddy MA, Jervey TY, Kohler CP, Staley TL, Vanson CD, Jones TR, Iskenderian AC, Anders DG, Stenberg RM. Multiple regulatory events influence human cytomegalovirus DNA polymerase (UL54) expression during viral infection. J. Virol. 1996:70:373–382.

271. Kohler CP, Kerry JA, Carter M, Muzithras VP, Jones TR, Stenberg RM. Use of recombinant virus to assess human cytomegalovirus early and late promoters in the context of the viral genome. J. Virol. 1994:68:6589–6597.

272. Kim YE, Park MY, Kang KJ, Han TH, Lee CH, Ahn JH. Requirement of the N-terminal residues of human cytomegalovirus UL112-113 proteins for viral growth and oriLyt-dependent DNA replication. *J Microbiol*. 2015:53:561–569.

273. Cormack BP, Valdivia RH, Falkow S. FACS-optimized mutants of the green fluorescent protein (GFP). Gene. 1996:173(1):33–38.

274. Yang TT, Cheng L, Kain SR. Optimized codon usage and chromophore mutations provide enhanced sensitivity with the green fluorescent protein. Nucleic Acids Res. 1996:24:4592–4593.

275. Chalfie M, Tu Y, Euskirchen G, Ward WW, Prasher D. Green fluorescent protein as a marker for gene expression. Science. 1994:263:802-805.

276. Troy T, Jekic-McMullen D, Sambucetti L, Rice B. Quantitative comparison of the sensitivity of detection of fluorescent and bioluminescent reporters in animal models. Imaging. 2004:3(1):9–23.

277. Nagy SR, Sanborn JR, Hammock BD, Denison MS. Development of a Green Fluorescent Protein-Based Cell Bioassay for the Rapid and Inexpensive Detection and Characterization of Ah Receptor Agonists. Toxicological Sciences. 2002:65:200–210.

278. Aubin JE. Autofluorescence of viable cultured mammalian cells. J Histochem Cytochem. 1979:27:36–43.

279. Drezek R, Sokolov K, Utzinger U, Boiko I, Malpica A, Follen M, Richards-Kortum R. Understanding the contributions of NADH and collagen to cervical tissue fluorescence spectra: modeling, measurements, and implications. Journal of biomedical optics. 2001:6(4):385–396.

280. Billinton N, Knight AW. Seeing the wood through the trees: a review of tech-niques for distinguishing greenfluorescent protein from endogenous autofluores-cence. Anal. Biochem. 2001:291(2):175–197.

281. Banerjee B, Miedema BE, Chandrasekhar HR. Role of basement membrane collagen and elastin in the autofluorescence spectra of the colon. J Investig Med 1999:47:326-32.

282. Benson RC, Meyer RA, Zaruba ME, McKhann GM. Cellular autofluorescence - is it due to flavins? The journal of histochemistry and cytochemistry : official journal of the Histochemistry Society. 1979:27:44 - 48.

283. Ishii N, Maier D, Merlo A, Tada M, Sawamura Y, Diserens A C, Van Meir EG. Frequent co-alterations of TP53, p16/CDKN2A, p14ARF, PTEN tumor suppressor genes in human glioma cell lines. Brain pathology (Zurich, Switzerland). 1999:9(3):469–479.

284. https://www.lgcstandards-atcc.org/Global/FAQs/C/F/U373_MG_ATCC_HTB17-1055.aspx?geo_country=gb

285. Croce AC, Bottiroli G. Autofluorescence spectroscopy and imaging: a tool for biomedical research and diagnosis. Eur J Histochem. 2014:12:58(4):2461.

286. Bindels D, Haarbosch L, van Weeren L. Postmas M, Wiese KE, Mastop M, Aumonier S, Gotthard G, Royant A, Hink MA, Gadella TWJ. mScarlet: a bright monomeric red fluorescent protein for cellular imaging. Nat Methods. 2017:14:53–56.

287. Moore CB, Guthrie EH, Huang MTH, Taxman DJ. Short Hairpin RNA (shRNA): Design, Delivery, and Assessment of Gene Knockdown. Methods Mol Biol. 2010:629:141-158.

288. Enomoto M, Hirai T, Kaburagi H, Yokota T. Efficient Gene Suppression in Dorsal Root Ganglia and Spinal Cord Using Adeno-Associated Virus Vectors Encoding Short-Hairpin RNA. In: Shum K., Rossi J. (eds) SiRNA Delivery Methods. Methods in Molecular Biology. 2016:364.

289. Khvorova A, Reynolds A, Javasena SD. Functional siRNAs and miRNAs Exhibit Strand Bias. Cell. 2003:2993:115(2):209-216.

290. Schwarz DS, Hutvagner G, Du T, Xu Z, Aronin N, Zamore PD. Asymmetry in the Assembly of the RNAi Enzyme Complex. Cell. 2003:115(2):199-208.

291. https://www.invivogen.com/sirnawizard/guidelines.php

292. Cortese M, Calò S, D'Aurizio R, Lilja A, Pacchiani N, Merola M. Recombinant Human Cytomegalovirus (HCMV) RL13 Binds Human Immunoglobulin G Fc. Plos One. 2012:7(11):e50166.

293. Elbashir SM, Martinez J, Patkaniowska A, Lendeckel W, Tuschi T. Functional anatomy of siRNAs for mediating efficient RNAi in Drosophila melanogaster embryo lysate. EMBO J. 2001:20:6877-6888.

294. Jackson AL, Bartz SR, Schelter J, Kobayashi SV, Burchard J, Mao M, Li B, Cavet G, Linsley PS. Expression profiling reveals off-target gene regulation by RNAi. Nat. Biotechnol. 2003:21:635-637.

295. Amarzguioui M, Holen T, Babaie E, Prydz H. Tolerance for mutations and chemical modifications in a siRNA. Nucleic Acids Res. 2003:31:589-595.

296. Yu JY, DeRuiter SL, Turner DL . RNA interference by expression of short-interfering RNAs and hairpin RNAs in mammalian cells. PNAS. 2002:99(9):6047-52.

297. Mäkinen PI, Koponen JK, Kärkkäinen AM, Malm TM, Pulkkinen KH, Koistinaho J, Turunen MP, Ylä-Herttuala S. Stable RNA interference: comparison of U6 and H1 promoters in endothelial cells and in mouse brain. J Gene Med. 2006:8(4):433-41.

298. Kunkel GR, Maser RL, Calvet JP, Pederson T. U6 small nuclear RNA is transcribed by RNA polymerase III. Proc. Natl Acad. Sci. USA. 1986:83: 8575-8579.

299. Gandara C, Affleck V, Stoll EA. Manufacture of third-generation lentivirus for preclinical use, with process development considerations for translation to Good Manufacturing Practice (GMP). Human Gene Therapy Methods. 2018:29(1):1-15.

300. Hanenberg H, Xiao XL, Dilloo D, Hashino K, Kato I, Williams DA. Colocalization of retrovirus and target cells on specific fibronectin fragments increases genetic transduction of mammalian cells. Nat Med. 1996:2:876-882.

301. Fire A, Xu S, Montgomery MK, Kostas SA, Driver SE, Mello CC**.** Potent and specific genetic interference by double-stranded RNA in C. elegans. Nature. 1998:391**:**806-811.

302. Hamilton AJ, Baulcombe DC. A species of small antisense RNA in post-transcriptional gene silencing in plants. Science. 1999:286:950–952.

303. Kennerdell JR, Carthew RW. Use of dsRNA-mediated genetic interference to demonstrate that frizzled and frizzled 2 act in the wingless pathway. Cell. 1998:95:1017–1026.

304. Hammond SM, Bernstein E, Beach D, Hannon GJ. An RNA-directed nuclease mediates post-transcriptional gene silencing in Drosophila cells. Nature. 2000:404:293–296.

305. Elbashir SM, Harborth J, Lendeckel W, Yalcin A, Weber K, Tuschl T. Duplexes of 21±nucleotide RNAs mediate RNA interference in cultured mammalian cells. Nature. 2001:411:494-498.

306. Harborth J, Elbashir SM, Bechert K, Tuschl T, Weber K. Identification of essential genes in cultured mammalian cells using small interfering RNAs. J Cell Sci. 2001:114:4557-4565.

307. https://www.thermofisher.com/uk/en/home/references/gibco-cell-culture-basics/transfection-basics/choosing-transfection-strategy.html.

308. Leuschner PJF, Ameres SL, Kueng S, Martinez J. Cleavage of the siRNA passenger strand during RISC assembly in human cells. EMBO Rep. 2006:7(3):314–320.

309. Wang XJ, Li Y, Huang H, Zhang XJ, Xie PW, Hu W, Li DD, Wang SQ. A Simple and Robust Vector-Based shRNA Expression System Used for RNA Interference. Plos One. 2013:8:e56110.

310. Elbashir SM, Martinez J, Patkaniowska A, Lendeckel W, Tuschl T. Functional anatomy of siRNAs for mediating efficient RNAi in Drosophila melanogaster embryo lysate. EMBO J. 2001:20:6877–6888.

311. Jackson AL, Bartz SR, Schelter J, Kobayashi SV, Burchard J, Mao M, Li B, Cavet G, Linsley PS. Expression profiling reveals off-target gene regulation by RNAi. Nat. Biotechnol. 2003:21:635–637.

312. Amarzguioui M, Holen T, Babaie E, Prydz H. Tolerance for mutations and chemical modifications in a siRNA. Nucleic Acids Res. 2003:31:589–595.

313. Baldanti F, Paolucci S, Campanini G, Sarasini A, Percivalle E, Revello MG, Gerna G. Human cytomegalovirus UL131A, UL130 and UL128 genes are highly conserved among field isolates. Archives of Virology. 2006:151:6:1225-1233.

314. Bannister SC, Wise TG, Cahill DM, Doran TJ. Comparison of chicken 7SK and U6 RNA polymerase III promoters for short hairpin RNA expression. BMC. Biotechnol. 2007:7:79.

315. Lambeth LS, Wise TG, Moore RJ, Muralitharan MS, Doran TJ. Comparison of bovine RNA polymerase III promoters for short hairpin RNA expression. Anim Genet. 2006:37:369–372.

316. Lee, S. K., Dykxhoorn, D. M., Kumar, P., Ranjbar, S., Song, E., Maliszewski, L. E., François-Bongarçon, V., Goldfeld, A., Swamy, N. M., Lieberman, J., & Shankar, P. (2005). Lentiviral delivery of short hairpin RNAs protects CD4 T cells from multiple clades and primary isolates of HIV. Blood, 106(3), 818–826.

317. Wang H, Lui X, Wu,J, Wu G, Yu L, Yang CHH, Xie, Y, Xia X, He, H Bovine fetal epithelium cells expressing shRNA targeting viral VP1 gene resisted against foot-and-mouth disease virus. Virology. 2013:439(2):115-121.

318. Ye C, Chen M, Chen E, et al. Knockdown of FOXA2 enhances the osteogenic differentiation of bone marrow-derived mesenchymal stem cells partly via activation of the ERK signalling pathway. Cell Death Dis. 2018:9(8):836.

319. Tanioka M, Mott KR, Hollern DP. et al. Identification of Jun loss promotes resistance to histone deacetylase inhibitor entinostat through Myc signaling in luminal breast cancer. Genome Med. 2018:10:86.

320. Moore, CB, Guthrie EH, Huang MTH, Taxman DJ. Short Hairpin RNA (shRNA): Design, Delivery, and Assessment of Gene Knockdown. Methods Mol Biol. 2010:629:141-158.

321. Reynolds A, Leake D, Boese Q, Scaringe S, Marshall WS, Khvorova A. Rational siRNA design for RNA interference. Nat. Biotechnol. 2004:22:326–330.

322. Amarzguioui M, Prydz H. An algorithm for selection of functional siRNA sequences. Biochem. Biophys. Res. Commun. 2004:316:1050–1058.

323. Ui-Tei K, Naito Y, Takahashi F, Haraguchi T, Ohki-Hamazaki H, Juni A, Ueda R, Saigo K. Guidelines for the selection of highly effective siRNA

sequences for mammalian and chick RNA interference. Nucleic Acids Res. 2004:32:936–948.

324. Takasaki S, Kotani S, Konagaya A. An effective method for selecting siRNA target sequences in mammalian cells. Cell Cycle. 2004:3:790–795.

325. Luo KQ, Chang DC. The gene-silencing efficiency of siRNA is strongly dependent on the local structure of mRNA at the targeted region. Biochem. Biophys. Res. Commun. 2004:318:303–310.

326. Heale BS, Soifer HS, Bowers C, Rossi JJ. siRNA target site secondary structure predictions using local stable substructures. Nucleic Acids Res. 2005:33:e30.

327. Mittal V. Improving the efficiency of RNA interference in mammals. Nat. Rev. Genet. 2004:5:355–365.

328. Sandy P, Ventura A, Jacks T. Mammalian RNAi: a practical guide. Biotechniques. 2005:39:215–224.

329. Gong D, Ferrell JE Jr. Picking a winner: new mechanistic insights into the design of effective siRNAs. Trends Biotechnol. 2004:22(9):451–454.

330. Xu XM, Yoo MH, Carlson BA, Gladyshev VN, Hatfield DL. Simultaneous knockdown of the expression of two genes using multiple shRNAs and subsequent knock-in of their expression. Nat Protoc. 2009:4(9):1338–1348.

331. Chai L, QiaoZ, Wang J, Lui M, Wang Y, Wang X, He M, Li W, Yu Q, Han Y, Ren S. Optimization and establishment of RNA interference-mediated knockdown of the progestagen-associated endometrial protein gene in human metastatic melanoma cell lines. Molecular medicine reports. 2013:1390-1396.

332. Akter P, Cunningham C, McSharry BP, Dolan A, Addison C, Dargan DJ, Hassan-Walker AF, Emery VC, Griffiths PD, Wilkinson GW, Davison AJ. Two novel spliced genes in human cytomegalovirus. J. Gen. Virol. 2003:84:1117-1122.

333. Maele BV, De Rijck J, De Clercq E, Debyser Z. Impact of the Central Polypurine Tract on the Kinetics of Human Immunodeficiency Virus Type 1 Vector Transduction. Journal of Virology. 2003:77(8):4685-4694.

334. Mwiniarska M, Nowis D, Firczuk M, Zagozdzon A, Gabrysiak M, Sadowski R, Barankiewicz J, Dwojak M, Golab J. Selection of an optimal promoter for gene transfer in normal B cells. Molecular Medicine Reports. 2017:16:3041-48.

335. Fechner H, Wang X, Wang H, Jansen A, Pauschinger M, Scherübl H, Bergelson JM, Schultheiss H-P, Poller W. Trans-complementation of vector replication versus Coxsackie-adenovirus-receptor overexpression to improve transgene expression in poorly permissive cancer cells. Gene Therpay. 2000:7:1954-68.

336. Legrand V, Spehner D, Schlesinger Y, Settelen N, Pavirani A, Mehtali M. Fiberless Recombinant Adenoviruses: Virus Maturation and Infectivity in the Absence of Fiber. J Virol. 1999 Feb; 73(2): 907–919.

337. Jorba N, Coloma R, Ortín J. Genetic trans-Complementation Establishes a New Model for Influenza Virus RNA Transcription and Replication. Plos pathogens. 2009:(5):e1000462.

338. Min J, Yang D, Kim M, Haam K, Yoo A, Choi JH, Schrami BU, Kim YS, Kim D. Kang SJ. Inflammation induces two types of inflammatory dendritic cells in inflamed lymph nodes. Experimental & Molecular Medicine. 2018:50:458.

339. Palucka K, Banchereau J. Cancer immunotherapy via dendritic cells. Nat Rev Cancer. 2012:22:12(4):265-77.

340. Hertel L. Human cytomegalovirus tropism for mucosal myeloid dendritic cells. Rev Med Virol. 2014:24(6):379-95.

341. Banchereau J, Steinman R. Dendritic cells and the control of immunity. Nature. 1998:392:245–252.

342. Serbina NV, Salazar-Mather TP, Biron CA, Kuziel WA, Pamer EG. TNF/iNOS-producing dendritic cells mediate innate immune defense against bacterial infection. Immunity. 2003:19:59–70.

343. Romani N, Gruner S, Brang D, Kampgen E, Lenz A, Trockenbacher B, Konwalinka G, Fritsch PO, Steinman RM, Schuler G. Proliferating dendritic cell progenitors in human blood. J. Exp. Med. 1994:180:83.

344. Sallusto F, Lanzavecchia A. Efficient presentation of soluble antigen by cultured human dendritic cells is maintained by granulocyte/macrophage colony-stimulating factor plus interleukin 4 and downregulated by tumor necrosis factor alpha. J. Exp. Med. 1994:179:1109.

345. Steinman RM, Idoyaga J. Features of the dendritic cell lineage. Immunological Reviews. 2010:234.

346. Collin M, Bigley V. Human dendritic cell subsets: an update. Immunology. 2018:154(1):3-20.

347. Segura E, Amigorena S. Inflammatory dendritic cells in mice and humans. Trends Immunol. 2013:34:440-445.

348. Kuznetsova AV, Kurinov AM, Aleksandrova MA. Cell models to study regulation of cell transformation in pathologies of retinal pigment epithelium. J Ophthalmol. 2014:2014:801787.

349. Dunn KC, Aotaki-Keen AE, Putkey FR, Hjelmeland LM. ARPE-19, a human retinal pigment epithelial cell line with differentiated properties. Experimental Eye Research. 1996:62(2):155–169.

350. Rambhatla L, Chiu C-P, Glickman RD, Rowe-Rendleman C. In Vitro Differentiation Capacity of Telomerase Immortalized Human RPE Cells. Investigative Ophthalmology & Visual Science. 2002:43:622-1630.

351. Luo Y, Zhuo Y, Fukuhara M, Rizzolo LJ. Effects of culture conditions on heterogeneity and the apical junctional complex of the ARPE-19 cell line. Investigative Ophthalmology and Visual Science. 2006:47(8):3644–3655.

352. Revello MG, Baldanti F, Percivalle E, Sarasini A, De-Giuli L, Genini E, Lilleri D, Labò N, Gerna G. In vitro selection of human cytomegalovirus variants unable to transfer virus and virus products from infected cells to polymorphonuclear leukocytes and to grow in endothelial cells. J Gen Virol. 2001:82(Pt 6):1429-1438.

353. Wang D, Shenk T. Human cytomegalovirus UL131 open reading frame is required for epithelial cell tropism. J Virol. 2005:79:10330-10338.

354. Wang D, Shenk T. Human cytomegalovirus virion protein complex required for epithelial and endothelial cell tropism. Proc Natl Acad Sci. USA. 2005:102:18153–18158.

355. Ryckman BJ, Jarvis MA, Drummond DD, Nelson JA, Johnson DC. Human cytomegalovirus entry into epithelial and endothelial cells depends on genes UL128 to UL150 and occurs by endocytosis and low-pH fusion. J Virol 2006:80:710–722.

356. Lei H, Rheaume MA, Velez G, Mukai S, Kazlauskas A. Expression of PDGFRalpha is a determinant of the PVR potential of ARPE19 cells. Invest Ophthalmol Vis Sci. 2011:52:5016–5021.

357. https://cmvaction.org.uk/about-us/counting-cost-cmv

358. Stratton KR, Durch JS, Lawrence RS (editors). Vaccines for the 21st Century: A Tool for Decisionmaking. Committee to Study Priorities for Vaccine

Development. Division of Health Promotion and Disease Prevention, Institute of Medicine. The National Academies Press 2000.

359. Suárez NM, Wilkie GS, Hage E, Camiolo S, Holton M, Hughes J, Maabar M, Vattipally SB, Dhingra A, Gompels UA, Wilkinson GWG, Baldanti F, Furione M, Lilleri D, Arossa A, Ganzenmueller T, Gerna G, Hubáček P, Schultz TF, Wolf D, Zavattoni M, Davison AJ. Human cytomegalovirus Genomes Sequenced Directly From Clinical Material: Variation, Multiple-Strain Infection, Recombination, and Gene Loss. J Infect Dis. 2019:31:220(5):781-791.

360. Human cytomegalovirus haplotype reconstruction reveals high diversity due to superinfection and evidence of within-host recombination
Cudini J, Roy S, Houldcroft CJ, Bryant JM, Depledge DP, Tutill H, Veys P, Williams R, Worth AJJ, Tamuri AU, Goldstein RA, Breuer J. Proceedings of the National Academy of Sciences. 2019:116(12):5693-5698.

361. Chou SW. Reactivation and recombination of multiple cytomegalovirus strains from individual organ donors. J Infect Dis. 1989:160(1):11-5.

362. Dunn W, Chou C, Li H, Hai R, Patterson D, Stolc V, et al. Functional profiling of a human cytomegalovirus genome. Proc Natl Acad Sci U S A. 2003:100(24):14223-8.

363. Ourahmane A, Cui X, He L, Catron M, Dittmer DP, Al Qaffasaa A, Schleiss MR, Hertel L, McVoy MA. Inclusion of Antibodies to Cell Culture Media Preserves the Integrity of Genes Encoding RL13 and the Pentameric Complex Components During Fibroblast Passage of Human Cytomegalovirus. Viruses. 2019:11:221.

364. Hitt DC, Booth JL, Dandapani V, Pennington LR, Gimble JM, Metcalf J. A flow cytometric protocol for titering recombinant adenoviral vectors containing the green fluorescent protein. Mol Biotechnol. 2000:14:197-203.

365. Gueret V, Negrete-Virgen JA, Lyddiatt A, Al-Rubeai M. Rapid titration of adenoviral infectivity by flow cytometry in batch culture of infected HEK293 cells. Cytotechnology. 2002:38:87-97.

366. Jackson AL, Linsley PS. Recognizing and avoiding siRNA off-target effects for target identification and therapeutic application. Nature Reviews: Drug Discovery. 2010:9:57-67.

367. Tomasec P, Wang EC, Davison AJ, Vojtesek B, Armstrong M, Griffin C, McSharry BP, Morris RJ, Llewellyn-Lacey S, Rickards C, Nomoto A, Sinzger c, Wilkinson GWG. Downregulation of natural killer cell-activating ligand CD155 by human cytomegalovirus UL141. Nat. Immunol. 2005:6:181–188.

368. Sinzger C, Hahn G, Digel M, Katona R, Sampaio KL, Messerle M, Hengel H, Koszinowski U, Brune W, Adler B. Cloning and sequencing of a highly productive, endotheliotropic virus strain derived from human cytomegalovirus TB40/E. J. Gen. Virol. 2008:89:359–368.

369. Vo M, Aguiar A, McVoy MA, Hertel L. Cytomegalovirus Strain TB40/E Restrictions and Adaptations to Growth in ARPE-19 Epithelial cells. Microorganisms. 2020:8:615.

370. Prod'homme V, Sugrue DM, Stanton RJ, Nomoto A, Davies J, Rickards CR, Cockrane D, Moore M, Wilkinson GW, Tomasec P. Human cytomegalovirus UL141 promotes efficient downregualtion of the natural killer cell activating ligand CD112. J Gen Virol. 2010:91:2034-2039.

371. Nemčovičová I, Benedict CA, Zajonc DM. Structure of human cytomegalovirus UL141 binding to TRAIL-R2 reveals novel, non-canonical death receptor interactions. PLoS Pathog. 2013:9:e10032242013.

372 Zou F, Lu ZT, Wang S, Wu S, Wu YY, Sun ZR. Human cytomegalovirus UL141 protein interacts with CELF5 and affects viral DNA replication. Mol Med Rep. 2018:17: 4657-4664.

373. Naing Z, Hamilton ST, van Zuylen WJ, Scott GM, Rawlinson WD. Differential Expression of PDGF Receptor-α in Human Placental Trophoblasts Leads to Different Entry Pathways by Human Cytomegalovirus Strains. Sci Rep. 2020:10:1082.